STANFORD ELECTRONICS LABORATORIES

DEPARTMENT OF ELECTRICAL ENGINEERING
STANFORD UNIVERSITY · STANFORD, CA 94305

STUDY OF THE ELECTRONIC SURFACE STATE OF III-V COMPOUNDS

FINAL TECHNICAL REPORT

W. E. Spicer, Principal Investigator
Telephone: (415) 497-4643

15 October 1978

NIGHT VISION LABORATORY
U.S. Army Electronics Command
Fort Belvoir, Virginia 22060

Sponsored by

DEFENSE ADVANCED RESEARCH PROJECTS AGENCY
DARPA ORDER NO. 2182
PROGRAM CODE NO. 4D10

CONTRACT NO. DAAK02-74-C-0069

(6) STUDY OF THE ELECTRONIC SURFACE STATE OF III-V COMPOUNDS.

(9) FINAL TECHNICAL REPORT.

(10) W. E. Spicer, Principal Investigator
Telephone: (415) 497-4643

(11) 15 Oct 78

NIGHT VISION LABORATORY
U.S. Army Electronics Command
Fort Belvoir, Virginia 22060

(12) 259

Sponsored by

DEFENSE ADVANCED RESEARCH PROJECTS AGENCY
DARPA ORDER NO. 2182
PROGRAM CODE NO. 4D10

(15) [redacted] DAAK02-74-C-0069 ; ARPA Order-2182

Effective: 1973 September 01 Expiration: 1978 September 30 ($742,742)

STANFORD ELECTRONICS LABORATORIES
STANFORD UNIVERSITY
STANFORD, CALIFORNIA 94305

The views and conclusions contained in this document are those of the authors and should not be interpreted as necessarily representing the official policies, either expressed or implied, of the Defense Advanced Research Projects Agency of the U.S. Government.

332 400

SUMMARY

In the past few years, we have made intensive studies of the physics of compound semiconductor interfaces. This report contains the most important results obtained during the contract period and is divided roughly into three parts dealing with Schottky-barrier formation, oxygen chemisorption, and cesium and cesium oxide overlayers. Following the Overview, Chapter 2 presents a model for the surface structure of GaAs which is now accepted. The next chapter demonstrates that Schottky-barrier pinning is due not to intrinsic surface states but to metal induced extrinsic states. Chapter 4 describes synchrotron radiation studies of Au Schottky-barrier formation on the IV-V semiconductors and presents a model of Schottky-barrier pinning based on defect formation induced by the Au overlayer. This model is expanded and generalized in Chapter 5, where a unified model for Schottky-barrier and III-V-insulator interface states formation is discussed. Chapters 6 and 7 deal with core level and valence band studies of oxygen chemisorption and oxide formation on GaAs, GaSb, and InP. Chapter 8 contains a study of thick Cs oxides (on a Cu substrate) at liquid nitrogen temperature, using photon energies lower than 11 eV, while Chapter 9 describes a synchrotron radiation study of the interaction of oxygen with cesiated GaAs at room temperature, where it is shown that conventional models of negative electron affinity devices are likely to be inadequate. A list of the papers published under the support of this contract is given in the Appendix. Reprints of these publications are available.

CONTENTS

		Page
1.	OVERVIEW	1
2.	SURFACE STATE BAND ON THE GaAs (110) FACE	4
3.	COMMENT ON "RELATION OF SCHOTTKY BARRIERS TO EMPTY SURFACE STATES ON III-V SEMICONDUCTORS	15
4.	PHOTOEMISSION STUDY OF Au SCHOTTKY BARRIER FORMATION ON GaSb, GaAs, AND InP USING SYNCHROTRON RADIATION	22
	Introduction	23
	Experimental	26
	Results	29
	SXPS Spectra	29
	UPS and CFS Spectra	41
	Discussion	62
5.	A NEW AND UNIFIED MODEL FOR SCHOTTKY-BARRIER AND 3-5-INSULATOR INTERFACE STATES FORMATION	75
	Introduction	78
	Do Intrinsic States Move into the Band Gap?	79
	A Mechanism for Fermi Level Pinning by Metal or Oxygen Deposition	82
	General Approach	82
	Fermi Level Pinning Versus Metal Coverage	83
	Similarity of Fermi Level Pinning for Oxygen and Metals	83
	Are Pinning Levels Produced Indirectly by Adatoms?	84
	The Model for Interface States Formed by Adatoms	85
	Indirect Evidence for Lattice Defect Formation	88
	During Oxygen Uptake	88
	During Schottky-Barrier Formation	90
	Comparison with Thick "Device" Oxides or Schottky Barriers	92
	Schottky Barriers	92
	Correlation with Practical "Device" Oxides	94
	Summary and Conclusions	97

CONTENTS (Cont)

Page

6. CHEMISORPTION AND OXIDATION STUDIES OF THE (110) SURFACES OF GaAs, GaSb, AND InP 124

Introduction 126

Experimental 130

Apparatus 130

Procedure 132

Results 134

Discussion 141

Interpretation of Chemical Shifts 141

Model for Oxidation of GaAs (110) 148

Determination of the Escape Depth 152

Surface Chemical Shift 153

7. VALENCE BAND STUDIES OF CLEAN AND OXYGEN EXPOSED GaAs (110) SURFACES 176

Introduction 177

Experimental 180

Apparatus and Procedure 180

Results 182

Discussion and Conclusions 190

8. THE OXIDATION OF Cs - UV PHOTOEMISSION STUDIES 220

Introduction 221

Experimental Details 222

Results 224

Introduction 224

Low Oxygen Exposure (Regions I and II) 224

Regions of Large Oxygen Exposure (Regions II, III and IV) 226

Conclusions 227

9. OXYGEN CHEMISORPTION ON Cs COVERED GaAs (110) SURFACES 242

APPENDIX: Publications 250

Chapter 1

OVERVIEW

For the last few years, we have devoted much effort towards the study of the physics and chemistry of the III-V semiconductor surface. The compounds we examined in detail are GaAs, GaSb, and InP. Major areas of research include surface states on the clean surface, Schottky-barrier formation, oxygen chemisorption and oxide formation, and cesium oxides on semiconductor and metal substrates. The majority of our work has been on the cleaved (110) surface, since this surface is easier to reproduce and has a high degree of perfection (e.g., nonstoichiometry is not a problem) and an understanding of this surface should provide a solid stepping-stone towards the understanding of other, more complex, faces. The early experiments were conducted at the Stanford Electronics Laboratories using a hydrogen discharge lamp. While much useful information was obtained, the relatively low photon energies available ($h\nu < 12$ eV) meant somewhat less than optimum surface sensitivity and also limited the accessible range of electronic structure to the top half of the valence band. The completion of the Stanford Synchrotron Radiation Laboratory expanded our capability enormously since we are now able to probe both core levels and the valence band with great surface sensitivity. Most of the experiments performed in the last three years used synchrotron radiation as the light source.

Filled surface states in Si were first observed with photoemission in 1972 by Wagner and Spicer[1] and by Eastman and Grobman.[2] Eastman and Grobman[2] also observed filled surface state emission from GaAs. However, much work in this laboratory failed to reproduce these observations and led instead to the formulation of the GSCH (Gregory, Spicer, Ciraci, Harrison) model for the GaAs (110) surface described in Chapter 2. In this

model, the As surface atoms are relaxed outward and the Ga surface atoms inward, with the dangling bond electrons associated with the surface As. The empty and filled surface states are separated by a large band gap, with the filled states located below the valence band maximum. The major features of this model is now accepted as correct, although the empty states located near midgap in the first experiments were later found to be extrinsic, due probably to defects, while the intrinsic empty surface states were actually higher up in energy, being above the conduction band edge.

Experiments on the Cs Schottky barrier on GaSb led to the conclusion that intrinsic surface states are not responsible for Schottky-barrier pinning. Rather, the pinning is due to extrinsic states induced by the metal. Naturally, the next step is to discover the nature of these metal-induced states. Our work on the Au Schottky barrier (using synchrotron radiation) led to the suggestion that these states are defect related. The heat of adsorption of the metal on the semiconductor is sufficient to generate some defects. Localized states associated with these defects then pin the Fermi level. In Chapter 5, the "defect" model is generalized to apply to not only the metal-semiconductor interface but also to the oxide-semiconductor interface. Suggestions are also made as to their nature. The pinning levels have the following locations relative to the valence band maximum: GaAs, 0.7 and 0.5 eV; InP, 0.9 and 1.2 eV. The first energy is associated with a missing anion and the second with a missing cation. For GaSb, only an acceptor due to a missing Sb has been located at 0.1 eV.

Studies of the core levels and valence bands of the III-V compounds are discussed in Chapters 6 and 7, respectively. In these studies, it is

found that oxygen excited by a hot filament gauge gives rise to very different surface chemistry compared to when unexcited, molecular oxygen is used. By observing the changes in the core level positions and heights, the formation of As_2O_3, As_2O_5, free As, and Ga_2O_3 at different stages of oxidation using excited oxygen, and the sublimation of As_2O_3, may be followed. In the valence band studies, by correlating band bending, photoemission and partial yield (constant final state) measurements, it is found that Fermi level pinning at midgap on GaAs is caused by extrinsic states. It is also found that small amounts ($<<1\%$) of oxygen coverage can cause the photoemission spectra to show sharper structure, implying that the oxygen has long-range effects. In fact, with a coverage of about 5%, oxygen causes the valence band structure to smear, indicating disorder.

The last two chapters deal with the study of Cs-O. The object of the work is to obtain information on bulk Cs oxides and correlate this with the Cs-O-GaAs surface in an effort to understand the physics of negative electron affinity surfaces on photocathodes. Surprisingly, synchrotron radiation studies of the oxidation of cesiated GaAs reveal that Cs caused the adsorption rate of oxygen on GaAs to accelerate by as much as six orders of magnitude, while it is by no means clear whether any Cs oxides or suboxides formed. This suggests that previous models of the negative electron affinity GaAs surface, which assume formation of Cs oxides, may be inadequate. Further work is called for.

References

1. L. F. Wagner and W. E. Spicer, Phys. Rev. Lett. 28, 1381 (1972).
2. D. E. Eastman and W. D. Grobman, Phys. Rev. Lett. 28, 1378 (1972).

Chapter 2

SURFACE STATE BAND ON THE GaAs (110) FACE

P. E. Gregory, W. E. Spicer, Department of Electrical Engineering*
and
S. Çıracı, W. A. Harrison, Department of Applied Physics+
Stanford University, Stanford, CA. 94305

ABSTRACT: Careful photoemission studies of surface states on the cleavage GaAs (110) detect no filled states in the band gap. However, empty states pin the surface Fermi level on n-type GaAs at mid-band gap. Filled states are placed below the valence band maximum and empty surface states in the upper half of the band gap. Calculations, using the Bond Orbital Model, agree with these results and associate the empty and filled bands with Ga and As, respectively.

Recently through experimental[1,2,3] and theoretical[4] studies, major advances have been made in the understanding of Si surface states. Through photoemission studies, a good measure of the density of filled states[1,2,3] and their dependence[3] on crystal face has been obtained. However, contradictory results have been reported concerning the clean GaAs cleavage (110) plane. Eastman and Grobman[2](EG) have reported filled surface states lying in the bottom half of the band gap; whereas, Van Laar and Scheer[5] (VLS) and Dinan, Galbraith, and Fischer[6](DGF) found no filled states there. Here we report: (1) very careful experimental work which shows the bottom half of the valence band to be free of surface states (i.e., the filled states lie below the valence band maximum), and empty surface states extending down to the middle of the band gap, in agreement with DGF; and (2) theoretical work which explains the large band gap between the filled and empty surface states and relates this to the electronic population of surface atoms. Brief comments are made concerning the effects of oxygen and of Cs on the surface states and surface atoms.

The surface of GaAs has been studied by ultraviolet photoemission spectroscopy, using a technique similar to that used by Wagner and Spicer[1] to study Si surface states. The cleaved (110) surfaces were usually very smooth, but two roughly cleaved surfaces (i.e., surface containing many steps) were purposely made. The samples studied are described in Table I. Energy distribution curves (EDCs) are given in Figs. 1a and b. In most cases, the pressure was below 5×10^{-11} Torr, and measurements were begun within 15 to 30 minutes after the cleave was made.

For GaAs as Si, three methods were used to identify surface states. In one, the cleaved surface was exposed to oxygen and examined for structure near the band gap which is preferentially affected. In contrast to Si, where strong changes due to removal of surface states were found, oxidation did not preferentially remove any states in the band edge (see Fig. 1b). This suggests the absence of normally filled surface states. Another test, is to look for surface state pinning as a function of bulk doping. As Fig. 1a illustrates, no pinning was found on p^{++} GaAs. This indicates the absence of normally filled (donor) surface states. For the n-type samples,

the Fermi level was pinned at midgap independent of doping. This indicates normally empty (acceptor) surface states extending down to midgap.

The third test is to identify structure in the EDCs which cannot be explained in terms of bulk band structure[7]. EDCs were taken every few tenths of an eV from 5.6 to 11.8 eV and no such structure was observed. The position in energy of all observed structure was found to depend on $h\nu$ as expected, if due to bulk band structure. No structure was found, such as that in Si, whose energy was independent of $h\nu$. Note in Fig. 1a that for the n-type samples, there is no emission originating from near the Fermi level and that for p-type, the Fermi level comes at the valence band maximum. This position of the Fermi level for p-type material was also found by DGF on more lightly doped p-type samples. This gives further evidence against normally filled (donor) states lying in the band gap.

Our GaAs data is consistent with the model shown in Fig. 2. For sake of comparison, the Si (111) surface states have also been indicated. Note that the GaAs surface states are split into a normally filled and empty band separated by an appreciable band gap. Within our experimental accuracy ($\pm$0.1 eV), we have obtained no evidence that the filled band extends into the band gap.

Since our results differ from those of EG, we have taken extreme care in measurements and have studied a number of samples[8]. Our results are in good agreement with DGF and, in concluding that the filled band lies below the valence band gap, agree with VLS.

The Bond Orbital Model[9] for the electronic structure of tetrahedrally coordinated solids gives us a simple approximate way of estimating the bands, and surface bands for these materials. The Bond Orbital Model is a tight binding calculation of the dangling bonds. Previous calculations[10] have left the energy matrix elements as parameters. The Bond Orbital Model, however, computes values for the parameters V_2 and V_3 from the bulk optical properties. V_1 is taken from the Herman-Skillman tables[11]. S is the overlap integral. We take S=.5, and the values of V_1, V_2, and V_3 are taken from the new formulation of the Bond Orbital Model[9]. For silicon we construct energies for individual

sp^3 hybrid on each atom as illustrated in Fig. 3a. We then form bond orbitals lowered in energy by $(1-S)V_2$ and antibonding orbitals higher by $(1+S)V_2$ in each bond with V_2= 2.2 eV in silicon. The surface, or dangling, hybrids do not, of course, form bonds. The bonding states then broaden into valence bands of width $4V_1$, with V_1 = 1.4 eV for silicon. The formation of conduction bands is not so simple but we take the conduction band edge above the top of the valence band by the observed gap of 1.14 eV. This leaves the dangling bond states, which broaden (due to coupling between dangling bonds through the back-bonds) into two bands, degenerate at certain symmetry directions of the surface Brillioun Zone[12]. (Surface reconstruction would split the occupied and unoccupied surface bands, but we will not consider that here.)

The electronic structure of GaAs is similarly constructed but begins with two types of hybrids, one for Ga ans one for As, differing in energy by $2V_3$ with V_3= 1.2 eV. The resulting bands, one completely in the bulk valence band and occupied, and the other one empty and in the energy gap, are as shown in Fib. 3b. As polarity increases in going to II-VI and I-VII compounds, V_3 will increase and therefore the gap between surface states could increase further in such materials.

In Fig. 4, we indicate in real space the approximate bulk and surface configurations deduced from this work. In the bulk, the Ga and As atoms have a rearrangement of charge because of the formation of the bond. At the surface, one of the four covalent bonds per atom is broken and three remain. As a result, the net change relaxes towards zero; i.e., a surface As has approximately five and Ga approximately three valence electrons. Each type of surface atom contributes three electrons to the covalent bond. This leaves each surface As with two excess electrons which form the filled surface band lying below the top of the valence band. All three Ga ele-trons are taken up in the covalent bond leaving none to populate surface states; thus, the empty surface band is formed primarily from the Ga states[13]. This model of a dangling electron pair associated with the As atom and no dangling electrons associated with the Ga atom is in qualitative agreement with the model proposed by Miller and Haneman[13a].

Brief mention will be made of studies of the oxidation of GaAs, since this bears on the above mentioned model. A more complete report will be given elsewhere. In Studying n-type GaAs, we found a very striking result: within ±0.1 eV, the pinning of the Fermi level by the empty surface states was unchanged by oxidation (see Fig. 1b). This is in strong contrast to Si where the surface state pinning is destroyed by oxidation[1]. We suggest that this result is due to oxygen combining with the two surface As electrons, reducing the energy of those electrons and removing the filled band while leaving the surface Ga atoms, and thus the empty surface band, largely unaffected. We would, therefore, expect the oxygen atoms to be located roughly over the As atoms and a stable monolayer to be formed with 50% atomic coverage of the GaAs corresponding to oxidation of only the As surface atoms.

One also needs to relate the surface states reported here for clean GaAs to the Schottky barrier work on GaAs metal interfaces where surface state pinning about 0.5 eV above the top of the valence band is typically found.[14] We have done preliminary work with CS on p^{++} GaAs and find that the Cs produces surface states in the band within 0.5 eV of the valence band maximum. In particular, we find that these states pin the surface Fermi level about 0.5 eV above the valence band maximum in agreement with Uebbing and Bell.[15] We believe that extensions of this work will have important implications for practical "negative electron affinity" photocathodes.[16]

TABLE I

Sample	Doping		Bulk Fermi level Position above Vm(eV)	No. of Cleaves Studied
18 n	1.7×10^{18} cm^{-3}	n-type	1.4	2
14 n	6×10^{14} cm^{-3}	n-type	1.2	4
19 p	3×10^{19} cm^{-3}	p-type	0	1

References

Useful discussions with Dean Eastman, Traugott Fischer, H. LÜth, and Jack Rowe are gratefully acknowledge.

* This research was supported by the Advanced Research Projects Agency of the Department of Defense and monitored by Night Vision Laboratory, USAECOM under contract DAAK02-74-C-0069.

+ Work supported in part by NSF.

1. L. F. Wagner and W. E. Spicer, Phys. Rev. Lett. 28, 1381 (1972); and Phys. Rev. B9, 1512 (1974)
2. D. E. Eastman and W. D. Grobman, Phys. Rev. Lett. 28, 1378 (1972)
3. J. W. Rowe and H. Ibach, Phys. Rev. Lett. 32, 421 (1974)
4. J. A. Appelbaum and D. R. Hamann, Phys. Rev. Lett. 31, 106 (1973)
5. J. Van Laar and J. J. Scheer, Surface Science 8, 342 (1967)
6. J. H. Dinan, L. K. Galbraith and T. E. Fischer, Surface Science 26, 587 (1971)
7. R. C. Eden, Ph.D. dissertation, Stanford Univ., 1967 (unpublished); W. E. Spicer and R. C. Eden, 1968, Proc. IX International Conf. on Phys. of Semiconductors (Publishing House, "Nauka"), page 65.
8. Dean Eastman, private communication, and his coworkers have studied other GaAs samples since their original work and have obtained results in agreement with those reported here (see for example, Phys. Rev. Lett. 29, 5208, 1972). Since the sample of Eastman and Grobman (Ref. 2) was characterized by a bad cleave (i.e., many cleavage steps), we purposely made bad cleaves. These did not show the surface states reported in Ref. 2.
9. W. A. Harrison, Phys. Rev. B 8, 4487 (1973), and a reformulation by W. A. Harrison and S. Ciraci, to be published, in which the effect of overlaps of two hybrids in one band is included.
10. J. Koutecky and M. Tomasek, Phys. Rev. 120, 1212 (1960)
11. F. Herman and S. Skillman, Atomic Structure Calculations, Prentice-Hall, Englewood Cliffs, N.J. (1963).

12. R. O. Jones, Phys. Rev. Lett. 20, 992 (1968).

13. This division of surface states into anion-like and cation-like behavior is well known (c.f. J.D. Levine and S. Freeman, Phys. Rev. B2, 3253 (1970)

14. C. A. Meade, Solid State Electronics 9, 1023 (1966)

15. J. J. Uebbing and R. L. Bell, Appl. Phys. Lett. 11, 357 (1967)

16. R. L. Bell and W. E. Spicer, Proc. IEEE, 58, 1788 (1970)

FIGURE CAPTIONS

FIG. 1a EDC for $h\nu = 10.2$ eV for n- and p-type GaAs samples. The zero of energy is taken at the valence band maximum. E_F indicates the Fermi level position.

1b Effect of oxygen exposure on n-type GaAs. Note that the Fermi level (E_f) is uneffected by the oxidation.

FIG. 2 Models for surface states on the cleavage faces of Si and GaAs.

FIG. 3 Diagram showing the formation of bulk (bold lines) and (110) surface (dashed lines) band structure of tetrahedrally coordinated semiconductors.

a) Silicon Energy parameters $V_1 = 1.4$ eV, $V_2 = 2.2$ eV, $V_3 = 0$

b) GaAs Energy parameters $V_1 = 1.7$ eV, $V_2 = 2.1$ eV, $V_3 = 1.2$ eV

FIG. 4 GaAs surface and bulk atoms. At the surface, Ga has approximately three valence electrons and As approximately five. The filled surface band is associated principally with the As surface atoms; the empty surface band principally with the Ga surface atoms.

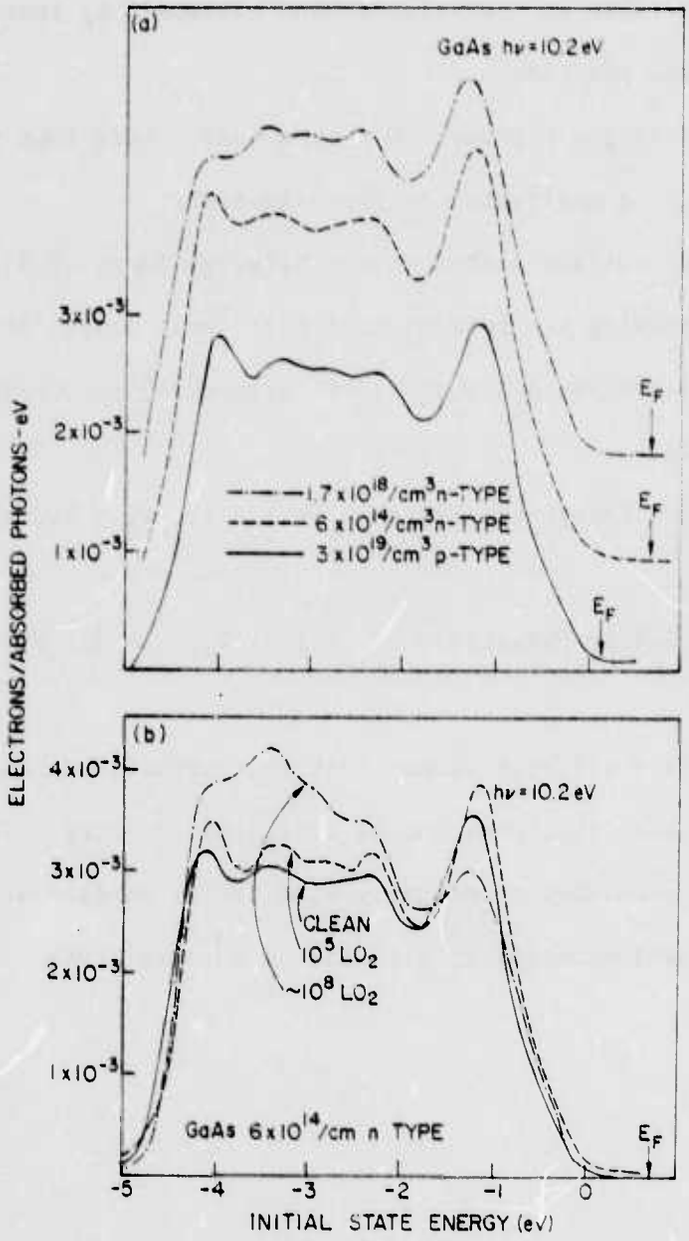
(a)
GaAs hν=10.2eV
3x10⁻³
2x10⁻³
1x10⁻³
E_F
E_F
E_F
1.7x10¹⁸/cm³ n-TYPE
6x10¹⁴/cm³ n-TYPE
3x10¹⁹/cm³ p-TYPE
(b)
4x10⁻³
3x10⁻³
2x10⁻³
1x10⁻³
hν=10.2eV
CLEAN
10⁵ LO₂
~10⁸ LO₂
GaAs 6x10¹⁴/cm n TYPE
E_F
-5
-4
-3
-2
-1
0
INITIAL STATE ENERGY (eV)
ELECTRONS/ABSORBED PHOTONS - eV

Fig. 1

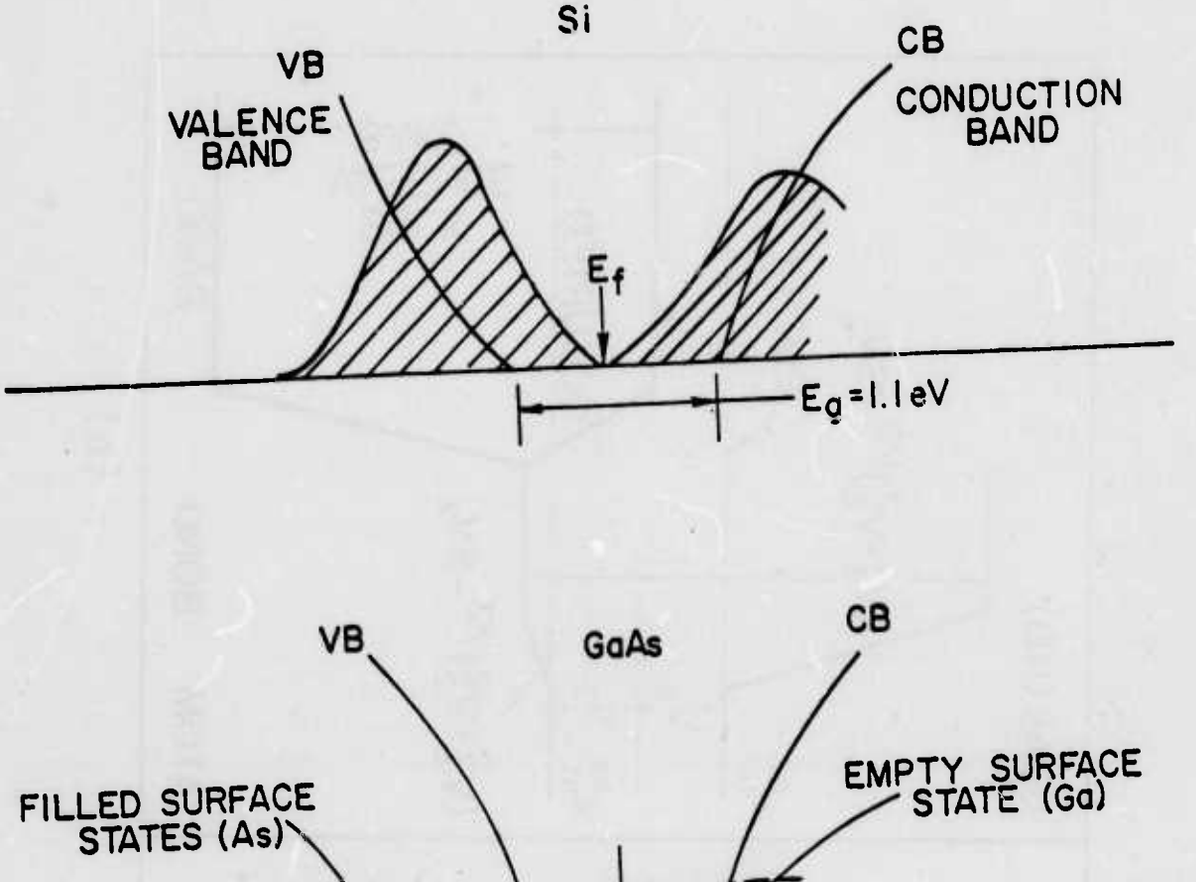
Si
VB
VALENCE BAND
CB
CONDUCTION BAND
E_f
E_g=1.1 eV
VB
GaAs
CB
FILLED SURFACE STATES (As)
EMPTY SURFACE STATE (Ga)
E_g=1.4 eV

Fig. 2

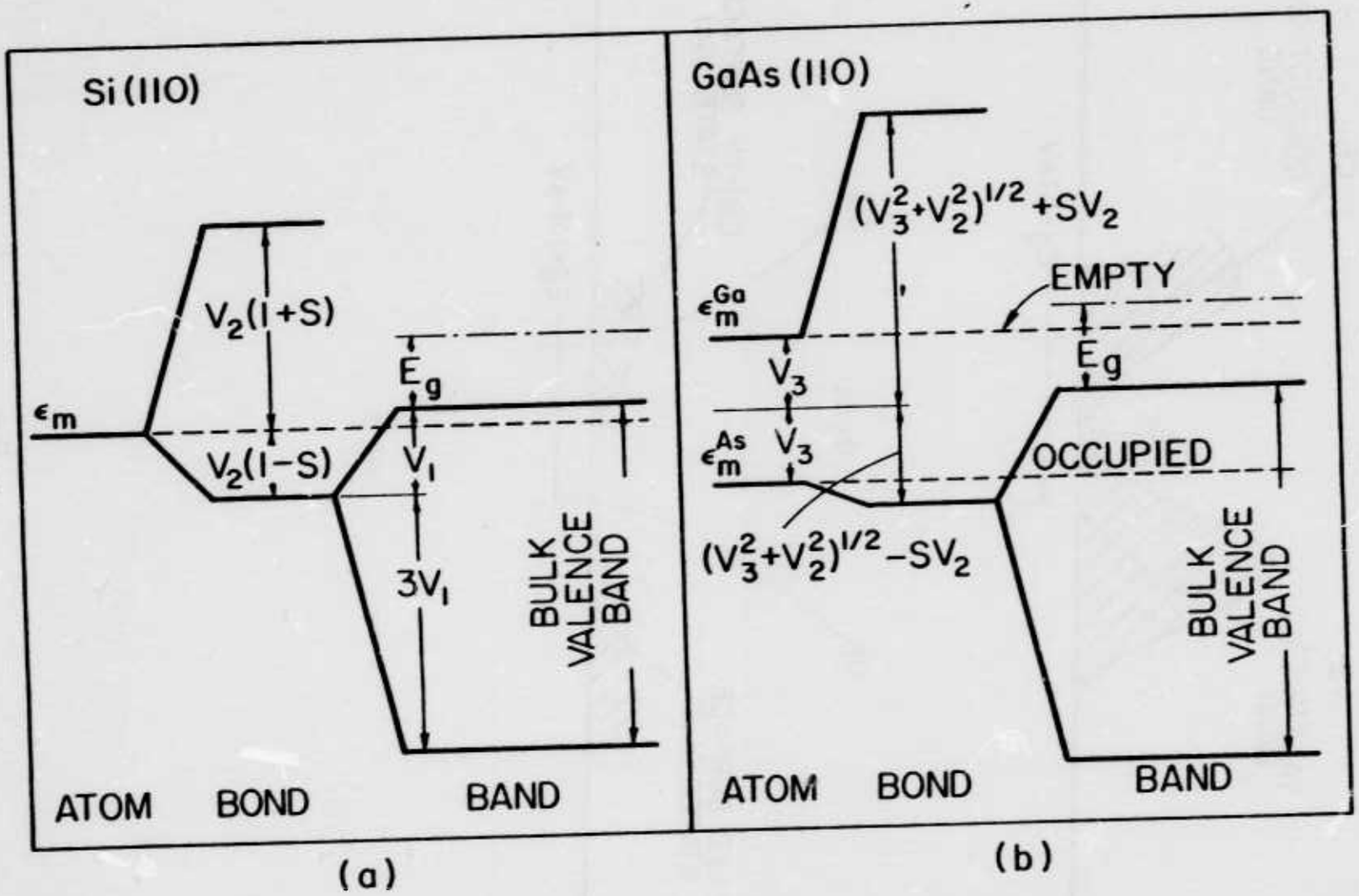
Si (110)
$V_2(1+S)$
E_g
ϵ_m
$V_2(1-S)$
V_1
$3V_1$
BULK VALENCE BAND
ATOM
BOND
BAND
(a)
GaAs (110)
$(V_3^2+V_2^2)^{1/2}+SV_2$
EMPTY
ϵ_m^{Ga}
V_3
E_g
ϵ_m^{As}
V_3
OCCUPIED
$(V_3^2+V_2^2)^{1/2}-SV_2$
BULK VALENCE BAND
ATOM
BOND
BAND
(b)

FIG. 3

Chapter 3

Comment on "Relation of Schottky Barriers to Empty Surface States on III-V Semiconductors" by D. E. Eastman and J. L. Freeouf

GaSb Surface States and Schottky Barrier Pinning*

by

P. W. Chye, I. A. Babalola,+ T. Sukegawa++ and W. E. Spicer

Stanford Electronics Laboratories
Stanford University
Stanford, Ca. 94305

ABSTRACT

Photoemission measurements on GaSb indicate no surface states in the bandgap. Deposition of Cs to form a Schottky barrier on n-GaSb moves the Fermi level 0.55 eV and produces pinning within the bandgap. Thus, for the first time, Schottky barrier pinning without the presence of intrinsic surface states in the gap is directly demonstrated.

Surface state studies of clean cleaved (110) GaSb and of cesium on (110) GaSb are reported. These results which represented work of two cleaves on an n-type[1] and one cleave of a p-type GaSb crystal are in disagreement with recent results published by Eastman and Freeouf[2] (EF) and modification of their generalizations concerning Schottky barriers appears necessary.

Figure 1 shows the high energy portions of photoelectron energy distribution curves (EDCs) for clean and cesiated n-type (carrier concentration 1.1×10^{18} cm^{-3}) and clean p-type (carrier concentration 1.6×10^{17} cm^{-3}) (110) GaSb at an incident photon energy of 10.2 eV. In Fig. 1, a Cs monolayer is defined as the coverage which gives

+ On leave from Physics Department, University of Ibadan, Nigeria

++ On leave from Research Institute of Electronics, Shizuoka University, Hamamatsu, Japan

minimum photoemission threshold.[3] Further experimental details are available elsewhere.[3,4] The EDC's are presented with the peaks due to direct transitions in the bulk superimposed. Fermi level positions determined to within ±0.1 eV using a Cu reference emitter are marked near the high energy edges. The difference in energy of the positions of the Fermi level on the clean n- and p-type samples is 0.65 eV, which is almost the full bandgap. An additional determination of the n-type Fermi level based on yield measurements and the observed width of the EDC of the clean sample, is in agreement with Fig. 1 putting the surface Fermi level, E_f, on n-type GaSb at the conduction band minimum (CBM). This corresponds to a flat band situation with the forbidden bandgap free of empty intrinsic surface states which would cause pinning. EF, on the other hand, showed empty surface states on GaSb as having a peak near the CBM with a tail extending below midgap and located the Fermi level on their n-type sample 0.4 eV below the CBM.

Further evidence for the intrinsic n-type Fermi level location being near the CBM is given by following the Fermi level movement with Cs addition. It is evident that with cesiation the Fermi level moved towards the valence band maximum (VBM) and eventually moved through the bandgap by 0.55 eV and stabilized near the VBM[5], in accordance with the Fermi level position for bulk Schottky barriers[6]. If the intrinsic Fermi level position on an n-type sample were located about 0.4 eV below the CBM as reported by EF, such a large movement would be impossible[7].

It appears possible to reconcile the present results with that of EF. Lapeyre[9] has suggested that excitonic effects may be important in the Ga 3d transition used by EF to detect their empty surface states. This would result in a measured empty surface state position appreciably below that of its true energy, and could explain the difference between EF's location of the empty surface states using photoemission partial yield spectroscopy and our results. EF have considered possible excitonic or correlation effects but it appears that the energy lowering associated with these effects are probably somewhat more than the $\sim$ 0.1 to 0.2 eV suggested by them.

There is a large variation reported in the literature for the surface Fermi level position on cleaved GaSb. Viljoen et al.[10] found a variation of 0.6 eV across the surface of a newly cleaved sample with E_f finally stabilizing at 0.1 eV above the VBM after several days. EF found E_f to lie about 0.3 eV above VBM. As is described below, we believe these pinning positions have been affected by the unusually high sensitivity of GaSb E_f to oxygen (and presumably other gases). Recent studies of the effects of oxygen on clean GaSb by Chye et al.[11] show that the position of E_f can be affected by quite small amounts of oxygen. Movement is seen even at 10L O_2 exposure. At 10^4L O_2 the E_f moved downward by about 0.5 eV. Sensitivity to other gases might be even greater.[12]

Using MacRae and Gobeli's sticking probability of less than 10^{-5} for oxygen,[13] these exposures correspond to less than 10^{-4} and 10^{-1} monolayer coverage respectively. In agreement with MacRae and Gobeli's low sticking probability, no structure due to oxygen was found in the EDCs ($h\nu \leq 11.6$ eV) for these exposures. We therefore suggest that this unusually high sensitivity of E_f to exposure to oxygen (and presumably other gases) is due to the lack of any intrinsic surface state pinning. In GaAs[14] and InP[15] where empty intrinsic surface states were present in the bandgap no such sensitivity was found.

The present work shows that surface state pinning may be produced at a metal-semiconductor contact even when empty intrinsic surface states are not present. It also shows that the Fermi level pinning position may be far removed from the bottom of the conduction as well as the empty surface state band when these surface states lie in the conduction band. Thus, it appears that the conclusion of EG that intrinsic surface states play a predominant role in determining Schottky barriers in III-V semiconductors must be reexamined. In particular, their conclusion seems only clearly applicable when empty surface states lie in the bandgap. The present work shows directly for the first time that Schottky barrier pinning can be obtained in the gap even when no intrinsic surface states lie in the gap.

The assistance of Hideo Sunami is gratefully acknowledged.

REFERENCES

* This research was supported by the Advanced Research Projects Agency of the Department of Defense and monitored by Night Vision Laboratory, USAECOM under Contract No. DAAK 02-74-C-0069.

1. The clean work is also in agreement with one cleave on a second n-type crystal. However, no Cs was added to that crystal.

2. D. E. Eastman and J. L. Freeouf, Phys. Rev. Lett. 34, 1624 (1975)

3. P. Gregory and W. E. Spicer, Phys Rev. B 15 (in press, tentatively scheduled for Sept. 15, 1975 issue).

4. L. F. Wagner and W. E. Spicer, Phys. Rev. Lett 28, 1381 (1972); L.F. Wagner and W. E. Spicer, Phys Rev. B 9, 1512 (1974); P. E. Gregory, W. E. Spicer, S. Ciraci and W. A. Harrison, App. Phys. Lett. 25, 511 (1974).

5. Similar results were obtained with potassium deposition.

6. T. C. McGill, J. Vac. Sci. Technol, 11, 935 (1974).

7. Two other striking differences were found between Cs on GaSb and Cs on GaAs (Refs. 3 and 8) and InP (Ref. 8). First for Cs coverages < 0.3 (as defined here, < 0.1 as defined in Ref. 3 and 8), strong upward movement of the leading edge of the EDCs into the bandgap were noted; this was absent for GaSb. Second, the Cs coverage giving minimum $e\phi$ was time stable on GaAs and InP and not on GaSb, i.e., Cs evaporated from GaSb. We attribute both effects to stronger interaction with Cs when empty surface states are in the bandgap.

8. W. E. Spicer, P. Gregory, P. Chye, I. A. Babalola and T. Sukegawa, Appl. Phys. Lett., in press.

9. G. T. Lapeyre and J. Anderson, Phys. Rev. Lett 35, 117 (1975).

10. P. E. Viljoen, M. S. Jazzar and T. E. Fischer, Sur. Sci 32, 506 (1972).

11. P. Chye, T. Sukegawa, I. A. Babalola, H. Sunami, P. Gregory and W. E. Spicer, to be published.

12. Oxygen does not stick well to GaSb (Ref. 13); other gases may. The rate of contamination at a given pressure was found to be greatly increased when an unshielded hot filament was located near the sample. To avoid this effect, a Redhead gauge was routinely used in this work.

13. A. U. MacRae and G. W. Gobeli, J. Appl. Phys. 35, 1629 (1964).

14. P. Gregory and W. E. Spicer, Surface Science, in press

15. P. Chye, I. A. Babalola, T. Sukegawa and W. E. Spicer, to be published.

FIGURE CAPTION

Fig. 1 The high energy portions of clean and cesiated GaSb EDCs. The Fermi level (E_F) of the n-type sample shows a large movement with cesiation and the Fermi levels of the clean p- and n-type samples differ in energy by 0.65 eV. This shows that the Fermi level of the n-type sample lies near the CBM and indicates the absence of empty intrinsic surface states which would cause pinning.

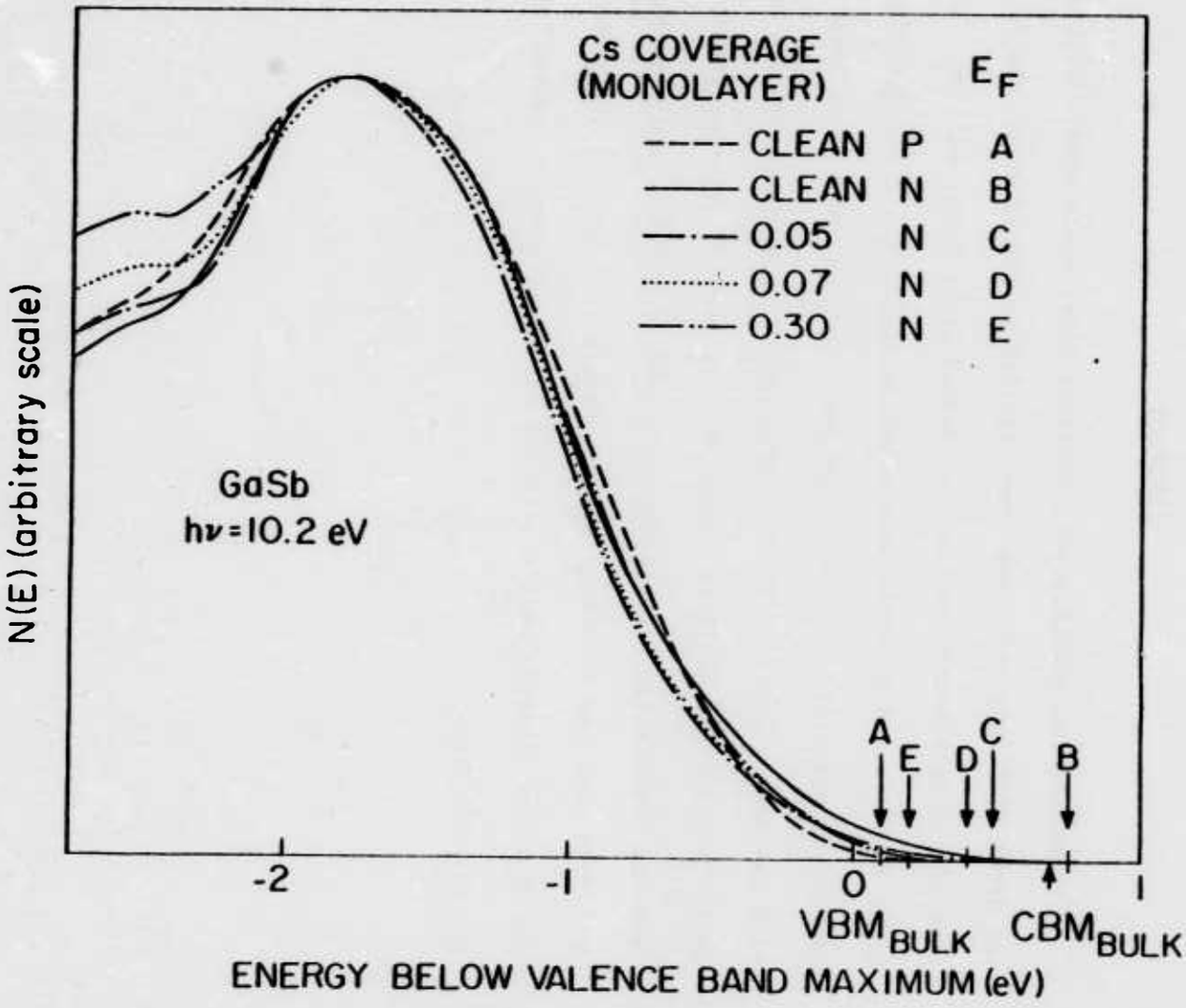
Cs COVERAGE
(MONOLAYER)
E_F
---- CLEAN P A
—— CLEAN N B
—·— 0.05 N C
..... 0.07 N D
—··— 0.30 N E
GaSb
hν=10.2 eV
N(E) (arbitrary scale)
A
E
D
C
B
-2
-1
0
1
VBM_{BULK}
CBM_{BULK}
ENERGY BELOW VALENCE BAND MAXIMUM (eV)

Fig. 1

Chapter 4

PHOTOEMISSION STUDY OF Au SCHOTTKY BARRIER FORMATION ON GaSb, GaAs, AND InP USING SYNCHROTRON RADIATION

ABSTRACT

Photoemission spectroscopy, constant final state spectroscopy, and ion depth profiling techniques were applied to the study of the formation of the Au Schottky barrier on cleaved GaSb, GaAs, and InP. It was found that the deposited Au interacted strongly with the semiconductors, causing decomposition of their surfaces. Further, the Fermi level pinning was nearly complete at <0.2 monolayer Au coverage, when the Au was still "atomic-like." It is suggested that defect states at the interface are responsible for the Schottky barrier pinning, and a mechanism for their creation is proposed. It appears that many of the known phenomena on Schottky barriers can be explained using a "defect" model as proposed here.

I. Introduction

In the fabrication of semiconductor devices, a metal overlayer is often used in making interconnections, ohmic contacts, or Schottky contacts. Because of its importance, the Schottky barrier (SB) has been the subject of numerous theoretical and experimental investigations. Much of the earlier experimental work may be summarized in a set of empirical rules. For covalent semiconductors, Mead and Spitzer[1] showed that a "two-thirds" rule often applies; that is, the electron barrier height ϕ_B is approximately equal to two-thirds of the energy gap, E_g. The exceptions are InAs, GaSb, and InP. The barrier energies of the covalent materials are relatively insensitive to the metal used in forming the barrier. In contrast, on the more ionic materials, Mead et al[2,3] observed a strong dependence on the metal used. They showed[3] that the separation between the covalent and ionic behavior (ionic-covalent transition) came at an electronegativity difference of 0.6. The index of interface behavior S is then defined by $S = d\phi_B/d\chi_M$ where χ_M is the metal electronegativity. The covalent semiconductors then have $S \sim 0.1$, while insulators such as SiO_2 have $S \sim 1.0$; however, the latter has very recently been questioned by Schlüter[4] who argued that $S > 1$ for the insulators. Recently, McCaldin et al[5] pointed out that, for III-V and II-VI compounds, the SB height for holes is dependent only on the particular anion and is roughly a linear function of the anion electronegativity. This "anion rule" applies also to materials which do not follow the "two-thirds" rule and to more ionic compounds such as ZnS which has $S \approx 1.0$. The aluminum compounds are the exceptions.

Back in 1947, Bardeen[6] proposed that, on (covalent) semiconductors, intrinsic surface states of sufficiently high density in the band gap stabilize the Fermi level (E_F), and the barrier height is then largely independent of the metal. Many years later, Heine[7] suggested that metallic like states with wave functions decaying into the semiconductor--the tails of the metal wave functions--are responsible for E_F pinning. Photoemission and constant final state (CFS) experiments on group III-V compounds[8,9] at first appeared to support the Bardeen model, but it was soon realized that E_F pinning due to imperfections and strong excitonic effects in the CFS spectra led to incorrect conclusions on GaSb. For example, Chye et al[10] demonstrated directly SB pinning without the presence of intrinsic surface states in the band gap. It is now believed that there are no intrinsic surface states in the band gap of most group III-V semiconductors, and therefore the SB pinning cannot be due to intrinsic surface states.[11-13] Rowe et al[14-18] did much work on group III metal overlayers on semiconductors and reported metal-induced surface states. They also showed that the first metal overlayer is important in determining the interface behavior and emphasized the need for a microscopic theory of chemical bonding. It was suggested that the metal forms covalent bonds with the semiconductor surface, giving rise to the observed metal-induced states which pin E_F.

Since the early stages of SB formation are so important, experiments were performed to study the effects of metal overlayers from submonolayer amounts to relatively thick coverages. In this paper, we report experimental results for Au overlayers on the III-V semiconductors GaAs, GaSb, and InP. The cleaved (110) surfaces were studied in ultrahigh vacuum in order to avoid complications arising from irreproducibility or

nonstoichiometry of the initial surface (e.g., on heat-cleaned or sputter-annealed surfaces) or from surface contamination by oxides or carbon. The experimental methods are outlined in the next section. Section III presents the experimental results which are further discussed in Section IV where a "defect" model for Schottky barrier pinning is presented.

II. Experimental

Several spectroscopic techniques were used in this study: UV and soft X-ray photoemission spectroscopy (UPS and SXPS), constant final state (CFS) spectroscopy,[19] and Auger electron spectroscopy (AES) used in conjunction with ion sputtering to yield composition profiles with depth. All the surfaces were prepared by cleaving in stainless steel chambers with base pressures $\sim 10^{-10}$ torr, exposing the (110) surfaces which were usually 5 × 5 mm in area. The UPS, SXPS, and CFS experiments were all performed at the 8° and 4° beam lines at the Stanford Synchrotron Radiation Laboratory (SSRL) where continuous radiation up to 600 eV is available. The photoelectrons were energy-analyzed with a PHI double-pass cylindrical mirror analyzer (CMA) set to 0.3 eV resolution and the spectrum recorded using a Tracor-Northern Digital Signal Averager. Au deposition was made by one of two methods: (1) by rotating the sample through a stream of Au emerging from an evaporator consisting of a shield and a Au bead suspended on W wire, and (2) by placing the sample in front of an evaporator and opening a shutter. To avoid heating of the sample surface in method 2, the shutter was never left open for more than 20 sec (typically, 10 sec exposures were used). The evaporation rates were monitored in method 2 by means of a quartz crystal thickness monitor placed to the side of the evaporator in front of an opening cut in the side of the evaporator shield. This monitor was previously calibrated in a separate pump-down against another placed in front of the evaporator near the sample position. The coverage in monolayers (θ) is then determined from the Å's of Au evaporated, with 1 monolayer defined to be one Au atom/surface atom. Evaporation rates were not monitored in method 1,

but very rough estimates may be made from the current input to the evaporator since the evaporation rate was subsequently calibrated with the quartz oscillator as a function of current input.

Pressure during evaporation was generally $<10^{-9}$ torr. AES on a different portion of the surface from that studied in photoemission showed no contamination from oxygen or carbon. The ion-profiling experiments were performed in a system manufactured by Varian Associates and used a single-pass CMA as the energy analyzer.

In photoemission spectroscopy, it is important to be able to establish a meaningful reference level to set the energy scale. In these experiments, reference spectra were taken from Au evaporated onto a stainless steel substrate attached to the same sample carousel as the semiconductors. The sample carousel is grounded to the analyzer. The electron energy (E_e) measured is relative to the Fermi energy E_F of the analyzer. The binding energy relative to E_F, E_B^F, is then

$$E_B^F = h\nu - E_e - e\phi_A \qquad (1)$$

where $h\nu$ = photon energy and ϕ_A = work function of analyzer. The location of E_F (and hence ϕ_A) may be found from the Fermi edge of the Au reference. However, in a semiconductor, E_F is not the best reference level, as it shifts around in the band gap at the surface, due to changes in band-bending and type (n or p) of semiconductor. Nor is the vacuum level a good reference, as electron affinities are not well known and also change with the addition of adsorbates. The binding energy of a core level in a semiconductor does not change with band-bending when measured relative to the valence band maximum (VBM) at the surface, and

we shall use this binding energy E_B^{VBM}. However, when the semiconductor dissociates and the individual components become metallic, the meaningful reference level becomes the metal E_F. Thus, one needs to be careful in interpreting spectra from mixed metallic and semiconducting states and in comparing binding energies made on metals and semiconductors (e.g., Ga metal and Ga in GaAs). It is important to remember that E_B^F in a semiconductor may vary from sample to sample, whereas E_B^{VBM} is constant. Thus, the band-bending of a semiconductor with small amounts of adsorbates may be followed using the movement of the core level since ϕ_A is very stable. That is, from (1), $\Delta E_B^F = \Delta E_e$. At higher coverages, other factors need to be considered, e.g., charge transfer, changes in screening, conversion into metallic form due to dissociation, and so on, which will give extra contributions to ΔE_B^F.

At the lower photon energies, E_F and its position relative to the VBM may be very accurately determined. Our procedure is to use photoelectron energy distribution curves (EDC's) at $h\nu = 10.2$ eV to study E_F movement and locate the VBM.[10] The electron escape depth is a function of electron kinetic energy[20] and is relatively long (≈ 20 Å) near 10 eV but is short compared to the depletion-layer width of several hundred angstroms at the doping levels used here. Thus, bulk band structure features remain up to relatively thick coverages of adsorbates. By aligning the bulk peaks, the amount of E_F movement can be measured by locating E_F on the different spectra using the Au reference. The position of E_F relative to the VBM is obtained from the clean sample. The VBM on the more heavily Au covered surface where VBM is masked by Au emission can be obtained from knowledge of E_F movement obtained from the 10.2 eV EDC's.

III. Results

A. SXPS Spectra

Figures 1, 2, and 3 show SXPS spectra (taken on the 4° beam line) of the outer core levels of Au and the III-V semiconductor substrates as the Au coverage is gradually increased. Evaporation method 1 was used. Parts of Figs. 1 and 3 have been published in a previous paper[20] in somewhat less detail. These samples are all n-type. The photon energies used were 165 eV for GaAs, 120 eV for GaSb, and 120 eV for the In-4d and 165 eV for P-2p. At 165 eV, the cross section for Au-4f is much larger than at 120 eV, and the escape depth for the photoelectrons[21,22] is also shorter (4 vs 10 Å at 120 eV). However, the 4d cross section is very small at 165 eV--the Cooper minimum[23]--thus, it was necessary to use the lower photon energy for studying GaSb. The escape depths of the core levels presented here are all estimated to be between 5 to 10 Å, based on escape depth curves published by Pianetta et al[22] and Lindau and Spicer.[21] Thus, SXPS is extremely surface sensitive (the escape depths here may be compared to those for ESCA which are generally $\gtrsim$ 20 Å). Immediately obvious from Figs. 1, 2, and 3 is that, while for GaAs and InP both anion and cation core level emissions decrease at roughly the same rate until a residual level is reached, for GaSb, the Ga emission is attenuated as Au is deposited and decreases rapidly, while the Sb emission remains strong. This increase in the Sb/Ga ratio is already quite pronounced at a few monolayers coverage.

Chye et al[20] interpreted the Au-GaSb spectra as showing selective removal of Sb from the interface such that a layer of Sb "floats" to the surface of the Au. One can give an explanation of this based on known

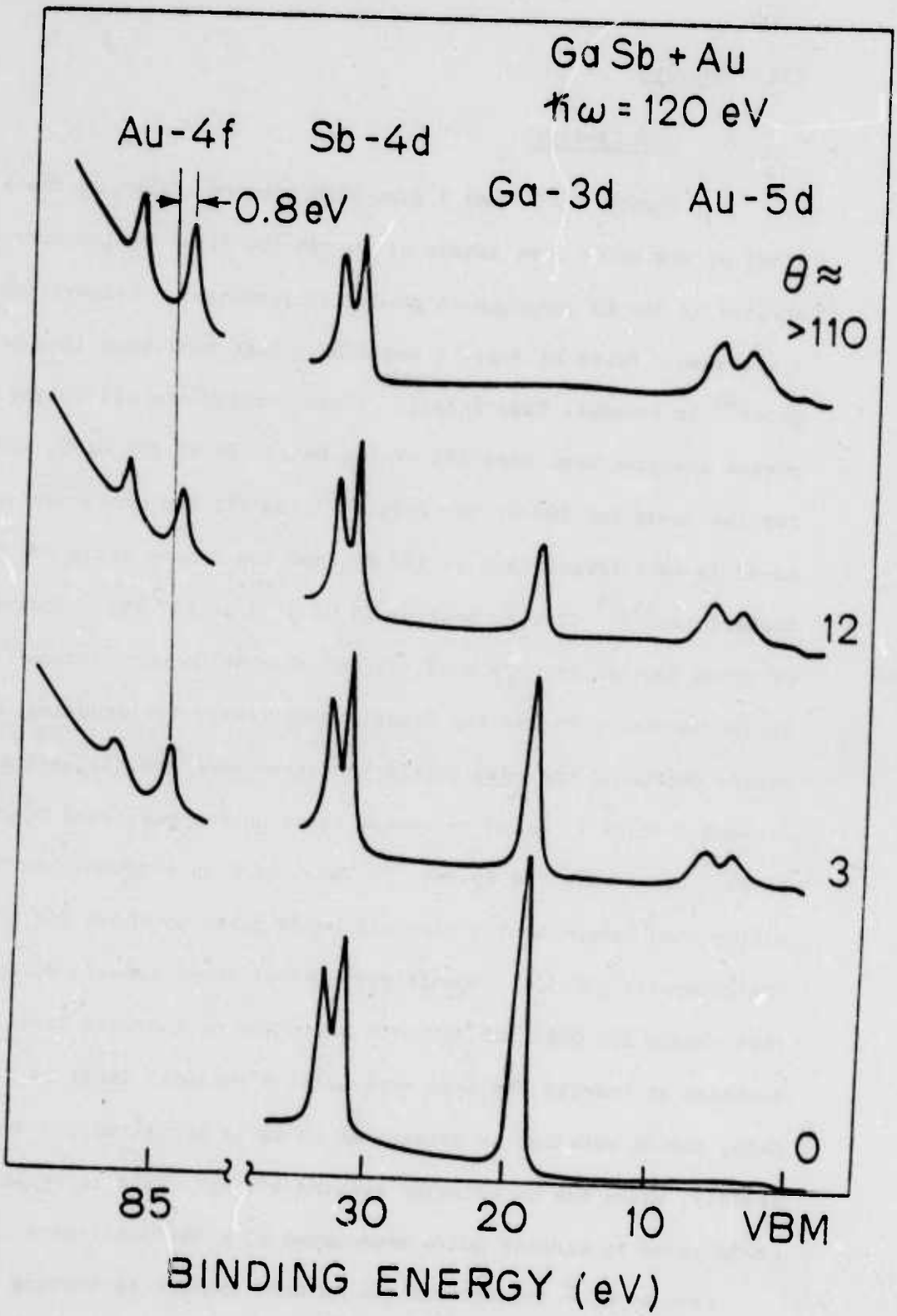

Fig. 1. PHOTOEMISSION SPECTRA TAKEN AT A PHOTON ENERGY OF 120 eV FOR GaSb WITH DIFFERENT Au COVERAGES.

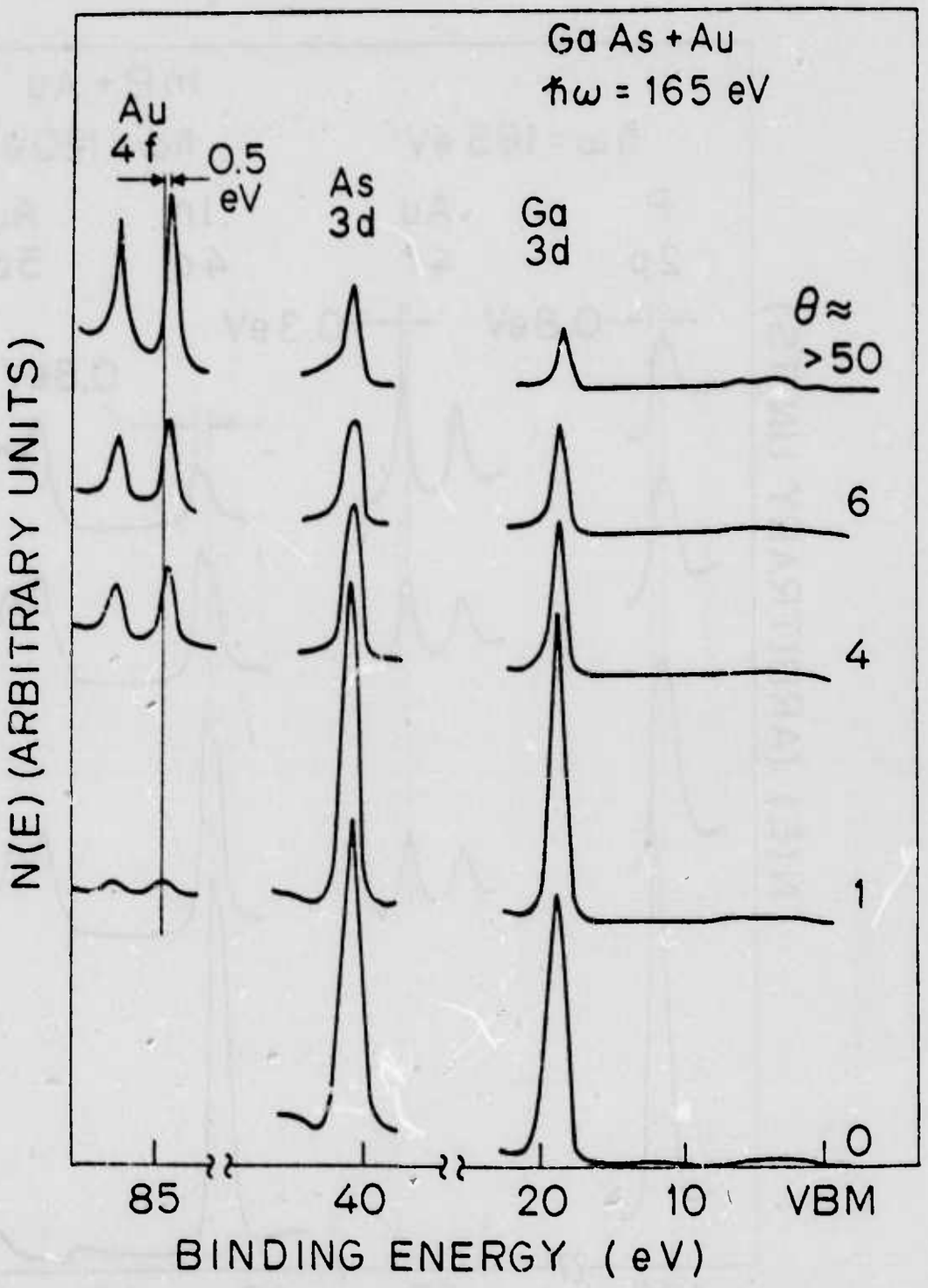

Fig. 2. PHOTOEMISSION SPECTRA TAKEN AT A PHOTON ENERGY OF 165 eV FOR GaSb WITH DIFFERENT Au COVERAGES.

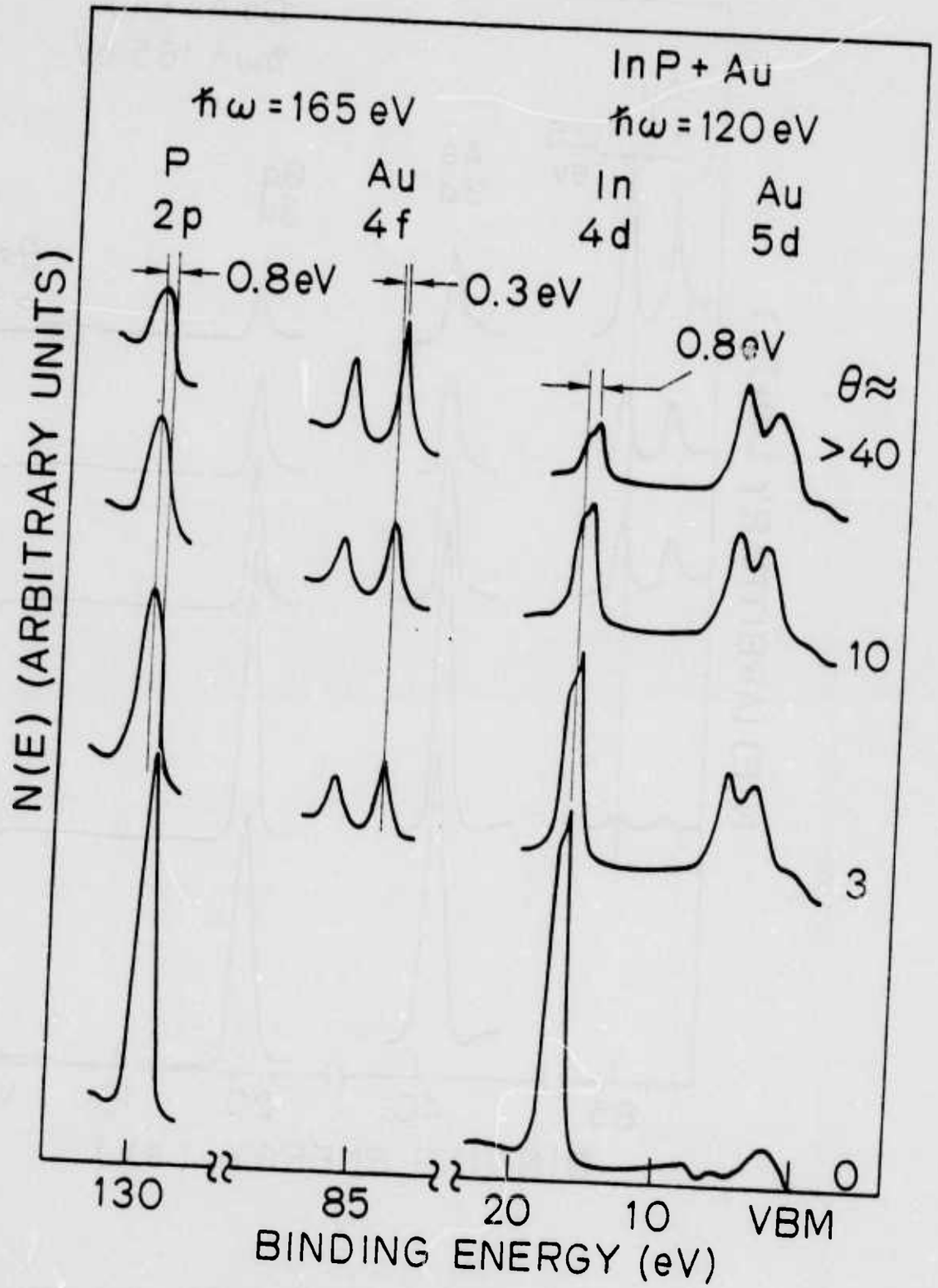

Fig. 3. PHOTOEMISSION SPECTRA TAKEN AT THE PHOTON ENERGIES 120 eV (In 4d, Au 5d) AND 165 eV (P 2p, Au 4f) FOR InP WITH DIFFERENT Au COVERAGES.

bulk properties. In bulk GaSb, it is well known[24-27] that crystals tend to grow nonstoichiometric with an excess of Ga. Thus, GaSb may favor removal of the Sb at the surface. It is also well known from alloy studies[28] that the surface composition is different from the bulk composition in an alloy and that the component with the smallest surface free energy is normally enhanced at the surface. Thus, the Sb the GaSb gave up upon Au deposition moves to the surface since it has the smallest surface free energy. Some caution must be exercised since the system studied here is a very thin film and equilibrium probably has not been attained. Therefore, bulk phase diagrams and properties can only serve as rough guides. Semiconductor components are also present on the surface of Au-GaAs and Au-InP and may be there for the same reason of minimizing the surface free energy.

At thick Au coverage, there is an apparent enhancement of the As/Ga ratio. This may be due to a preferential removal of As from the semiconductor or may be due to several factors which become important as the Au thickness becomes appreciable. One factor is the relative solubility of the semiconductor elements in the Au layer. Another factor is the relative tendency to form compounds or alloys with the Au. A third factor is the relative diffusion rate. This last factor is quite unlikely here as Ga diffuses rather rapidly in Au.[29] It seems more likely that Ga form compounds or alloys, thus remaining in the Au layer. One may conclude from the increase in As/Ga ratio that at least partial dissociation of Ga from As has occurred. It is also important to realize that, on GaSb, the Sb/Ga enhancement is apparent at low coverages when the complicating factors mentioned above are not yet significant. Thus, while it is clear that, on Au-GaSb, Sb is removed preferentially, it is more difficult to

tell on GaAs whether preferential removal of the As has taken place. The present data favor near stoichiometric removal. In order to study the composition versus depth, ion depth profiling studies were made and the results shown in Figs. 4 and 5.

Evaporation method 2 was used without a thickness monitor. The amount of Au evaporated in Fig. 4 is known to be ~50 to 70 Å based on a calibration run using the same evaporator after this depth profile was taken. The ion beam is incident on the surface at a grazing angle near 80° (normal incidence = 0°). The Ar^+ current density is measured using a Faraday cup at an angle of 53.5° to the beam. A simple geometrical correction was applied. The sputtering rate, calculated from sputtering yields for Au in the literature for 1 keV ions,[30] was 13.4 Å/min. The profile was measured after the Au-covered sample was allowed to sit in vacuum (2×10^{-10} torr) for 20 hr.

The profile unambiguously shows a layer of Sb forming the top few monolayers. This layer may be in the form of Sb metal, $AuSb_2$, a mixture of the two, or an Sb-Au alloy. Since the increase in Au signal is slight as the top layer is sputtered away, it is likely that Au is present in this top layer. The apparent interface width (90 to 10 percent Au) is 110 Å, neglecting broadening factors. Broadening due to finite escape depth is small (<10 Å) and, at the glancing ion incidence used here, knock-on mixing effects should be less important. In any event, even allowing for a 30 Å broadening due to knock-on, the interface is still quite wide. It is possible that substantial intermixing of semiconductor and Au has occurred at room temperature. One other broadening factor which may be important here is the well known tendency of Au to form islands or "clump." If the Au film were nonuniform in thickness, then

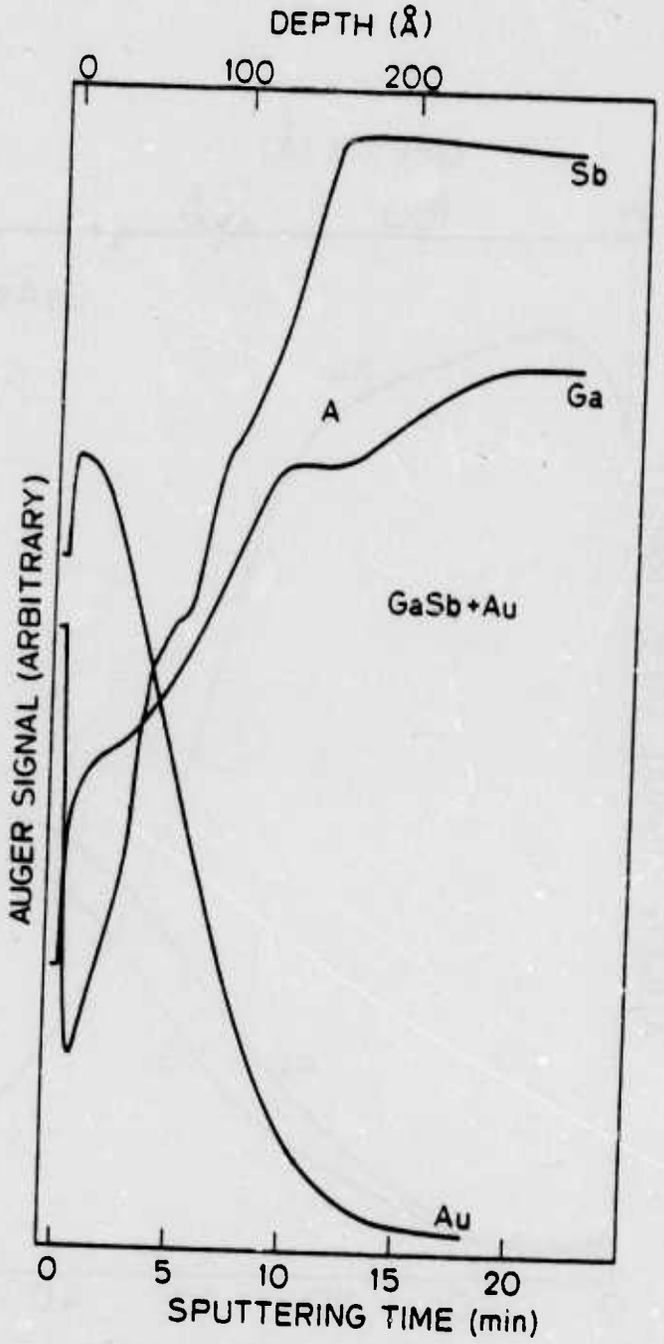

Fig. 4. COMPOSITIONAL DEPTH PROFILE OF Au COVERED GaSb OBTAINED USING AUGER ELECTRONIC SPECTROSCOPY IN COMBINATION WITH ARGON ION ETCHING.

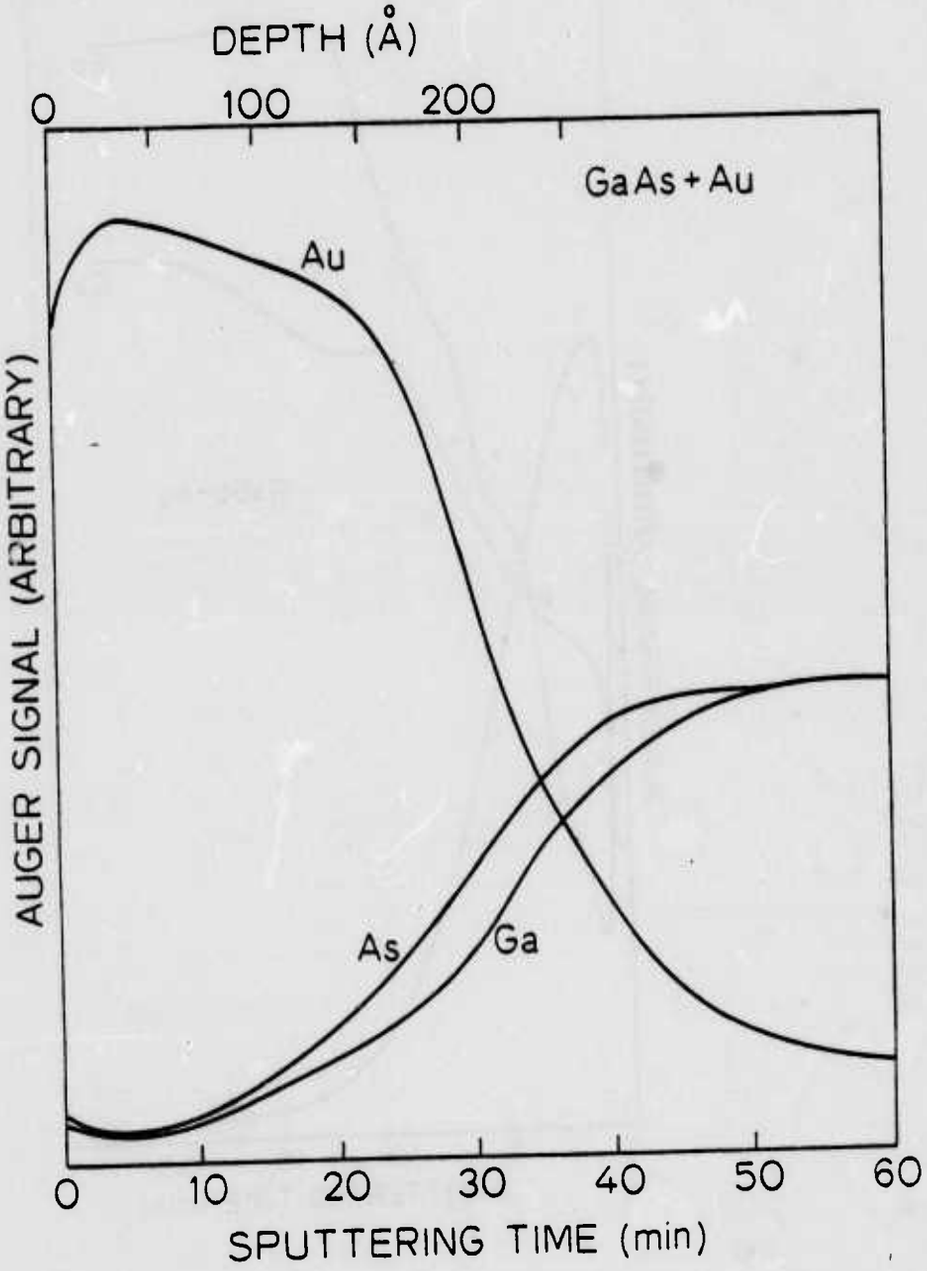

Fig. 5. COMPOSITIONAL DEPTH PROFILE OF Au COVERED GaAs OBTAINED USING AUGER ELECTRON SPECTROSCOPY IN COMBINATION WITH ARGON ION ETCHING.

the interface would appear broadened. This "clumping" may not be very pronounced at room temperature. The existence of region A in Fig. 4 also argues against significant "clumping." In this region, the Ga signal stays constant while the Sb signal increases steadily. This region also was observed on a second Au-GaSb sample with thicker Au coverage. If there was clumping, then one should just observe a steady increase in both the Ga and Sb signal. (If such a steady increase were observed as in Fig. 5, one would not be able to distinguish between broadening by intermixing or by "clumping.") In this region, too, nonstoichiometry is likely since one semiconductor component is steadily increasing while the other is constant. This region is roughly 30 Å wide. For comparison, the depth profile for Au-GaAs is shown in Fig. 5. The sputtering rate is 6.7 Å/min. Here, nothing similar to region A is seen. Other workers[31-33] have also studied Au-GaAs depth profiles with various techniques and observed interdiffusion, particularly at high temperatures. In general, more Ga than As was found to be on the surface. For example, Hiraki et al[33] studied Au overlayers on semiconductors and insulators and found that, at room temperature, the surface is Ga rich, with an "alloyed" interface while, for Au-insulator systems, the interface is sharp. Figure 3 shows the presence of both Ga and As on the surface, with somewhat more As at the higher coverages. The discrepancy may be explained by difference in initial surface preparation (Hiraki et al[33] used ion-sputter and anneal methods rather than cleaving), by a probable difference in crystal face (which they did not specify but was not likely to be (110)), and possibly by differences in Au evaporation techniques. The most significant thing in their findings is the absence of an "alloyed" interface on insulators. Further discussion will be postponed till Section IV.

A close examination of Figs. 1, 2, and 3 shows that some levels are shifted and some are broadened. The Au-$4f_{7/2}$ level has a binding energy (BE) of 84 eV relative to E_F at thick coverages, in agreement with measurements on bulk Au. However, at low coverages, the 4f's have a higher BE. This increase is as large as 0.8 eV on GaSb, possibly larger at still lower coverages. The shift is 0.6 eV on GaAs (partially masked by band-bending: these spectra are plotted with the VBM aligned) and 0.3 eV on InP. As will be shown below, at low coverages, the Au is in a dispersed or "atomic-like" state. Thus, it appears that the Au-4f's are higher in BE relative to E_F by >0.8 eV in the dispersed or "atomic-like" state and move continuously toward lower BE as more Au is deposited. The shift of a core level may be due to chemical effects such as charge transfer or due to configuration changes or differences in screening and relaxation. Since Au is quite electronegative,[34] shifts due to chemical effects should be towards higher BE as bulk Au is formed, so the observed shift is probably due to changes in screening and relaxation.

On the GaSb cleave of Fig. 1, E_F appears to be pinned near midgap after cleaving. While E_F is usually unpinned on n-GaSb, occasionally, extrinsic states cause pinning either over the whole crystal surface or over parts of it, as in Fig. 9. As Au coverage is increased, there is little change in the position of the core peaks relative to VBM. There may be a small shift (~0.2 eV) of the Sb-4d towards higher BE, but it is difficult to be certain with the present experimental resolution. The full width at half maximum (FWHM) of these levels also show negligible change. The Sb-$4d_{5/2}$ in metallic Sb has a BE of 32.1 eV (referred to E_F) according to ESCA measurements.[35] Here, the surface

$Sb\text{-}4d_{5/2}$ has a binding energy of 31.9 eV (relative to E_F) and, for clean GaSb, a binding energy of 31.6 eV (relative to VBM). The difference in BE between ESCA and the present measurements is within experimental uncertainties, so it is not possible to tell whether Sb, $AuSb_2$, or an alloy is at the surface. However, the relatively strong intensity of the Au emission and the absence of bulk Au structure favor $AuSb_2$ or an alloy, with perhaps some metallic Sb mixed in. Although the bulk phase diagram[36] for Au-Sb indicates that only Sb + $AuSb_2$ is possible at high concentration of Sb at room temperature, the surface phase diagram is likely to be different. In addition, the present system may not have reached equilibrium.

In GaAs, the Ga-3d and As-3d levels are broadened by ~0.5 eV (FWHM) for this particular cleave immediately after cleaving although most GaAs cleaves do not show this. This is a good example of inhomogeneous band-bending over the surface. Further examples will follow in the next subsection. This pinning due to extrinsic states from the cleaving process has caused considerable confusion in the past, leading to erroneous conclusions that intrinsic surface states are responsible for the SB pinning.[8-13] The inhomogeneity in band-bending disappears with the addition of Au, since Au causes pinning at the same energy position over the entire surface. Thus, the core levels narrow with Au deposition. There is no observable change in the peak position of either core level (relative to VBM) although, at thick Au coverage, a tail toward higher BE in the As-3d can be clearly seen. This tail falls at the right energy for bulk As-3d, which has slightly higher binding energy. Once again, since valence band spectra (Figs. 13 and 16) show that bulk Au is not present at the surface, the surface layer is likely to be As, Ga-Au alloys, or

compounds such as $AuGa_2$ or AuGa, and perhaps some free Ga. The surface composition is probably such that the surface free energy is minimized. Our preliminary data on Ga + GaAs indicate that the BE of Ga-3d in Ga metal (relative to E_F) is close to that for Ga-3d in GaAs (relative to VBM), so any Ga metal here would be difficult to distinguish.

For InP, the behavior of the P level with Au deposition indicates the possible presence of free P. The P-2p level broadens by ~0.4 eV (FWHM) with the addition of several monolayers of Au and, at thick coverage, the peak position has shifted by 0.8 eV towards higher BE. No such broadening is observed in the In-4d level, although a shift by 0.8 eV towards lower BE is observed. Once again, valence band spectra indicate formation of compounds or alloys of Au. These are probably Au-In alloys or compounds such as $AuIn_2$ or AuIn, and the lack of broadening indicates that there is one dominant compound or alloy. However, the broadening of the P-2p indicates the presence of (at least) two different species of P--possibly free P and a Au-P alloy. There is a suggestion of excess P since, even though the P amplitude decreases at roughly the same rate as In, it is broadened. This may be due to a true excess of P removed from the semiconductor since this excess is already observed at several monolayer coverage.

The important conclusions to be drawn from this subsection is (1) Au interacts strongly even at room temperature with the semiconductor when deposited, causing large amounts of intermixing with some surface enhancements, (2) the semiconductor material removed from the crystal may be partially or totally dissociated and may remain in the free state or form compounds or alloys with Au, and (3) the semiconductor components may be removed nonstoichiometrically, and the excess elements appear to

be Sb and (to a lesser extent) P in GaSb and InP, respectively. Ga and As appear to be removed in nearly stoichiometric amounts in GaAs.

B. UPS and CFS Spectra

From previous work,[10,37] one knows that a small fraction of a monolayer of Cs can cause E_F pinning on GaSb. Rowe et al's experiments[16,17] for group III metals on Si (111)(7×7) indicate that 70 percent of E_F stabilization takes place for the first monolayer of metal coverage. It is therefore extremely important to follow the pinning change and the surface electronic structure for the first monolayer of metal coverage. With the photon energies available on the 8° line at SSRL (5 to 35 eV), one can carry out such studies easily. In this subsection, unless otherwise noted, Au deposition method 2 was used.

In Figs. 6, 7, and 8, the position of E_F in the band gap as a function of Au coverage is plotted for the three semiconductors studied. The most striking thing is the extreme sensitivity of E_F to Au. It is apparent that, for coverages <0.2 monolayer, E_F has already stabilized near the positions for bulk Au on cleaved surfaces reported by Mead and Spitzer.[1] This sensitivity is high both for GaSb and InP, which are unpinned here after cleaving, and for GaAs, which has E_F pinned at midgap. (Occasionally, on "good" cleaves, E_F on GaAs is unpinned.[13]) It is perhaps more accurate to refer to GaSb as mostly unpinned after cleaving, since band-bending varies over the surface with most areas being unpinned. This will be discussed below. The behavior of E_F on GaSb with adsorbate is similar to that observed for Cs on GaSb[37] where ~ 0.1 monolayer is sufficient to pin E_F at the VBM. The barrier height is similar to that of Au-GaSb, even though these metals

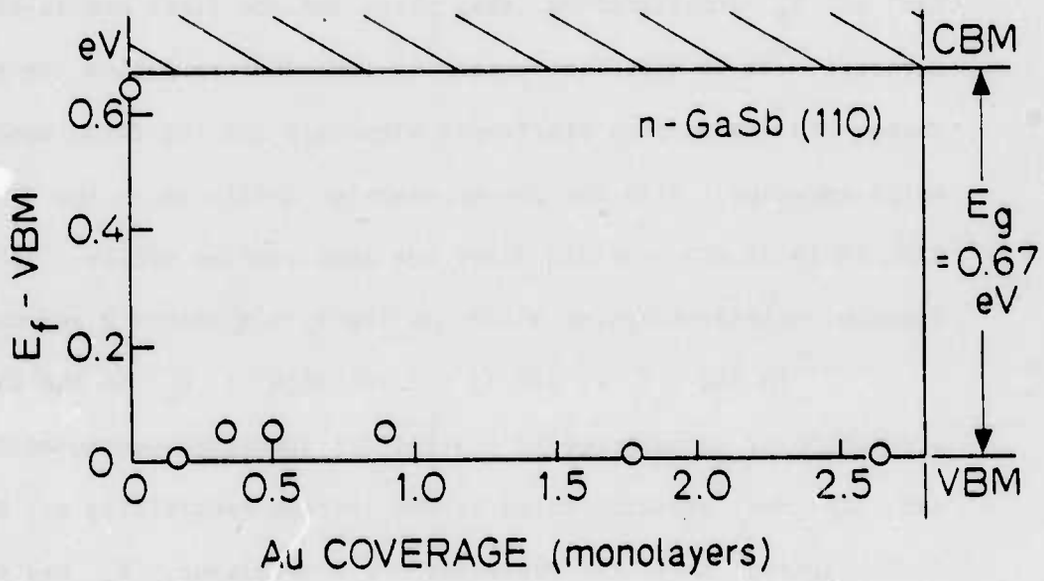

Fig. 6. POSITIONS OF THE SURFACE FERMI LEVEL RELATIVE TO THE VALENCE BAND MAXIMUM ON GaSb, PLOTTED AS A FUNCTION OF Au COVERAGE.

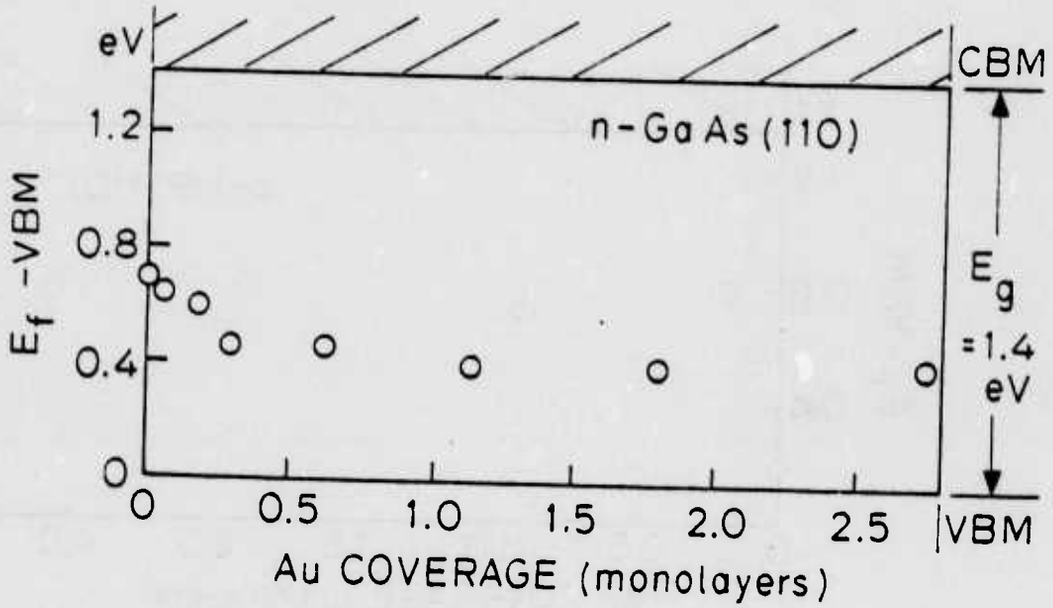

Fig. 7. POSITIONS OF THE SURFACE FERMI LEVEL RELATIVE TO THE VALENCE BAND MAXIMUM ON GaAs, PLOTTED AS A FUNCTION OF Au COVERAGE.

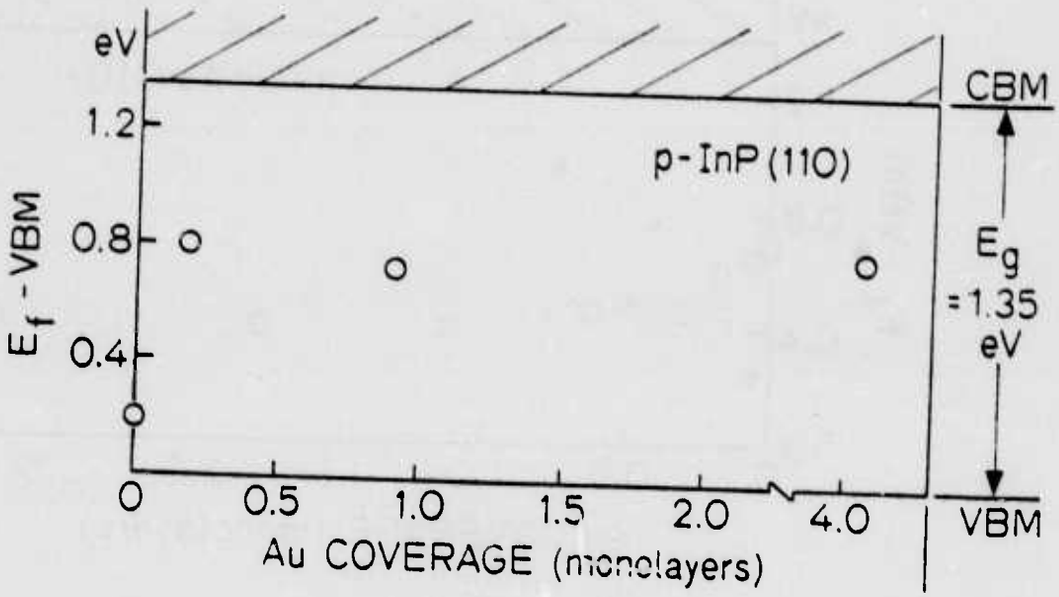

Fig. 8. POSITIONS OF THE SURFACE FERMI LEVEL RELATIVE TO THE VALENCE BAND MAXIMUM ON InP, PLOTTED AS A FUNCTION OF Au COVERAGE.

have very different electronegativities. The barrier heights on the other two semiconductors are slightly lower for Cs than for Au; the difference is $\lesssim 0.2$ eV, however.

We have established here that < 0.2 monolayer of Au at room temperature is sufficient to stabilize E_F near the bulk metal overlayer position so that a microscopic or "atomic-scale" model involving a very small number of states is needed to explain the experimental observations. This is important since practical devices are made with bulk metal overlayers, but the relevant layer is the first 0.2 monolayer or less so that one needs to concentrate on understanding the first few monolayers to solve the problem of E_F pinning and the SB height. The SB height is, of course, only part of the difficult problem in the study of SB's. The electrical behavior (e.g., departure from ideality, $n \neq 1$), reverse current characteristics, and degradation of the barrier may all be related to the complex phenomena at thick layers such as widening of the interface, enhanced intermixing, compound formation in the metal layer, and so on.

At $\hbar\omega > 25$ eV, the semiconductor valence band matrix elements and the photoelectron escape depth decrease. On the other hand, the Au 5-d matrix elements increase. These factors enable small amounts of Au to be easily observed. It is usually important to know whether the Au is well dispersed on the surface. By following the development of the Au-5d bands, one can gather such information. From photoemission work on Au alloys,[38] it is known that, when Au atoms are well dispersed as in a dilute Au alloy, the splitting of the Au-5d peaks is reduced from the bulk value of 2.3 eV until it approaches the value for atomic Au (1.5 eV). In addition, there is a shift towards higher binding energy of these bands.

Therefore, the Au distribution may be probed by following the details of the 5d bands. If Au islands of appreciable size form, then one would expect to see bulk Au valence bands, which includes a shoulder to the lower binding side of the upper d-band and larger splittings (>2 eV) of the 5d-peaks. Because of band structure effects at these photon energies, the splitting of the peaks in the 5d bands is a function of photon energy.[39] The splitting at $\hbar\omega = 21$ eV is small (2.0 eV, Fig. 16), but a very strong shoulder is present on the low binding side of the upper 5d-peak. The splitting at 28 eV is larger--2.3 eV--but the shoulder is less pronounced. This shoulder is characteristic of pure bulk Au at these photon energies. In Figs. 9 and 11, one can see that the splitting for <0.2 monolayer is 1.7 and 1.6 eV for GaSb and InP, respectively. The splitting for 0.17 monolayer of Au on GaAs is larger--1.9 eV--but still is less than the bulk value. The shoulder mentioned above is also absent. Thus, we may conclude that, <u>when E_F has stabilized, the Au on the surface is still well dispersed and has not formed large "clumps" so that it remains rather "atomic-like</u>."

This observation makes all "jellium" theories of SB's suspect. Obviously, there can be no <u>bulk</u> metal wave function tails that penetrate into the semiconductor; rather, any theories would have to depend on a much more "atomic" model of the metal atom. At higher coverages, the splitting increases, but the valence bands still do not resemble bulk Au, with the shoulder still absent. This is especially clear in the 21 eV EDC's shown later in this section. This is due to the formation of compounds or alloys with the semiconductor components, so the Au atoms do not assume the lattice structure of metallic Au.

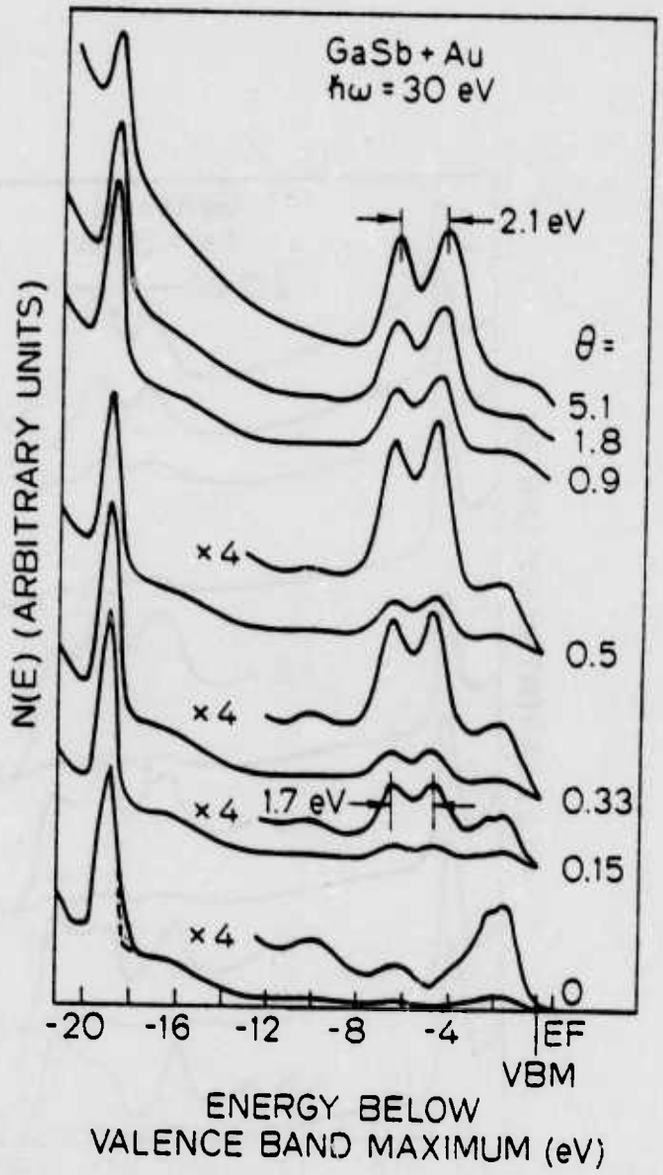

Fig. 9. EDC'S OF GaSb AT A PHOTON ENERGY OF 30 eV AS A FUNCTION OF Au COVERAGE.

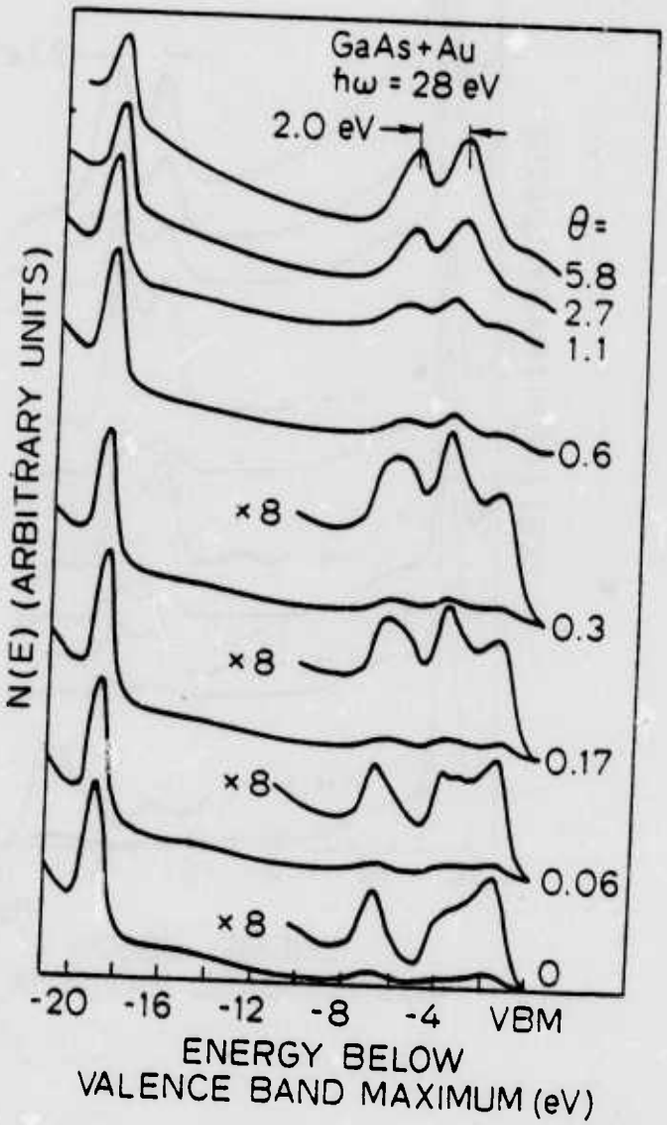

Fig. 10. EDC'S OF GaAs AT A PHOTON ENERGY OF 28 eV AS A FUNCTION OF Au COVERAGE.

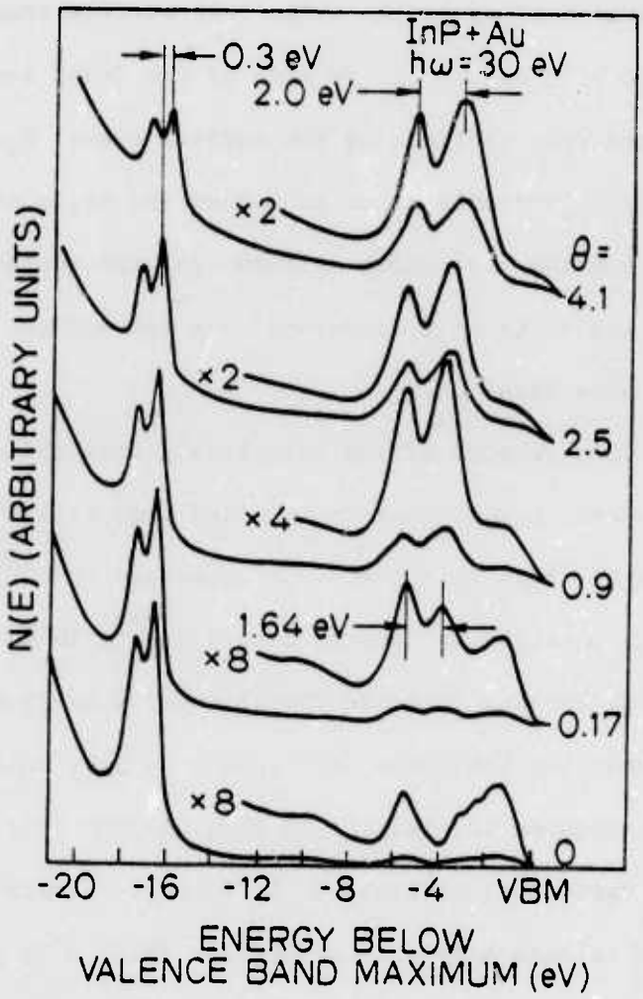

Fig. 11. EDC'S OF InP AT A PHOTON ENERGY OF 30 eV AS A FUNCTION OF Au COVERAGE.

Another way to determine the dispersion of the Au atoms is to look for nonuniform band-bending, i.e., "patch" effects, from the broadening of the Ga or In levels. If Au "clumps," then pinning will be nonuniform over the surface and the core levels will be broadened. This method works extremely well when E_F changes in energy position by large values with deposition of Au. A striking example of the effects of nonuniform band-bending is the clean GaSb surface studied here. In Fig. 9, there is a tail on the low BE side of the Ga-3d level (shaded area), due to emission from portions of the surface where E_F is pinned. The deposition of 0.15 monolayer of Au caused the tails to disappear, suggesting that the pinning has become uniform over the surface, once again indicating that the Au is well dispersed over the surface. The CFS spectra (Fig. 17) also show this.

Observation of the core levels show that the In-4d level moves upward towards lower BE as Au is added and, at 4.1 monolayers, has shifted up by 0.3 eV, less than the 0.8 eV observed in SXPS at much higher coverage. This possibly is because a more dilute In-Au alloy shows a larger In-4d shift and may indicate formation of a Au-In alloy. The Ga-3d levels on the other two semiconductors appear to have no resolvable shift.

Figures 12, 13, and 14 show the EDC's of GaAs, GaSb, and InP at 21 eV at various Au coverages. At 21 eV, the matrix elements of the semiconductor valence band are much larger than at 30 eV while the Au 5d matrix elements decrease. There is the question of whether submonolayers (or even several monolayers) of metal atoms can be considered as metallic. One common feature in these spectra is the absence of a Au Fermi edge near E_F up to about two monolayers. To show this more clearly, the top 3 eV of Fig. 14 is reproduced in Fig. 15. Note, in particular, the lack of

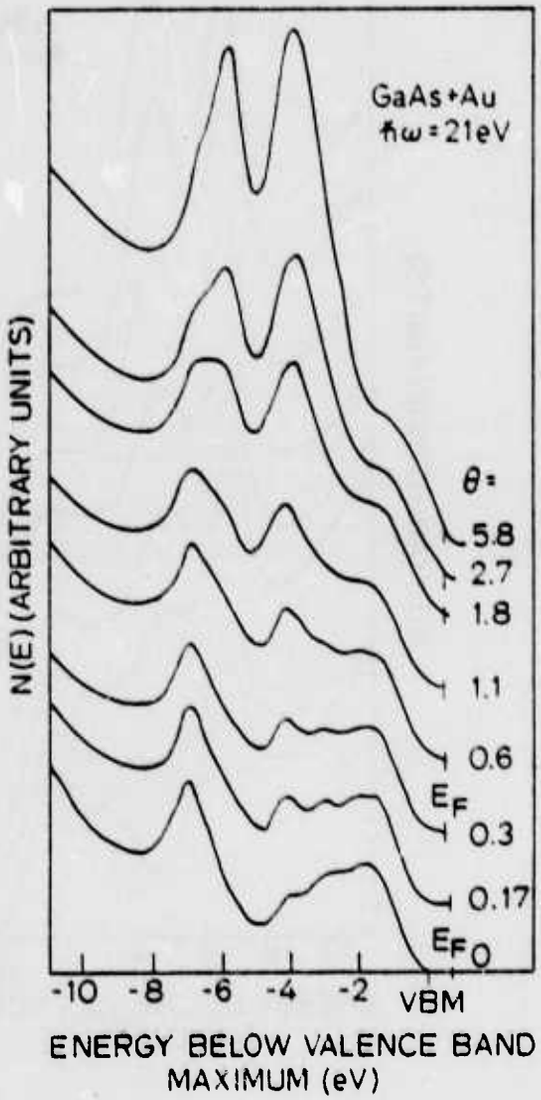

Fig. 12. EDC'S OF GaAs AT A PHOTON ENERGY OF 21 eV AS A FUNCTION OF Au COVERAGE.

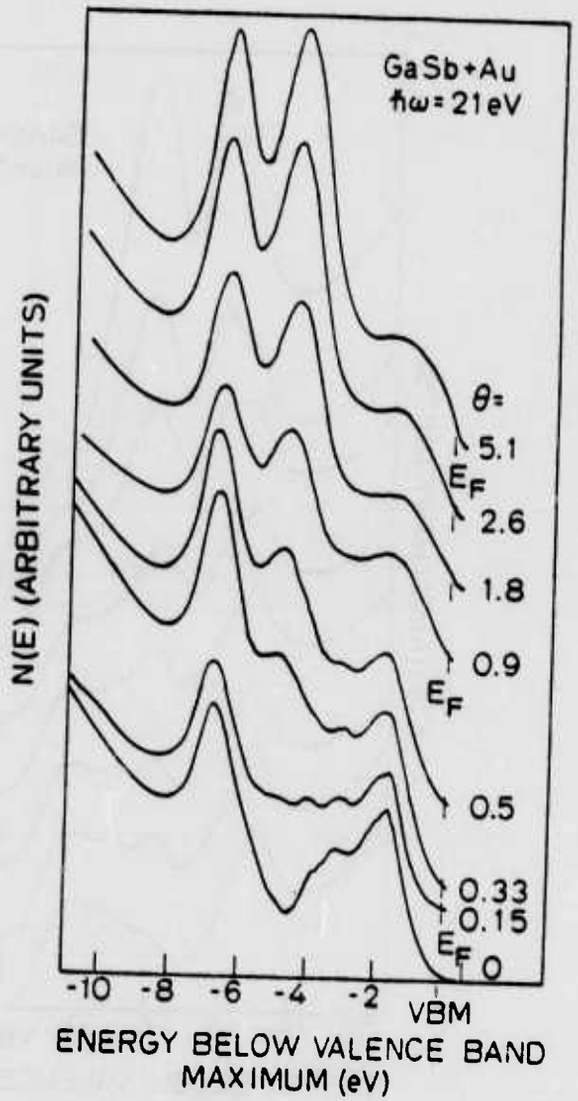

Fig. 13. EDC'S OF GaSb AT A PHOTON ENERGY OF 21 eV AS A FUNCTION OF Au COVERAGE.

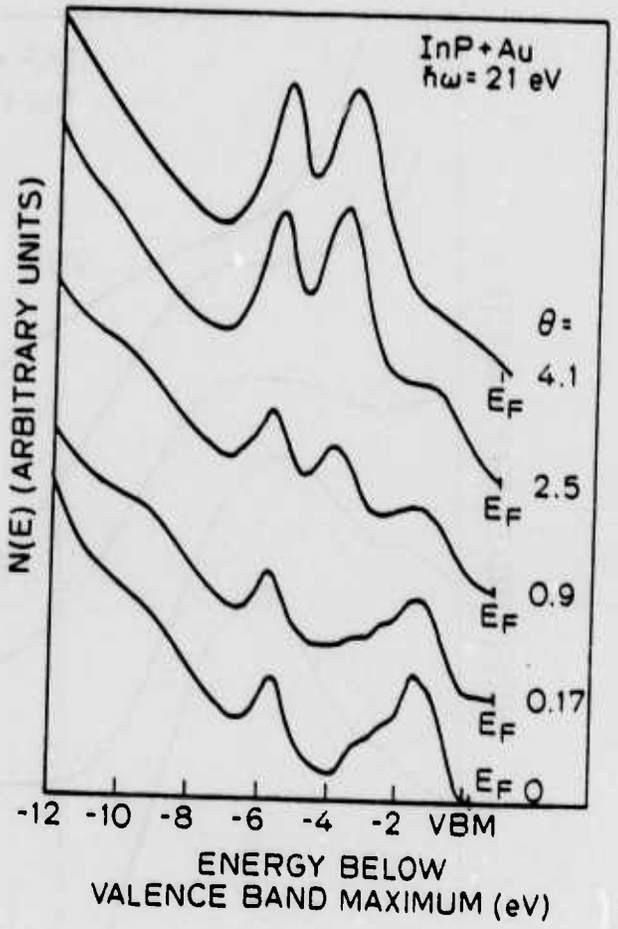

Fig. 14. EDC'S OF InP AT A PHOTON ENERGY OF 21 eV AS A FUNCTION OF Au COVERAGE.

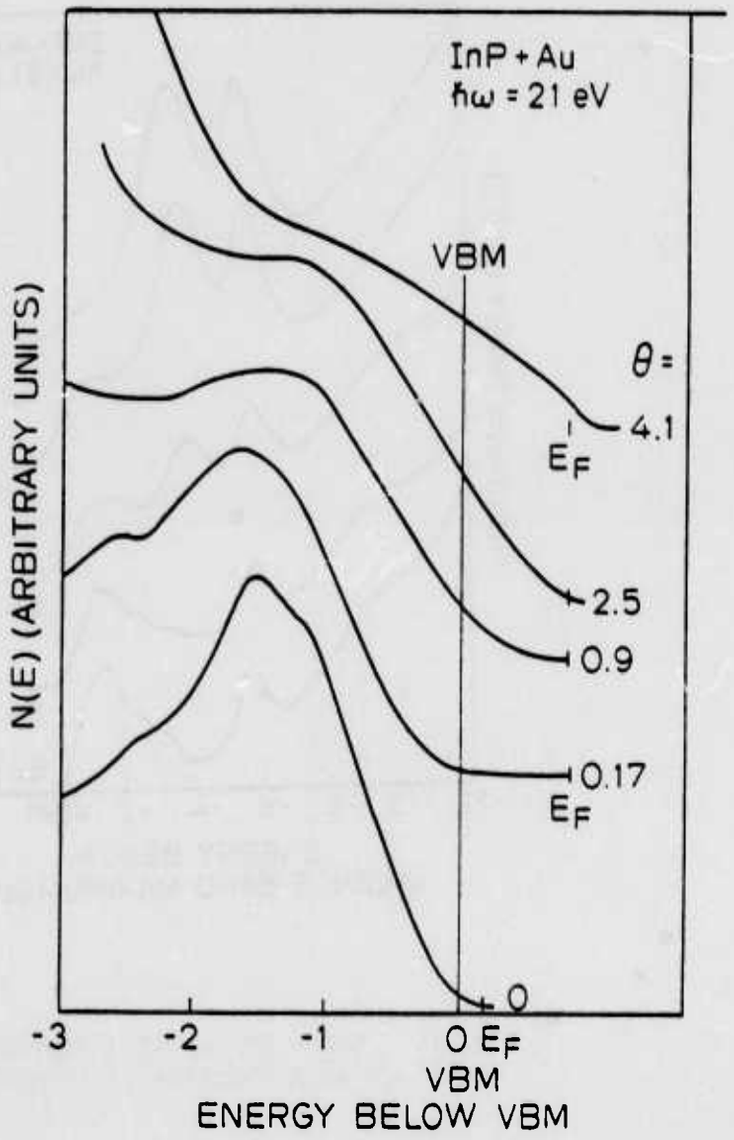

Fig. 15. TOP 3 eV OF THE InP VALENCE BAND AT A PHOTON ENERGY OF 21 eV AS A FUNCTION OF Au COVERAGE.

emission near E_F below 1.1 monolayer when the barrier is already formed. Since the escape depth near E_F for $\hbar\omega = 21$ eV is ~10 Å, there should be sufficient surface sensitivity to detect any emission. This further argues against a "jellium" type model of the SB. The evidence is that the adlayer does not become metallic till coverages of 4 to 5 monolayers, quite possibly because of intermixing or diffusion. Emission in the band gap is gradually appearing at 0.6 monolayer and is probably from the Au 6s electrons. At coverages near half a monolayer, the structure in the semiconductor valence bands have disappeared, indicating that the surface layers have become severely disordered and possibly amorphous. Note that the Au emission at 0.6 monolayer is not sufficiently strong to mask the semiconductor valence band emission; note too, at several monolayers, the emission from the top 3 eV in the EDC is from both Au and the semiconductor components, as the emission is much higher than is observed for Au. The EDC's at $\hbar\omega = 21$ eV for thicker coverages deposited using method 1 for these semiconductors are shown together with one for Au in Fig. 16. The striking thing is that, even for fairly thick layers, the Au-5d bands from the overlayers still do not closely resemble that from Au--note the absence of the shoulder mentioned previously. The metal Fermi edge is well established in these EDC's.

We have supplemented our photoemission measurements with constant final state spectroscopy[8,9] (CFS). In CFS, one monitors the secondary electron yield at a constant final state energy (constant retarding voltage) while varying the photon energy incident on the sample. At photon energies which cause transitions from the Ga or In d levels, d core holes are created. Recombination of electrons with these holes

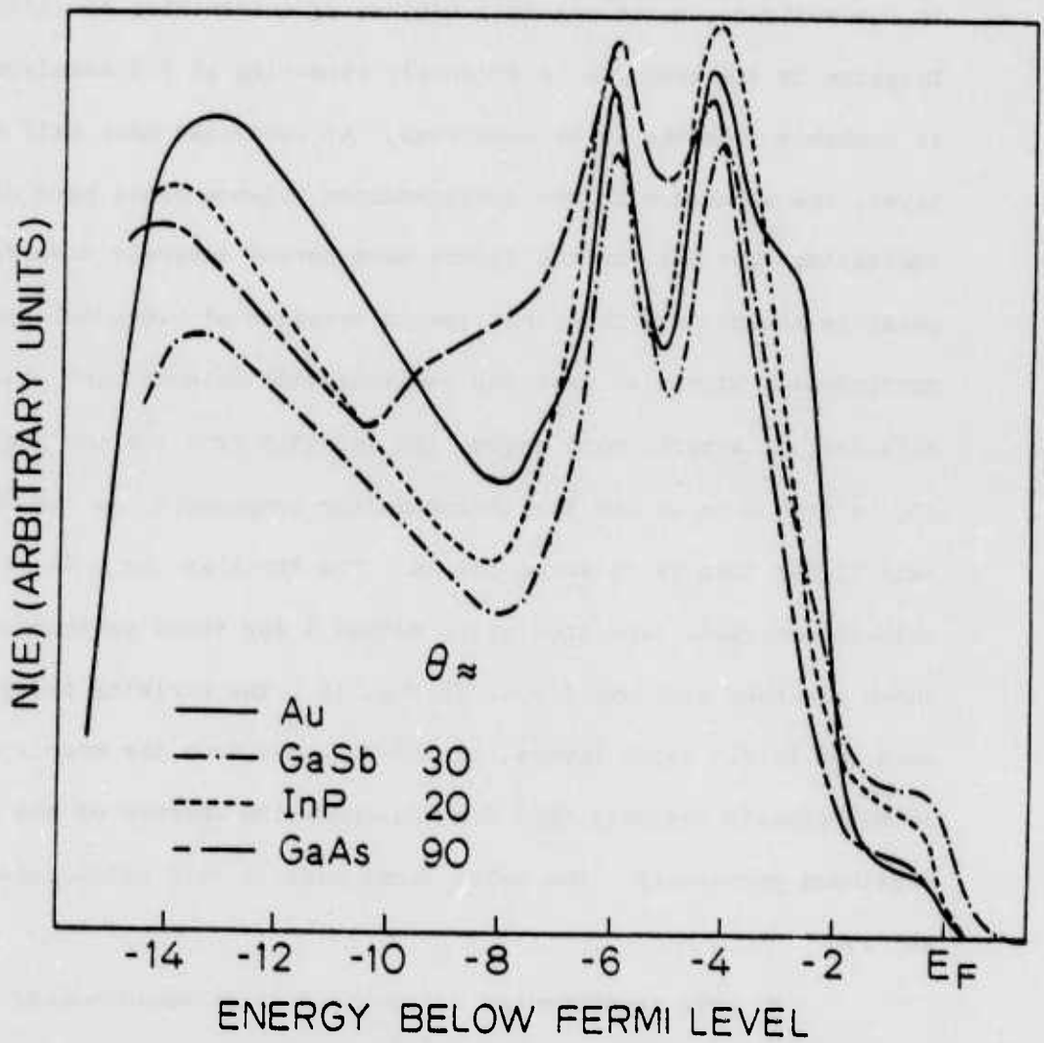

Fig. 16. EDC'S OF Au AND OF THICKER Au LAYERS ON GaAs, GaSb, AND InP AT A PHOTON ENERGY OF 21 eV.

gives rise to secondary Auger electrons whose final state energy does not change with photon energy. The final state energy chosen here is 4 eV.

In Figs. 17, 18, and 19, CFS spectra for GaSb, GaAs, and InP are shown. The double peak structure near 19 eV are believed to be excitonic levels involving transitions from the spin orbit split anion d-core level (Ga-3d and In-4d) and empty states--possibly surface states--above the conduction band minimum.[40] The energy necessary to cause a transition into them is lowered by the exciton binding energy (~0.5 to 1.0 eV). The transition strength is matrix element dependent.[41] The broad peaks at higher photon energies are due to transitions into the bulk conduction band, reflecting the density of states. At still higher photon energies in Figs. 17 and 19, the sharp peaks are due to sweeping of the core d-level (primary) photoelectrons through the final state energy of 4 eV.

In Fig. 17, the Ga-3d peak near 28 eV shows the tail (shaded) mentioned earlier (Fig. 9). After 0.15 monolayer of Au, the peak shifts by 0.6 eV due to movement of E_F by that amount, and the tail disappears since pinning is now uniform over the surface (see earlier discussion on Fig. 9). Further deposition of Au fails to cause any extra E_F movement, once again demonstrating that pinning is complete at 0.15 monolayer. Note, however, that, even though pinning is complete at 0.15 monolayer, the surface excitons are little affected and, in particular, remain at the same energy, showing that the final states are not shifted by the presence of Au. By 0.9 monolayer, however, much of the excitonic structure has disappeared. The coverage for exciton extinction appears slightly higher for the other two semiconductors; but, when pinning is complete,

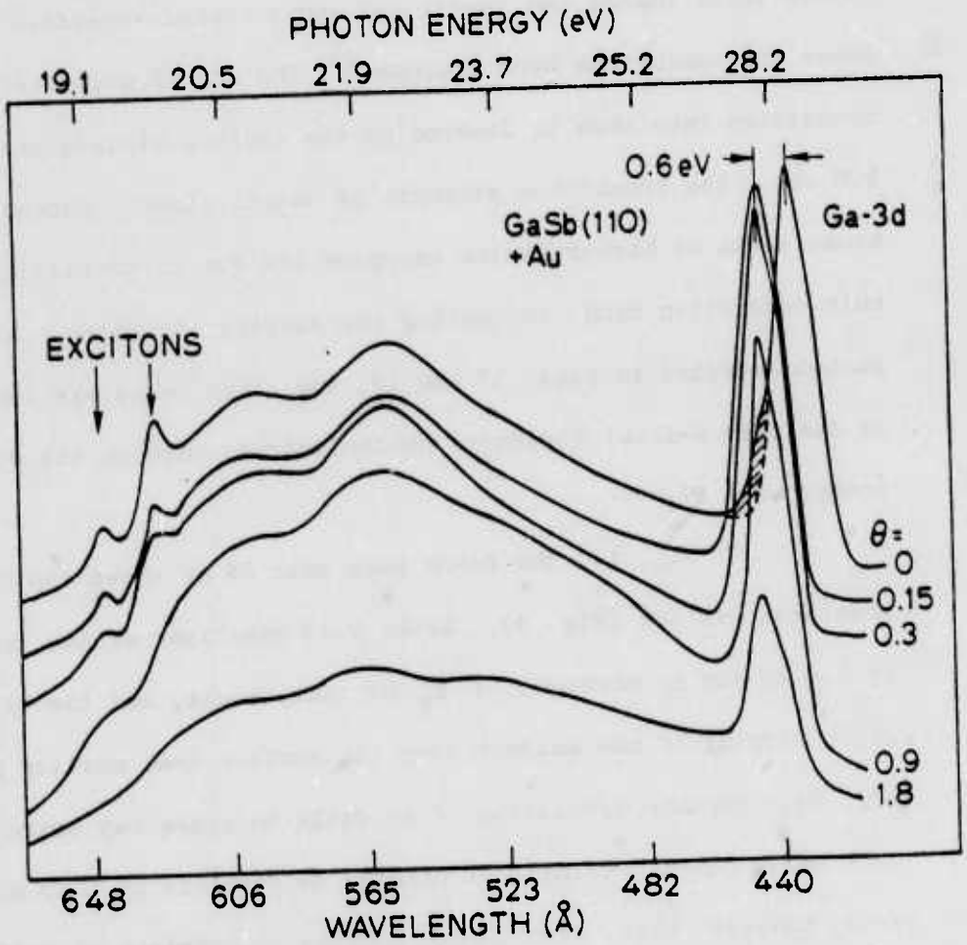

Fig. 17. CONSTANT FINAL STATE SPECTRA OF GaSb AS A FUNCTION OF Au COVERAGE.

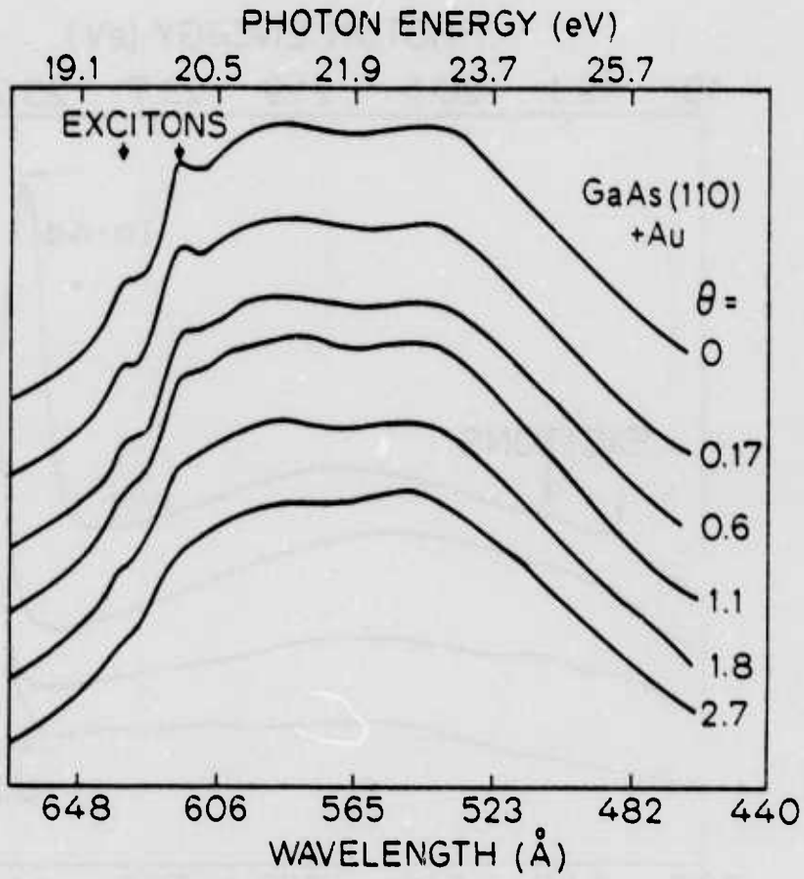

Fig. 18. CONSTANT FINAL STATE SPECTRA OF GaAs AS A FUNCTION OF Au COVERAGE.

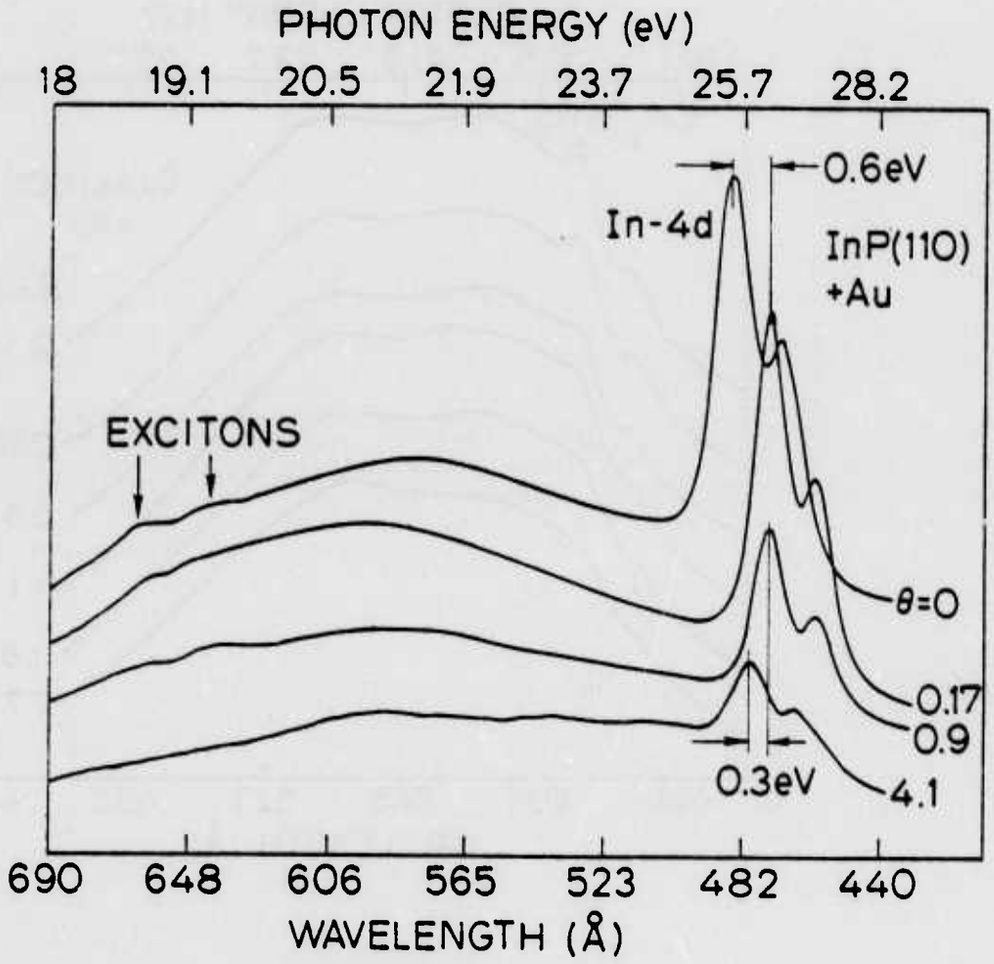

Fig. 19. CONSTANT FINAL STATE SPECTRA OF InP AS A FUNCTION OF Au COVERAGE.

the excitons are little affected. Note that, in Fig. 19, the shift in the In-4d is due initially to E_F movement, but the shift (0.3 eV) at 4.1 monolayer is due not to E_F movement but to compound or alloy formation.

Our results here are in contrast to Eastman and Freeouf's[8,9] for Pd overlayers on GaAs (110) and In overlayers on GaAs (110), GaSb (110), and InAs (110) where the surface excitons were little affected by 2 to 3 metal layers. Our results are similar to Rowe et al's for group III metal overlayers on Ge, Si, and GaAs (110) and (100) surfaces.[14-18] Rowe et al had proposed that the (110) surface is anomalous; our results here indicate that it is not. Possibly, the discrepancy is due to some peculiarity of Pd and In overlayers; further experiments are needed to resolve this discrepancy.

One question that might be asked is whether the Au creates any new empty levels. The data here show no clear evidence of new levels arising from the deposition of Au. One explanation is that the density of new empty states created (metal induced states) is low since $<10^{12}$ states/cm^2 are sufficient to pin E_F. However, if Au forms covalent bonds with the surface atoms, as proposed for group III metals on Si (111),[16] then one would expect creation of $\sim 10^{15}$ states/cm^2 and introduce new levels into the CFS spectra. The absence of these levels near 1 monolayer suggests that covalent bonding may not be the correct description for the materials studied here.

IV. Discussion

It is appropriate at this point to summarize what is now known about SB's, both from other work and from the present study. (1) SB heights in covalent semiconductors are nearly independent of the metal work function Φ_M and, with a few exceptions, are equal to two-thirds of the band gap (the two-thirds rule); however, for ionic materials, strong Φ_M dependence is observed.[2,3] (2) The anion rule proposed by McCaldin et al,[5] which states that the SB height for holes is dependent only on the anion, applies to both covalent and more ionic materials such as CdSe, ZnSe, CdS, and ZnS. Materials which are the exceptions to the two-thirds rule such as InP and GaSb obey the anion rule. (3) Observations 1 and 2 are made on atomically clean surfaces. However, barrier heights on "real" surfaces with native oxides and other contaminants appear to be very similar and are not strongly affected by moderate heat treatment. For example, Kim et al[32] found that, for Au-GaAs, heating up to 400°C for seven minutes only changed the barrier height by 0.02 eV. The measurements were made at room temperature. At 500°C, the barrier height drops by ~0.26 eV compared to room temperature, and there is a large increase in the ideality factor n defined in the thermionic emission current equation for emission over the barrier:

$$J = A^*T^2 \exp(-q\phi_B/kT)[\exp(qV/nkT) - 1]$$

where J = diode current density, A^* = effective Richardson constant, ϕ_B = barrier height, and V = applied voltage. For an ideal barrier, $n = 1$; departures of n from unity are always to higher values. (4) ϕ_B does not change very much going from submonolayer or monolayer

coverage to hundreds of monolayers, and, as this work shows, E_F is stabilized by the first 0.15 monolayer (or less) of metal on the III-V semiconductors, i.e., before a clearly metallic layer forms; thus, a microscopic or "atomic-scale" model based more on the interaction of Au atoms with the semiconductor than with a well-formed Au metallic layer is necessary to explain the data. (5) Since it is now believed that, for most III-V semiconductors, there exist no intrinsic surface states in the band gap, metal-induced states must be responsible for E_F stabilization. Our observations lead us to the conclusion that they are extrinsic states. Here, it is wise to define what one means by extrinsic. We define extrinsic states to be those states not present on a clean, perfect, defect-free surface. The surface may have a reproducible reconstruction, e.g., Si (111) 2×1. Extrinsic states may be induced by surface strain or defects introduced by surface preparation or by the presence of foreign atoms on the surface. (6) From CFS data, the excitonic transition involving final states above the CBM are barely affected when E_F has stabilized at <0.2 monolayer coverage, and ~1 monolayer of metal is required to remove this transition. At one monolayer coverage, no new transitions into final states in the band gap can be seen. (7) There apparently is a large amount of intermixing of metal and semiconductor although, for insulators, Hiraki et al[33] observed no "alloyed" junction. There is thus a (possibly nonstoichiometric) removal of semiconductor material at the interface. For example, Sb is removed to the surface of the Au layer on Au-GaSb to leave an excess of Ga at the interface.

A successful model for SB formation must be able to explain or, at the very least, not be inconsistent with the above observations. While

it is not possible at this time to present a definitive model which accounts for all the known phenomena, many of the observations can be explained by a "defect" model. Confirmation of this model will require much further experimentation; hopefully, presentation of the model here will stimulate interest in performing work to test it.

This model is motivated largely by observation 7 above. Removal of semiconductor materials from the interface is likely to give rise to large numbers of defects which can pin E_F. Although a departure from stoichiometry is unnecessary for E_F pinning (see below), it is almost certain that there is a nonstoichiometric interface in Au-GaSb and quite probable in some others, although small departures from stoichiometry (e.g., 1 percent) will be nearly impossible to detect with the techniques used in this paper although they are sufficient to produce pinning.

The bulk growth properties of GaSb support an interpretation of nonstoichiometry. It has long been known[24-27] that high purity undoped GaSb is p-type due to nonstoichiometry. The acceptors in that semiconductor are related to a Ga excess or an Sb deficiency, are related to vacancies, and are fairly immobile. van der Meulen[26] ruled out the possibility of a simple defect and suggested that the complex center $Ga_{Sb}V_{Ga}$, that is, a Ga vacancy associated with an antisite defect of Ga on an Sb site, gives rise to these acceptors. These same acceptors may be responsible for pinning E_F at the VBM at the surface. It appears that GaSb surface is highly p-type, and the deposited Au provides the energy to create the acceptors. One point to note is that the semiconductors are dissociated by the Au causing considerable intermixing; this indicates that a substantial amount of energy is deposited by the Au. Now, what is the source of this energy?

When Au is evaporated, it is in a higher energy state, with an energy equal to the heat of sublimation (89 kcals/mole = 3.87 eV/atom) above the metallic state at room temperature. Upon arrival at the semiconductor surface, the Au atoms go into a lower energy state, releasing large amounts of energy. The amount of energy each condensed Au atom gives up will depend on the strength of binding to the substrate, that is, whether it forms a compound with the semiconductor, chemisorbs, sits interstitially, goes substitutionally into the semiconductor lattice, or bonds weakly to the semiconductor surface or to other Au atoms. This energy will--especially for the first monolayer of Au--be different from the heat of sublimation of Au since, in the previous section, we have seen that bulk Au structure is not obtained until tens of monolayers have been deposited. For example, the initial heat of adsorption of Cs on GaAs (110) is ~60 kcal/mole, while the heat of sublimation of bulk Cs is ~19 kcal/mole.[42] The excess energy carried by the deposited Au is released in a localized volume, thus, causing a "thermal spike" which can create defects. Van Vechten[43] has calculated the enthalpies in forming various bulk defects and, for vacancies, the values are typically 2 to 3 eV for III-V semiconductors. At the surface, these values will be reduced because of reduced area in his macroscopic "cavity" thus lowering the surface energy. Another way of looking at this is that, at the surface, fewer bonds need to be broken to form a defect. Brillson[44] and Lindau et al[45] have presented plots of the Index of Interface Behavior S versus the heat of formation (HF) of numerous covalent and ionic compounds, and there is a striking relation. The more ionic compounds have high HF and $S = 1$, while the covalent compounds have low HF and small S (indicating weak dependence on ϕ_M). From this, one might argue that

the defects formed with metal deposition are more numerous when HF is small and that these defects are more important than the particular metal used in determining the pinning, consistent with observations 1 and 3, although the metal used still affects the pinning position slightly. (This may be due to interactions between the metal and defects.) For more ionic compounds with higher HF, fewer defects are formed, so the dependence on Φ_M is stronger.

Although the defects that pin E_F are probably complex (see below), one may consider as a reasonable approximation that simple vacancies are first formed which later interact with other lattice atoms or impurities to form complexes. Van Vechten's calculations[43] show that, in general, the enthalpies for anion and cation vacancies are different. Therefore, it is likely that more vacancies of one component will be formed. In his simple model, the larger the covalent radius, the greater the enthalpy for vacancy formation. For the semiconductors studied here, GaSb, InP, and GaAs, respectively, $\Delta H(V_{Sb}) = 2.56$ eV, $\Delta H(V_{Ga}) = 2.03$ eV; $\Delta H(V_P) = 2.17$ eV, $\Delta H(V_{In}) = 3.04$ eV; $\Delta H(V_{As}) = \Delta H(V_{Ga}) = 2.59$ eV. These estimates predict that V_{Ga} should be more numerous than V_{Sb}, but, as mentioned previously, the Sb goes to the surface of the Au. Estimates for antisite defects[46] predict that the enthalpy to put a larger atom at the site of a smaller atom is greater and vice versa. Thus, it is more likely for Ga_{Sb} (Ga atom in an Sb site) than Sb_{Ga} to form. Some of the Ga atoms then move into vacant Sb sites to form $V_{Ga}Ga_{Sb}$. Now, an anion vacancy is believed to be a donor while a cation vacancy is believed to be an acceptor; a cation on an anion site is an acceptor, whereas an anion on a cation site is a donor. Thus, the $V_{Ga}Ga_{Sb}$ complex in GaSb would give rise to acceptor levels.

Assuming that the defects formed introduce acceptor and donor levels into the band gap, we can gain some insight into the behavior of E_F by considering two simple situations discussed in Blakemore[47] (and references therein). Consider first the case of an n-type semiconductor. When N_A acceptors are introduced at the energy $E_C - E_A$ into the band gap (E_C = energy of CBM) by making the interface nonstoichiometric, then compensation occurs until N_A exceeds N_d, the concentration of dopants. (Note that compensation may reduce the energy needed to create a defect.) At that point, E_F drops very rapidly and locks onto the acceptor level. This is probably the case for GaSb.

A second case is when N donor and an equal number of acceptor levels are introduced (for example, through creation of As and Ga vacancies) at energies E_D and E_A measured relative to the CBM. For an n-type semiconductor, E_F would drop very rapidly when N approaches the dopant concentration of the crystal and, when N is much larger than the dopant concentration, E_F would come to rest at an energy intermediate between E_D and E_A. Thus, it is not necessary for nonstoichiometry to exist before pinning occurs.

What are the kind of defects found at or near the surface or interface after metal deposition? Many types of defects can occur in the compound AB. The simplest ones are vacancies ($V_{A,B}$) and antisite defects (A_B, B_A). These can interact with each other or with the metal (e.g., Au) to form complexes. All these defects may form as Au is deposited, but one or two types of defects are likely to dominate E_F pinning and particularly the more immobile ones as more mobile defects can diffuse away from the interface. Thus, as mentioned above, the $V_{Ga}Ga_{Sb}$ complex is likely to be responsible for pinning E_F in GaSb. On GaAs, Lang et al[48]

measured eight different levels in the band gap, two (located near midgap and a few tenths eV below midgap) of which are present before irradiation of the semiconductor with 1 MeV electrons. It is generally accepted[48] that, in isochronal annealing experiments, the lowest-temperature stages are associated with simple defects which have high mobility, while the highest-temperature stages are associated with defect clusters or impurity complexes which have low mobility. Also, it is known that simple defects in GaSb and InSb are unstable above 200°K. Although simple defects may exist in GaAs and InP, judging from isochronal annealing data which show that materials which have higher Debye temperatures have defects with lower mobility,[48] the evidence argues against their playing an important role in SB pinning. Lang et al[48] identified one level as being a simple Ga vacancy level. This level, however, lies in the top part of the band gap, away from the SB pinning position. A level H1 which they believe is related to impurities may be responsible for SB pinning since it lies at approximately the right energy position. Also, as mentioned earlier, the more mobile simple defects are likely to diffuse away from the interface with time, so it is more probable that the nonmobile complexes or clusters which remain near the interface are responsible for SB pinning. Measurement of defect level positions in other semiconductors such as InP should prove very useful.

The "defect" model presented above will explain many of the observations summarized at the beginning of this section. It explains Observation 1 from a consideration of HF and explains Observation 3 since adsorbates with sufficient heats of condensation or adsorption will create defect levels which are characteristic of the semiconductor and depend only weakly on the particular metal deposited. Observation 2 is more

difficult to explain but, if, for GaSb and GaAs, we assume the presence of V_{Ga} or a complex depending strongly on V_{Ga}, then the dangling bonds in the vacancy are anion bonds; since the VBM is anion-like, it is quite reasonable for the energy separating between the defect level (due to anion dangling bonds) to be dependent only on the particular anion. The "defect" model is also a microscopic or "atomic-scale" model, and it is not unreasonable for sufficient defect states to have formed with <0.2 monolayer of metal to pin E_F (Observations 4 and 5). Observation 6 may provide evidence for rejecting a model based on formation of covalent bonds between the metal and the semiconductor surface in the III-V semiconductors (other semiconductors, e.g., group IV semiconductors, may behave differently). Since covalent bonding is expected to provide $\sim 10^{15}$ surface states/cm^2, one might expect to see new transitions due to these states in the CFS spectra. None were observed. The absence of pinning in Ga-GaAs (described below) also argues against covalent bonding since Ga should also form covalent bonds with GaAs and thus pin E_F whereas, if Ga created Ga defects, it might heal these defects and remove the pinning. Note that, since only a very small fraction of the Au atoms create a defect state, new structure in CFS spectra is not expected. Finally, Observation 7 is related to Observation 1 and is explained quite readily by the present model since HF is much higher for the insulators and the metal is unable to create defects and remove material.

Experimentally, much work will have to be done to test the "defect" model. One possible experiment would be to use the appropriate column III or V metal as overlayer in the hope of eliminating pinning due to the deficit of one of the components. Bachrach[49] has studied Ga on p-GaAs and observed no pinning. Woodall et al[50] also reported a suppression

of pinning on n-GaAs. These experiments suggest that the pinning is Ga related, possibly due to Ga vacancies as Ga metal should readily heal V_{Ga} and thus supports the model. In has also been reported[51] to form ohmic contacts to InP. If antisite defects were involved, it is no longer clear what might happen. Other work might be done using very pure undoped material to eliminate the donor-vacancy complex. Theoretically, a good calculation of the enthalpies for surface defect formation would be very helpful. Estimates of the defect level energy positions would be invaluable.

Acknowledgment

The technical support of the Stanford Electron Tube Laboratory, in particular that of Jack McGowan, is gratefully acknowledged.

References

1. C. A. Mead and W. G. Spitzer, Phys. Rev. 134, A 713 (1973).
2. C. A. Mead, Solid State Electron. 9, 1023 (1966).
3. S. Kurtin, T. C. Mc Gill, and C. A. Mead, Phys. Rev. Lett. 22, 1433 (1969).
4. M. Schlüter, Proc. 5th Annual Conf. on the Physics of Compound Semiconductor Interfaces, 1978.
5. J. O. Mc Caldin, T. C. Mc Gill, and C. A. Mead, Phys. Rev. Lett. 36, 56 (1976).
6. J. Bardeen, Phys. Rev. 71, 717 (1947).
7. V. Heine, Phys. Rev. 138, A 1689 (1965).
8. D. E. Eastman and J. L. Freeouf, Phys. Rev. Lett. 34, 1624 (1975).
9. J. L. Freeouf and D. E. Eastman, CRC Crit. Rev. Solid State Sci. 5, 245 (1975).
10. P. W. Chye, I. A. Babalola, T. Sukegawa, and W. E. Spicer, Phys. Rev. Lett. 35, 1602 (1975).
11. A. Huijser and J. van Laar, Surface Sci. 52, 202 (1975); J. van Laar and A. Huijser, J. Vac. Sci. Technol. 13, 769 (1976).
12. W. Gudat and D. E. Eastman, J. Vac. Sci. Technol. 13, 831 (1976).
13. W. E. Spicer, I. Lindau, P. E. Gregory, C. M. Garner, P. Pianetta, and P. W. Chye, J. Vac. Sci. Technol. 13, 780 (1976).
14. J. E. Rowe, S. B. Christman, and G. Margaritondo, Phys. Rev. Lett. 35, 1471 (1975).
15. G. Margaritondo, S. B. Christman, and J. E. Rowe, J. Vac. Sci. Technol. 13, 329 (1976).
16. G. Margaritondo, S. B. Christman, and J. E. Rowe, Phys. Rev. B 14, 5396 (1976).

17. J. E. Rowe, J. Vac. Sci. Technol. 13, 798 (1976).

18. J. E. Rowe, G. Margaritondo and S. B. Christman, Phys. Rev. B 15, 2195 (1977).

19. Also known as Partial Yield Spectroscopy.

20. P. W. Chye, I. Lindau, P. Pianetta, C. M. Garner, and W. E. Spicer, Phys. Rev. B 17, 2682 (1978).

21. I. Lindau and W. E. Spicer, J. Electron Spectrosc. 3, 409 (1974).

22. P. Pianetta, Ph.D. Thesis, Stanford University, 1976; P. Pianetta, I. Lindau, C. M. Garner, and W. E. Spicer, Phys. Rev. B, in press.

23. J. W. Cooper, Phys. Rev. 128, 681 (1962).

24. Y. J. van der Meulen, Solid-State Electron. 7, 767 (1964).

25. D. Effer and P. J. Etter, J. Phys. Chem. Solids 25, 451 (1964).

26. Y. J. van der Meulen, J. Phys. Chem. Solids 28, 25 (1967).

27. H. Miki, K. Segawa, and K. Fujibayashi, Japan J. Appl. Phys. 13, 203 (1974).

28. S. H. Overbury, P. A. Bertrand, and G. A. Somorjai, Chemical Rev. 75, 547 (1975); G. A. Somorjai and S. H. Overbury, Faraday Discussions of the Chemical Society, No. 60, p. 279 (1975).

29. V. Simić and Ž. Marinković, Thin Solid Films 34, 179 (1976).

30. Handbook of Thin Film Technology, McGraw-Hill, 1970.

31. A. K. Sinha and J. M. Poate, Appl. Phys. Lett. 23, 666 (1973).

32. H. B. Kim, G. G. Sweeney, and T. M. S. Heng, Inst. Phys. Conf. Ser. No. 24, 307 (1975).

33. A. Hiraki, K. Shuto, S. Kim, W. Kammura, and M. Iwani, Appl. Phys. Lett. 31, 611 (1977).

34. L. Pauling, The Nature of the Chemical Bond, Cornell University Press, New York, 1967.

35. R. B. Shalvoy, G. B. Fisher, and P. J. Stiles, Phys. Rev. B 15, 1680 (1977).

36. M. Hansen, Constitution of Binary Alloys, McGraw-Hill, New York, 1958.

37. P. W. Chye, T. Sukegawa, I. A. Babalola, H. Sunami, P. E. Gregory, and W. E. Spicer, Phys. Rev. B 15, 2118 (1977).

38. P. W. Chye, I. Lindau, P. Pianetta, C. M. Garner, and W. E. Spicer, Phys. Lett. 63A, 387 (1977).

39. J. Freeouf, M. Erbudak, and D. E. Eastman, Solid State Commun. 13, 771 (1973).

40. J. Lapeyre and J. Anderson, Phys. Rev. Lett. 35, 117 (1975).

41. R. S. Bauer, J. Vac. Sci. Technol. 14, 899 (1977).

42. J. Derrien and F. Arnaud D'Avitaya, Surface Sci. 65, 668 (1977).

43. J. A. Van Vechten, J. Electrochem. Soc. 122, 419 (1975).

44. L. J. Brillson, Phys. Rev. Lett. 40, 260 (1978); Proc. 5th Annual Conf. on the Physics of Compound Semiconductor Interfaces, 1978.

45. I. Lindau, P. W. Chye, C. M. Garner, P. Pianetta, C. Y. Su, and W. E. Spicer, Proc. 5th Annual Conf. on the Physics of Compound Semiconductor Interfaces, 1978.

46. J. Van Vechten, J. Electrochem. Soc. 122, 423 (1975).

47. J. S. Blakemore, Semiconducting Statistics, Pergamon Press, London, 1962.

48. D. V. Lang, R. A. Logan, and L. C. Kimerling, Phys. Rev. B 15, 4874 (1977).

49. R. Z. Bachrach, Proc. 5th Annual Conf. on the Physics of Compound Semiconductor Interfaces, 1978.

50. J. M. Woodall, C. Lanza, and J. L. Freeouf, Proc. 5th Annual Conf. on the Physics of Compound Semiconductor Interfaces, 1978.

51. R. H. Williams, R. R. Varma, and A. McKinley, J. Phys. C 10, 4545 (1977).

Chapter 5

A NEW AND UNIFIED MODEL FOR SCHOTTKY-BARRIER AND 3-5-INSULATOR INTERFACE STATES FORMATION*

W. E. Spicer,† P. W. Chye,
P. R. Skeath, C. Y. Su, and I. Lindau
Stanford Electronics Laboratories
Stanford University
Stanford, California 94305

*Supported by the Advanced Research Projects Agency of the Department of Defense and monitored by the Office of Naval Research under Contract No. DAAK 02-74-C-0069 and by the Office of Naval Research, ONR N00014-75-C-0289. Part of the work was performed at SSRL which is supported by the National Science Foundation, NSF DMR73-07692, in cooperation with the Stanford Linear Accelerator Center and the Department of Energy.

†Stanford W. Ascherman Professor of Engineering.

ABSTRACT

For n- and p-doped 3-5 compounds, Fermi level pinning and accompanying phenomena of the (110) cleavage surface have been studied carefully using photoemission at $h\nu \lesssim 300$ eV (so that core as well as valence band levels could be studied). Both the clean surfaces and the changes produced, as metals or oxygen are added to those surfaces in submonolayer quantities, have been examined. It is found that, in general, the Fermi level stabilizes after a small fraction of a monolayer of either metal or oxygen atoms have been placed on the surface. Most strikingly, Fermi level pinning produced on a given semiconductor by metals and oxygen are similar. However, there is a strong difference in these pinning positions depending on the semiconductor: The pinning position is near (1) the conduction band maximum (CBM) for InP, (2) mid-gap for GaAs, and (3) the valence band maximum (VBM) for GaSb.

The similarity in the pinning position on a given semiconductor produced by both metals and oxygen suggests that the states responsible for the pinning resulted from interaction between the adatoms and the semiconductor. Support for formation of defect levels in the semiconductor at or near the surface is found in the appearance of semiconductor atoms in the metal and in disorder in the valence band with a few percent of oxygen. Based on the available information on Fermi energy pinning, a model is developed for each semiconductor with two different electronic levels which are produced by removal of anions or cations from their normal positions in the surface region of the semiconductors. The pinning levels have the following locations, with respect to the VBM: GaAs, 0.7 and 0.5 eV; InP, 0.9 and 1.2 eV. The first energy given is associated

with a missing anion and the second with a missing cation. For GaSb, only an acceptor due to a missing Sb has been located at 0.1 eV. Our work is found to correlate well with that on practical Schottky barriers.

A detailed comparison is made with interface state positions and densities found by others on practical MIS structures, and it is suggested that the large density of these states on 3-5's as compared to Si is due to extrinsic interface states created by stoichiometric deficits of the 3-5 semiconductor. For GaAs, the dominant state is found at 0.7 eV and is associated with an As deficit. For InP, the major interface level is about 0.1 eV below the CBM. These positions are in good agreement with the existing data obtained from a wide variety of samples.

I. INTRODUCTION

At the 1976 Physics of Compound Semiconductor Interface (PCSI) Meeting, all experimental groups reported[1,2,3] agreed that, on the (110) faces of GaAs (and other smaller band-gap 3-5 semiconductors), there were no intrinsic[4] surface states in the band gaps. Since the classic work by Mead et al[5] was also done on cleavage (110) faces of these semiconductors, this had strong implications for Schottky-barrier formation. From LEED[6] and bonding considerations,[7] it appeared likely that the surface states were moved out of the band-gap region by electronic and lattice rearrangement at the surface. Work since then has firmly established that this is the case.[8,9] Figure 1 schematically shows the rearrangement and the electronic structure.[10] The lack of intrinsic states in the band gap had immense implications for the understanding of Schottky barriers (SB) since it established that the free surface contained no intrinsic surface states which could pin the Fermi level at the metal-semiconductor in the manner suggested by Bardeen[11] and applied by Mead et al.[5]

This left quantum mechanical interaction between metal and semiconductor as the most popular mechanism of Schottky-barrier pinning. Heine[12] had first pointed out such a possibility and had emphasized the tunneling of electrons from the metal into the band gap of the semiconductor. In the period of approximately 1976 to 1978, there have been a number of theoretical papers exploring in a more quantitative manner this possibility as well as looking into related many-body effects.[13] These papers had one aspect in common: they assumed an ideal planar junction between the semiconductor and metal. Recent experimental work strongly suggests that the situation is not so simple.[14,15,16]

In this paper, we will propose a detailed and unified model not only for Schottky-barrier pinning but for the interface states at the semiconductor-insulator interface of MIS (metal-insulator semiconductor) structures.[17] This is an extension of our work as reported by Lindau et al[15] at last year's PCSI. Our general approach has been to (1) develop experiments in which the interaction between the adatoms (metal or oxygen) can be followed on an atomic scale, particularly in the early stages of Fermi-level pinning, i.e., very low (small fractions of a monolayer) coverages, (2) systematically study the Fermi level pinning at both semiconductor-metal and semiconductor-oxide interfaces on both n- and p-doped semiconductors, and (3) compare results from thick device-type overlayers and those from the atomic scale studies. Thus, in this paper, we will draw extensively on data from our own studies of the first steps in oxygen adsorption[3,10,18,19,20] on GaAs, InP, and GaSb as well as on our work on Schottky-barrier formation.[14,15] In addition, we will draw on work of others[21-27] on thicker "device"-type oxides.

II. DO INTRINSIC STATES MOVE INTO THE BAND GAP?

As emphasized in the introduction, it became clear between 1976 and 1978 that, on the (110) face of GaAs and smaller band gap 3-5 compounds, the intrinsic surface states were swept out of the band gap due to the rearrangement of the atoms near the surface. At once, we became concerned that the pinning we and others[28,29] had seen consistently on clean cleaved (110) n-type GaAs might be due to intrinsic surface states brought into the band gap by a new and different reconstruction of the surface.[2]

Starting in 1976,[3] we have continuously attempted to test the hypothesis that intrinsic surface states might move into the band gap due to new surface rearrangements. We will briefly review that work since the negative results obtained played an important role in developing the model of interface states which will be presented here.

First, it was recognized by ourselves and Peter Mark that all of the LEED work had been done on sputter-annealed (110) GaAs surfaces and that such clean surfaces always showed Fermi level pinning near mid-gap for n-type samples. In contrast, no LEED had been done on cleaved surfaces and these were the only surfaces which showed[1,2,3] no surface Fermi level pinning (i.e., cleaved surfaces sometimes showed no pinning, whereas sputter-anneal surfaces always showed pinning. Thus, LEED work was done on a number of cleaved GaAs (110) surfaces and compared to the sputter and annealed work.[30,31] No measurable difference was found, establishing that the same surface rearrangements did take place on both types of surfaces. This and related work was reviewed by Skeath et al in last year's PCSI.[30]

The overall conclusion is that the pinning which is often observed on clean cleaved n-GaAs (110) is due to extrinsic states produced by defects formed in the cleaving process. Any comprehensive model for extrinsic states must satisfactorily explain these states.

Monch[32] has pointed out that bulk doping impurities may produce extrinsic states at the surface; however, the density of these is not, in general, suificient to explain the observed pinning; thus, defect states must be invoked, in addition. However, the bulk doping can reduce the number of defects needed.

Another more general method for studying the empty surface states is the constant final state (CFS) or partial yield spectroscopy developed by Lapeyre[33] and Kunz[34] and their coworkers and ingeniously applied to the surface state problem by Eastman and coworkers.[35] It is now clear that the original interpretation of such work[35] erred by not taking excitonic effects into account. However, in the studies we undertook, we were most interested not in the absolute energy of the final state involved in the transition but in decreases in this energy which would be associated with the empty intrinsic surface states moving[36] into the band gap to produce the observed surface Fermi level pinning. This movement, since it should be an electron volt or more, would produce an easily detected decrease in the excitation energy for the exciton. Since these studies have been reported in detail elsewhere, we will restrict ourselves here to giving examples and discussing the results and appropriate references.

A first question (also addressed above) was whether the pinning sometimes observed on n-type cleaved samples was due to intrinsic surface states moving into the band gap region. Our CFS measurements showed no difference in excitation energy for the exciton on pinned surfaces and unpinned surfaces.[3,37] This is taken as definitive evidence that the pinning which occurs on cleaving is due to extrinsic and not intrinsic surface states. As an example of this type of data, Fig. 2 compares spectra taken from cleavage surfaces which did and did not show pinning.[3,37]

The same test was made with regard to pinning due to placing of oxygen or metals on the surface. As the oxygen or metal is added in small quantities to a clean surface which shows no pinning, both the excitonic structure in the CFS spectra and the Fermi level pinning are followed as a function of coverage of the foreign atom.[38] Examples are given in Fig.

2 for oxygen addition. The paper by Skeath et al[39] in these proceedings gives an example for metals as does the work of Chye et al.[14] Again, no evidence is found for reduction of the exciton energy[3,18,19] as the overlayer is added, showing that the empty intrinsic surface states are not moving into the band gap. These data will be discussed in detail later in this article. Thus, we conclude that the pinning observed after deposition of metals or oxygen is not due to movement of the intrinsic states characteristic of the free surface into the band gap because of surface rearrangement produced by the addition of oxygen or metals to the surface. Mele and Joannopoulos[40] have proposed new interface states in the band gap due to Al on GaAs. It appears that, to detect these, one must look at the CFS structure using excitation from the Al core levels.

III. A MECHANISM FOR FERMI LEVEL PINNING BY METAL OR OXYGEN DEPOSITION

A. General Approach

Using photoemission, the Fermi level position at the surface can be measured directly.[39] It is important to make a clear distinction between such measurements and those (see, for example, Ref. 41) in which Fermi level is not measured directly, i.e., when methods such as contact potential (CPD) measurements are used.[41] In the latter case, the changes in the potential barrier at the surface must be successfully separated from those of band bending. On addition of any adatoms to the surface of a semiconductor, both the Fermi level position and the semiconductor electron affinity will, in general, change.[42] It is the sum of these two effects which are measured by CPD measurements. As the comments after Ref. 41 indicate, these are not always simple to sort out and serious

errors can be made in estimating the change in Fermi level at the surface. In contrast, the photoemission measurement, as mentioned above, obtains the Fermi level position directly. This is illustrated in more detail by Skeath et al.[39]

B. Fermi Level Pinning Versus Metal Coverage

Our general approach in this work has been to deposit metal in rather small increments and to determine the change of surface Fermi level position with coverage. Detailed data are present in these proceedings (Ref. 39), in last year's proceedings (Ref. 15), and elsewhere (Refs. 14 and 43). An example is given in Fig. 3a.[15] As can be seen, the change in Fermi level pinning due to the metal is essentially completed at only about 0.1 of a monolayer coverage. Detailed studies of the 5d bands of Au have indicated that the Au atoms are dispersed across the surface and essentially atomic in nature.[14,43] This is also the case for Cs. Thus, the pinning takes place before a metallic layer is formed. This brings into question those theoretical calculations that start from the model of a metal on a semiconductor.

C. Similarity of Fermi Level Pinning for Oxygen and Metals

It is interesting to note that there is surprisingly little difference (~0.3 eV on GaAs, less on GaSb) in the pinning position[14] for Cs and Au despite the very large difference in the nature of the outermost valence wave functions of the atoms of these two metals. Even more striking is the similarity of the Fermi level pinning position due to oxygen and the metals. In Fig. 3b, we present Fermi level position

due to oxygen on GaSb. As can be seen, the final Fermi level pinning position is almost identical to that of the metals and the pinning is completed at a small fraction[44] of a monolayer.[45] Similar results have been obtained on GaAs and InP.[3,18,19,44,51,52,53,64,65]

In Fig. 4, we present our data on the pinning position for a number of metals and oxygen on GaAs, InP, and GaSb. This figure has two striking characteristics. First, the oxygen pinning position falls within the scatter of surface Fermi level positions from the metals. Second, the pinning positions for each semiconductor fall in a distinct and separate part of the band gap: InP in the upper part of the gap, GaAs near mid-gap, and GaSb near the valence band maximum.

D. Are Pinning Levels Produced Indirectly by Adatoms?

Why would both metals and oxygen produce levels at approximately the same energy? It is very difficult, if not impossible, to rationalize this in terms of energy levels produced directly by the adatoms. This statement is based on the gross differences in atomic energy levels (as well as chemistry) between the various adatoms. On the other hand, if the pinning states are produced indirectly, for example, by the formation of vacancies or other defects, the energy levels of these defects would not necessarily depend on the details of the adatoms. Thus, it is attractive to think of the pinning produced by the adatoms as being due to defects produced at or near the surface of the semiconductor due to the deposition of the adatoms. These defects must then be created by the interaction of the adatoms with the semiconductor surface.

Such a suggestion raises at least two new questions: (1) Is there any experimental information suggesting the formation of such

defects and (2) where does the activation energy come from to form such defects? Last year,[15] we made some suggestions in this regard. In this paper, we will refine and generalize those original suggestions. In addition, we will make use of data in the literature which relate to interface states on thick-device-type oxides in order to test our suggestions. However, first, we will present a model of the interface states produced at the interface of InP, GaAs, and GaSb by metal deposition or oxygen exposure.

IV. THE MODEL FOR INTERFACE STATES FORMED BY ADATOMS

In Fig. 5, we present models for the interface states formed near the surface of GaAs, InP, and GaSb by addition of oxygen or metals to the surface. For each material, two levels are given and three quantities are associated with each of these levels: (1) the energy level (measured with respect to the valence band maximum (VBM)), (2) whether the defect is an acceptor or donor,[46] (3) a suggestion as to the nature of the defect. However, it is important to emphasize that the essence of the model is that pinning is dominated by defect levels formed due to the addition of metals or oxygen to the surface. As Fig. 4 shows and as will be shown when we examine practical oxides, the general systematics of pinning positions is in agreement with the specific energy levels in Fig. 5, i.e., the pinning levels lie in the upper part of the band gap for InP, near mid-gap for GaAs, and near the VBM for GaSb.

Two levels were used in Fig. 4, as this is the smallest number which can begin to give agreement with a large number of different experiments. However, once one starts creating defect levels, it should be recognized

that a large number of different defect combinations are possible (e.g., vacancies, anti-site defects, and various combinations of vacancies, etc.).[47] Therefore, the exact energy positions are, in general, not to be taken too seriously within a tenth of an electron volt. However, as emphasized above, the energy position within these limits is to be taken quite seriously.

Also indicated on Fig. 5 is the acceptor or donor nature of the defect. This has been deduced by the dependence of the pinning on doping type of the material. For example, there was a long experience of no pinning on cleaved p-type GaAs but pinning at 0.7 eV for n-type samples. This indicates an acceptor at 0.7 eV. Similarly, the pinning of n-type GaSb near the VBM (see Fig. 3) must be due to an acceptor level.

The experimental and theoretical data on bulk defect levels do not seem to be definitive enough to act as a strong guide to the nature of the defect. Thus, we will take a simple model and assume that donors are formed by anion (column 5) atoms in cation (column 3) sites and acceptors are due to the inverse situation with cation atoms in anion sites. These models should be considered as tentative.

As can be seen from the experimental results presented above (and that which will be presented below), one type of defect is often predominant in a given material after a specific treatment, e.g., the 0.7 eV level in GaAs after cleaving and the 0.1 eV level in GaSb after adsorption of oxygen or deposition of a metal. The pinning of the as-cleaved n-type material at 0.7 eV together with the lack of pinning on p-type GaAs give clear evidence of dominance of the 0.7 eV acceptor level for this surface. Figure 3 gives strong evidence for the dominance of the 0.1 acceptor level in GaSb. A similar level has long been associated with a deficit of Sb

which occurs in GaSb.[48] The nature of the second defect in GaAs and GaSb is tentatively assigned by the author's liking for symmetry and order. In GaSb, the Sb defect appears to dominate; pinning toward mid-gap only appears after several molecular layers of oxide have been grown. This casts some doubt on the second level for GaSb, as it may be associated with the oxide rather than interface. Thus, it is accompanied by a question mark in Fig. 6.

The second (0.5 donor) level in GaAs is deduced by the systematic difference in pinning position due to Al, Ga, and In on n- and p-type GaAs found by Skeath et al[39] and by a similar difference reported earlier for the pinning of n and p GaAs after the addition of a fraction of a monolayer of oxygen.[49] The energy levels on InP were deduced from studies of Chye et al[19,43,44] of the Fermi level position as a function of oxygen or metal coverage. In Fig. 6, we present data for InP exposed to oxygen. Again, we see that, at the larger oxygen exposures, the curves for n- and p-type material are parallel with the p curve displaced lower in energy by about 0.2 eV. This suggests, again, the presence of two states. Using both the oxygen and Schottky-barrier data, the levels are assigned as 1.2 and 0.9 eV. At least two factors suggest that the upper level is a donor. These are the facts that the p-type material rises above 0.9 eV for the highest oxygen exposure and that the Fermi level of the n-type material dips to about 1.0 eV at intermediate coverages before rising to 1.1 eV. Both of these results can only be explained if the donor is placed above the acceptor to make compensation possible. However, these should only be considered tentative conclusions. Using our detailed assignment of donors and acceptors discussed elsewhere, we assign the upper level to P in an In site and the lower to an In in a P site.

Williams,[50] on the other hand, would associate the upper level with a missing P based on his results. An open mind must be kept until more definitive data are available.

To summarize, the position of the levels in Fig. 5 is to be taken seriously within 0.1 eV. Under a given set of circumstances, one level may be dominant. The assignments in terms of acceptor or donor and the detailed nature of the defect level should be considered tentative and subject to much future examination.

V. INDIRECT EVIDENCE FOR LATTICE DEFECT FORMATION

A. During Oxygen Uptake

We were driven to the suggestion of defect formation by evidence we obtained (making full use of the capabilities of synchrotron radiation[3]) of disruption of the surfaces by oxygen or metal adlayers. In Fig. 7, we present energy distribution curves (EDC's) obtained from photoemission studies of the valence electronic states associated within the last few layers of GaAs at the surface[10,18,51,52] as a function of oxygen exposure. Note that there is a rather abrupt transition in the valence band for exposures of 10^6 to 10^7 L of oxygen (a few percent of a monolayer adsorbed oxygen). For exposures below 10^6 L, the sharp valence band structure is relatively unchanged. The transition to the disordered state is relatively abrupt for a given sample, but the point of transition varies by about an order of magnitude from sample to sample. This transition would make the formation of defects possible. It roughly corresponds to the coverage at which the pinning is completed.

The abrupt loss of surface valence band structure suggests strongly that the periodic structure at that surface is highly disturbed by the oxygen adsorption. In the introduction (see Fig. 1), we showed that the free surface is highly rearranged (i.e., distorted in a periodic way) from the bulk and emphasized that there was considerable strain between the surface and bulk of the crystal. Such strain might be relieved by defect formation. In Ref. 10, we discuss the fact that chemisorption of an oxygen atom will cause considerable local lattice rearrangement (driven by the electronic rearrangement) and increased local strain as well as producing local heating due to the heat of adsorption. Apparently, these effects are sufficient to cause a certain amount of lattice disorder to set in at a few percent of a monolayer of oxygen coverage (remember that, on the average, oxygens can be located only 5 or 10 lattice sites apart at this coverage). The oxygen uptake increases markedly at this point, and the Fermi level tends to stabilize its pinning position.[18,52,53] Thus, we have a process in which it is likely that defects will be formed.

In cases where thick oxides are formed, one probably first goes through this stage. In addition, because of the difference in the oxygen chemistry of Ga and As, it is highly likely that these materials will not be removed in exactly stoichiometric quantities from the interface. The complexity of this chemistry is well established.[18,51,53,54] Thus, conditions at the interface between the oxide or chemisorbed oxygen seems very favorable for formation of defects due to local removal of Ga or As atoms.

B. During Schottky-Barrier Formation

Making use of both synchrotron radiation[3,14,43] and sputter Auger techniques, we have consistently found sizable amounts of semiconductor material in the metal of the Schottky barriers. Figure 8 gives EDC's taken at SSRL with $h\nu = 120$ eV so that both the core levels of the semiconductor constituents as well as the valence levels and core levels of the gold could be followed.

The striking thing about Fig. 8 is that the Sb cores persist strongly even after about 110 monolayers of Au have been added. In contrast, no detectable Ga is found near the surface at this coverage. (It should be emphasized that the sampling depth in these experiments is about two atomic layers.) These experiments show clearly that Sb is removed from the semiconductor by the addition of the metal. (If pin holes in the metal were present, both the Ga and Sb core levels should have shown through with equal strength.) Confirmation of the movement of the semiconductor material into the metal is given by sputter-Auger[3,43] studies.

Closer examination of Fig. 8 shows that the Ga does not disappear as quickly with addition of Au as one would expect (taking the short sampling depth into account). The sputter-Auger also indicates Ga in the Au well away from the surface for a Au layer several hundred angstroms thick. The fact that Sb is found on the surface of thick layers can be understood in terms of minimizing surface energy (Sb has a much lower heat of evaporation than Au or Ga) and the kinetics which removed the 3-5 material into the semiconductor originally.

For GaAs and InP, both species are also moved into the metal.[3,14,43] Both species appear on the surface, although there appears to be slightly more As or P.

As was suggested last year,[3] we believe the driving force for dissolution of the 3-5 and its movement into the metal is the heat of absorption of the metal on the surface of the semiconductor. The heat of absorption or condensation has been habitually overlooked in considering such problems as this. It is the heat of bonding of the metal to the free semiconductor surface. It is not to be directly compared to any bulk compound formation; it is also much larger than the kinetic energy associated with the metal atom after evaporation. In general, data are only available for the metallic heat of condensation of metals on themselves. These numbers can be high (~87 Kcal/mole for Au). The heat of condensation of Cs on itself is smaller (~20 Kcal/mole); however, very beautiful measurements have been made by Derrien and Arnaud D'Avitoya[55] of the heat of condensation of Cs on GaAs; these give about 60 Kcal/mole at low coverages. Thus, on being absorbed on the semiconductor surface, the metal gives up energy comparable to or considerably larger than the heat of formation of the semiconductor.[3] This energy must be dissipated and, in so doing, will momentarily excite the semiconductor atoms near it. If a few atoms of the semiconductor are moved into the metal for each hundred metal atoms bound to the surface, this can account for the local departure from stoichiometry and resulting defect states which produce Schottky-barrier pinning.

This process is depicted in a pictorial way in Fig. 9. Note that, in that diagram, the defect levels are usually placed at least one lattice site beneath the surface. This is because a metal atom could

fill a vacancy at the surface (although not a simple anti-site defect). Again, we can not be sure of the nature of the defect, at this time, and thus must allow for various possibilities.

To summarize, experiment evidence for both oxygen uptake and Schottky-barrier formation on the clean semiconductor surface shows that the conditions are present for the formation of defect centers at or near the surface of the semiconductor. The similarity of the Fermi level pinning positions for very different metals and/or oxygen suggest strongly that such centers are formed and produce the Schottky-barrier pinning and interface states at the 3-5 oxide interface.

VI. COMPARISON WITH THICK "DEVICE" OXIDES OR SCHOTTKY BARRIERS

A. Schottky Barriers

The pinning positions we obtain are, to a first approximation (within a few tenths of an electron volt), in agreement with both the work obtained by Mead[5] (who used clean surfaces but very high metal deposition rates) and, for practical devices in which the sample, because of etching and transport through air, has at least a thin oxide outer layer. To put the results more emphatically, the pinning position we obtain with only 10 to 20 percent of a monolayer of metal is, to the first approximation, the same as that obtained for thick (thousands of monolayers of metal) Schottky barriers. Thus, it appears that the same basic pinning mechanism must occur in all cases.

The classical work on Schottky barriers by Mead et al[5] was performed in a slightly different manner than our own work.[14,43,44] The pressure in our preparation chamber was about four orders of magnitude

lower than that in Mead's chamber. As a result, we were able to make very "gentle" depositions (e.g., depositions in steps of 0.1 monolayer),[40,43,44] minimizing the chances of heating the crystal or creating a large density of defects (which may interact) in a short period of time. However, the general results of our work and those of Mead et al[5] as to pinning position are, on the average, quite close. The main difference[40] is that, after detailed studies of Al, Ga, and In on GaAs,[56,57,58] the pinning position on n-type material is found to be about 0.25 eV higher than on p-type material. This difference between the previous work and ours may be due to the details of deposition with the result that the defect levels formed are not the same. However, more work must be done to clarify this question.[59]

In the past, it has been hard to understand why the Schottky-barrier pinning positions were so similar for metal on atomically clean GaAs and on practical surfaces where the semiconductor was usually covered by at least a few layers of oxide. The present work resolves this question in showing that the oxide pinning position is approximately the same as that of the metal.

There is an interesting sidelight to the work presented here. Garner et al[60,61] have studied the effect of the chemical composition of the oxide present on the forward characteristics of Au Schottky barriers formed on n-type GaAs. His results indicate that the Schottky barrier is greatly reduced if an As oxide is present.[62] This is consistent with the pinning of n-type GaAs being due to an acceptor near 0.7 eV, resulting from a deficit of As. The As oxides are notoriously unstable, and free As may be produced by the thick Au deposition. Some free As might, in turn, be available for incorporation in the GaAs surface region,

reducing the pinning states to such a degree that the Schottky-barrier height is strongly reduced. The fact that excess As tends to remove the pinning but Ga does not must relate to the detailed hopping probability or other details of defect formation or reduction at room temperature.

To summarize, the model proposed here explains, to first order, a wide range of phenomena extending from Schottky-barrier pinning produced by a small fraction of a monolayer of metal to that obtained on a practical semiconductor surface with a region containing a few layers of oxides after a thick metallic deposition. This lends credance to the underlying physical model; however, much more work must be done to definitively establish this model and fill in all of the details which are now missing.

B. Correlation with Practical "Device" Oxides

One of the most fascinating aspects of this work has been the correlation of our fundamental studies of oxygen chemisorption and oxidation with the data on interface states obtained from "device-like" thick oxides intended for MOS (metal oxide semiconductor) as well as other device applications. Whereas, Schottky barriers on 3-5's have been used practically for many decades, the practical native oxide on 3-5's is a new development which has not yet reached the production stage. Thus, a recent object of our work has been to compare our results for oxygen adsorption in relatively small quantities on the clean, cleaved (110) surfaces with the work from MIS-type structures where the device qualities were sufficiently good so that a measure could be made of the interface state density. In Table I, we present a comparison of our data for the "saturated" pinning position obtained after the addition of a

few tenths of a monolayer or more of oxygen to the surface[3,5,6,44,53,63,64] to the zero bias or Fermi level pinning position for the "practical MIS devices."[21] Typical data of this showing the surface pinning position versus exposure for a clean surface is given in Fig. 10 for n-type GaAs.

In order to gain perspective, Fig. 10 also contains similar data on n-type Si (111). Whereas, the oxygen removes the surface states and pinning from the Si,[63] the situation is the opposite for GaAs (110).[3,18,53] For GaAs, one goes from an unpinned to a pinned situation, indicating creation of states in the gap by the oxygen adsorption. As outlined in Section II, this is not due to the movement of the intrinsic surface states back into the band gap, but must be due to the formation of extrinsic states in the gap. As Section III indicates, the levels do not appear to be associated with the oxygen, but to a level produced indirectly.

In Table I, the "thick practical" data was obtained from Ref. 20; Wieder and his coworkers[65] have recent indications of strong interface states at about 1.1 and 1.3 eV, in reasonable correlation with the pinning positions we obtain with a fraction of a monolayer of oxygen. Note that the spread of pinning position for either GaAs or InP is less than the systematic difference in pinning positions in the band gap between the two materials. Also given in Table I are Schottky-barrier pinning positions for a large range of metals on the clean, cleaved (110) faces of InP and GaAs (GaSb is not included in Table I since we could not find data for "device-type" oxides) to, once again, emphasize the similarity between the oxide and Schottky-barrier results.

In Fig. 11, we present plots of interface states density for a thick "device" oxide from the work of Koshiga and Sugano.[22] It is clear

that a state near 0.7 eV is playing a dominant role. Measurements of interface density above 0.7 eV have been difficult because of frequency effects. However, it is now clear that, because of the strength of the level near 0.7 eV, it is impossible to make[23,24,25,66] direct interface state density measurements much above 0.7 eV.

This is in contrast to the situation on InP where interface state density measurements can be made through most of the band gap. As mentioned earlier, there is evidence for interface states about 0.1 and 0.3 eV below the conduction band minimum;[65] however, these seem to be smaller in density than for GaAs since inversion can be achieved in InP but not GaAs.[65] In general, Wieder and his coworkers find the density of interface states in InP to be an order of magnitude less than in GaAs.[65]

Convincing evidence is not found in the work of Hasegama et al[23,66] or Koshiga and Sugano[22] of a peak in the density of interface states near 0.5 eV (there may be some suggestion of such a peak in Koshiga and Sugano's[22] unannealed sample). However, Meiners has obtained evidence of pinning in this region.[26,27] Thus, it appears that the treatments used to provide insulating layers on GaAs definitely tend to suppress the 0.5 eV level (which we tentatively associate with missing Ga) and enhance the 0.7 eV level which we associate with missing As.

In Fig. 12, we present a proposed density of semiconductor-oxide interface states for GaAs, InP, and GaSb. For the sake of comparison, Si is also included. These density of states are not to be taken seriously in detail; rather, one should concentrate on their general features.

Note that the density of interface states for Si is generally "U" shaped. (These states are usually associated with the strains due

to the lattice mismatch between the semiconductor and oxide.) For the 3-5's, we superimpose on these "U"-shaped background broad peaks. These are associated with the deficit centers proposed earlier due to missing anions or cations. It should be amphasized that the absolute values of these peaks depend on the method of providing the insulating layer. For example, the state near 0.7 eV in GaAs (associated with missing As) is clearly dominant in the "practical" samples mentioned here;[21-27,66] whereas, clear evidence of a level near 0.5 eV is only found in one study.[26,27] Thus, it appears that it is fairly easy to suppress the 0.5 eV level (associated with a Ga deficit) in preparing an MOS structure on GaAs, but that the level at 0.7 eV associated with a deficit of As is universally strong in the data studied to date.

A similar situation appears to occur for InP in which the level near 1.2 eV (tentatively associated by us with an In deficit) dominates. We found no MOS data for GaSb; however, in our own data, the 0.1 eV level (associated with missing Sb) clearly dominates at low oxygen coverages; however, there is an indication of a level near 0.3 eV at thicker coverages. This is also indicated in Fig. 12 and associated with a missing Ga; however, the lack of certainty is indicated by the question mark.

VII. SUMMARY AND CONCLUSIONS

Despite the fact that Schottky diodes have been of practical importance for over four decades, the mechanism for the Fermi level pinning which determines the height of the rectifying barrier has not been definitively determined. In this paper and that by Skeath et al,[39] as well as in the papers by Lindau et al[15] and Chye et al,[14] the previous

suggestions have been examined and rejected. Further, we have put forth a new model based on pinning by defect states. The defect formation is caused by the energy released when the metal atom is chemisorbed on the surface (see Fig. 9). One point of support for the model is the appearance of one or more constituents of the semiconductor in the metal (see Fig. 8).

Another critical result is that the pinning position for metals and oxygen is essentially identical. Based on the difference in the electronic configuration for oxygen and metals (as well as the difference in the metals themselves which extend from Cs to Au), it is suggested that this is only consistent with defects being produced indirectly by either oxygen or metal adsorption. Studies of the valence band structure at the surface (see Fig. 7) as a function of oxygen adsorption lend support to this.

Using our experimental data, we propose a general model shown in Fig. 5. In that model, which is the simplest one that is consistent with the available data, two energy levels are present in the band gap; one due to a missing anion is an acceptor, and the other, which is due to a missing cation, is a donor. A simple suggestion for the defects is that they are anti-site defects. In the case of the acceptor for GaSb, however, there is evidence that it arises from a more complex center such as Ga on an Sb site associated with a Ga vacancy.[48] It is clear that a major effort must be made both theoretically and experimentally to identify and understand these defects at or near the surface. Any possible interactions between the metallic wave functions and the defect levels also need investigation. One would think that the understanding of defects in the bulk of 3-5's could be drawn upon: however, it appears that

the electronic levels associated with bulk defects are not well enough understood to make such correlations. Clearly, the understanding of defects at the surface and in the bulk is an area where much more work is needed. Theory and such experiments such as spin resonance studies seem especially appropriate.

McCaldin et al[67] have noted that the Fermi level pinning position on p-type samples is determined principally by the anion. This is consistent with our model since a surface donor (needed to pin a p-type sample) is produced by removing a cation and/or placing a anion on a cation site, thus forming a center only containing anions. Thus, the pinning will be expected to be determined by the anion. GaSb is a special case, as it seems that Sb is preferentially removed, leaving many more acceptor states which lie below any donor states; thus, there is strong pinning on n-type GaSb but not on p-type material, in agreement with the findings of McCaldin et al[67] of a zero barrier on p-type GaSb.

Since our model by its very nature applies to semiconductor oxide interfaces as well as Schottky barriers, the detailed reasons for the difficulties in passivating the 3-5 as compared to Si become more apparent. In addition, we find that the peaks in the density of interface states in MIS devices correspond rather well with the states we have identified in our fundamental studies. Our models for the interface states are presented in Figs. 5 and 12. For GaAs, a state near mid-gap which we associate with an As deficit is found to dominate; whereas, for InP, the dominant state is near the conduction band minimum.

To conclude, there is evidence indicating that Schottky-barrier pinning on 3-5's as well as the interface states at 3-5 oxide interfaces are due to energy levels produced by defects formed by putting down the metal

or oxygen on the semiconductor. However, much more work must be done to tie down the detailed nature of these defects as well as to test and quantify the model.

An important aspect of this model is that it suggests ways by which both the Schottky-barrier height and the interface state density at the oxide interface may be changed, e.g., by treating the sample to reduce or otherwise modify the interface state density. The work of Garner et al possibly gives some evidence of this.[60,61]

It should be noted that we have compared Fermi level pinning and interface states on different crystal faces. The fact that agreement is found under such procedures gives further evidence that the states involved are defect states which are not strongly affected by the crystal face. This gives further evidence that the pinning defects probably lie just below the surface and are due to crystal defects. Heime's[68] review of deep "accidental" defects in bulk GaAs shows a broad peak about 0.7 eV. Thus, there may be a close connection to the pinning defects created near the surface by adlayers and defects in the bulk of the semiconductor.

REFERENCES

1. J. van Laar and J. J. Scheer, Surf. Sci. 8, 342 (1967); J. van Laar and A. Huijser, J. Vac. Sci. Technol. 13, 769 (1976).
2. W. Gudat and D. E. Eastman, J. Vac. Sci. Technol. 13, 831 (1976).
3. W. E. Spicer, I. Lindau, P. E. Gregory, C. M. Garner, P. Pianetta, and P. Chye, J. Vac. Sci. Technol. 13, 780 (1976).
4. In this article, we will use this terminology; by intrinsic surface states, we mean surface states characteristic of the "ideal" rearranged surface. The density of these intrinsic surface states should correspond to the total density of surface atoms. The term "extrinsic surface state" will be used for surface states induced by surface defects or impurities. The density of these states will normally correspond to the density of surface defects, imperfections, and impurities.
5. C. A. Mead and W. G. Spitzer, Phys. Rev. 134, A713 (1964); S. Kurten, T. C. McGill, and C. A. Mead, Phys. Rev. Lett. 22, 1433 (1969).
6. C. B. Duke, A. Lubinsky, B. W. Lee, and P. Mark, J. Vac. Sci. Technol. 13, 761 (1976); P. Mark, G. Cisneros, M. Bonn, A. Kahn, C. B. Duke, G. Patton, and A. R. Lubinsky, J. Vac. Sci. Technol. 14, 883 (1977); C. B. Duke, J. Vac. Sci. Technol. 14, 870 (1977).
7. A. U. MacRae and G. W. Gobeli, in Semiconductors and Semimetals, Vol. 2 of Physics of 3-5 Compounds (R. K. Willardson and A. C. Beer, eds.), Academic Press, New York, 1966, pp. 115-137; W. A. Harrison, Surf. Sci. 55, 1 (1976).
8. A. Kahn, E. So, P. Mark, C. B. Duke, and R. J. Meyer, J. Vac. Sci. Technol. 15, 1223 (1978); B. J. Mrstik, S. Y. Tong, and M. A. Van

Hove, these proceedings; C. B. Duke, R. J. Meyer, A. Kahn, E. So, and P. Mark, these proceedings.

9. D. J. Chadi, J. Vac. Sci. Technol. 15, 1244 (1978); A. Huijser, J. van Laar, and T. I. Van Rooy, Phys. Lett. 65A, 335 (1978); J. R. Chelikowsky, S. G. Louie, and M. L. Cohen, Phys. Rev. B 14, 4724 (1976).

10. W. E. Spicer, I. Lindau, J. N. Miller, D. T. Ling, P. Pianetta, P. W. Chye, and C. M. Garner, Physica Scripta 16, 388 (1977).

11. J. Bardeen, Phys. Rev. 71, 717 (1947).

12. V. Heine, Phys. Rev. 138, A1689 (1965).

13. J. C. Inkson, J. Phys. C5, 2599 (1972); C6, 1350 (1973); J. Vac. Sci. Technol. 11, 943 (1974); S. G. Louie, J. R. Chelikowsky, and M. L. Cohen, Phys. Rev. B15, 2154 (1977); J. M. Andrews and J. C. Phillips, Phys. Rev. Lett. 35, 56 (1975); C. Tejedor, F. Flores, and E. Louis, J. Phys. C10, 2163 (1977); E. J. Mele and J. D. Joannopoulos, J. Vac. Sci. Technol. 15, 1370 (1978); H. I. Zhang and M. Schlüter, J. Vac. Sci. Technol. 15, 1384 (1978); W. A. Goddard III and John J. Barton, J. Vac. Sci. Technol. 15, 1273 (1978).

14. P. W. Chye, I. Lindau, P. Pianetta, C. M. Garner, and W. E. Spicer, Phys. Rev. B17, 2682 (1978); P. W. Chye, I. Lindau, P. Pianetta, C. M. Garner, C. Y. Su, and W. E. Spicer, Phys. Rev. B18, 5545 (1978).

15. I. Lindau, P. W. Chye, C. M. Garner, P. Pianetta, C. Y. Su, and W. E. Spicer, J. Vac. Sci. Technol. 15, 1332 (1978).

16. L. J. Brillson, Phys. Rev. Lett. 40, 260 (1978); Phys. Rev. B18, 2431 (1978); J. Vac. Sci. Technol. 15, 1378 (1977).

17. Since, in all cases known to the authors, at least several monolayers of native oxide (i.e., oxide formed from the semiconductor material) occur on the semiconductor before a subsequent deposition of a second insulator film, interface states formed in conjunction with native oxide growth will be of universal importance. Thus, we will concentrate our attention on these states in this paper. However, if the native oxide is successfully removed before the new insulator is deposited, it is anticipated that the same general mechanism of interface state formation will occur due to the difficulty of chemically bonding the insulator to the semiconductor.

18. P. Pianetta, I. Lindau, P. E. Gregory, C. M. Garner, and W. E. Spicer, Surface Sci. 72, 298 (1978); P. Pianetta, I. Lindau, C. M. Garner, and W. E. Spicer, Phys. Rev. B18, 2792 (1978).

19. P. W. Chye, C. Y. Su, P. Skeath, I. Lindau, and W. E. Spicer (submitted for publication).

20. P. W. Chye, C. Y. Su, I. Lindau, P. Skeath, and W. E. Spicer, J. Vac. Sci. Technol. (these proceedings).

21. H. H. Wieder, Thin Solid Films (in press), and references therein.

22. Fusrko Koshiga and Takuo Sugano, Surface Sci. (in press).

23. H. Hasegawa, T. Sawada, and T. Sakai, Surface Sci. (in press).

24. A. Shimano, A. Moritani, and J. Nakai, Japan J. Appl. Phys. 15, 939 (1977).

25. C. R. Zeisse, L. J. Messick, and D. L. Lile, J. Vac. Sci. Technol. 14, 957 (1977).

26. L. G. Meiners, Appl. Phys. Lett. 33, 747 (1978).

27. H. H. Weider, L. G. Meiners, and D. L. Lile, private communication.

28. P. Gregory and W. E. Spicer, Phys. Rev. B12, 2370 (1975).

29. G. W. Gobeli and F. G. Allen, Phys. Rev. 137, A245 (1965); J. H. Dinan, L. K. Galbraith, and T. E. Fisher, Surface Sci. 26, 587 (1971); D. E. Eastman and J. L. Freeouf, Phys. Rev. Lett. 34, 1624 (1975).

30. P. Skeath, W. A. Saperstein, P. Pianetta, I. Lindau, and W. E. Spicer, J. Vac. Sci. Technol. 15, 1219 (1978).

31. P. Mark, P. Pianetta, I. Lindau, and W. E. Spicer, Surface Sci. 69, 735 (1977).

32. W. Monch and H. J. Clemens, these proceedings.

33. G. J. Lapeyre, R. J. Smith, J. Knapp, and J. Anderson, J. Physique Colloq. 39, C4-149 (1978).

34. W. Gudat and C. Kunz, Phys. Rev. Lett. 29, 169 (1972).

35. D. E. Eastman and J. L. Freeouf, Phys. Rev. Lett. 33, 1601 (1974).

36. The soft x-ray transitions studied by these methods involve formation of an exciton (see the paper by M. Altarelli, G. Bachelet, and R. Del Sole, these proceedings) during excitation from the filled Ga 3d core levels into the lowest available empty states. These final states will certainly be the empty surface states provided that they lie in or near the band gap. The problem is more difficult when the empty states lie above the CBM as appears to be the case for the rearranged GaAs (110). However, if any new surface reconstruction moves the surface states into the band gap, this will certainly produce an easily detected reduction in the photon energy necessary to excite the exciton. For metals and oxygen exposures, the surface Fermi level has moved by large amounts before the excitonic transition is removed by the adsorption.

37. I. Lindau, P. Pianetta, W. E. Spicer, and C. M. Garner, Proc. Seventh Intl. Vacuum Congress and the Third Intl. Conf. on Solid Surfaces, Vienna, Austria, 12-16 Sep 1977, p. 615 (R. W. Dobrozemsky, F. G. Rüdenauer, F. P. Viehböck, and A. Breth, eds.).

38. P. W. Chye, P. Pianetta, I. Lindau, and W. E. Spicer, J. Vac. Sci. Technol. 14, 917 (1977).

39. P. R. Skeath, C. Y. Su, P. W. Chye, I. Lindau, and W. E. Spicer, these proceedings.

40. E. J. Mele and J. D. Joannopoulos, these proceedings.

41. L. J. Brillson, Phys. Rev. Lett. 42, 397 (1979), and these proceedings; see also comments on Brillson's article in these proceedings.

42. For example, the maximum change of electron affinity found on putting Cs on GaAs is about 3.0 eV compared to a maximum change in Fermi level of about 0.7 eV. This is an extreme case, but it illustrates how large the change in electron affinity can be compared to the Fermi level motion at the surface.

43. P. R. Skeath, I. Lindau, P. Pianetta, P. W. Chye, C. Y. Su, and W. E. Spicer, to be published.

44. Patrick Chye, Ph.D. dissertation, Stanford University, 1978 (unpublished).

45. When several monolayers of oxide are grown on GaSb (see Refs. 18 and 44), the oxide position rises to near mid-gap. It is not yet clear whether this represents the oxide surface Fermi level or that at the oxide-semiconductor interface.

46. The usual definition is used for acceptors and donors, i.e., an acceptor is uncharged when containing no electron(s) and a donor is uncharged when it is filled with electron(s).

47. In addition, since the defects are near the surface (we will discuss their position with regard to the surface or interface in more detail later), some interaction with the tunneling wave functions of the metal atoms may also be important.

48. Y. J. Van der Meulen, J. Phys. Chem. Solids 28, 25 (1967).

49. See Fig. 8 of Ref. 3.

50. R. H. Williams, these proceedings.

51. W. E. Spicer, P. Pianetta, I. Lindau, and P. W. Chye, J. Vac. Sci. Technol. 14, 885 (1977).

52. I. Lindau, P. Pianetta, W. E. Spicer, P. E. Gregory, C. M. Garner, and P. W. Chye, J. Electron Spectrosc. and Related Phenomena 13, 155 (1978).

53. Piero Pianetta, Ph.D. dissertation, Stanford University, 1976 (unpublished).

54. C. C. Chang, P. H. Citrin, and B. Schwartz, J. Vac. Sci. Technol. 14, 943 (1977); G. P. Swartz, J. E. Griffiths, and B. Schwartz, these proceedings.

55. Jacques Derrien and Francois Arnaud D'Avitoya, Surface Sci. 65, 668 (1977).

56. It is particularly interesting that Al and In act so similar. Al displaces Ga in the first layer of GaAs (forming AlAs and Ga) where In does not. However, the pinning positions are very similar. This and much other information (Ref. 57) establishes that the displacement reaction of Al in GaAs does not play a key role in establishing the Schottky-barrier height as suggested by Brillson (Ref. 16).

57. See comments by T. McGill and W. E. Spicer after the paper (Ref. 16) presented by Brillson in these proceedings.

58. As can be seen from the data of Ref. 40, Ga may be different from In and Al in that it takes a large coverage to reach the final pinning point. However, more work must be done before this point is clear.

59. A second-order but important question is the difference in pinning position between Au and more electro-positive metals and Al and Cs.

60. C. M. Garner, J. Appl. Phys. (in press).

61. C. M. Garner, Ph.D. dissertation, Stanford University, 1978 (unpublished).

62. The Schottky-barrier characteristics become very "soft" and can not be fit by the ideal Schottky-barrier equations. This is probably due to a large amount of "patchiness" in the surface.

63. L. F. Wagner and W. E. Spicer, Phys. Rev. B 9, 1512 (1974).

64. W. E. Spicer, I. Lindau, P. Pianetta, P. W. Chye, and C. M. Garner, Thin Solid Films 56, 1 (1979); W. E. Spicer, P. W. Chye, C. M. Garner, I. Lindau, and P. Pianetta, Surface Sci. (in press).

65. H. H. Wieder, private communication.

66. H. Hasegawa and T. Sawada, these proceedings.

67. J. O. McCaldin, T. G. McGill, and C. A. Mead, Phys. Rev. Lett. 36, 56 (1976); J. Vac. Sci. Technol. 13, 802 (1976).

68. K. Heime, Proc. NATO Summer School, "Non-destructive Testing of Semiconductor Materials," Frescati, Italy, 1978 (J. Zemel, ed.) (in press).

Figure Captions

1. A schematic drawing of the lattice and electronic structure of the GaAs (110) face after rearrangement (relaxation). The As surface atoms have taken up a p^3 bonding arrangement (with two electrons in a $4s^2$ filled state), while the Ga has gone from the bulk sp^3 to a sp^2 arrangement. Since the p^3 bond angles are more acute than the bulk sp^3 bonds, the As moves outward; conversely, the Ga moves inward. The movements are large (large fractions of an angstrom). This rearrangement moves the filled and empty surface states out of the band gap. However, since the surface lattice is no longer lattice match to the bulk, there is strong strain at the surface.

2. Measurements of the exciton produced by optical excitation from the Ga 3d core level to the lowest lying intrinsic empty states at the surface. For sample LD1C, the Fermi level was not pinned at the surface; whereas, in sample MCPB, it was. As can be seen, the position of surface excitons are the same, independent of pinning. This establishes that the pinning is not due to intrinsic surface states. The upper curves in each panel indicate the change in the exciton as a function of oxygen exposure. By an exposure of 10^6 to 10^7 L (a few percent of a monolayer), the exciton is no longer seen. This is roughly the exposure at which the valence band disorders (as will be shown in Fig. 7).

3. Starting with a clean cleavage face (110) of an n-type GaSb crystal, Cs (panel a) or oxygen (panel b) is added as indicated on the abscissa. In both cases, the surface Fermi level position moves through the band gap and pins at about 0.1 eV above the VBM for submonolayer coverages. Similar motion of the surface Fermi level is seen in GaAs and InP with oxygen and metals. However, the final pinning positions are different.

4. A summary of the final surface Fermi level pinning positions obtained by experiments similar to those detailed in Fig. 3 for a wide variety of metals and oxygen on GaAs, InP, and GaSb. The positions are located no better than $\pm$0.1 eV. Note the striking differences in the surface Fermi level positions between the three semiconductors.

5. A model of extrinsic states produced near or at the surface by perturbing the surface through addition of metals or oxygen to the surface. Each level is tentatively associated with a deficit of a anion or cation; however, it is unlikely that the defect is a vacancy. More likely, it is an anti-site or more complicated defect.

6. The surface Fermi level position for n- and p-type InP as a function of oxygen exposure (and approximate coverage). The initial cleaved surfaces were pinned due to extrinsic defects; however, this appears to have no effect on the final pinning position. The last oxygen exposure (10^{12} L, then $+10^{7}$ L EO) was made with oxygen excited by turning on an ionization gauge (see Refs. 3 and 18).

7. Energy distribution curves (EDCs) from the valence states of GaAs within a few atomic layers of the surface as a function of oxygen exposure. Up to 10^6 L, the structure is relatively sharp and unchanged by the oxygen. Near 10^6 L, there is an abrupt loss of structure for $E > -5$ eV. This is associated with a partial disordering of the surface in which lattice defects may be formed.

8. EDCs taken as Au is very slowly (see Ref. 14) deposited on GaAs. $h\nu = 120$ eV so that one can clearly see the Sb 4d and Ga 3d core levels as well as the Au 5d valence levels. The sampling depth is about two layers. Note that, even after many layers of Au have been applied, the Sb 4d signal is relatively strong but there is no Ga signal. This establishes the movement of Sb from the semiconductor to the surface. Both anions and cations are seen to move to the metal surface when GaAs and InP are studied in the same manner.

9. Schematic of suggested defect mechanism due to deposition of metal atoms on clean 3-5 surfaces. This process (i.e., a defect must be formed) needs occur only about once for every hundred metal atoms striking the surface in order to explain the Fermi level pinning.

10. The movement of the surface Fermi level in n-type cleaved Si and GaAs. The clean Si is pinned by intrinsic surface states which are removed by approximately a monolayer of oxygen and the band bending disappears. In contrast, the clean GaAs (110) is originally unpinned but becomes pinned with the addition of a small amount of oxygen.

11. Interface states from a thick MOS layer formed and measured by Koshiga and Sugano (Ref. 22).

12. Model of interface states for GaAs, InP, and GaSb MIS Structures based on the present work.

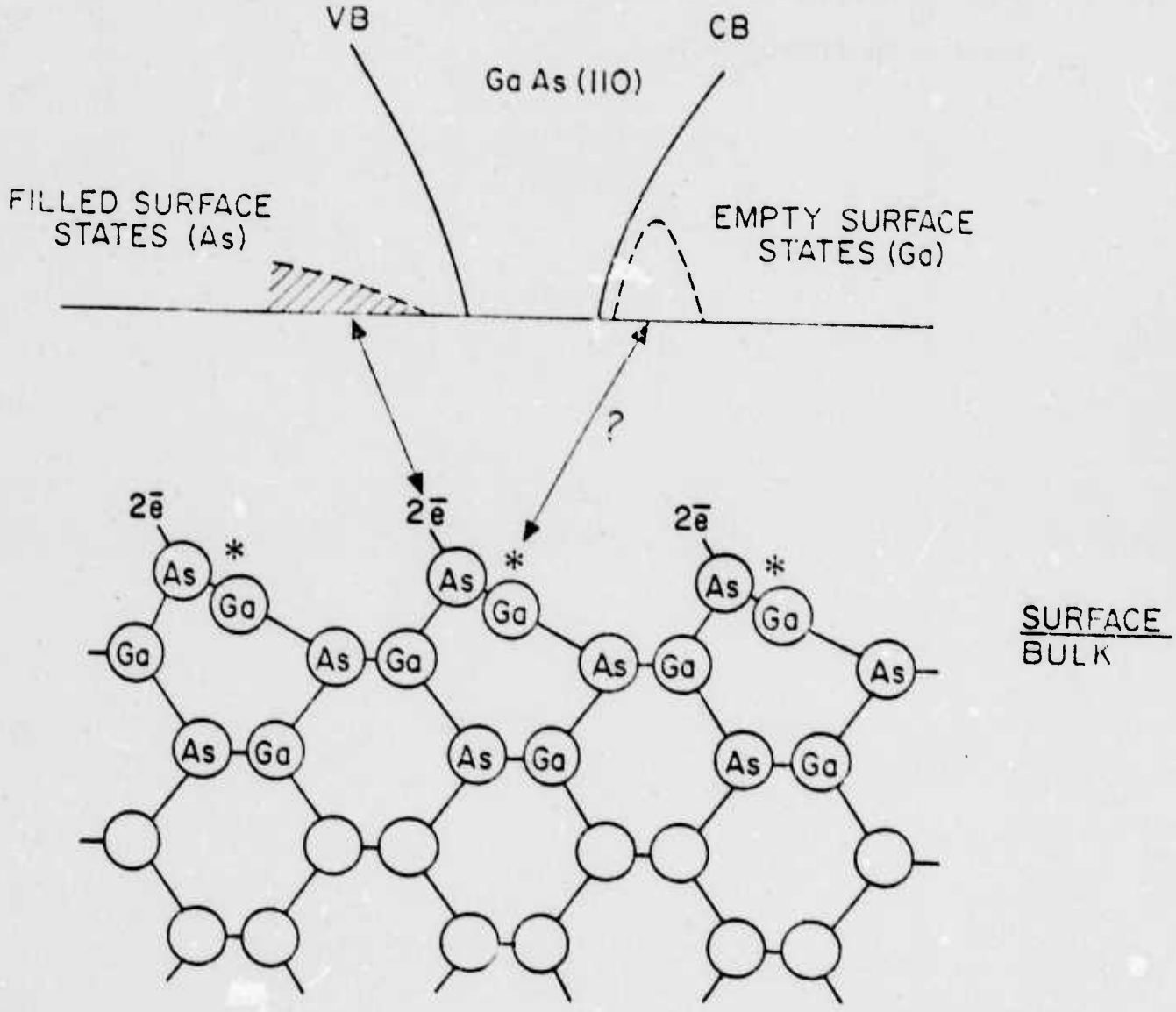

* LOCATION OF EMPTY SURFACE STATE

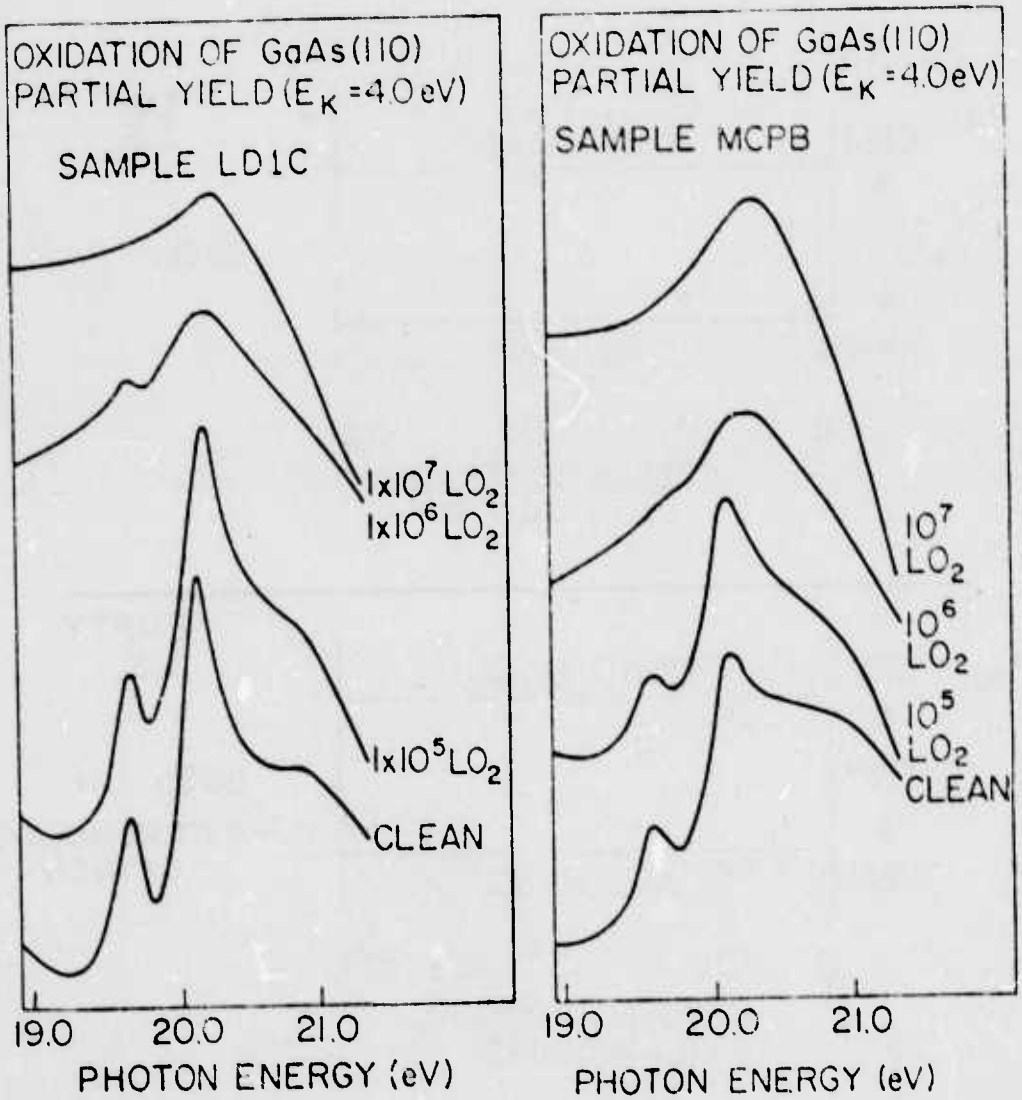
OXIDATION OF GaAs(110)
PARTIAL YIELD (E_K =4.0 eV)
SAMPLE LD1C
1x10^7 LO$_2$
1x10^6 LO$_2$
1x10^5 LO$_2$
CLEAN
19.0
20.0
21.0
PHOTON ENERGY (eV)
OXIDATION OF GaAs(110)
PARTIAL YIELD (E_K =4.0eV)
SAMPLE MCPB
10^7 LO$_2$
10^6 LO$_2$
10^5 LO$_2$
CLEAN
19.0
20.0
21.0
PHOTON ENERGY (eV)

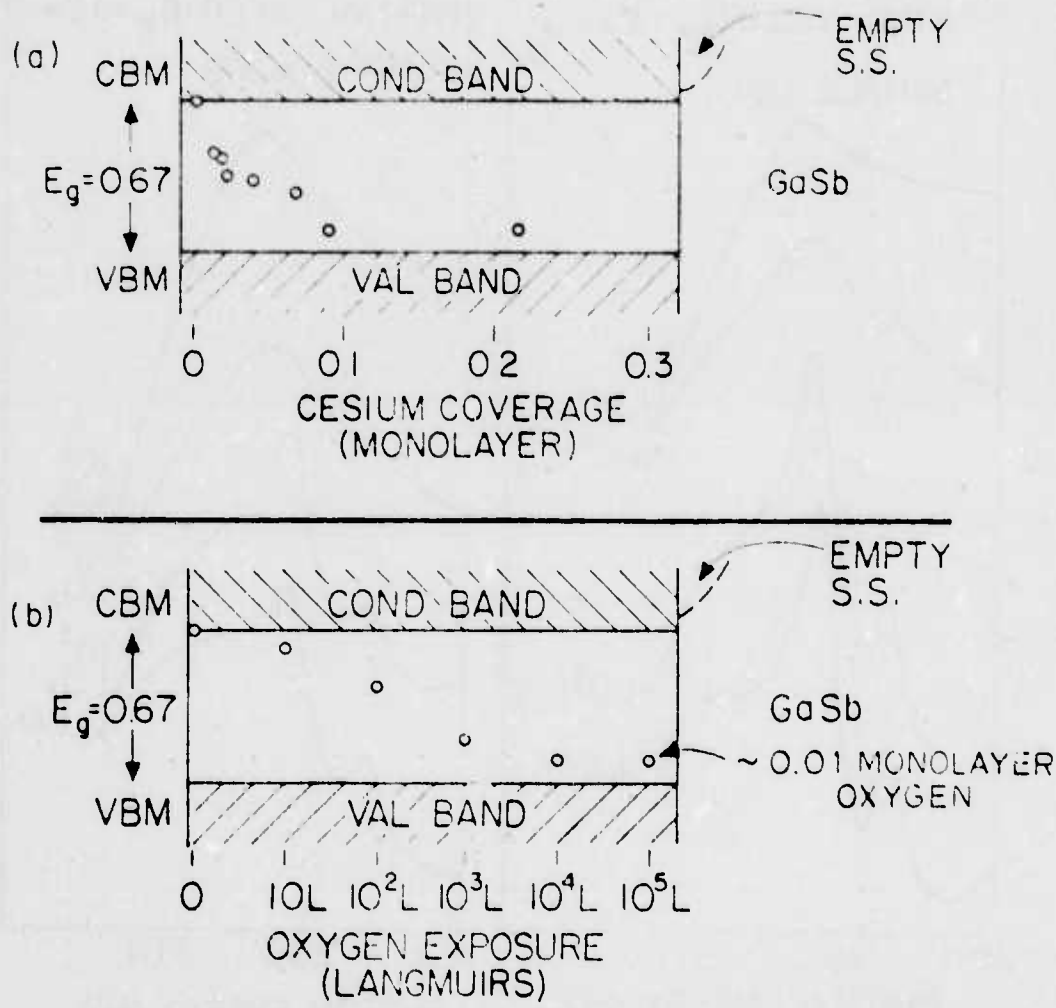
(a)
CBM
COND BAND
EMPTY
S.S.
E_g=0.67
GaSb
VBM
VAL BAND
0
0.1
0.2
0.3
CESIUM COVERAGE
(MONOLAYER)
(b)
CBM
COND BAND
EMPTY
S.S.
E_g=0.67
GaSb
~ 0.01 MONOLAYER
OXYGEN
VBM
VAL BAND
0
1L
10^2L
10^3L
10^4L
10^5L
OXYGEN EXPOSURE
(LANGMUIRS)

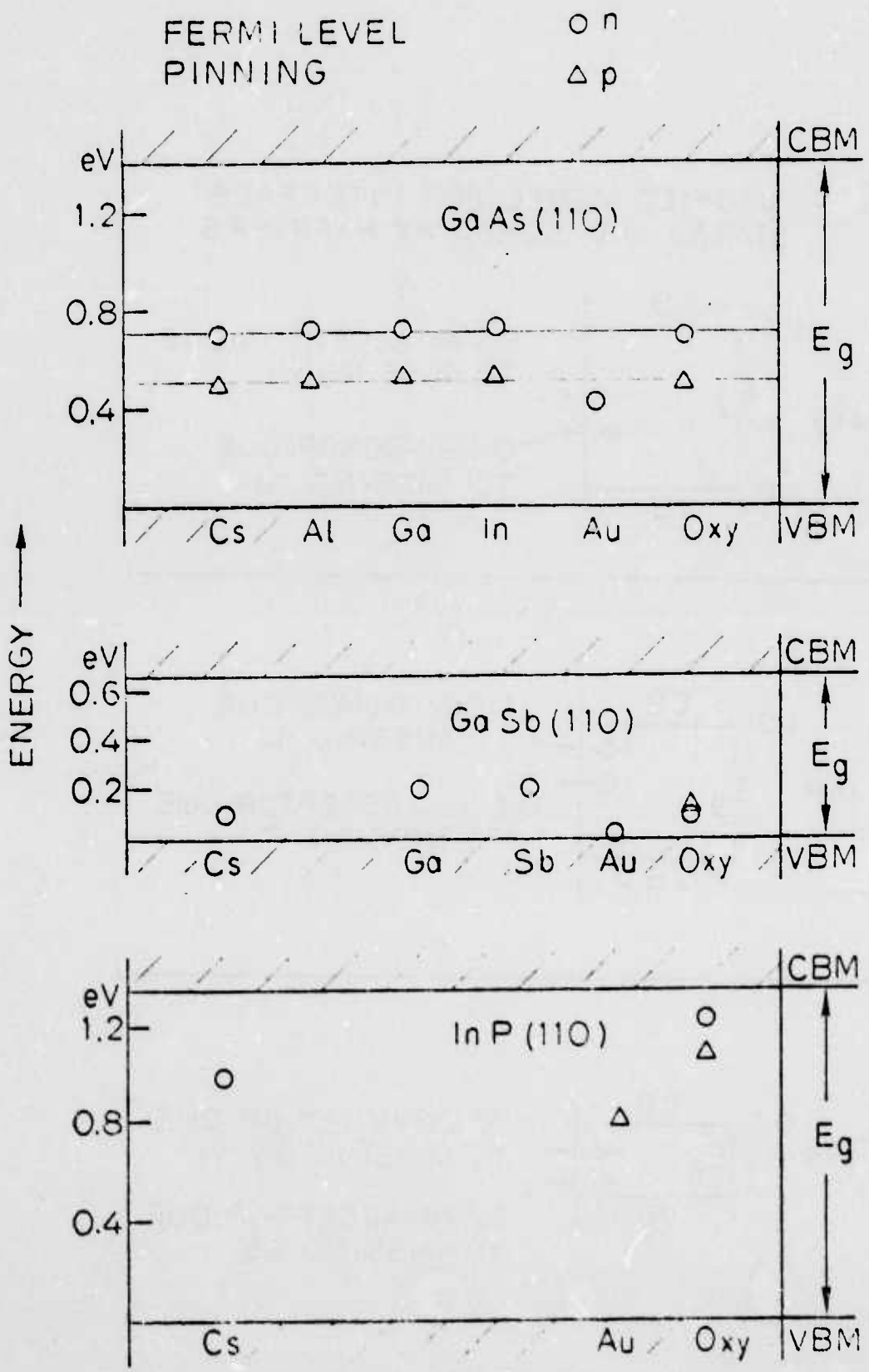

OVERLAYER PRODUCING PINNING (Sub - Monolayer)

UNIFIED MODEL FOR INTERFACE STATES AND SCHOTTKY BARRIERS

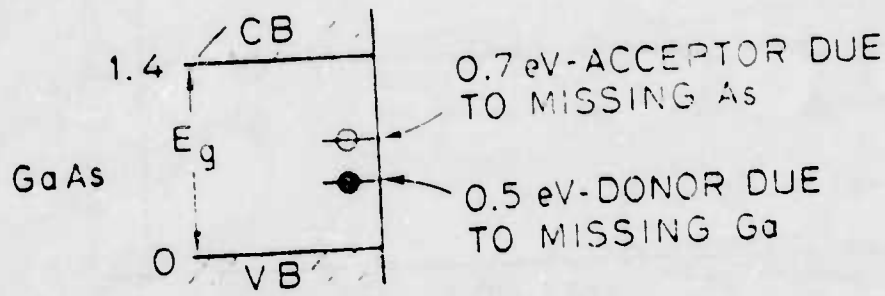

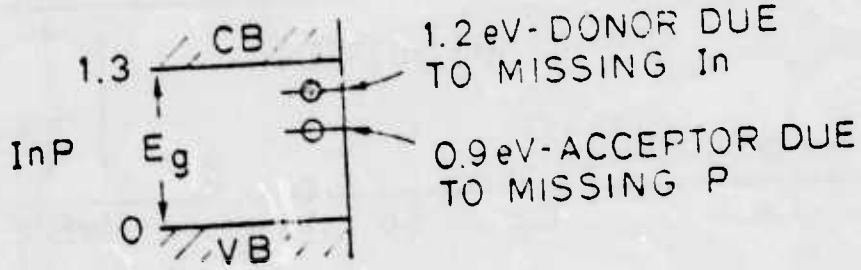

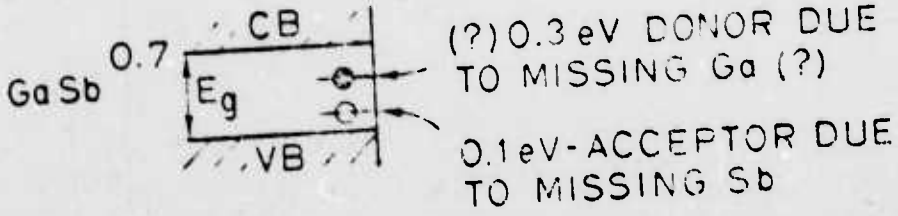

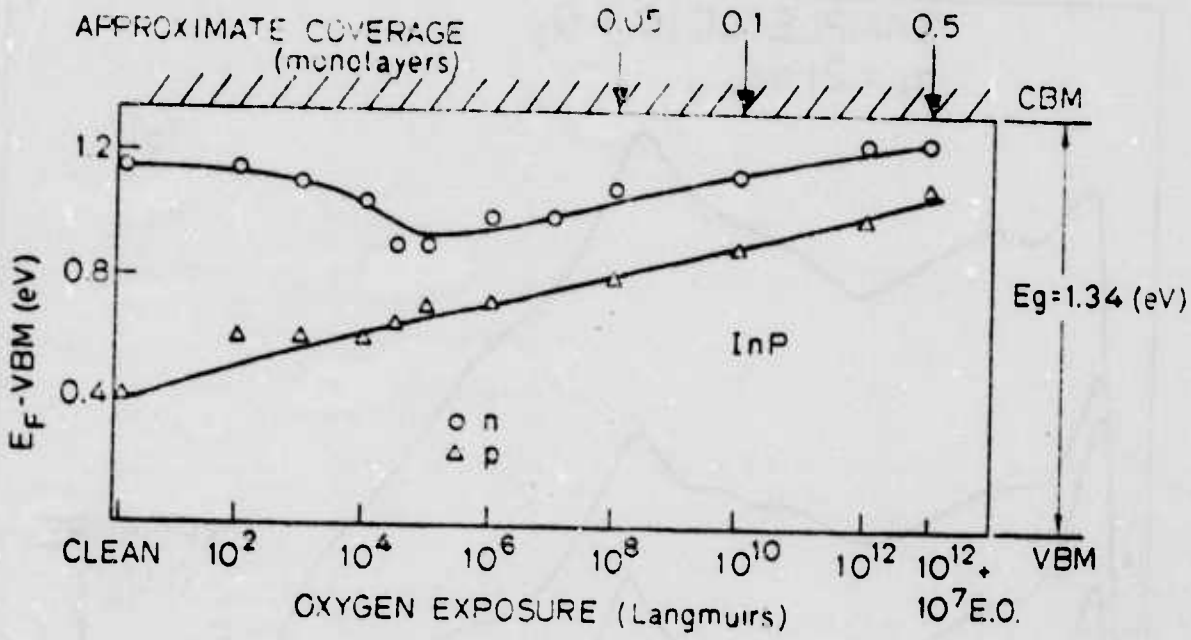
APPROXIMATE COVERAGE
(monolayers)
0.05
0.1
0.5
CBM
VBM
Eg=1.34 (eV)
1.2
0.8
0.4
E_F-VBM (eV)
InP
o n
Δ p
CLEAN
10^2
10^4
10^6
10^8
10^{10}
10^{12}
10^{12}+
10^7E.O.
OXYGEN EXPOSURE (Langmuirs)

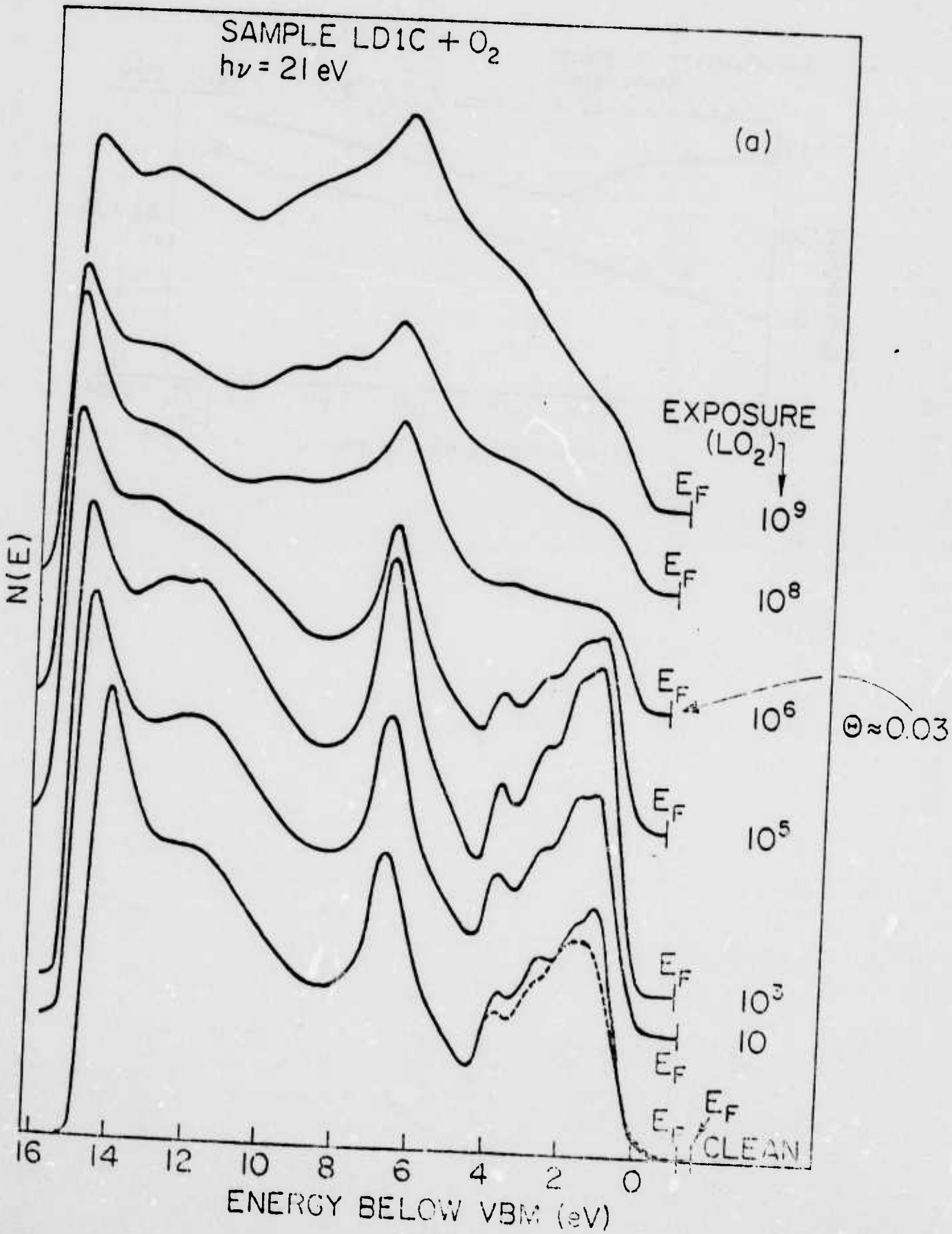
SAMPLE LD1C + O_2
$h\nu$ = 21 eV
(a)
EXPOSURE (LO_2)
E_F
10^9
10^8
10^6
10^5
10^3
10
CLEAN
$\Theta \approx 0.03$
N(E)
16
14
12
10
8
6
4
2
0
ENERGY BELOW VBM (eV)

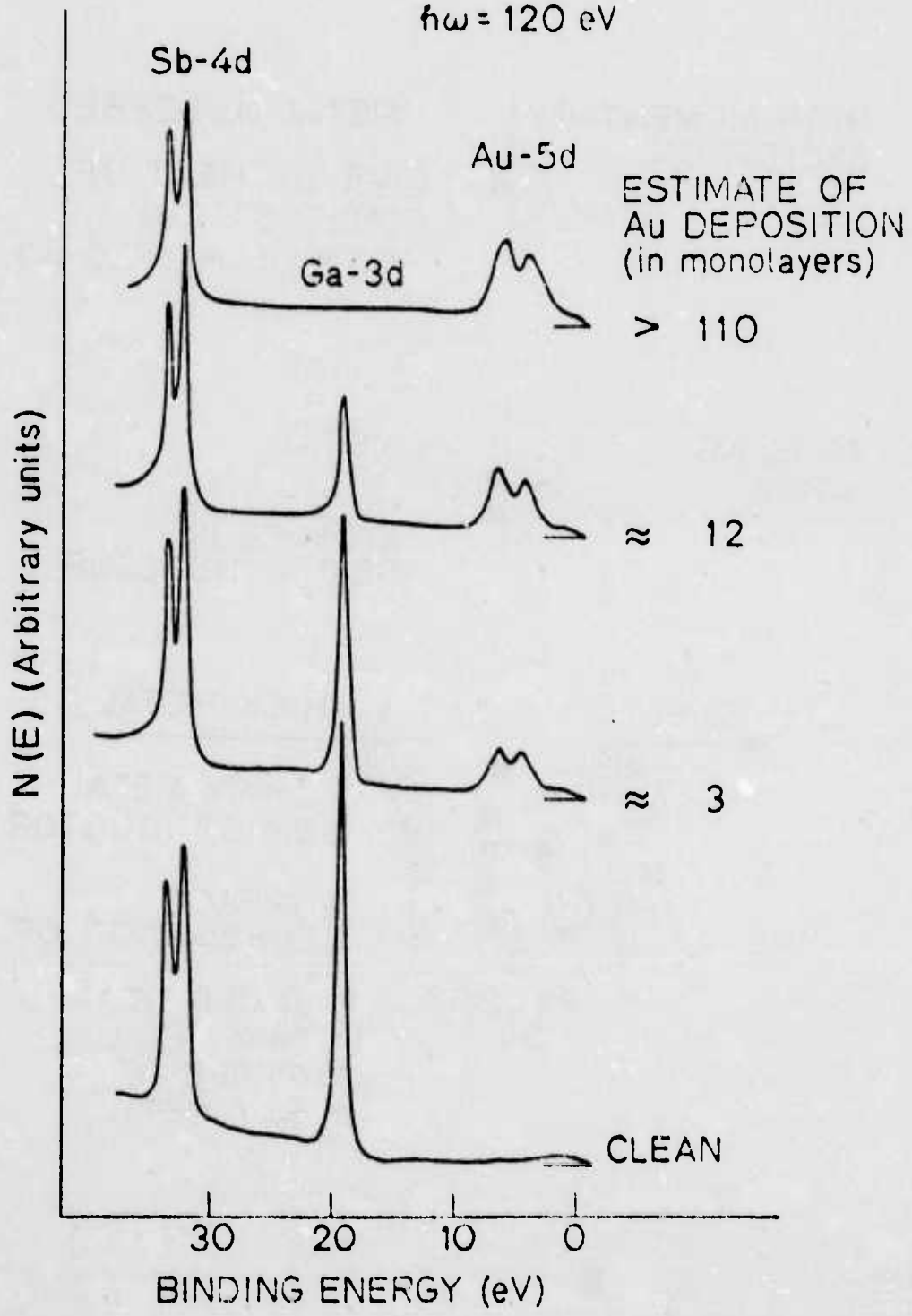
ħω = 120 eV
Sb-4d
Au-5d
Ga-3d
ESTIMATE OF
Au DEPOSITION
(in monolayers)
> 110
≈ 12
≈ 3
CLEAN
N(E) (Arbitrary units)
30
20
10
0
BINDING ENERGY (eV)

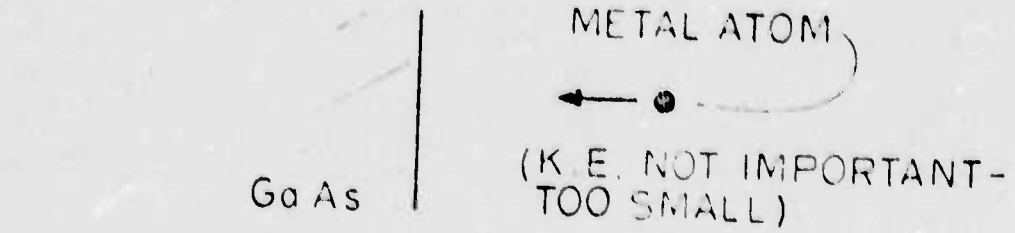
METAL ATOM
Ga As
(K.E. NOT IMPORTANT-
TOO SMALL)


HIGH MOMENTARY
EXCITATION
METAL-ADSORBED
GIVE UP HEAT OF
CONDENSATION
~60 K cal/mol. (2.5 eV)

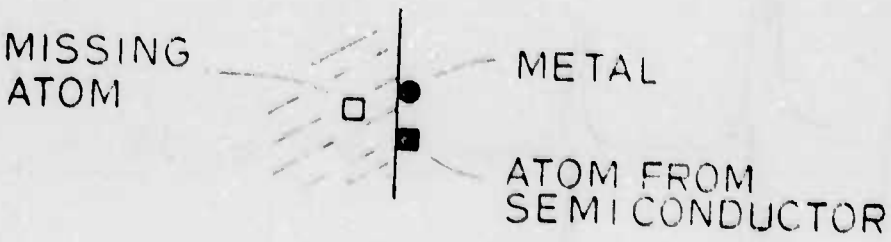
MISSING
ATOM
METAL
ATOM FROM
SEMICONDUCTOR

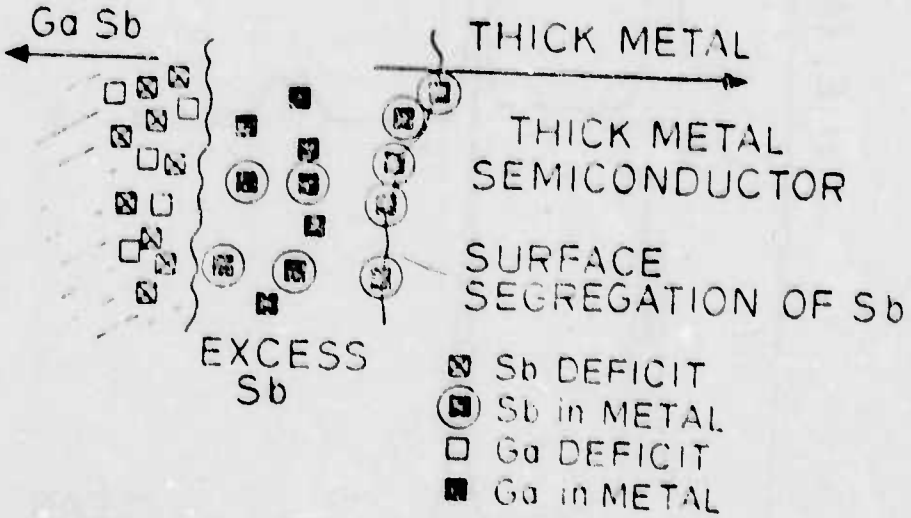
Ga Sb
THICK METAL
THICK METAL
SEMICONDUCTOR
SURFACE
SEGREGATION OF Sb
EXCESS
Sb
Sb DEFICIT
Sb in METAL
Ga DEFICIT
Ga in METAL

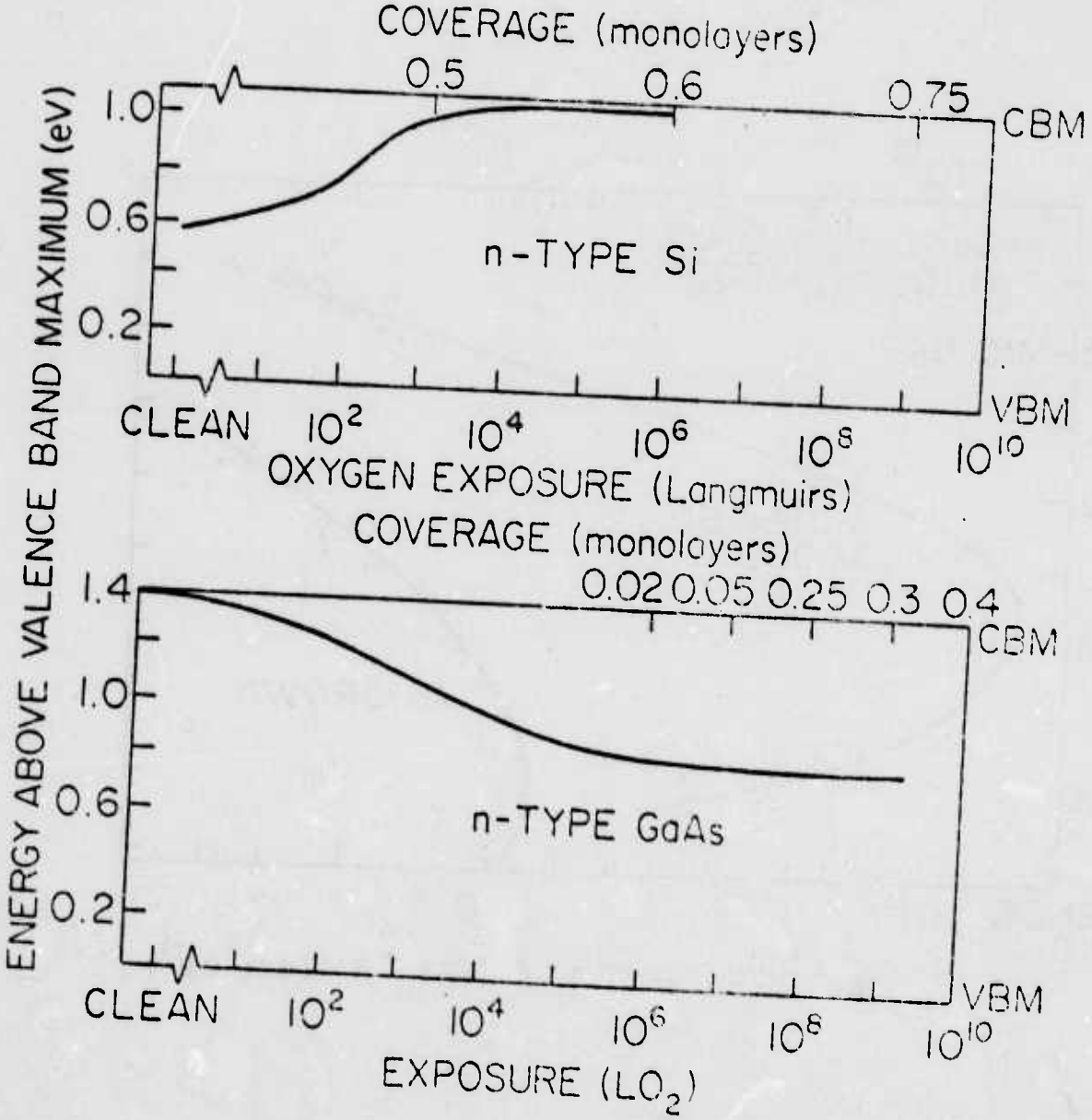
COVERAGE (monolayers)
0.5
0.6
0.75
CBM
1.0
0.6
0.2
n-TYPE Si
VBM
CLEAN
10^2
10^4
10^6
10^8
10^{10}
OXYGEN EXPOSURE (Langmuirs)
COVERAGE (monolayers)
0.02 0.05 0.25 0.3 0.4
CBM
1.4
1.0
0.6
0.2
n-TYPE GaAs
VBM
CLEAN
10^2
10^4
10^6
10^8
10^{10}
EXPOSURE (LO_2)
ENERGY ABOVE VALENCE BAND MAXIMUM (eV)

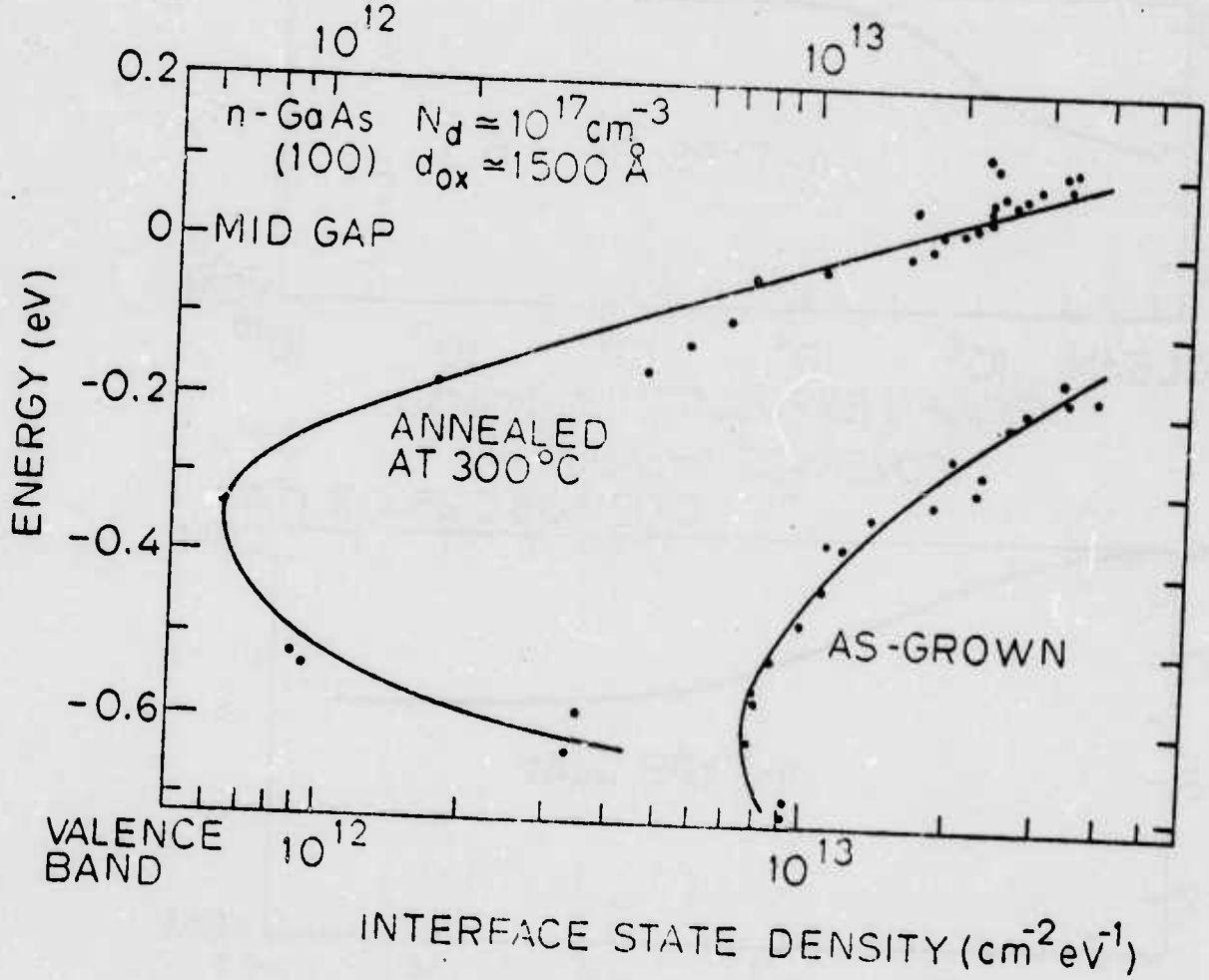
10^{12}
10^{13}
0.2
n-GaAs $N_d \simeq 10^{17} cm^{-3}$
(100) $d_{ox} \simeq 1500$ Å
0
MID GAP
-0.2
-0.4
-0.6
ENERGY (eV)
ANNEALED
AT 300°C
AS-GROWN
VALENCE
BAND
10^{12}
10^{13}
INTERFACE STATE DENSITY ($cm^{-2}eV^{-1}$)

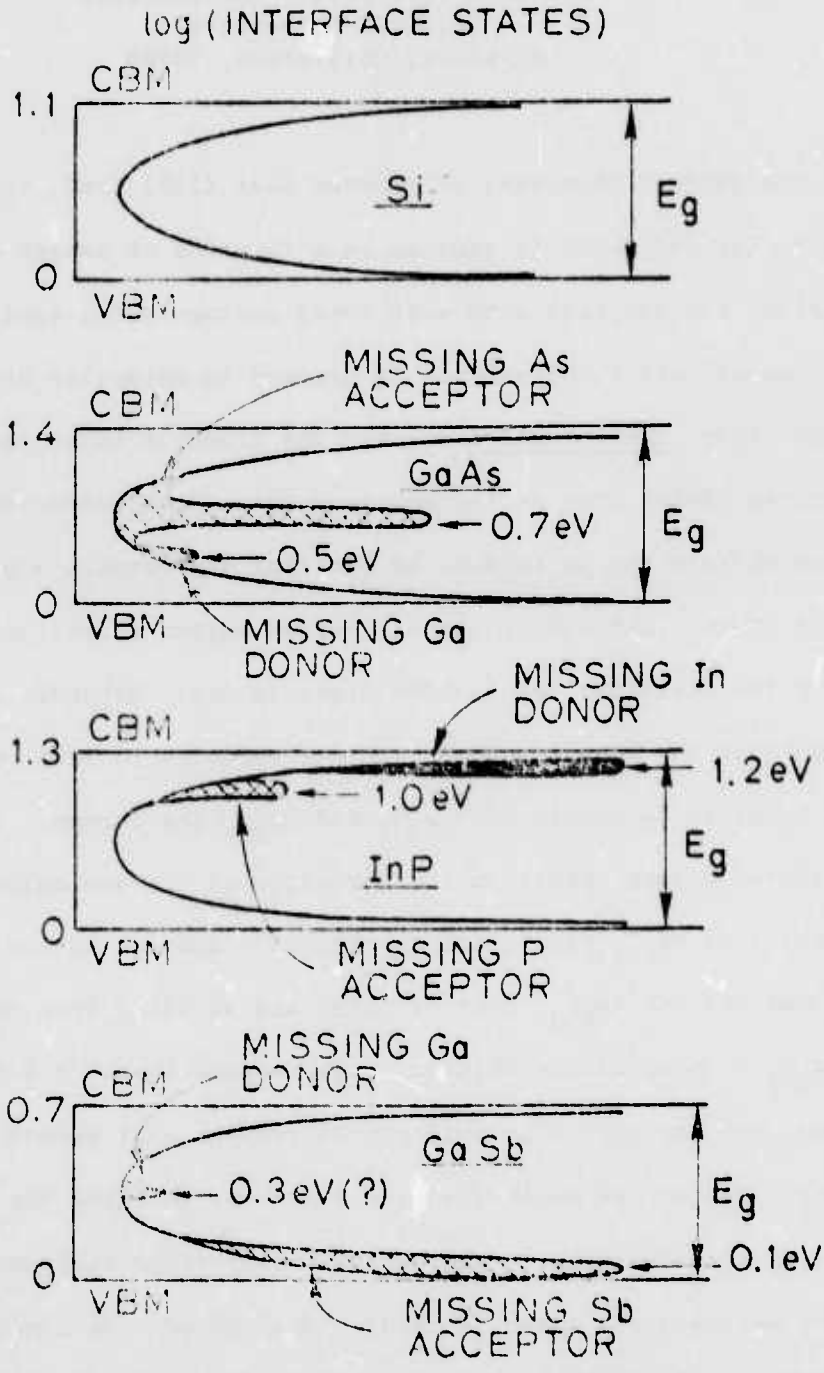

INTERFACE STATE : SEMICONDUCTOR OXIDE

Chapter 6

CHEMISORPTION AND OXIDATION STUDIES OF THE (110) SURFACES OF GaAs, GaSb, AND InP†

P. Pianetta, I. Lindau,
C. M. Garner, and W. E. Spicer
Stanford Electronics Laboratories
Stanford University
Stanford, California 94305

The surface chemistry of cleaved GaAs (110) (and, to a lesser extent, InP and GaSb) is studied as a function of oxygen exposure (both unexcited and excited) with soft X-ray photoemission spectroscopy. When the cleaved GaAs (110) surface is exposed to molecular oxygen in the ground state, chemisorption to only the arsenics takes place. No back bonds are broken even for large exposures. Room temperature oxidation of the surface can be induced by exciting the oxygen, e.g., by an ionization gauge. The adsorption of excited oxygen is initially the same as for the unexcited, except 500 times faster. However, after >20% of a monolayer has been adsorbed, further exposure to excited oxygen causes back bonds to be broken and As_2O_5 and Ga_2O_3 are formed. Larger doses of excited oxygen result in the formation of thicker oxides composed primarily of Ga_2O_3 with small amounts of elemental As (or As bound to only one Ga) and As_2O_3, most of which has sublimed from the surface. No As_2O_5 is seen in the thicker oxide because there is a deficiency of oxygen, and any partially oxidized Ga present will reduce the arsenic oxides. The escape depth for GaAs (110) was measured for electron kinetic energies between 20 and 200 eV. This range includes the minimum in the escape depth which is about 6 Å at 60 eV. No chemical shift in the core levels between the atoms on the surface and in the bulk was observed. GaSb (110) and InP (110) surfaces were also studied. InP

behaves like GaAs, whereas the GaSb is oxidized immediately even when exposed to only unexcited oxygen. The oxygen uptake curves for GaSb and GaAs were compared and found to be quite different with a sticking coefficient, at zero coverage, of 2×10^{-4} for GaSb and 8×10^{-10} for GaAs.

---

†Work supported by the Advanced Research Projects Agency of the Department of Defense monitored by Night Vision Laboratory, U.S. Army Electronics Command under Contract No. DAAK 02-74-C-0069 by the Office of Naval Research Contract No. N00014-75-C-0289; by the National Science Foundation Contract No. DMR 73-07692 A02 in cooperation with the Stanford Linear Accelerator Center and the U.S. Energy Research and Development Administration.

I. INTRODUCTION

The surface physics and chemistry of III-V compound semiconductors have attracted considerable interest, both experimental and theoretical. One of the things that makes III-V compounds such as GaAs so interesting from a fundamental point of view is the effect of the polar nature of the fundamentally covalent Ga-As bond on the surface properties of the crystal. III-V compounds also have important practical applications such as infrared detectors, high frequency MOS devices, and light emitting diodes. One of the major obstacles in fabricating GaAs MOS devices, as well as in many other applications, is that it is very difficult to passivate the surface. Much work has been done in this area, but no oxides with the favorable properties characteristic of silicon based devices have yet been developed. Thus, it is very important to gain more insight into the chemistry of the oxide semiconductor interface.[1]

Crystals of the III-V compounds have the zincblende structure, and we should note that, in terminating the lattice to create the ideal surfaces, one covalent bond per surface site has been broken, leaving three intact.[2] On the (110) surface, which is the cleavage face of the III-V semiconductors, a rearrangement of charge takes place and it becomes energetically favorable for the surface atoms to seek a bonding configuration more characteristic of their covalent bonding in small molecules. To be more precise, a simplified version of the currently accepted model is that the surface Ga now has only three electrons (in an sp^2 configuration), all involved in back conding, while the As has five electrons (in a p^3s^2 configuration), three of these electrons take part in the back bonds (p^3) and the remaining two (s^2) are the "dangling bond orbitals."[2-4] This charge rearrangement has two important consequences. First, the change

in the bonding configuration of the surface atoms results in a distortion of the lattice at the surface consistent with the planar sp^2 Ga back bonds and the prismatic p^3 As back bonds, Fig. 1 (we should note this relaxation is not total).[3,5,6] Secondly, since all of the electrons on the surface Ga are used in forming the back bonds, the Ga has no filled surface state orbitals. The surface As atoms, on the other hand, have two available electrons to contribute to the filled surface state band which lies well below the valence band maximum.[1,2] The position of the filled and empty surface states on an energy level diagram is also shown in Fig. 1 after Gregory et al.[2,3,7-10]

The basic aspects of this model can also be applied to the polar faces in order to explain the greater chemical activity of the As-terminated ($\overline{111}$) face with respect to the Ga-terminated (111) face. However, the experimental situation for the polar faces is not as well defined as for the cleaved (110) surface since the surface atoms on the polar surfaces probably have some unsaturated bonds. This situation could be caused by deficiencies in the available surface preparation techniques or fundamental problems arising from the polar nature of these surfaces.[3,4,11,12]

One of the major predictions of the model of Fig. 1 is that, for the (110) surface, oxygen is adsorbed preferentially on the arsenic atoms by interacting with the filled surface states. Furthermore, since all the bonding electrons associated with the surface gallium atoms are involved in the back bonds, the oxygen will bond to the gallium only after one or more of the back bonds are broken.[2,7,13] The oxidation of GaAs has been studied extensively by ultraviolet photoemission spectroscopy (UPS),[2,14] ellipsometry,[15] electron energy loss spectroscopy (EELS),[16,17] Auger electron spectroscopy (AES),[12,14,15,18] and low energy electron diffraction

(LEED).[5,15] The early experimental work on the cleaved (110) surface gave results that were consistent with the predictions outlined above,[2,15,16] whereas recent results on the polar surfaces have been interpreted to mean that the oxygen sticks preferentially to the surface Ga atoms.[12,17] However, the conclusions from one of the studies[17] on the polar surfaces are based on indirect evidence whose interpretation is open to question.[19] The interpretation given in the second set of studies[12] is probably correct, but the polar faces used had unsaturated Ga bonds so that adsorption on the Ga sites does not necessarily disagree with the model of Fig. 1 (this point will be discussed at the end of Section III.B).

In our recent work[7,13] on the GaAs (110) surface, we showed definitively that there is a charge transfer from surface As atoms to chemisorbed oxygen. We interpreted this to mean that the oxygen is bound preferentially to surface As atoms, in agreement with the earlier work cited above. We have also shown that InP behaves in the same way as GaAs, whereas the oxidation of GaSb proceeds in an entirely different manner. In GaSb, the oxygen bonds both species breaking the Ga-Sb back bonds.[7] This latter effect can then be compared to the situation when the GaAs (110) surface is exposed to excited oxygen.[20]

In this paper, we will present a detailed analysis of our previously reported results and new data on the very heavily oxidized surface of GaAs (110), which gives us greater insight into the oxidation of GaAs.

All the results presented here were obtained with soft X-ray photoemission spectroscopy (SXPS) using synchrotron radiation from the "4° line" at the Stanford Synchrotron Radiation Project in the photon energy range $32 \text{ eV} \leq h\nu \leq 350 \text{ eV}$.[21] This photon energy range is interesting because it allows us to observe both the valence band and

several core levels from both the Ga and As at high resolution (0.25 eV). By tuning through the available photon energies, we are able to adjust the kinetic energies of the various levels to be roughly between 20 and 200 eV. This is possibly the most significant aspect of our experiments because the escape length of electrons in a material is strongly dependent on the electron kinetic energy, and this escape depth goes through a minimum of $\lesssim$10 Å for kinetic energies between 50 and 150 eV for most materials.[22]

The experimental methods, such as LEED, AES, and UPS, that were used in the earlier oxidation studies all have high surface sensitivity. However, they lack the chemical information which can be obtained from X-ray photoemission (XPS) studies of core level shifts.[23] AES can be used to look at chemical shifts, but the use of an e-beam as the excitation source can desorb the oxygen or destroy the integrity of the surface.[18,20,24] This damage is minimized when using UV light or X-rays. However, conventional XPS ($h\nu$ = 1486.7 or 1253.6 eV) lacks the necessary surface sensitivity.[22] With SXPS, not only can we study the chemical shift of core levels upon forming a chemical bond, but we can also perform these studies at submonolayer coverages due to the inherent surface sensitivity of the technique.[7,13] In our experiment, we adsorb oxygen on GaAs, GaSb, or InP and observe any core level shifts that take place upon adsorption. We then measure the magnitude of the core level shifts and correlate these shifts with chemical shift measurements made on bulk oxides using conventional XPS. This correlation allows us to determine the type of oxides forming at the surface in a relatively straightforward way.[23] The ratio of the area of the shifted to unshifted peaks can be used to determine coverages versus exposure as well as escape depth information.

In Section II, we will discuss the experimental apparatus, procedure, and results. Section III will contain the discussion. In this section, we will correlate the chemical shifts obtained from the surface oxidation of GaAs (110) to the shifts obtained from ESCA measurements of bulk oxides. These correlations will then be used to give a model for the oxidation of GaAs (110), starting from surface chemisorption and ending with the formation of actual bulk oxides. We will also determine the escape depth for GaAs as a function of photon energy as well as show a difference in adsorption kinetics between GaAs (110) and GaSb (110).

II. EXPERIMENTAL

A. Apparatus

The experimental chamber consists of a stainless steel UHV bell jar and base pressure $<1 \times 10^{-10}$ torr. The pumping system is a 240 L/sec ion pump plus titanium cryopump with a poppet valve for sealing the pump from the main chamber. The chamber contains a double pass cylindrical mirror analyzer (Physical Electronics), a cleaver, and a sample manipulator capable of holding four samples for cleaving, one sample for heat cleaning ($T_{max} \approx 2000°C$) and a substrate upon which Au or Cu may be evaporated for Fermi level (and thus binding energy) determinations.[25] An evaporator which contains copper and gold beads is also housed in the chamber.

Research grade oxygen was admitted into the vacuum system through a bakeable leak valve. For large exposures (pressures up to 750 mm O_2), an auxiliary pumping system was used to return the main chamber to pressures below $\sim 10^{-8}$ torr. This system consisted of vacsorb pumps,

an ion pump, and all the necessary gauging to measure pressures for the gas exposures.

Pressures between 10^{-11} and 10^{-5} torr were measured by a Redhead cold cathode ionization gauge (NRC) located in the main vacuum system. This pressure range was used for exposures up to 10^{4} L (1 L = 10^{-6} torr/sec) where the exposure time was no longer than 10^{3} sec. A hot filament ionization gauge with Thoria coated iridium filaments (Varian) was also located in the main vacuum system. This gauge was used initially to check the cold cathode gauge and, more importantly, as a source of excited oxygen when used during a gas exposure. The effect of the ion gauge on the oxidation will be treated in a later section.

Pressures between 10^{-5} and 0.6 torr were measured by a millitorr gauge (Varian) located in the auxiliary pumping system. This pressure range gives exposures between 10^{4} L and $\approx 10^{9}$ L. A thermocouple gauge (Hasting DV-4) again in the auxiliary pumping system, was used for pressures between 1 and 20 torr, giving exposures between 10^{9} L and 2×10^{10} L. For larger exposures of up to 10^{12} L, a mechanical vacuum gauge (Wallace and Tiernen) was used, measuring pressures up to 800 torr.

The synchrotron radiation is monochromatized by a grazing incidence monochromator (resolution 0.2 Å) with a refocusing mirror located after the exit slit.[26] The radiation enters the chamber through a bakeable straight through valve. The energy of the photoemitted electrons is then determined by the double-pass cylindrical mirror analyzer operated in the retarding mode. This mode ensures a constant resolution which is equal to 0.6% of the electron pass energy through the analyzer. In these experiments, we used a pass energy of 25 eV, giving an electron energy resolution of 0.15 eV. At $h\nu$ = 100 eV, typical counting rates

on the Ga 3d levels are about 5×10^3 counts per second for a circulating electron current in SPEAR of 20 ma.

The signals from the electron energy analyzer are amplified and fed into a 2048 channel signal averager (Tracor Northern) used as a multichannel scaler. The energy of the detected electrons was controlled by the signal averager through a voltage ramp synchronized with the memory sweep.

The samples that were studied in these experiments are Te doped, n-type GaAs ($n = 3.5 \times 10^{17}$ cm^{-3} and $n = 0.5 \times 10^{18}$ cm^{-3})[27] and Zn doped p-type GaAs ($p = 6 \times 10^{18}$ cm^{-3}) from Laser Diode (LD) Corporation; Te doped n-type GaSb ($n = 1.1 \times 10^{18}$ cm^{-3}) from Asarco;[28] and Zn doped p-type InP ($p = 2 \times 10^{18}$ cm^{-3}) from Varian Associates. The GaAs and GaSb samples were rectangular prisms $5 \times 5 \times 10$ mm^3, and the InP was $2 \times 5 \times 10$ mm^3. In all the samples, the (110) axis was along the long dimension.

B. Procedure

First, the samples were cleaved along the (110) planes by slowly squeezing the sample between the annealed copper anvil and tungsten-carbide knife of the cleaver. The cleaved sample is then inspected visually to ensure the cleave has a mirror-like finish. A set of spectra is taken for $32 \leq h\nu \leq 300$. Now the sample is ready to be exposed to oxygen. The pump is valved off from the main chamber with the poppet valve, partially for exposures below 10^4 L and completely for larger exposures. The gas is admitted and the pressure monitored. After the desired exposure is reached, the majority of the gas is removed with the auxiliary pumping system. When the chamber reaches a pressure below

$\sim 10^{-8}$, the poppet valve is opened and the main pump takes the chamber to pressures below $5 \sim 10^{-10}$ torr for all gas exposures that are performed. During these exposures, the straight through valve into the grazing incidence monochromator has been closed and is not opened until the pressure in the chamber $< 1 \times 10^{-9}$ torr. With this scheme for making the gas exposures, the chamber is returned to its base pressure very quickly. Using the technique described above, the majority of the gas is pumped out in the first 15 sec and working pressure is achieved within 10 to 15 minutes, giving a minimum of down time between spectra.

The exposures with excited oxygen are performed with the ion gauge in the main chamber turned on.[29] This gauge is out of line of sight of the sample so that the gas molecules must strike at least two surfaces before hitting the sample. However, for the larger exposures, it is also possible that the oxygen is deflected to the sample through collisions with other gas molecules since the mean free path of the molecules is between 1 and 10 cm for the pressures used in the ion gauge exposures (10^{-2} to 10^{-3} torr). Two different ion gauge emission currents were used in the exposures. One emission current seting was 4.0 ma (for pressures below 10^{-4} torr), and the other was 0.4 ma (for pressures between 10^{-2} and 10^{-3} torr). We did not directly determine if there was a tenfold increase in the amount of excited oxygen in going from the 0.4 to 4.0 ma emission currents, but the results of the oxidation indicate that this should be the case.[30]

The binding energies in these studies are measured relative to the valence band maximum of the clean surface. Binding energies with respect to the Fermi level can be determined by referring the unknown binding energies to either the 4f levels of Au (binding energy = 84.0 eV) or

the Fermi level of a gold film evaporated in situ on a substrate in electrical contact with the sample.[25]

In all the figures that follow, in which we show spectra for clean and oxidized samples on the same graph, the horizontal binding energy scale refers to the clean spectrum. The spectrum of the oxidized samples are adjusted so that the various unshifted peaks line up consistently. This must be done because the Fermi level pinning for these samples changes as a function of oxygen exposure so that binding energies referenced to the Fermi level vary.[7,31] Furthermore, the structure in the valence band also changes considerably with oxidation so that the unshifted core levels must again be used as standards. Beyond 10^7 LO_2, the position of the Fermi level has stopped moving so that we may use the measured energy positions of the peaks as a consistency check.

C. Results

In Fig. 2, we show spectra for the clean and oxidized GaAs (110) surface at $h\nu = 100$ eV. As we expose the surface to oxygen, we see a single peak ($E_B = 43.7$ eV) growing 2.9 eV below the As-3d peak ($E_N = 40.8$ eV) with a proportionate decrease in the As-3d intensity. This is a chemically shifted peak indicating a transfer of charge from the surface As atoms to the adsorbed oxygen. Concurrent with the appearance of the shifted arsenic peak, we see the O-2p resonance level at a binding energy of about 5 eV. As we go to higher exposures, the shifted As-3d peak and O-2p level grow simultaneously until saturation is reached between 10^9 and 10^{12} LO_2. We interpret the filling in of the valley between the shifted and unshifted peaks as due to the overlap between these two peaks since all the observed structure can be accounted

for by this overlap without introducing any intermediate states. The elimination of any such intermediate states has important implications when it comes to understanding the type of ligand which gives rise to the AsI peak.

An estimate of the relative amount of oxidized As atoms on the surface can be obtained by comparing the areas under the shifted and unshifted peaks. This is done in Fig. 3, where we plot the area in relative units under the shifted and unshifted peaks as a function of exposure. Here, the sum of the areas under the shifted and unshifted peaks were normalized to unity. As expected, the amount of oxidized arsenic increases while the unoxidized decreases for increasing exposure. At 10^6 LO_2, where we first start to see the effect of oxygen in the valence band as well as seeing a chemically shifted As-3d level, the coverage is only about 2% of saturation.

If we consider only the points up to an exposure of 5×10^9 LO_2 in Fig. 3, saturation seems to have been reached at about 10^9 LO_2. If, however, we include the point at 10^{12} LO_2, which gives a 1.7 times increase in coverage over that at 10^9 LO_2, the apparent saturation exposure is increased by three orders of magnitude. At present, we will not place too much emphasis on this one point because the spectrum for 10^{12} LO_2 was obtained by exposing a freshly cleaved surface (sample LD1) to 10^{12} LO_2 <u>in one step</u>, whereas all the other spectra were obtained by exposing sample LD3 <u>gradually</u> to increasing amounts of oxygen.

The relative oxygen coverages can also be obtained by measuring the area under the O2p resonance in the valence band. The major drawback to this technique is that the valence band and the O2p signal overlap so that it is difficult to get reliable coverage information below exposures

of about 5×10^7 LO_2. Even above this exposure, the GaAs valence band is still a significant fraction of the total emission, so care must be used in separating out the oxygen contribution from that of the GaAs. These problems are seen rather clearly in Fig. 4 where we show a blow-up of the GaAs valence band for various oxygen exposures. The coverage, as determined from the shifted arsenic level, gives a measure of the relative amount of oxygen that has chemically combined with the surface arsenic atoms. The coverage obtained from the O2p signal gives a measure of the <u>total</u> amount of oxygen sticking to the surface. Thus, comparison of the oxygen uptake determined in these two ways can be used to give additional information on the kinetics of the adsorption as well as the nature of the adsorbate. Our initial studies on sample LD3 indicate that the two methods give similar results. However, the 10^{12} LO_2 exposure on sample LD1 shows that the number of shifted arsenic atoms has increased by a factor of 1.7, while the oxygen coverage has not changed appreciably from the coverage at 10^9 LO_2. This could be interpreted to mean that the oxygen has been adsorbed dissociatively because the higher pressure of the exposure has changed the adsorption kinetics. This is a very interesting point, but we will not pursue it further here because more experimental work needs to be done on the exposures between 10^{10} and 10^{12} LO_2 before definitive conclusions may be drawn. We will limit our discussion of chemisorption mechanisms to the exposures below 10^{10} LO_2.

For this work, the significance of the curve for 10^{12} LO_2 is that, even for this very large exposure (this corresponds to an exposure of <u>one</u> atmosphere of O_2 for 20 minutes!), no major shift in the gallium 3-d level is observed. The only effect on the gallium peak is a 0.4 eV

broadening. Part of this broadening is due to a nonuniformity in work function across the face of the sample since the unshifted arsenic peak is broadened by 0.1 eV. For the exposures below 10^{10} LO_2, the Ga 3-d broadens symmetrically by ±0.12 eV, and the shift to higher binding energy is less than 0.03 eV.

The oxidation of the GaSb (110) surface is shown in Fig. 8 for $h\nu$ = 100 eV. As in the case of GaAs, all the spectral features of interest can be obtained at the same photon energy and in one spectrum, thus facilitating comparisons. The valence band extends approximately 12 eV below the valence band maximum. The Ga-3d level is at a binding energy of 19.4 eV, the Sb-4d doublet is at 32.1 eV ($4d_{5/2}$) and 33.2 eV ($4d_{3/2}$). We are able to clearly see the spin orbit splitting in the Sb-4d levels, whereas we were not able to see it at these energies for the Ga and As levels, primarily because the splitting of the Sb-4d levels is much larger than that of the 3d levels of As or Ga. We should also note that the As and Ga levels are 3d's, while that of Sb is a 4d. This point is important for the choice of photon energy since the variation of cross-section for the 4d levels versus photon energy is rather dramatic, as indicated in Fig. 6. Here, we show spectra of oxidized GaSb for several different photon energies. Notice that almost all the intensity is lost from the 4d levels over a very small photon energy range. The variation in cross section of the 3d's is not as dramatic, but is nevertheless also large.[32] Consequently, we are forced to use photon energies below about 120 eV.

As we oxidize the GaSb surface, we start to see changes in the spectra at about 5×10^5 LO_2. This is about a factor of two sooner than with the GaAs. But, more importantly, as we increase the exposure to 5×10^7 LO_2, we start to see a definite broadening of the Ga-3d level

toward higher binding energy. In fact, even by 5×10^8 LO_2, a definite shifted Ga-3d peak is seen (ΔE_B = 1.1 eV). Of course, the shifted Sb-4d (ΔE_B = 2.5 eV) level has also been growing at the expense of the unshifted level. The shifted peaks for both Sb and Ga completely dominate the unshifted peaks for exposures above 5×10^9 LO_2. In Figs. 2 and 5, we can see the obvious differences between the oxidation of GaAs and GaSb. In GaAs, only the As peak is shifted while the Ga peak is broadened. In GaSb, both the Sb and Ga are definitely shifted, indicating that charge transfer from both surface Sb and Ga atoms to the oxygen has taken place. This implies that bonds are broken between neighboring surface Ga and Sb atoms.

Another striking difference is seen if the coverage (area under shifted Sb peak or O-2p level) is plotted with respect to exposure (Fig. 7). The rate of oxygen adsorption from Fig. 7 does not show the saturation behavior which is characteristic of the GaAs surface as seen in Fig. 3.

Spectra for the clean and oxygen exposed p-type InP (110) surface are shown in Fig. 8. In this case, we used two different photon energies to optimize the surface sensitivity and cross section for the levels of interest. The P-2p levels are measured at $h\nu$ = 160 eV and the In-4d levels at $h\nu$ = 80 eV. The indium levels, being 4d levels, have the same general behavior versus photon energy as the Sb-4d levels. Therefore, they too have a rather large variation in cross section, forcing us to choose a photon energy not too high above threshold. As seen from Fig. 8, the InP (110) surface behaves like GaAs (110), with possible differences in the adsorption kinetics which will not be dealt with here. One subtle difference is that we are able to resolve the spin orbit splittings in both the phosphorous and indium levels for the clean surface. However, they smear out upon oxygen adsorption. No shifts are observed in the

In-4d levels, and a shifted P-2p level (ΔE_B = 4.4 eV) is observed which grows with oxygen exposure. Similar results have been seen in InAs by Gudat and Eastman.[34]

All the previous exposures were done with unexcited molecular oxygen. In the section that follows, we will consider the effect of excited oxygen on the adsorption process.[20] In Fig. 9, we show what happens when the GaAs (110) surface is exposed to excited oxygen. In these spectra, the exposure was carried out in exactly the same way as the previous exposures except that the ion gauge was on during the exposure with an emission current of 4 ma (the exposures at 10^6 and 10^7 L used an emission current of 0.4 ma). Comparing these spectra to those in Fig. 2, we see that the sticking probability has become much larger. It only takes an exposure of 10^5 L excited oxygen to give the same effect as an exposure of 5×10^7 LO_2. This is an increase in oxygen adsorption by a factor of 500! The fact that oxygen, which has been excited in some way, will stick more readily to semiconductor surfaces has been documented in the literature.[15,33] What has not been seen before is the change in chemical state due to bonding of such excited oxygen.[20] As we expose the surface to even more excited oxygen, a rather striking thing happens. At an exposure of 5×10^5 L excited oxygen, the first shifted peak (ΔE_B = 2.9 eV) stops growing, and a second shifted peak with a binding energy shift of 4.5 eV starts to grow and soon dominates the first shifted peak. But, what is even more striking is that the gallium peak starts to broaden also at 5×10^5 L excited oxygen. At higher exposures, we can see that the initial broadening at 5×10^5 L excited oxygen is due to a shifted gallium peak (ΔE_B = 1.0 eV) which grows concurrently with the second shifted arsenic peak.[13] This

simultaneous growth is very much like what was seen for the oxidation of GaSb in Fig. 5. We also see in these spectra the O-2s at 24 eV and the O-2p at 5 eV below the valence band maximum.

In Fig. 10, we give examples of the effects of very large doses of excited oxygen on the GaAs (110) surface. The top two curves are spectra for clean GaAs (110) and for the clean surface plus 10^{12} LO_2. The spectrum labeled "heavily oxidized" was obtained by exposing the surface, which had previously been exposed to 10^{12} LO_2, to 5×10^5 L excited oxygen with the ion gauge running at 0.4 ma emission current. Notice that the binding energies of the peaks in this spectrum are the same as those of Fig. 9. There are two oxidation states of As, and there is a shifted gallium peak. The fourth spectrum of Fig. 10 labeled "very heavily oxidized" was obtained by exposing clean GaAs (110) to 5×10^5 L excited oxygen with the emission current of the ionization gauge set at 4.0 ma (giving a significantly larger amount of excited oxygen than in the previous case). In this case, we see no unshifted gallium peak; only the shifted one. There is no unshifted arsenic peak, but there are two other peaks shifted 0.4 and 3.2 eV with respect to the unshifted peak (if it were present). Note the drastic decrease in emission from the arsenic derived levels and that the emission from the O-2p and O-2s levels has gone down with respect to that in the second and third spectra.

The significance of these observations will be discussed in the next section, where we will present a model for the oxidation of the GaAs (110) surface from the chemisorption stage to the formation of bulk oxides. In Tables I and II, we summarize the binding energies and chemical shifts (for GaAs) discussed above.

III. DISCUSSION

A. Interpretation of Chemical Shifts

In this section, we will concentrate on trying to determine which oxidation states of the As and Ga give rise to the chemically shifted peaks that are observed in the photoemission spectra. Considerable information can be obtained from the chemical shift measurements by assuming that ligands of any given type each shift the core levels of the central atom by the same amount.[23] Thus, the total shift, ΔE_{tot}, is simply given as the sum of the individual ligand shifts, ΔE_{ligand}, i.e.,

$$\Delta E_{tot} = \sum_{\substack{\text{all} \\ \text{ligands}}} \Delta E_{ligand} \quad . \tag{1}$$

The magnitude of the ligand shift may be determined by measuring the binding energies of several compounds containing different numbers of these ligands. In our case, this is very useful for the case of nonstoichiometric oxides. For stoichiometric oxides, the obvious thing to do is to use the bulk oxides as standards. Here, we will do both in order to determine the chemical species present on the surface after initial chemisorption and further oxidation.

In Table III, we present binding energy shifts for the Ga and As 3d levels in the compounds that will be used as standards. These values are taken from the literature and, rather than give absolute binding energies, we choose instead to give the binding energy differences between the levels in the various compounds. This, in effect, avoids many of the problems in choosing an appropriate reference level when comparing the results from several sources. Through the work of Bahl et al,[35] we

were able to determine the 3d level binding energy shifts for As_2O_5 and As_2O_3 with respect to As. We then calculated the difference between the Ga and As 3d levels of As_2O_3, Ga_2O_3, GaAs, and Ga by referring to the work of Leonhardt et al.[36] The Ga_2O_3/Ga shift was found to agree with Schön's measurements to within 0.1 eV.[37] The binding energies of Ga_2O_3 and GaAs were also measured for us by an independent laboratory (using a Hewlett-Packard 5950A ESCA spectrometer).[38]

The ligand shifts for the standard compounds may be calculated from the chemical shifts given in Table III. This is done in Table IV. In the first column of Table IV, we list the compounds. In the second column, we list the shifts of the As or Ga 3d levels in these compounds with respect to their binding energy for the free element. A positive chemical shift is defined as a shift to higher binding energy. Columns four and five give the number and type of ligand for the compounds in the first column. In GaAs, each gallium (or arsenic) has four arsenic (or gallium) ligands. As_2O_3 has three single oxygen single bonds per arsenic atom. Ga_2O_3 is coordinated by six oxygens. As_2O_5 has three oxygen single bonds and one oxygen double bond per arsenic. $GaAsO_4$ has a quartz-like structure[39] with the silicon atoms replaced by alternating Ga and As. This results in each gallium and arsenic having four oxygen ligands.

The ligand shifts, ΔE_j, are the shifts due to the particular ligand j and are obtained most simply by dividing the total shift (column two) by the number of ligands (column four). When there are two types of ligands in the compound in question, such as A_2O_5 which has three $-O$ and one $=O$, we use another compound, As_2O_3 in this case, to determine one set of the shifts and then we solve for the second. In the last two

rows of Table IV, we have calculated, using the experimentally determined shifts with Eq. (1), the shifts that we would expect from $GaAsO_4$. We should note, in comparing the ligand shifts of Table IV with those given in Table V of Ref. 35, that the shifts quoted here are only 3-d shifts, whereas those used by Bahl et al[35] are the average of the shifts of all the core levels. There will be a slight discrepancy if this point is not realized.

As mentioned in the previous discussion, when the GaAs (110) surface is exposed to unexcited oxygen, only one shifted arsenic peak, AsI, is seen for all coverages. This implies that only a single site is involved in the chemisorption of unexcited oxygen. Thus, we must conclude that the AsI peak, with a shift of 2.9 eV with respect to GaAs (2.3 eV with respect to elemental As), is due to one oxygen atom or molecule bonded to a surface arsenic atom. The shift of the AsI peak is much larger than either the shift due to a single As-O bond (ΔE_B = 0.87 eV with respect to GaAs) or of an oxygen-arsenic double bond (ΔE_B = 1.7 eV with respect to GaAs). In fact, the experimentally determined shift of 2.9 eV is closer to the shift expected from three oxygens singly bonded to each surface arsenic atom, necessitating the breaking of back bonds. However, this latter situation implies that <u>three</u>, not one, chemically shifted As 3-d peaks (ΔE_B with respect to GaAs $\approx$ -0.87, -2.04, and -3.06 eV) should be observed corresponding to the three possible oxidation states which the surface arsenic atoms would then have. We would expect to see the -0.87 and -2.04 eV peaks for low and intermediate coverages and the -3.06 eV peak almost exclusively for the high coverages. This is clearly <u>not</u> what we observe experimentally and, because of the high surface sensitivity of our measurement, we would be able to see

such intermediate states. Therefore, we must conclude that the AsI peak is due to a single arsenic oxygen bond that gives a binding energy shift three times larger than what is expected from an As-O bond in an arsenic oxide. In the case of As_2O_3, the oxygens are more electronegative than the arsenic, so there is an equal transfer of charge away from the arsenic along each ligand. In the case of oxygen chemisorbed to the GaAs surface, the gallium back bonds transfer charge to the arsenic so the oxygen is the only ligand in which there is charge transfer away from the arsenic. That is, the single oxygen ligand does not have any competition for the charge on the arsenic. Consequently, the oxygen ligand in this case could give a much larger shift than would be predicted by a simple ligand shift analysis where the different electronegativities of the various ligands have not been taken into account. These same arguments, now used to estimate the shift of the Ga-3d due to a chemisorbed oxygen, would imply that the shift should be less than 0.33 eV (the ligand shift due to a single oxygen ligand in Ga_2O_3). Consequently, we would not expect to see a distinct chemically shifted peak for the case of oxygen chemisorption on the surface gallium atoms. We would, however, expect to see an asymmetric broadening of the Ga-3d level. For exposures below 10^{10} LO_2, as mentioned in Section III.A, there is no asymmetric broadening of the Ga-3d level to better than 0.03 eV. We can also exclude the possibility of bonding oxygen to the surface gallium atoms by breaking back bonds because, in this situation, we should definitely see an asymmetric broadening of the Ga 3-d level along with intermediate oxidation states of the arsenic atoms, neither of which is observed experimentally.

The AsII peak in the "heavily oxidized" curve of Fig. 10 is shifted 4.6 eV with respect to the arsenic in GaAs (or 4.0 eV with respect to elemental As). This value is bracketed by the experimentally determined value of 4.9 eV (4.3 eV with respect to elemental As) for As_2O_5 and the calculated value of 4.1 eV (3.5 eV with respect to elemental As) for $GaAsO_4$. The average of these two shifts gives 4.5 eV (3.9 eV with respect to elemental As), very close to the value measured in this work. This seemingly fortuitous result may be interpreted as follows. There are three single bonds and one double bond in As_2O_5, whereas $GaAsO_4$ contains four single bonds. The fact that the shift we measure lies between these two shifts is significant because, first, it indicates there are four oxygens bound to the As and, secondly, these bonds must have some double bond character. In the rest of the discussion, we will simply refer to this compound as As_2O_5. There are, however, no peaks in the spectra corresponding to $GaAsO_4$. As mentioned above, with reference to Fig. 9, the gallium peak starts to shift as soon as the AsII peak appears. The magnitude of the gallium shift is 1 eV which corresponds to Ga_2O_3 (compare Tables II and III). The fact that we start forming oxides of Ga and As at the same time clearly indicates that back bonds are being broken and true oxidation of the surface is occurring. We should note again that we do not observe any intermediate oxidation states for the gallium.

In the "very heavily oxidized" spectrum of Fig. 10, the gallium peak, GaI, is still shifted by 1 eV, indicating the presence of bulk Ga_2O_3. But, now, the peak labeled AsIII is shifted 0.4 eV with respect to the unshifted arsenic peak, Ga(As). The shift we expect between free arsenic and arsenic in GaAs is 0.6 eV. Thus, this peak

could be due to free As or, equally likely, arsenic bound to only one gallium atom (see the -Ga ligand shifts in Table IV for Ga(As)). The latter case would give a shift of about 0.4 eV. Therefore, it is plausible that this peak is due to either free arsenic or arsenic bound to, at most, one gallium atom. The second arsenic peak in this spectrum, labeled AsIV, is shifted 2.6 eV with respect to the As in GaAs. This is exactly the same as the shift observed for bulk As_2O_3 (Table III).

As mentioned above, InP behaves exactly like GaAs in the chemisorption stage. As in the case for the AsI peak, the chemical shift in the P-2p (ΔE_B = 4.4 eV) is much larger than one would expect by simply adding an -O or =O group. The shifts in these two cases are 0.24 and 1.38 eV, respectively.[40] This larger shift is again probably due to increased charge transfer from the phosphorous to the oxygen because of the low electronegativity of the surrounding indium atoms. Thus, the same arguments used above for GaAs may be used here.

The case of GaSb (110) is much simpler than that of InP or GaAs. Both the Ga and Sb peaks shift simultaneously. Therefore, bonds are being broken in order to allow charge transfer from both the gallium and antimony atoms, resulting in the simultaneous formation of both gallium and antimony oxides. This difference in the mechanisms of oxygen adsorption is also reflected as a difference in the adsorption kinetics between GaAs and GaSb. This is most clearly seen by comparing the oxygen uptake curves of Figs. 3 and 7. We can immediately make two observations. First, the shapes of these two curves for oxygen coverage <u>versus</u> exposure are rather different and, secondly, the GaSb adsorbs oxygen more readily than the GaAs. The second observation can be understood by considering the ionicities of Ga, As, and Sb. There is a larger electronegativity

difference between Ga and As than between Ga and Sb. This would imply that the GaAs bond is stronger than that of GaSb, giving a surface that is more resistant to chemisorption of oxygen. In view of this argument, we would expect that InP would behave like GaAs since the electronegativity difference between In and P is also large. This is indeed the case, as was shown above in Fig. 8. The dependence of oxygen uptake with electronegativity difference that we see here agrees with the work of Mark and Creighton[41] in which they observe a decrease in oxygen uptake with increasing bonding ionicity.

The difference in shape between the two curves in Figs. 3 and 7 seems to be very closely tied to the fact that oxygen chemisorbs to the GaAs surface, leaving it intact while, for GaSb, the oxygen actually breaks back bonds and forms oxides. Thus, for GaAs, we expect saturation at half monolayer coverage with the rate of oxygen uptake being a function of the coverage. For GaSb, on the other hand, the coverage does not stop at half monolayer, as seen by the vertical scale of Fig. 7 (this scale was determined by comparing the oxygen coverages on the GaAs and GaSb spectra from the O2p intensity and assuming half monolayer coverage at saturation for GaAs). In fact, the oxygen uptake for GaSb should be controlled mainly by diffusion of oxygen through the oxide layer to the unoxidized substrate.

At zero coverage, the approximate sticking coefficient is 2×10^{-4} for the GaSb surface and 8×10^{-10} for the GaAs surface. The measured sticking coefficient for GaAs is about five orders of magnitude smaller than what is reported in the literature for the cleaved GaAs (110) surface.[15] The larger sticking probability reported in the literature could possibly be due to the fact that the precautions exercised[15] to

avoid effects of excited oxygen[20] were not sufficient or that the surfaces used were not perfect enough.[12,24] Furthermore, in the other studies, saturation is seen at 10^6 LO_2, whereas at this exposure we see less than 10% of saturation coverage (see Fig. 3).

B. Model for Oxidation of GaAs (110)

The sequence of events leading to the formation of a thick oxide layer on GaAs may be summarized as follows: (1) the (excited or unexcited) oxygen is first chemisorbed on the surface As atoms with no breaking of back bonds; (2) addition of excited oxygen leads to the breaking of bonds between the first and second layers in the crystal

and the formation of less than two layers of As_2O_5/AsO_2 and Ga_2O_3; (3) further exposure to oxygen (excited) causes the oxidation to proceed further into the bulk, allowing the newly formed arsenic oxides to sublime and leave an oxide layer mainly composed of Ga_2O_3 with small amounts of bulk As_2O_3 and free As.

The chemisorption step, which is identical for both excited and unexcited oxygen, seems to be a necessary precursor to the breaking of back bonds. In order to break the Ga-As back bonds, we not only need excited oxygen, but also the presence of an oxygen chemisorbed to the arsenic dangling bond. Therefore, the energy carried to the surface by the excited oxygen must be coupled to the strain energy due to the previously chemisorbed oxygen. In fact, if a saturation coverage of oxygen is preadsorbed on the surface and then that surface is exposed to excited oxygen, <u>two</u> layers of GaAs can be oxidized by an exposure <u>20 times less</u> than was necessary to gradually oxidize only the <u>top layer</u> (compare the top curve of Fig. 9 with the "heavily oxidized curve" of Fig. 10).

The initial oxidation results in the formation of the most oxygen rich oxide of arsenic, satisfying all four of the possible arsenic bonds. This oxide, rather than As_2O_3, is formed because the part of the substrate being oxidized is in direct contact with the gaseous oxygen present in the chamber during exposure and enough oxygen is present to fully oxidize both the surface arsenic and gallium atoms. If the surface is oxidized even further, the substrate peaks are no longer visible, indicating that more than three or four molecular layers of oxide have been formed. This step in the oxidation is then the start of true oxide formation in which there is no longer a direct bonding between the GaAs lattice and most of the oxide and interface layer. In such a situation,

as soon as a gallium or arsenic atom has broken its bonds to the underlying lattice due to oxidation of a neighboring site, it is no longer constrained to follow the chemistry of the GaAs surface. Instead, the gallium and arsenic atoms are now free to follow their elemental chemistries. In the case of gallium and arsenic, the formation of Ga_2O_3 is favored over arsenic oxide formation, as seen by comparing their respective heats of formation.[42] Consequently, elemental gallium is oxidized more readily than elemental arsenic. Since there is now a layer of oxide through which the oxygen must diffuse in order to reach the substrate crystal, the amount of oxygen available for oxidation is limited and, consequently, the gallium will be oxidized first and then the arsenic. This is indeed the case, as seen by the fact that the thick oxide contains elemental arsenic as well as bulk As_2O_3. No elemental Ga is seen in the spectrum for the "very heavily oxidized" surface, indicating that the Ga may even be able to reduce As_2O_3 to elemental As. This could explain the presence of elemental As and no elemental Ga in the thick oxide. No As_2O_5 is present because oxygen is now scarce and the formation of the lower oxide of arsenic is more favorable. If the substrate were heated, resulting in a greater oxygen mobility through the oxide and, thus, a greater oxygen concentration at the interface, the situation would be much like that for the "heavily oxidized" spectrum, so As_2O_5 should then be present in the oxide layer.

Finally, there is very little arsenic (elemental or oxide) present in the thick oxide, indicating that the volatile As_2O_3 does sublime from the surface leaving an oxide rich in Ga_2O_3 with small amounts of As_2O_3 and elemental arsenic.

Caution should be exercised in trying to generalize these results to the polar faces or even (110) faces prepared by different techniques. For example, the work of Ranke and Jacobi[12] on the polar faces prepared either by ion bombardment and annealing or molecular beam epitaxy suggests that oxygen sticks to the surface gallium atoms. However, the sticking coefficients reported in those studies were significantly higher than those for the cleaved (110) surface. These larger sticking coefficients were attributed to the presence of Ga atoms on the polar surface with unsaturated bonds.[12] From our results on the oxidation of GaAs (110) with excited oxygen, we saw that, as soon as a Ga-As bond is broken, i.e., as soon as an unsaturated Ga bond is created, the Ga atom immediately becomes oxidized. Thus, if the polar surfaces studied by Ranke and Jacobi do indeed have unsaturated Ga bonds, it is not at all surprising that oxygen bonds preferentially to the Ga atoms. In fact, it would be entirely consistent with the results of our work. Therefore, it seems clear that the chemisorption properties of the various faces are very dependent on the integrity of the surface which is a function of both the fundamental properties of the particular face as well as the surface preparation technique. The resistance to oxidation exhibited by the cleaved GaAs (110) surfaces compared to the other surfaces or (110) surfaces prepared by techniques other than cleavage implies that the cleaved surfaces are more intact, i.e., all the surface atoms have saturated bonds, since the resistance to oxidation is characteristic of a low density of unsaturated bonds.

C. Determination of the Escape Depth

The relative escape depth for electrons with kinetic energies between 20 and 200 eV may be determined from our experimental results quite simply and elegantly by merely plotting the ratio of the areas under the shifted and unshifted arsenic peaks, As/AsI, as a function of photon energy. This curve is given in Fig. 11. The horizontal scale gives the kinetic energies of the electrons in the crystal. The photon energies that were used for each point are obtained by adding 40 eV (the approximate As-3d binding energy) to the given kinetic energies. The right-most vertical scale gives the actual ratio of the areas of the unshifted to shifted As-3d peaks as measured from the spectra of GaAs (110) + 10^{12} LO_2 for various photon energies. The minimum in the escape depth curve occurs around 60 eV kinetic energy ($h\nu = 100$ eV). The error bars associated with the points are due to the uncertainties in measuring the areas under the peaks.

One assumption that allows us to calculate the absolute escape depth, L(E), is that there is one oxygen molecule (or atom, for this discussion the nature of the adsorbed species is irrelevant) per surface arsenic atom by an exposure of 10^{12} LO_2. It seems adequately clear that saturation is reached at 10^{12} LO_2, but we have yet done no measurements to determine the actual oxygen coverage at this exposure. However, from the oxidation data of Fig. 2, it does seem to be a reasonable assumption. The major source of error is introduced into the calculation when we try to fix the absolute value of the escape depth. This entails estimating the thickness, x_1, of the topmost GaAs plus chemisorbed oxygen layer. This one thickness will then allow us to give an absolute value to the escape depth.

Consider a system composed of two uniform layers, surface and bulk. Here, we neglect the fact that the surface layer is only one molecular layer and thus not uniform. But, in the spirit of the calculation, this assumption will not introduce an unreasonable amount of error. Assuming exponential attenuation of the emitted electrons and that the number of emitted electrons is proportional to the area under the appropriate peak in the photoemission spectrum, we may write

$$L(E) = \frac{x_1}{\ell n\ (As/AsI)^{-1} + 1}$$

Using tabulated values for the radii of arsenic and oxygen, we let $x_1 = 4 \pm 1.5$ Å.[42] Inserting this into the above equation gives the L(E) scale on the left-hand side of Fig. 11. The second scale on the right of Fig. 12 giving the molecular layers is obtained by dividing the nominal escape depth by the distance between the (110) planes which is approximately 4 Å. At the minimum, the escape depth is 5.8 ± 1.5 Å or approximately 1.5 molecular layers, substantiating our claims of a very large surface sensitivity. With this value for the escape depth, simple calculations show that a spectral feature from the bulk can no longer be seen if it is more than five molecular layers from the surface (this assumes a detectability limit of about 2% for well-separated peaks; if the peaks are close together, we must assume a higher detectability limit).

D. Surface Chemical Shift[43]

During the course of this work, we have studied the Ga-3d levels from the clean GaAs (110) surface over a wide range of photon energies ($35\ eV \leq h\nu \leq 240\ eV$). This photon energy range enables us to probe

between approximately 1.5 and 3 molecular layers giving, first, primarily surface and, second, more bulk contributions to the spectra. If an appreciable chemical shift in the core levels between the atoms on the surface and in the bulk were present, it would definitely show up as a change in the full width at half maximum of the Ga-3d levels when a photon energy corresponding to a different escape depth was used. The fact is that we see no such effect to better than ±0.1 eV. In view of the surface state model of Fig. 2, these results indicate that there must be enough redistribution of charge along the back bonds, possibly involving several molecular layers, to keep the total charge densities around the surface atoms the same as in the bulk. This charge redistribution may, in fact, be one of the reasons for the smearing of the spin orbit splitting of the Ga and As 3-d levels.

The lack of chemical shift between the surface and bulk atoms also implies that the ligand shifts due to each back bond, i.e., the bonds connecting the surface layer to the rest of the crystal, will be 4/3 larger than the shifts due to the bonds in the bulk. The reason for this is, of course, that the same shift is due to three bonds for the atoms at the surface compared to four in the bulk. This again fits in well with the surface state model of Fig. 1 since the arsenic atoms at the surface must have more charge and the gallium atoms less than the corresponding atoms in the bulk.

ACKNOWLEDGMENT

We would like to thank Prof. W. A. Harrison for helpful discussions and the staff of the Stanford Synchrotron Radiation Project for their cooperation and assistance in this study.

REFERENCES

1. For a review of the latest developments in the field of GaAs surfaces and devices, consult the Proceedings of the 3rd Annual Conference on the Physics of Compound Semiconductor Interfaces in J. Vac. Sci. Technol. 13, No. 4 (1976).
2. P. E. Gregory, W. E. Spicer, S. Ciraci, and W. A. Harrison, App. Phys. Lett. 25, 511 (1974); P. E. Gregory and W. E. Spicer, Phys. Rev. B 13, 725 (1976) and Surf. Sci. 54, 229 (1976); W. E. Spicer and P. E. Gregory, Crit. Rev. Solid State Sci. 5, 231 (1975).
3. W. A. Harrison, Surf. Sci. 55, 1 (1976).
4. H. C. Gatos and M. C. Lavine, J. Electrochem. Soc. 107, 427 (1960); H. C. Gatos, J. Appl. Phys. 32, 1232 (1961); H. C. Gatos, J. Electrochem. Soc. 122, 287C (1975).
5. A. U. Mac Rae and G. W. Gobeli, in Semiconductors and Semimetals, Vol. 2, Physics of III-V Compounds, Eds., R. K. Willardson and A. C. Beer (Academic Press, New York, 1966), pp. 115-137; A. U. Mac Rae, Surf. Sci. 4, 247 (1966).
6. A. R. Lubinsky, C. B. Duke, B. W. Lee, and P. Mark, Phys. Rev. Lett. 36, 1058 (1976); C. B. Duke, A. R. Lubinsky, B. W. Lee, and P. Mark, J. Vac. Sci. Technol. 13, 761 (1976).
7. W. E. Spicer, I. Lindau, P. E. Gregory, C. M. Garner, P. Pianetta, and P. W. Chye, J. Vac. Sci. Technol. 13, 780 (1976).
8. J. D. Levine and S. Freeman, Phys. Rev. B 2, 3255 (1970).
9. D. J. Miller and D. Haneman, Phys. Rev. B 3, 2918 (1971).
10. R. Ludeke and L. Esaki, Phys. Rev. Lett. 33, 653 (1974) and R. Ludeke and A. Koma, Phys. Rev. Lett. 34, 817 (1975).

11. R. W. Nosker, P. Mark, and J. D. Levine, Surf. Sci. 19, 291 (1970).

12. W. Ranke and K. Jacobi, Surf. Sci. (in press), and references given therein.

13. P. Pianetta, I. Lindau, C. M. Garner, and W. E. Spicer, Phys. Rev. Lett. 35, 1356 (1975), and P. Pianetta, Ph.D. Thesis, Stanford University, 1976 (unpublished).

14. K. Jacobi and W. Ranke, J. Elect. Spectrosc. 8, 225 (1976).

15. R. Dorn, H. Lüth, and G. J. Russell, Phys. Rev. B 10, 5049 (1974).

16. H. Froitzheim and H. Ibach, Surf. Sci. 47, 713 (1975).

17. R. Ludeke and A. Koma, Crit. Rev. Solid State Sci. 5, 259 (1975), and J. Vac. Sci. Technol. 13, 241 (1976).

18. W. Ranke and K. Jacobi, Surf. Sci. 47, 525 (1975).

19. The objections to the interpretation presented in Ref. 17 are explained in: P. W. Chye, P. Pianetta, I. Lindau, and W. E. Spicer, 4th Annual Conference on the Physics of Compound Semiconductor Interfaces, Princeton, New Jersey, Feb 1977.

20. P. Pianetta, I. Lindau, C. M. Garner, and W. E. Spicer, Phys. Rev. Lett. 37, 1166 (1976), and references given therein.

21. S. Doniach, I. Lindau, W. E. Spicer, and H. Winick, J. Vac. Sci. Technol. 12, 1123 (1975).

22. I. Lindau and W. E. Spicer, J. Electron Spectrosc. 3, 409 (1974); M. Klasson, J. Hedman, A. Berndtsson, R. Nilsson, and C. Nordling, Physica Scripta 5, 93 (1972).

23. K. Siegbahn, J. Electron Spectrosc. 5, 3 (1975); U. Gelius, Physica Scripta 9, 133 (1974); T. D. Thomas, J. Am. Chem. Soc. 92, 4184 (1970); J. M. Hollander and D. A. Shirley, Ann. Rev. Nucl. Sci. 20, 435 (1970).

24. H. Ibach, Surf. Sci. 53, 444 (1975).

25. G. F. Derbenwick, D. T. Pierce, and W. E. Spicer, Methods of Experimental Physics (Academic Press, New York, 1974), Vol. 11, pp. 89-92.

26. F. C. Brown, R. Z. Bachrach, S. B. M. Hagstrom, N. Lien, and C. H. Pruett, in Vacuum Ultraviolet Radiation Physics, Eds., E. E. Koch, R. Haensel, and C. Kunz (Pergamon, New York, 1974), pp. 785-787.

27. The sample with $n = 0.5 \times 10^{18}$ cm^{-3} will be referred to sample LD1. It was used in the work of Refs. 7 and 20. In Ref. 7, it was called sample II. The sample with $n = 3.5 \times 10^{17}$ cm^{-3} will be called sample LD3; it was used in the work of Refs. 7 (Fig. 1), 13, and 20.

28. This sample was also used in the work described in Refs. 7, 20, and the work of P. W. Chye, I. A. Babalola, T. Sukegawa, and W. E. Spicer, Phys. Rev. Lett. 35, 1602 (1975).

29. The Thoria-coated iridium filament in the ion gauge allows lower filament temperatures ($< 800°C$) for a given emission current, relative to a Tungsten filament, so that no CO is generated by the hot filament.

30. In all the discussions that follow, we will refer to the molecular, unexcited oxygen simply as oxygen or O_2. We will refer to the oxygen excited by the ion gauge only as excited oxygen since the detailed nature of excited oxygen has never been established. Certainly, many forms must be considered, e.g., oxygen ions, atomic oxygen, ozone, molecular oxygen in excited form, etc.

31. A. Huijser and J. van Laar, Surf. Sci. 52, 202 (1975), and J. van Laar and A. Huijser, J. Vac. Sci. Technol. 13, 769 (1976).

32. I. Lindau, P. Pianetta, and W. E. Spicer, Phys. Lett. 57A, 225 (1976), and Proceedings of the International Conference on the Physics of X-ray Spectra, 30 Aug-2 Sep 1976, National Bureau of Standards, Gaithersburg, Maryland.

33. H. Ibach, K. Horn, R. Dorn, and H. Lüth, Surf. Sci. 38, 433 (1973); R. J. Archer and G. W. Gobeli, J. Phys. Chem. Sol. 26, 343 (1965).

34. W. Gudat and D. E. Eastman, J. Vac. Sci. Technol. 13, 831 (1976).

35. M. K. Bahl, R. O. Woodall, R. L. Watson, and K. J. Irgolic, J. Chem. Phys. 64, 1210 (1976).

36. G. Leonhardt, A. Berndtsson, J. Hedman, M. Klasson, R. Nilsson, and C. Nordling, Phys. Stat. Sol. (b) 60, 241 (1973).

37. G. Schön, J. Electron Spectrosc. 2, 75 (1973).

38. Surface Science Laboratories (Palo Alto, Ca.), ESCA Analytical Service Report #9-576.

39. R. W. G. Wyckoff, Crystal Structures (Interscience, New York, 1965) Volumes 2 and 3.

40. J. Hedman, M. Klasson, R. J. Lindberg, and C. Nordling, Electron Spectroscopy, D. A. Shirley, Ed. (North Holland, Amsterdam, 1972), p. 681.

41. P. Mark and W. F. Creighton, Appl. Phys. Lett. 27, 400 (1975).

42. Handbook of Chemistry and Physics, R. C. Weast, Ed. (The Chemical Rubber Company, Cleveland, Ohio, 1972), pp. D-45 and E-55.

43. J. E. Houston, R. L. Park, and G. E. Laramore, Phys. Rev. Lett. 30, 846 (1973), and references contained therein for other studies on surface chemical shifts.

Table I

EXPERIMENTAL BINDING ENERGIES REFERENCED TO THE VALENCE BAND MAXIMUM. The experimental accuracy is estimated to be ±0.05 eV with the largest uncertainty being in the determination of the valence band maximum. See text for discussion on difficulties in determining the binding energies with respect to the Fermi level.

Compound	Level	E_B (eV)
GaAs	Ga 3d	19.0
	As 3d	40.8
GaSb	Ga 3d	19.4
	Sb 4d 5/2	32.1
	Sb 4d 3/2	33.2
InP	In 4d	17.7
	P 2p	128.4

Table III

EXPERIMENTAL BINDING ENERGY DIFFERENCES (eV), FROM THE REFERENCES CITED, BETWEEN THE SHIFTED AND UNSHIFTED Ga AND As 3d LEVELS FOR VARIOUS COMPOUNDS OF Ga AND As. The data is presented in the same format as that of Table II.

ΔE_B (eV)	As_2O_3 35,36	Ga(As) 36,38,40,41	As 35,36	Ga_2O_3 36,37,38	(Ga)As 36,38,50,41	Ga 36,37
As_2O_5	1.7	4.9	4.3	25.7	26.6	27.7
As_2O_3		3.2	2.6	24.0	24.9	26.0
Ga(As)[a]			-0.6	20.8	21.7	22.8
As				21.4	22.3	23.4
Ga_2O_3					0.9	2.0
(Ga)As						1.1

(a) See text for the discussion about reliably determining the shifts between the semiconductor compounds and the other compounds in this table.

Table II

EXPERIMENTAL BINDING ENERGY DIFFERENCES (eV), FROM THIS WORK, BETWEEN THE SHIFTED AND UNSHIFTED Ga AND As 3d LEVELS FOR THE CLEAN AND OXIDIZED GaAs (110) SURFACE. The entries were obtained by subtracting the binding energies of the levels in the top row from those in the left most column.

ΔE_B (eV)	AsIII	AsII	AsI	Ga(As)	GaI	(Ga)As
AsIV[a]	2.8	-1.4[c]	0.3	3.2	24.0	25.0
AsIII		-4.2	-2.5	0.4	21.2	20.2
AsII			1.7	4.6	25.4	26.4
AsI				2.9	23.7	24.7
Ga(As)[b]					20.8	21.8
GaI						1.0

(a) The designations AsI, AsII, etc. refer to the labeling of Fig. 10.

(b) Ga(As) refers to As in GaAs; similarly, (Ga)As refers to Ga in GaAs.

(c) The negative shift means that AsII has a larger binding energy than AsIV.

Table IV

EXPERIMENTAL LIGAND SHIFTS OF THE Ga AND As 3d LEVELS FOR THE COMPOUNDS WHOSE SHIFTS WERE GIVEN IN TABLE III

Compound	ΔE_e (eV)[a]	ΔE_j (eV)[b]	n_j[c]	Ligand
As_2O_5	4.3	0.87	3	- O
		1.7	1	= O
As_2O_3	2.6	0.87	3	- O
Ga(As)	-0.6	-0.15	4	- Ga
Ga_2O_3	2.0	0.33	6	- O
(Ga)As	1.1	0.28	4	- As
$Ga(As)O_4$[d]	3.5	0.87	4	- O
$(Ga)AsO_4$[d]	1.3	0.33	4	- O

(a) ΔE_e is the binding energy shift with respect to the free element.

(b) ΔE_j is the ligand shift referenced to the free element where $\Delta E_e = n_j \Delta E_j$, summed over all j.

(c) n_j is the number of ligands of the given kind.

(d) Note these are not experimentally determined shifts; these shifts are calculated for the ideal structures using the ligand shifts given in the rest of the table.

FIGURE CAPTIONS

Fig. 1. The reconstructed (110) surface with an energy level diagram showing the location of the filled (As-derived) and empty (Ga-derived) surface states.

Fig. 2. EDC's of clean and oxygen exposed n-type GaAs (110) at $h\nu$ = 100 eV. The exposure of 1×10^{12} LO_2 (1 L = 10^{-6} torr-sec) was made on sample LD1, while the smaller exposures were all on sample LD3.

Fig. 3. The relative oxygen uptake of the GaAs (110) surface as a function of exposure determined from the area under the shifted As-3d levels ($\triangle$). The area of the unshifted As-3d levels (∇) is also plotted. The scale on the right assumes saturation is reached at 10^{12} LO_2.

Fig. 4. The valence band of clean n-type GaAs (110) and the same surface exposed to the indicated exposures. These curves are blow-ups of the valence band region of Fig. 2.

Fig. 5. EDC's of clean and oxygen exposed n-type GaSb (110) at $h\nu$ = 100 eV. Notice that both the Ga and Sb shift simultaneously with increasing oxygen exposure.

Fig. 6. EDC's of GaSb exposed to 5×10^{8} LO_2 for three photon energies showing the variation in the cross section of the Sb-4d levels <u>versus</u> photon energy.

Fig. 7. The relative oxygen uptake of the GaSb (110) surface as a function of exposure, determined from the area under the O-2p level. The vertical scale is obtained by comparing the areas under the O-2p in the spectra of Fig. 5 to the areas under the O-2p in Fig. 2 for GaAs.

Fig. 8. EDC's of clean and oxygen exposed p-type InP (110). The In-4d level was measured at $h\nu = 80$ eV and the P-2p at $h\nu = 160$ eV.

Fig. 9. EDC's of clean p-type GaAs (110) and the clean surface exposed to excited oxygen at $h\nu = 100$ eV.

Fig. 10. EDC's of n-type GaAs (110), LD1, for the clean surface, the clean surface + 10^{12} LO_2, the previous surface + 5×10^5 L excited oxygen with a 0.4 ma ion gauge emission current ("HEAVILY OXIDIZED"), and the clean surface exposed to 5×10^5 L excited oxygen with 4.0 ma ion gauge emission current ("VERY HEAVILY OXIDIZED").

Fig. 11. Plot of the ratio of the unshifted to shifted As-3d levels as a function of electron kinetic energy for the GaAs (110) surface + 10^{12} LO_2 (right-most scale). The other two scales give the escape depth in Angstroms and molecular layers (see text).

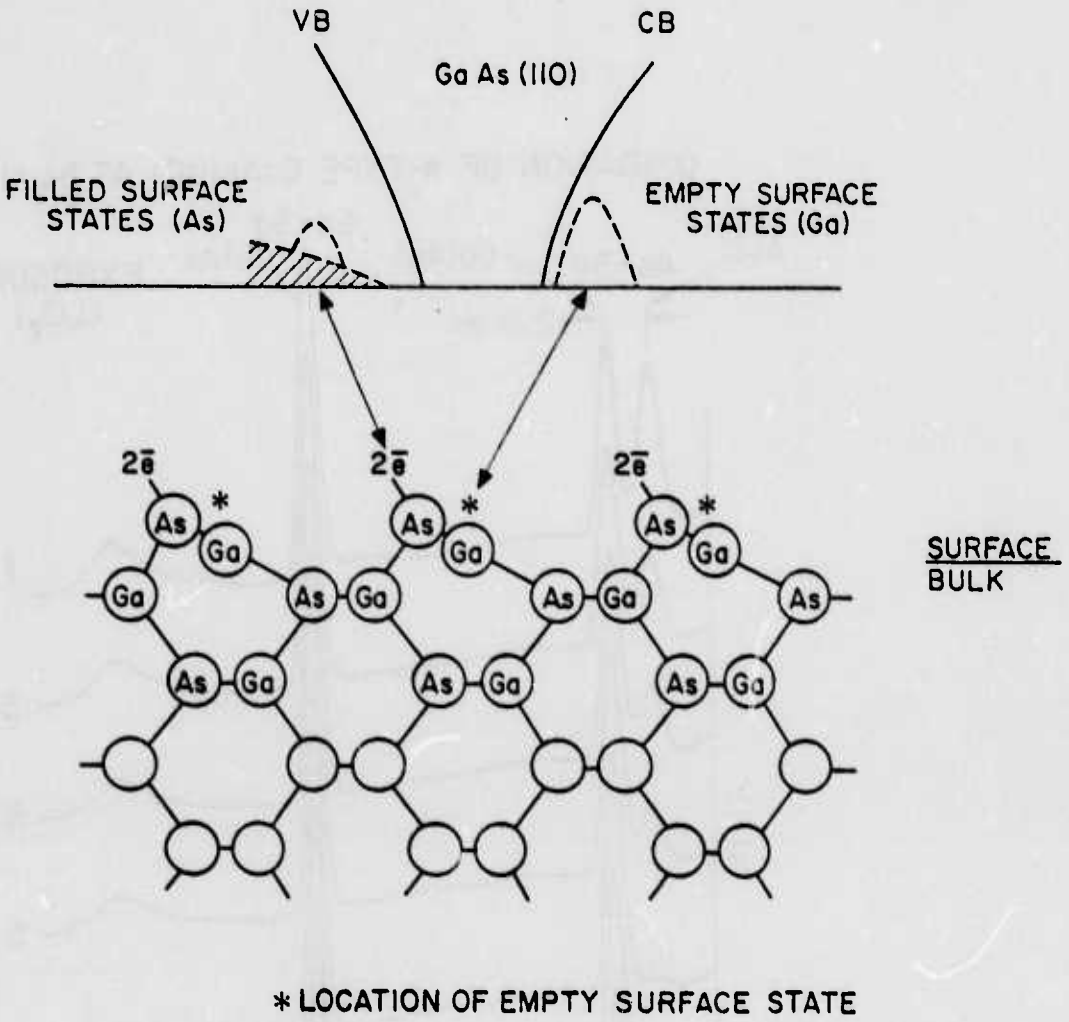
VB
CB
Ga As (110)
FILLED SURFACE STATES (As)
EMPTY SURFACE STATES (Ga)
2e
2e
2e
As
Ga
SURFACE
BULK
* LOCATION OF EMPTY SURFACE STATE

Fig. 1

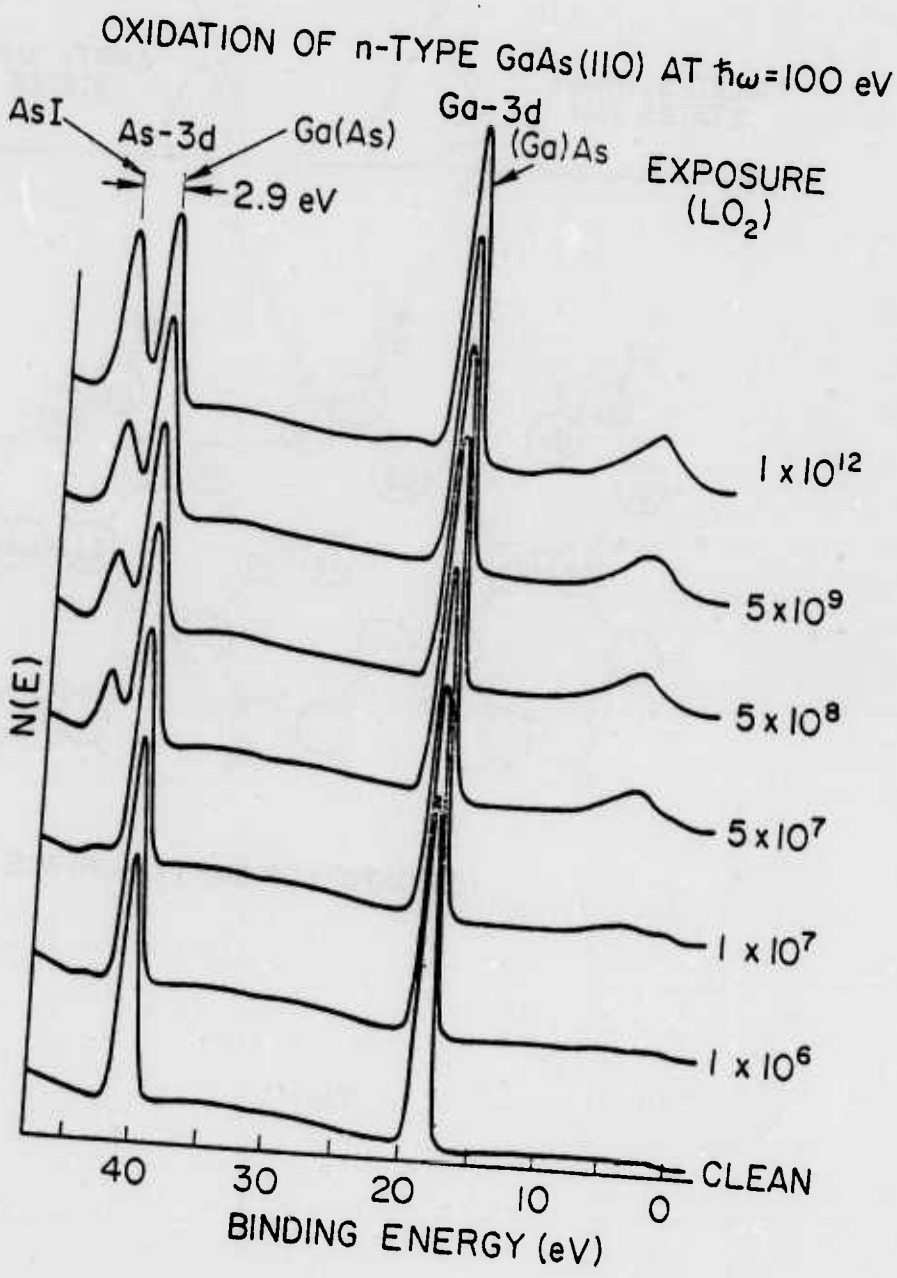
OXIDATION OF n-TYPE GaAs(110) AT ħω=100 eV
AsI
As-3d
Ga(As)
2.9 eV
Ga-3d
(Ga)As
EXPOSURE
(LO2)
1 x 10^12
5x10^9
5 x 10^8
5 x 10^7
1 x 10^7
1 x 10^6
CLEAN
N(E)
40
30
20
10
0
BINDING ENERGY (eV)

FIG.

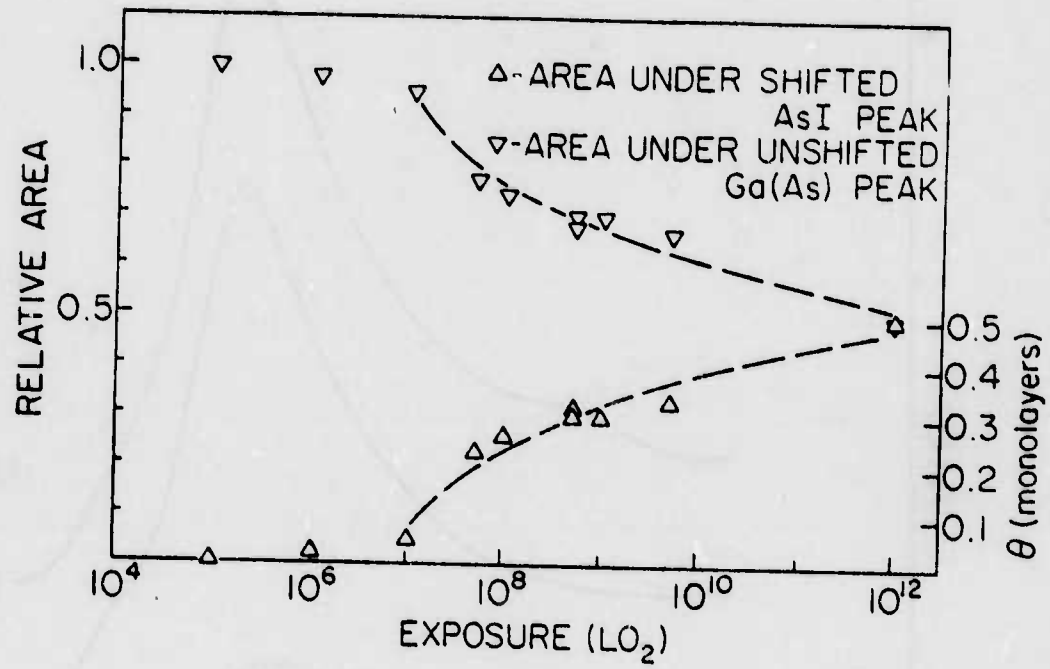
1.0
0.5
RELATIVE AREA
Δ-AREA UNDER SHIFTED
AsI PEAK
▽-AREA UNDER UNSHIFTED
Ga(As) PEAK
0.5
0.4
0.3
0.2
0.1
θ (monolayers)
10^4
10^6
10^8
10^10
10^12
EXPOSURE (LO2)

FIG.

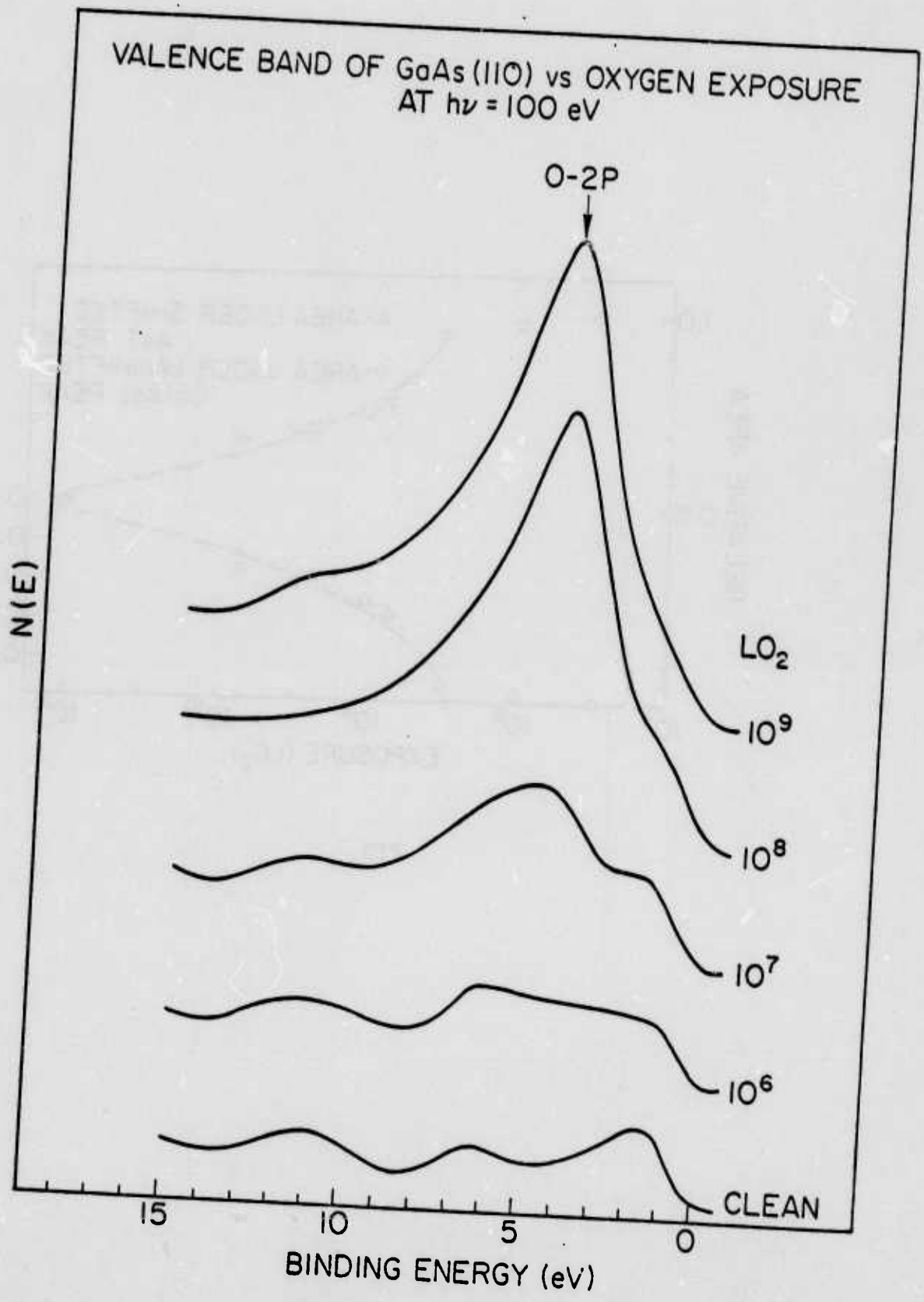
VALENCE BAND OF GaAs (110) vs OXYGEN EXPOSURE
AT hν = 100 eV
O-2P
N(E)
LO2
10^9
10^8
10^7
10^6
CLEAN
15
10
5
0
BINDING ENERGY (eV)

FIG. 4

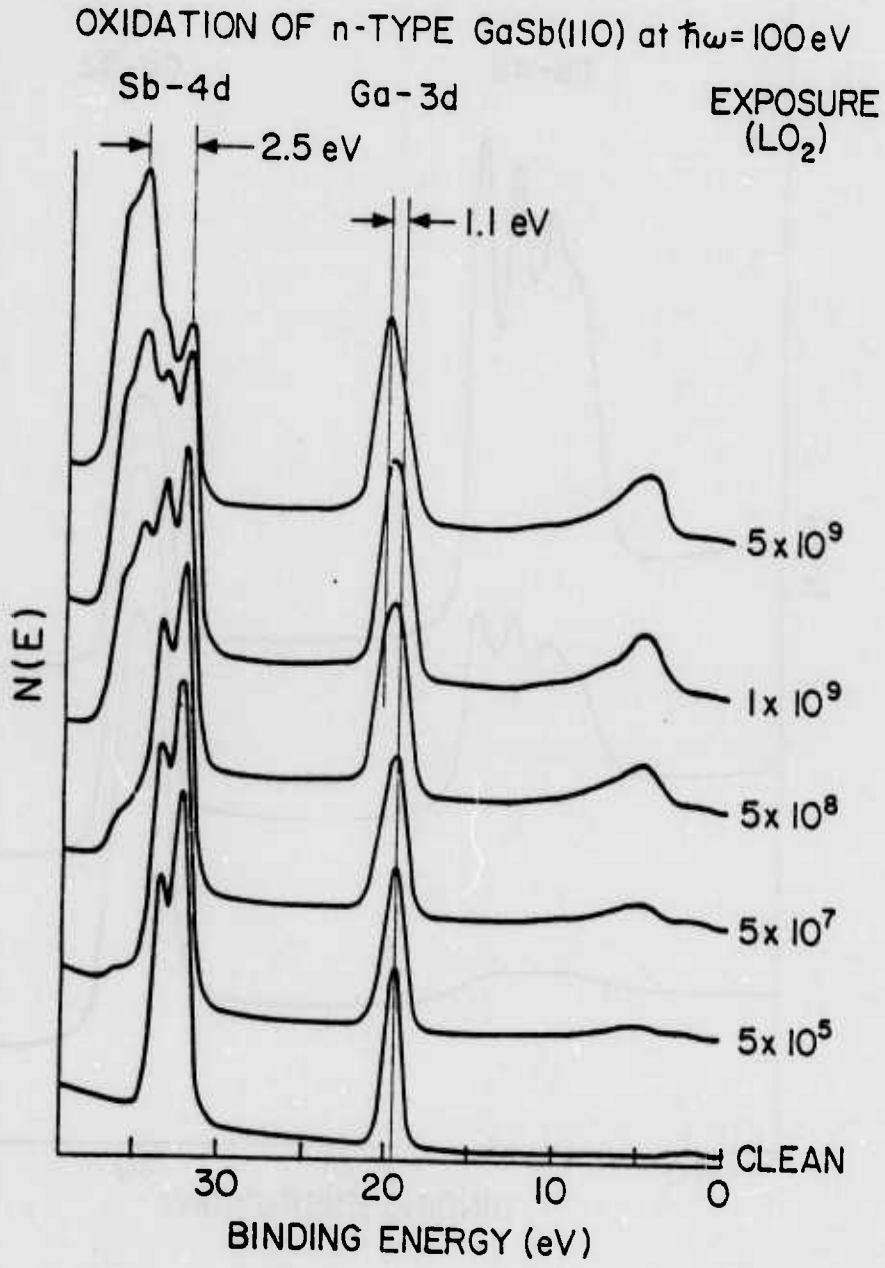
OXIDATION OF n-TYPE GaSb(110) at ħω = 100 eV
Sb-4d
Ga-3d
EXPOSURE
(LO2)
2.5 eV
1.1 eV
5x10^9
1x10^9
5x10^8
5x10^7
5x10^5
CLEAN
N(E)
30
20
10
0
BINDING ENERGY (eV)

Fig. 5

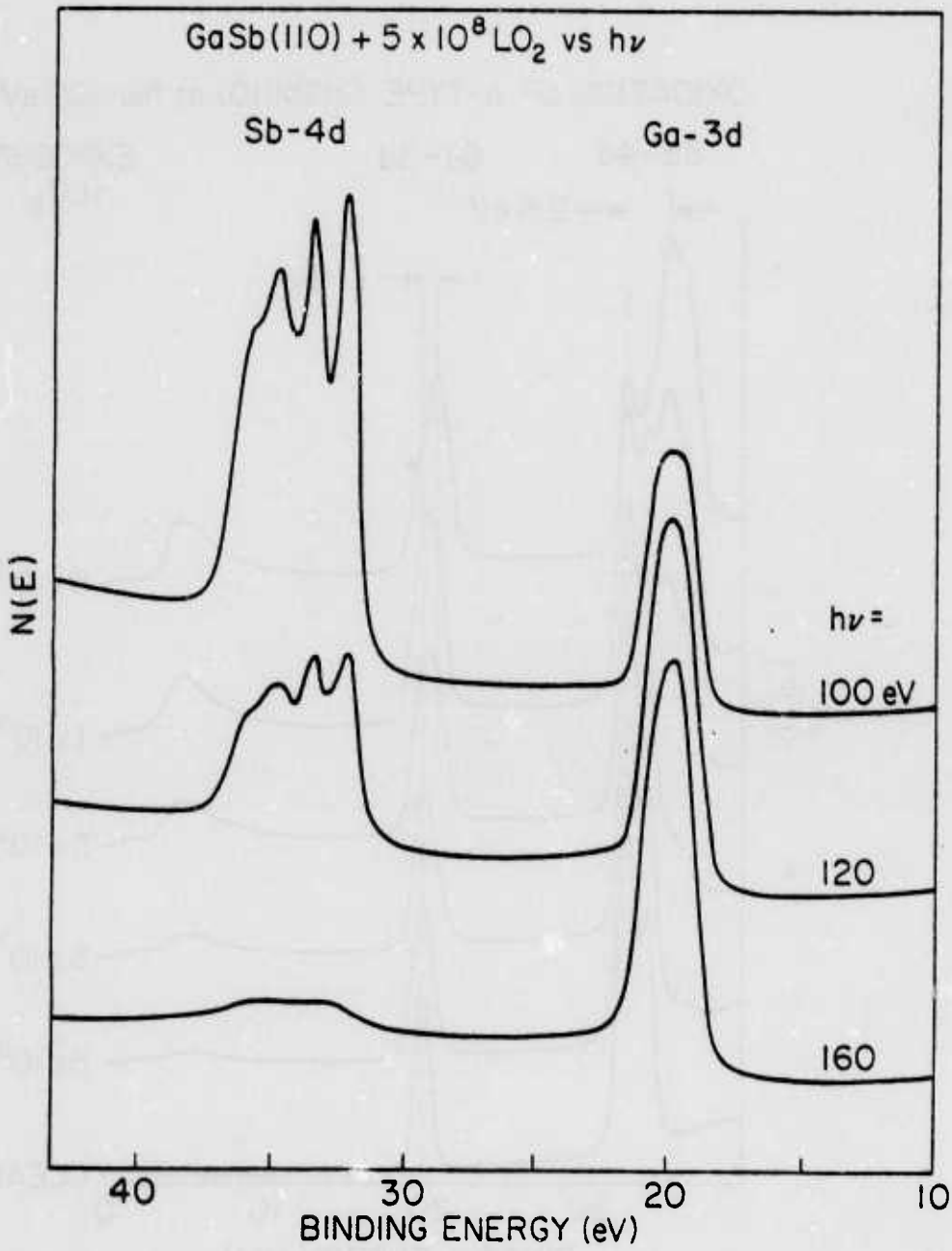
GaSb(110) + 5 x 10⁸ LO₂ vs hν
Sb-4d
Ga-3d
N(E)
hν =
100 eV
120
160
40
30
20
10
BINDING ENERGY (eV)

Fig. 6

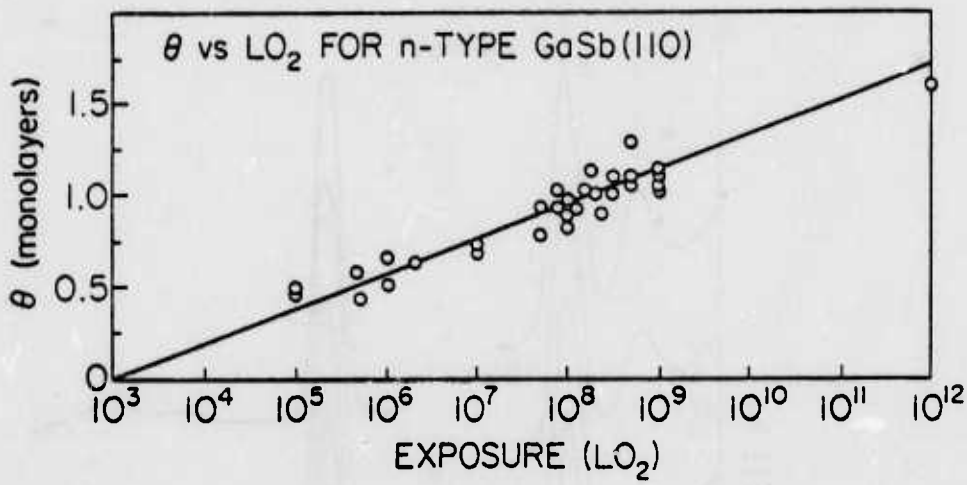
θ vs LO2 FOR n-TYPE GaSb(110)
θ (monolayers)
1.5
1.0
0.5
0
θ
10^3
10^4
10^5
10^6
10^7
10^8
10^9
10^10
10^11
10^12
EXPOSURE (LO2)

Fig. 7

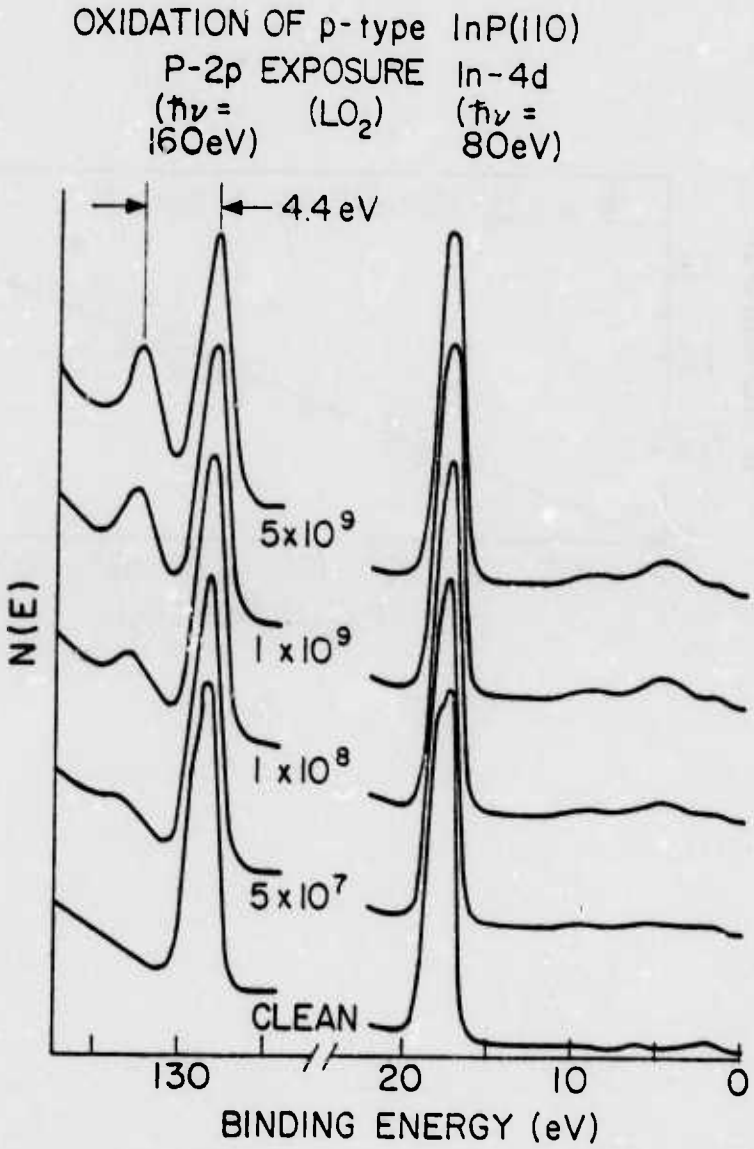
OXIDATION OF p-type InP(110)
P-2p EXPOSURE
(ħν = 160eV)
(LO2)
In-4d
(ħν = 80eV)
4.4 eV
5x10^9
1 x10^9
1 x10^8
5 x10^7
CLEAN
N(E)
130
20
10
0
BINDING ENERGY (eV)

FIG. 8

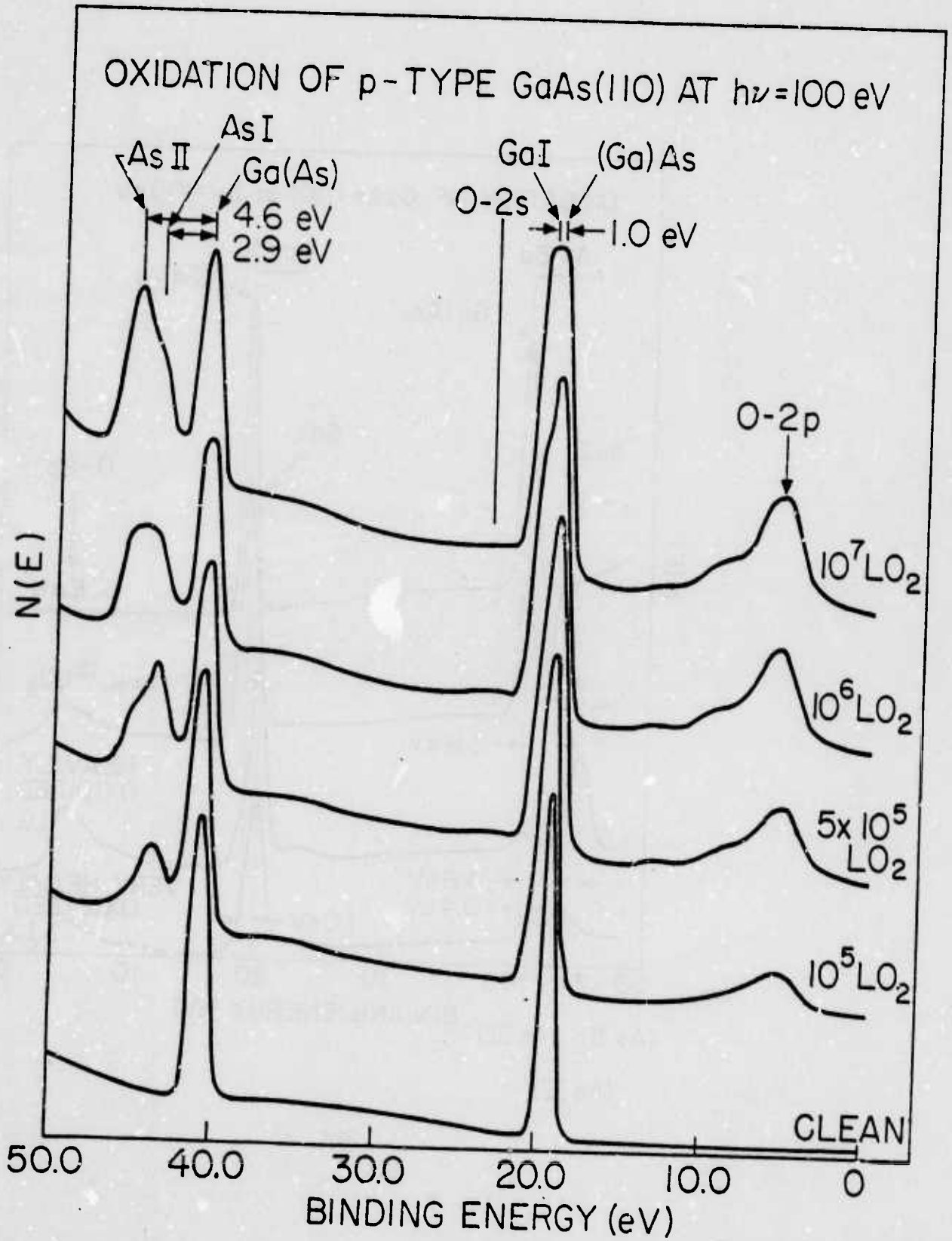
OXIDATION OF p-TYPE GaAs(110) AT hν=100 eV
As II
As I
Ga(As)
4.6 eV
2.9 eV
Ga I
(Ga) As
O-2s
1.0 eV
O-2p
N(E)
10^7 LO2
10^6 LO2
5x 10^5 LO2
10^5 LO2
CLEAN
50.0
40.0
30.0
20.0
10.0
0
BINDING ENERGY (eV)

FIG. 9

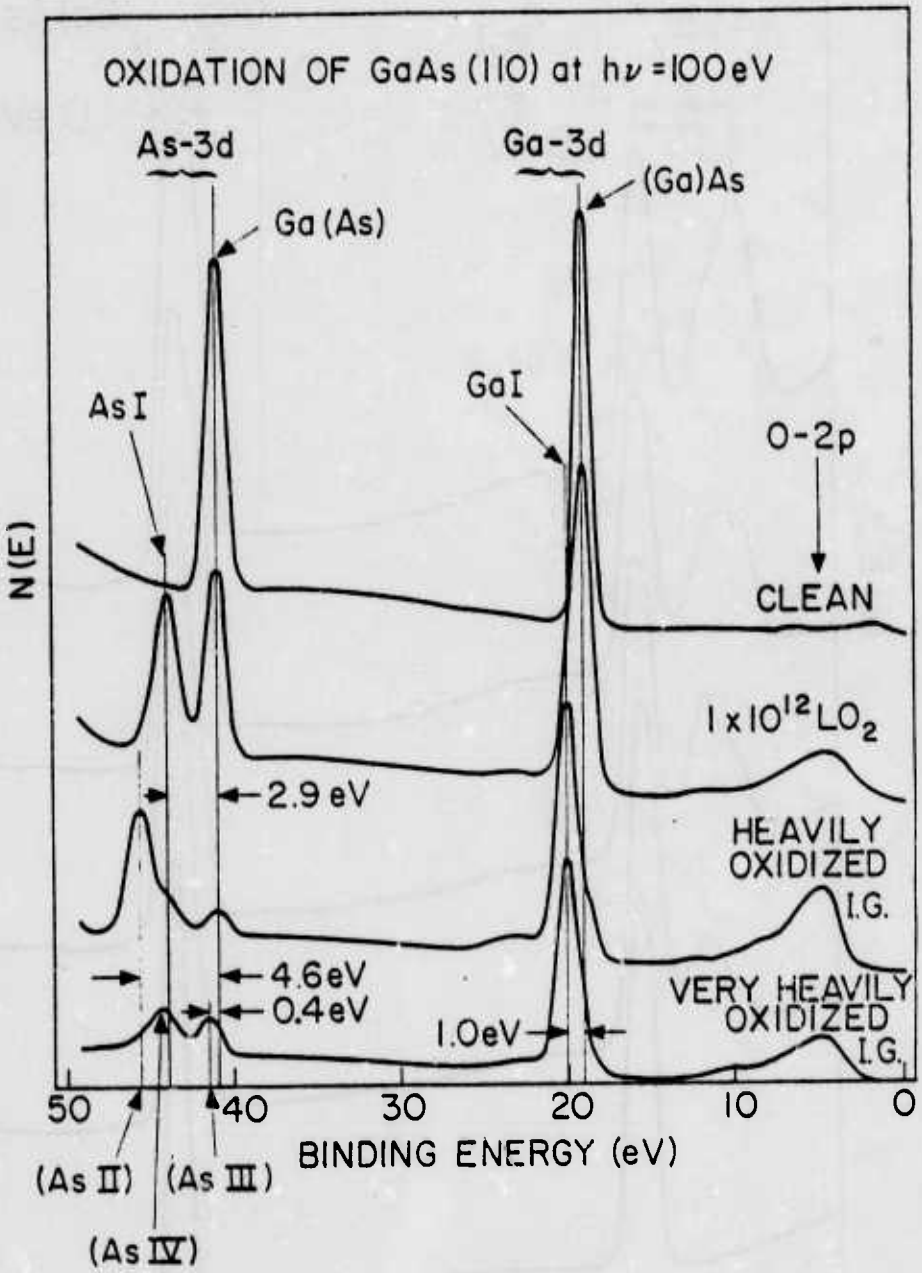
OXIDATION OF GaAs (110) at hν = 100eV
As-3d
Ga-3d
(Ga)As
Ga (As)
As I
Ga I
O-2p
CLEAN
1 x 10^12 LO2
2.9 eV
HEAVILY OXIDIZED
I.G.
4.6eV
0.4eV
1.0eV
VERY HEAVILY OXIDIZED
I.G.
N(E)
50
40
30
20
10
0
BINDING ENERGY (eV)
(As II)
(As III)
(As IV)

FIG. 10

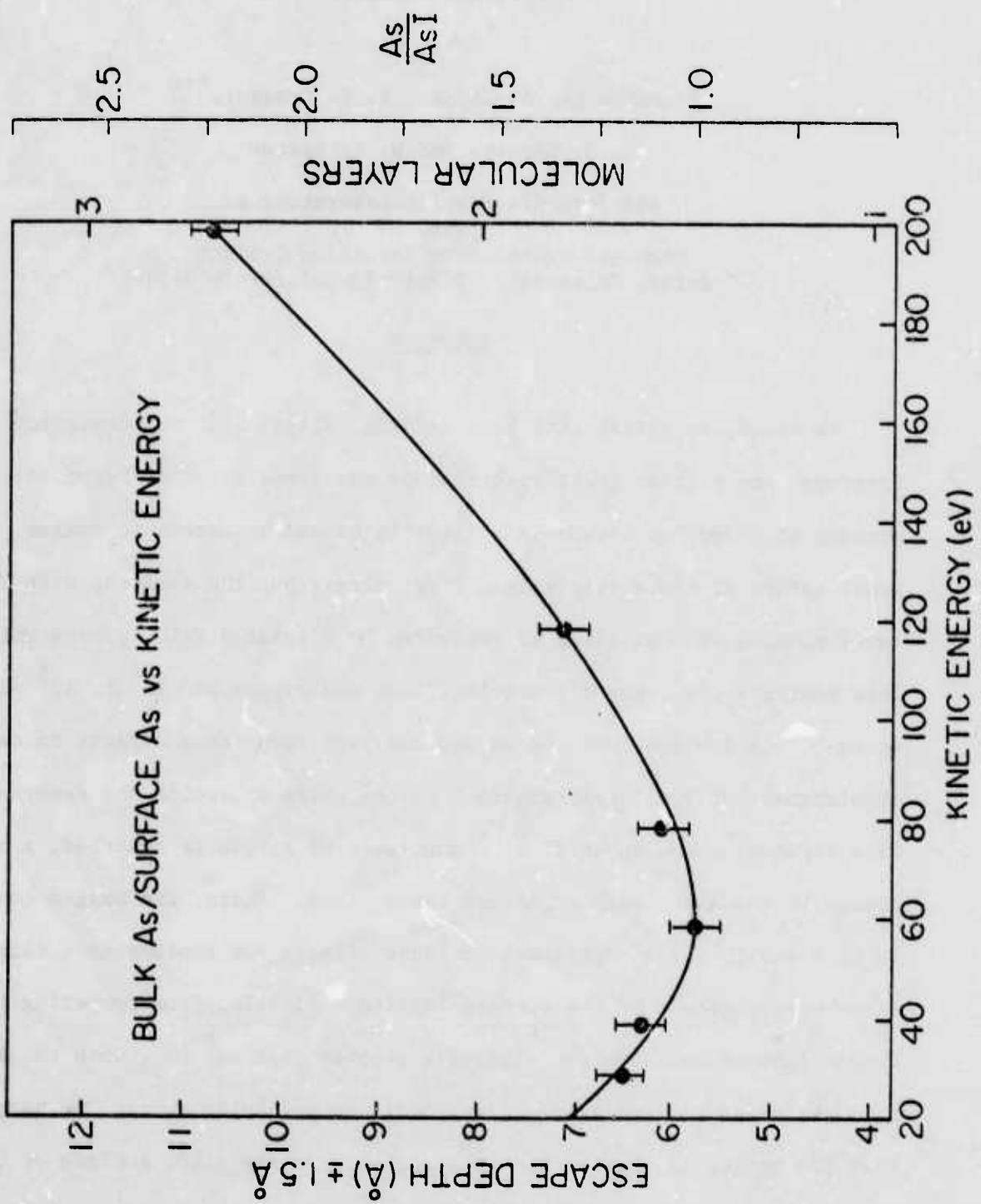
BULK As/SURFACE As vs KINETIC ENERGY
ESCAPE DEPTH (Å) ± 1.5 Å
KINETIC ENERGY (eV)
MOLECULAR LAYERS
As/AsI

Fig. 11

Chapter 7

VALENCE BAND STUDIES OF CLEAN AND OXYGEN EXPOSED GaAs (110) SURFACES*

by

P. Pianetta, I. Lindau, P. E. Gregory,**

C. M. Garner, and W. E. Spicer

Stanford Electronics Laboratories
and
Stanford Synchrotron Radiation Project
Stanford University, Stanford, California 94305

ABSTRACT

We found, by correlating band bending, ultraviolet photoemission spectroscopy, and partial yield spectroscopy measurements, that Fermi level pinning at midgap of n-type GaAs (110) is caused by extrinsic states. The exact nature of these states is not yet clear, but the surfaces with Fermi level pinning were strained as evidenced by a smeared valence band emission. This smearing was removed by as little as one oxygen per 10^4 to 10^5 surface atoms. This implies that the oxygen has very long range effects in causing spontaneous but small rearrangement of the surface lattice and removing surface strains. When about 5% of a monolayer of oxygen is adsorbed, a major change in the electronic structure takes place. Again, the oxygen coverage is very small, which suggests long range effects now leading to a fairly large rearrangement of the surface lattice. Finally, from comparing the oxygen induced emission for exposures greater than 10^7 LO_2, with the spectra from gas phase photoemission measurements on molecular oxygen, we suggest that the oxygen is chemisorbed as a molecule on the (110) surface of GaAs.

*Work supported by the Advanced Research Projects Agency of the Department of Defense monitored by Night Vision Laboratory, U.S. Army Electronics Command under Contract No. DAAK 02-74-C-0069; by the Office of Naval Research Contract No. N00014-75-C-0289; by the National Science Foundation Contract No. DMR 73-07692 A02 in cooperation with the Stanford Linear Accelerator Center and the U.S. Energy Research and Development Administration.

**Present address: Varian Associates, Palo Alto, California.

I. INTRODUCTION

The atomic structure of the GaAs (110) surface has been the object of numerous theoretical and experimental studies. LEED measurements[1] as well as theoretical predictions[2] have suggested that the GaAs (110) surface rearranges with the surface arsenic atoms moving out and the surface gallium atoms in. The exact values of these displacements are still under investigation. It is not clear how useful LEED is in detecting small changes in the surface rearrangement due to defects or oxygen adsorption. Recent calculations have shown that the valence band electronic structure of GaAs (110) surfaces depends markedly on the surface rearrangement.[3,4] It is difficult, at this point, to correlate differences in the experimentally determined valence band electronic structures to actual lattice distortions since the calculations that have been performed consider only the extreme cases of the fully relaxed and ideal surfaces. Small displacements from these two extremes have not yet been considered. Consequently, we will not attempt detailed comparisons with calculated surface densities of states; instead, we will concentrate on looking at the differences in the surface valence band electronic structure, as determined by photoemission, between a large number of samples as well as the effects of exposure to oxygen.[4]

The valence band of GaAs consists of four bands extending approximately 14 eV below the valence band maximum (VBM).[6] The lowest lying band (giving a peak 9 to 14 eV below the VBM) is primarily s-like and associated with the arsenic.[7,8] The next band (giving a peak centered 6.75 eV below the VBM) is composed of s-like states around the gallium and p-like states around the

arsenic.[7,8] The remaining two bands (giving the structure for the first 5 eV below the VBM and containing at least four peaks) are completely p-like around the arsenic.[7,8] The structures associated with these bands can be seen in Figs. 1-4 where we show energy distribution curves (EDC's) for the cleaved GaAs (110) surface taken at 21 eV (see below for detailed discussion of these spectra; here, we will just use them as examples of the general GaAs valence band structure). All the peaks are easily seen except for the one 9 - 14 eV below the VBM, both because it is masked by the scattering tail and because the cross-section for this peak (s-like) is less than that of the p-like peaks at this photon energy. We should also note that the band structure of GaAs has a large number of critical points in the upper 5 eV of the valence band compared to the region 5 - 14 eV below the VBM.[9,10] The critical points should be the part of the band structure that is the most sensitive to any changes in the surface lattice structure. Thus, we should expect the most significant changes to occur in the upper 5 eV of the EDC's. The calculations of Refs. 3 and 4 show that the top 5 eV of the valence band do indeed show the most changes due to a rearrangement of the surface.

Another very sensitive technique which can be used to characterize semiconductor surfaces is the measurement of band bending.[11,12,13] The presence of band bending is seen as a difference in the position of the Fermi level at the surface with respect to that in the bulk which is determined by the doping. For GaAs (110), it has been recently shown from contact potential difference[13] measurements and photoemission[4,14] that the bands are flat all the way up to the surface within the experimental

uncertainty. This means that for p-type GaAs (110) the Fermi level is at the VBM, while for n-type it is at the conduction band minimum (CBM).

In earlier work,[11,12] however, Fermi level pinning was detected in n-type GaAs (110). This pinning was attributed to the existence of an empty band of intrinsic surface states in the middle of the gap.[11] These results were reinforced by partial yield measurements[15] showing strong transitions from the Ga-3d levels to states which seemed to be located in the middle of the gap (the partial yield results have since been re-interpreted to be consistent with the absence of band bending).[16]

The presence or absence of intrinsic states in the gap has important implications bearing on surface band structure calculations. For example, calculations based on the ideal surface result in an empty band of surface states in the gap,[7] whereas, those based on the rearranged surface give an empty band of surface states whose center of gravity is in the conduction band.[3] Therefore, it is important to clarify some of the present confusion as to the origin of the states that cause the Fermi level pinning in n-type GaAs (110). Some workers have assumed the pinning observed in the earlier work was always caused by surface roughness which was the result of bad cleaves.[13,14,17] However, some of our previous work has shown that pinning is observed in macroscopically good cleaves as well.[4,18] Thus, the Fermi level pinning could also be caused by states which are the result of surface strain or other microscopic defects in the crystal.

In order to investigate more systematically the possible relationship between the Fermi level pinning on clean n-type GaAs (110) with

surface defects or strains as well as the nature of the states causing the pinning (i.e., whether they are actually intrinsic or extrinsic), we performed a series of experiments where we studied photoemission and partial yield spectroscopy measurements from four different samples (16 total cleaves). We concentrated on the valence band electronic structure, particularly the top 5 eV, and correlated the changes in this structure with both the Fermi level pinning and partial yeild for the clean and oxygen exposed surfaces.

II. EXPERIMENTAL

A. Apparatus and Procedure

The experimental apparatus has been described in detail elsewhere,[5] and only details which are pertinent to this experiment will be described below.

We studied four separate samples from two suppliers. Three of the samples came from Laser Diode Corporation (LD). These will be designated samples LD1, LD2, and LD3. LD1 and LD2 were cut from the same boule. The third came from MCP Electronics in England (MCP). The samples were 5 mm × 5 mm × 12 mm with the (110) axis along the long dimension. All samples were n-type and had the following doping: LD1 and LD2, Te doped with $n = 0.5 \times 10^{18}$ cm^{-3}; LD3, Te doped with $n = 3.5 \times 10^{17}$ cm^{-3}; and, MCP, Te doped with $n = 1.7 \times 10^{18}$ cm^{-3}. The MCP sample was the same sample used by Gregory and Spicer in their earlier work.[11]

The sample chamber consists of a stainless steel UHV bell jar, base pressure $<1 \times 10^{-10}$ Torr. The pumping system is a 240 L/sec ion

pump plus titanium cryopump with a poppet valve for sealing the pump from the main chamber. The samples are mounted in a carousel being held at one end with a metal clamp which exerts a minimum amount of pressure on them. Four cleaves, each 2 mm thick, can be taken from each sample. The samples are cleaved by carefully squeezing them between an annealed copper anvil and a tungsten carbide blade. A cleave is judged to be "good" if it has a shiny, mirror-like surface. We have since performed preliminary optical measurements and found that the cleaves appear comparable to the "good" cleaves of Huijser and Van Laar in terms of step density.

All cleaves were performed at pressures $< 1 \times 10^{-10}$ Torr, and no hot filament or ionization gauges were used during the measurements or oxygen exposures except as specifically noted. Gas exposures were performed by admitting research grade oxygen into the vacuum system through a bakeable leak valve. For large exposures, an auxiliary pumping system was used to return the main chamber to pressures below $\sim 10^{-8}$ Torr.[5] Binding energies were measured with respect to the VBM and the position of the Fermi level with respect to the VBM was determined by referencing to the Fermi level of a gold film evaporated <u>in situ</u> on a substrate in electrical contact with the sample.[19]

Synchrotron radiation in the range 9 to 30 eV from the "8°" line at the Stanford Synchrotron Radiation Project[5] was used in this work. The radiation is first monochromated by a Seya-Namioka monochromator and then enters the chamber through a bakeable straight through valve. The energy of the photoemitted electrons is then determined by a double pass cylindrical mirror analyzer operated in the retarding mode. This mode insures a constant resolution which is equal to 0.6% of the electron pass energy. In these measurements, we used a pass energy of 25 eV,

giving an electron energy resolution of 0.15 eV. Counting rates over 2×10^4 C/sec in the GaAs valence band at $h\nu = 20$ eV were typical.

B. Results

In Figs. 1-4, we show EDC's taken at 21 eV (20 eV in Fig. 4) for several cleaves from each of samples LD1, LD2, LD3, and MCP. We will designate successive cleaves from a given sample as cleaves A, B, C, etc., and we will refer to cleave A from sample LD1 as "sample LD1A;" similarly, cleave A from sample MCP is "sample MCPA," and so on. The Fermi level at the surface is marked on each curve. The horizontal scale gives the energy below the VBM. The position of the Fermi level relative to the valence band maximum as well as to the peak at a binding energy of 6.75 eV is plotted in Fig. 5. (This figure will be discussed below.)

In Table I, we give a summary of the samples that were studied. This table includes the figure numbers where the spectra for the various samples are located, an indication as to the sharpness of the spectral features in the top 5 eV of the valence band for each sample and a classification of each sample based on the band bending.

The first thing we should notice from Figs. 1-4 is that the peak locations are constant from sample to sample and cleave to cleave. Relative peak heights, on the other hand, vary considerably. As an extreme example, compare sample LD1C, i.e., sample LD1, cleave C (Fig. 1) with samples MCPA & B (Fig. 4). In Sample LD1C, there is a large peak 1.75 eV below the VBM, whereas it is relatively small on MCPA. There is, however, better agreement in the shape of the valence band structure

when samples from the same boule are compared. For example, all cleaves from the same sample are similar and all cleaves from samples LD1 and LD2 (Fig. 2), which are different samples from the same boule, give similar results.

The next observation that will be made concerns the "sharpness" of the individual spectra for the clean samples. This is a very subjective judgement and open to question, but we feel that the observations are general enough that they should be of some use. In all cases, samples with the Fermi level located at the conduction band minimum are somewhat sharper, i.e., more structure can be resolved in the top 5 eV of the EDC. For example, compare LD1C to LD1A, B, or D; also, compare MCPA to MCPB or MCPC. LD3A, B, or C (Fig. 4) do not exhibit significant surface Fermi level pinning, and they have very well resolved structure in the top of the valence band. An exception is sample LD2. Cleaves A, C, and D from sample LD2 are as sharp as LD1C, yet they exhibit pinning while LD1C does not. Samples LD2B and E (not shown) had a very smeared out structure and exhibited Fermi level pinning. Thus, the most general statement we can make concerning these observations is that, if a sample has an unpinned Fermi level, the structure in the upper 5 eV of the valence band will be well defined. If the Fermi level is pinned, the majority of samples will have a smeared out valence band.

We should also note at this point that, in the case of LD1C, the structure in the top of the valence band became sharper after the sample had been in the vacuum system at 1×10^{-10} torr for 12 hours. In the case of MCPB, however, the structure did not change noticeably even after 20 hours at 10^{-10} torr. In both cases, there was movement of the

position of the Fermi level. We are not yet sure if the sharpening is due to some sort of surface lattice relaxation with time or if it is due to contamination. At a base pressure of $\sim 10^{-10}$ torr, the sharpened structure had an exposure of $\sim$ 4L to the residual gas in the chamber. As we will show below, definite effects in the valence band are observed with the addition of less than 100 L of oxygen (in some cases, effects are seen for exposures as low as 10 L). Consequently, the effect we are seeing could be due to contamination.

Before discussing the position of the Fermi level as a function of oxygen exposure, let us consider one more feature which all the samples have in common. In Figs. 6 to 14, we show the EDC's as a function of oxygen exposure for a representative number of cleaves from each sample. In all cases, changes take place in the top 5 eV of the valence band for exposures which are less than 10^3 L of O_2. In some cases, the changes take place for exposures as small as 10 L O_2 (see, for example, Figs. 10 and 11). When the EDC for the clean sample is smeared out, these changes take the form of a sharpening of the structure in the top 5 eV of the valence band (see Figs. 8 and 10). In other cases, where the EDC's show well resolved valence band structure in that region, the changes are more subtle, i.e., there might be a small variation in relative peak heights as shown in Figs. 6, 9, 13, and 14.

Now that we have taken care of these general considerations, we will group the spectra together according to the Fermi level pinning, and then we will describe each group in detail. The first group contains samples LD1C,[20] MCPA, and LD3A, B, C. In all these samples, the Fermi

level was located approximately at the conduction band minimum, i.e., no surface Fermi level pinning is observed. We have complete exposure data only for samples LD1C and LD3C which are shown in Figs. 7 and 14, respectively. There is only one exposure for sample MCPA, and this is shown in Fig. 9.

The first thing to notice is that the Fermi level is about 1.4 to 1.6 eV above the valence band maximum, which is approximately the location of the conduction band minimum since the band gap of GaAs is 1.4 eV. Thus, the Fermi level is at the bulk position, and there is no pinning.

As the surface is exposed to more and more oxygen, the Fermi level moves closer and closer to midgap until it stops moving downward by about 10^6 L O_2 (Figs. 7 and 14). These points are plotted in the lowest curve of Fig. 5. After the initial sharpening of structure in sample LD1C, notice that no large changes occur in the EDC's until we reach this critical exposure at 10^5 to 10^6 L O_2. Up until this point, the only changes seen were the changes in the top 5 eV of the valence band and a possible splitting in the band structure feature located 10-12 eV below the VBM (this happened for sample LD1C in Fig. 7; no such splitting was seen for LD3C in Fig. 14). At 10^5 to 10^6 LO_2, a significant amount of emission is lost from the top 3 eV of the valence band, and most of the sharp structure in top 5 eV is gone. The valleys located 4.5 and 8.3 eV below the VBM start filling. No definite peak is seen yet in the 4.5 eV valley. However, for LD1C (Fig. 7), two peaks can be clearly resolved at 8.3 and 9.7 eV below the VBM and, for LD3C (Fig. 14),

one peak is seen at 8.3 eV below the VBM. The peak at 6.75 eV has so far been unaffected by the oxygen. By 10^9 LO_2, the Fermi level has moved back towards the CBM by 0.15 eV (Fig. 5). The large exposures have led to a further decrease in the emission at the top of the valence band and an increase in emission from the adsorbed oxygen. Also, at 10^9 LO_2, a more definite oxygen level begins to appear 5 eV below the VBM. The emission from the GaAs is still so large with respect to the new emission that it is very difficult to find the precise location of the new structure.

The second group contains those cleaves which exhibit Fermi level pinning at about midgap. This group is the largest and contains LD1A, B, D; LD2A, B, C, D, E; and MCPC, D (Figs. 6, 8; 13, 15; and, 11, 12, respectively). In the majority of these cleaves, the Fermi level is pinned 0.9 ± 0.15 eV above the VBM, and it remains within these limits for all exposures. In two cases, LD1D (Fig. 8) and LD1C (Fig. 15), the initial pinning was 0.6 eV above the VBM (these two samples have not been included in Fig. 5). The effect of oxygen on the valence states at the surface is the same as for the first group when exposures $\geq 10^6$ LO_2 are reached. Again, oxygen emission begins to be seen at 10^9 LO_2 as for the first group. For the lower exposures, especially below 10^3 LO_2 in all of the LD1 and MCP samples, the top 5 eV of the EDC sharpened dramatically even, in one case, for an exposure as low as 10 LO_2. The LD2 samples, already somewhat being sharp, show more subtle effects.

The third "group" contains only one sample, MCPB,[20] and is shown in Fig. 10. In this case, the Fermi level for the just cleaved surface is located 0.7 eV above the VBM, putting it at midgap.

After being in the vacuum system at $\lesssim 1 \times 10^{-10}$ torr for 20 hours (giving an exposure of 7 L to residual gases), the Fermi level moves to 0.8 eV above the VBM. Upon exposure to oxygen, the Fermi level goes to the unpinned position (CBM) by 10 LO_2, remains at that position until an exposure of 10^2 LO_2, and then returns back to midgap by about 10^6 LO_2. The structure at the top of the valence band sharpens dramatically for an exposure of less than 100 LO_2, as for the group II samples, and the loss of intensity in the upper 5 eV of the EDC is seen as early as 10^5 LO_2, even before a significant filling of either of the two valleys (4.5 and 8.3 eV below the VBM) has taken place.

This sample presents a unique situation. If we measure the position of the Fermi level relative to the VBM, we get the behavior described above and shown in the bottom curve of Fig. 5. If, however, we measure the Fermi level with respect to the peak 6.75 eV below the VBM (labeled peak "A" in the example EDC on the top of Fig. 5), we find that the Fermi level moves up 0.9 eV from freshly cleaved to 1 LO_2 exposure and then remains at this position until 10^3 L (see top curve in Fig. 5). If we measure the distance from the 6.75 eV peak to the VBM and plot it vs exposure, we get the middle curve of Fig. 5 (x's), where we have included the same plot for sample LD1C (solid circles) for comparison. It becomes very clear from these curves that the width of the valence band at the surface is changing as well as having a change in the pinning. The decrease in width upon addition of oxygen implies that structure at the top of the valence band is removed with oxygen. Furthermore, the 6.75 eV peak becomes noticeably narrower by 10^2 LO_2. Neither effect was seen in the other samples. In those cases, the 6.75

eV peak remained constant in width, and the distance from the 6.75 eV peak and the VBM remained approximately constant for all oxygen exposures, as can be seen from the example given for sample LD1C. The broadening in the MCPB sample could be due to a very strained surface giving rise to new structures in the EDC, which disappear with oxygen, or simply to a nonuniform work function across the surface of the sample, or even a combination of both. However, since we observed this effect only once, it is very difficult to draw more definite conclusions.

We can make a general comment with reference to Fig. 5, although the top and bottom sets of curves are consistent with each other. Less scattering was obtained between the data points in the top set. This indicates some of the problems in using the VBM as a reference. Since the top 5 eV of the VB change in shape, using the upper edge as a reference is clearly less reliable than using a constant structure such as the 6.75 eV peak.

We now turn our attention to what happens when we use the hot filament ionization gauge during an exposure. These results are shown (for sample LD2C) in the dashed curves of Fig. 15. The solid curves were obtained using unexcited oxygen on sample LD2A and are shown for comparison. The excited oxygen speeds up the rate of chemisorption, as can be seen by comparing the dashed curve at 10^5 L (excited oxygen) exposure with the solid curve at 10^6 L (unexcited oxygen) exposure. In fact, the first large effects with excited oxygen are seen at 5×10^4 L while, with unexcited oxygen, the first large effects are seen between 10^6 and 10^7 L, an increase in activity by about a factor of 100. We have discussed the increase in the rate of adsorption in References 5 and 21. As in the exposures with unexcited oxygen, we see the appearance of oxygen induced emission, associated with the O-2p level, at exposures $>10^6$ L. In the case of excited oxygen, however, this emission is much more pronounced and eventually becomes the dominant feature of the EDC, located at approximately 5 eV below the VBM of the clean sample. With unexcited

oxygen, the oxygen emission is at most a shoulder at even 10^9 L. Also note that the position of the O-2p emission does not become well established until after an exposure of 10^7 L excited oxygen since, even at 10^5 L excited oxygen, it is not much bigger than the GaAs emission.

At 10^5 L, a peak is present at 8.2 eV below the VBM in both samples. A second peak at 9.9 eV below the VBM is seen for the sample exposed to excited oxygen, but does not appear for the sample exposed to unexcited oxygen until 10^7 LO_2. As can be seen from the figure, these two sets of peaks are the same for exposure to either excited or unexcited oxygen. We note, however, that at 10^7 L of excited oxygen, the two peaks at 8.2 and 9.9 eV below the VBM disappear and a single peak at 8.8 eV takes their place. The same sequence of exposures with excited oxygen for sample LD2C, taken at a photon energy of 25 eV, is shown in Fig. 16. This was done mainly to get a better look at any structure lower than 10 eV below the VBM which is obscured by the scattering peak for $h\nu = 21$ eV. By comparing Figs. 15 and 16, we see that the EDC's for the two photon energies are similar except for two major exceptions. First, the structure at 8.2 and 9.9 eV below the VBM is not visible at 10^6 L excited oxygen for the 25 eV spectrum, whereas it is present at 21 eV. The peak at 8.8 eV below the VBM is quite prominent at 10^7 L excited oxygen for both photon energies. Second, because of cross-section effects, the height of the O-2p derived emission relative to the GaAs valence band emission is much larger at 25 eV than 21 eV. Consequently, we are able to see direct emission from the oxygen more readily using 25 eV photons.

The next experimental results are those of partial yield spectroscopy measurements performed on samples LD1C, which shows no pinning and MCPB, which shows pinning at midgap. These spectra, shown in Figs. 17a and 17b, were performed concurrently with the data of Figs. 7 and 10. The two sets of spectra are essentially identical. There are some differences in relative peak heights and shapes, but the energy positions of all the peaks are identical. On the clean spectra, there are two sharp peaks at 19.7 and 20.2 eV and a third broad peak at 20.9 eV. Upon addition of oxygen, the three peaks remain unchanged in position and shape up to an exposure of 10^5 L of unexcited O_2. At 10^6 L, the peaks are almost gone, but there has been no shift in energy position. At 10^7 L, the fine structure is completely gone, leaving one broad peak at 20.1 eV. The behavior of partial yield spectra for other samples and cleaves was identical to the spectra shown, irrespective of any differences in the initial Fermi level pinning or behavior with oxygen exposure.

III. DISCUSSION AND CONCLUSIONS

In the discussion that follows, we will first condense the information obtained from our valence band, Fermi level pinning, and partial yield studies, and then correlate these results.

We have seen three main things in our data. First, Fermi level pinning occurred on surfaces that could be classified as good cleaves. This implies that pinning is not necessarily caused by high step densities or surface roughness,[13,14] but rather by more subtle types of defects. Exposure of the surface to oxygen caused the Fermi level to go

to midgap for unpinned samples and stay the same (at midgap) for the pinned samples.

Second, the top 5 eV of the EDC's were relatively sharp for unpinned samples, while for pinned samples the structure in this region was, in general, more smeared. The exposure of the surface to less than 10^3 LO_2 resulted in a sharpening of the smeared structure and more subtle changes in relative peak heights for the sharp EDC's. At exposures between 10^3 to 10^6 LO_2, the top 5 eV of the valence band was again affected, exhibiting both a loss of emission and smearing. For exposures above 10^6 LO_2, the top 5 eV of the EDC dropped even more and oxygen induced emission became noticeable. However, at 21 eV, the cross-sections are such that no clear peak from the oxygen can yet be seen 4 to 5 eV below the VBM. Through all this, the valence band structures lower than 5 eV below the VBM have remained essentially unchanged.

Third, the partial yield gave the same results for all samples, irrespective of the initial position of the Fermi level. Addition of as much as 10^5 LO_2 had no effect on the partial yield structure either in peak position or height. The peaks lose intensity at 10^6 LO_2 and disappear by 10^7 LO_2, with no shift in the peak positions.

As we mentioned in the introduction, the top 5 eV of the valence band should be strongly affected by the surface lattice structure, so that movements in the positions of the surface atoms would appear as changes in the top 5 eV of the EDC. If a surface is strained, the surface atoms at the strain points will be somewhat displaced from their ideal positions. Consequently, the EDC's from such a surface would be smeared, since the EDC would have contributions from both

the ideal and strained parts of the surface. The fact that surfaces with unpinned Fermi levels have sharp structures in the top 5 eV of the EDC, while samples with pinned Fermi levels are initially smeared and sharpen with exposure to oxygen, indicates that the unpinned surfaces are more perfect. That is, the surfaces exhibiting Fermi level pinning are probably strained. Furthermore, since we see no difference in the partial yield results from the samples with and without Fermi level pinning, the pinning must be due to extrinsic states.[4,13] Therefore by combining the photoemission and partial yield results, we can conclude that surface defects could be responsible for both the Fermi level pinning and the smearing of the valence band.

The sharpening of the EDC's with oxygen occurs for exposures less than 10^3 LO_2. From previous work,[5] we saw that at 10^6 LO_2 the coverage is only 5% of saturation. Assuming saturation at half monolayer (4.4×10^{14} oxygens/cm^2), the oxygen coverage causing sharpening of the EDC's would be on the order of one oxygen per 10^4 to 10^5 surface atoms. These rather long range effects associated with the oxygen can be interpreted to mean that the surface strains are rather unstable so that rearrangements can be triggered quite easily by very few oxygens. One oxygen per 10^4 to 10^5 surface atoms gives a concentration on the surface of approximately 4×10^9 to 4×10^{10} oxygens/cm^2. The typical concentration of dopant on the surface is on the order of 10^{10} atoms/cm^2 for a bulk doping of 10^{18} atoms/cm^3. It is interesting that these numbers are close enough to indicate a possible link between the dopant and the initial oxygen chemisorption. However, we should keep in mind that it does take at least 10^{12} to 10^{13} states/cm^2 to pin the Fermi level at

midgap.[11,12,13] Thus, although the dopant atoms at the surface could be responsible for triggering surface rearrangement upon oxygen chemisorption, they can not be the primary cause of the Fermi level pinning observed on the surfaces with the smeared EDC's. In addition, even though the already sharp EDC's (i.e., with no pinning) are affected by less than 10^3 LO_2, the Fermi level does not start to move towards midgap until exposures larger than 10^3 LO_2. This is more evidence which implies that the sites causing the pinning or strain and those that remove the strain are not necessarily the same.

Many of the conclusions that have been drawn so far have been rather speculative, but the most important point that must be reiterated is that the chemisorbed oxygen has long range effects on the surface, acting at coverages as small as one oxygen per 10^4 to 10^5 surface atoms. The fact that the oxygen has such large effects for very small coverages implies that oxygen stimulates spontaneous rearrangement of the surface by possibly removing strains. The cause of the pinning on the cleaved samples is extrinsic states whose source is not yet known. However, we suggest that surface defects cause both the pinning and the smearing of the EDC's.

Between 10^3 and 10^6 LO_2, the coverage goes from 1 oxygen in 10^4 to 10^5 surface atoms to 5% of saturation, and the Fermi level goes from the CBM to midgap (for group I samples). This latter coverage corresponds to about 10^{13} oxygen atoms/cm^2 which is approximately the number of states needed at the surface to pin the Fermi level. Thus, it is easy to see the origin of the Fermi level pinning with exposure to oxygen, provided, of course, that every chemisorbed oxygen gives rise to one new interface state. Besides pinning the Fermi level at midgap, an

oxygen exposure of 10^6 LO_2 results in the complete smearing of the top 5 eV of the EDC's.[4] Since the coverage is now only about one oxygen atom per 20 surface sites (i.e., 5% of saturation), the effects of the oxygen are again long range. The large changes in the EDC's imply a relatively large rearrangement of all the surface atoms, not just the ones at the strain sites, as was the case before.

With these large changes taking place in the valence band, we should also expect significant changes in the local dielectric constant (or screening properties) at the surface. Such changes would explain the disappearance of the partial yield peaks in going from 10^5 to 10^7 LO_2. If the screening at the surface changes, the excitonic binding energy, which determines the position of the peaks in the partial yield could change. If this happened, the partial yield from the clean surface would drop and new structure representative of the new excitonic binding energy would grow. We could not, however, see such new structure if it was too close to the valence band. Thus, the loss of the partial yield peaks could possibly be due to a rearrangement of charge in the surface layer rather than a direct interaction of the oxygen with the surface gallium atoms. The same arguments could be applied to explain the disappearance of the structure in electron energy loss measurements.[22]

With exposure to large amounts of oxygen, we saw further decrease in the intensity from the top 5 eV of the valence band with two new peaks 9.9 and 8.2 eV and a shoulder 4 to 5 eV below the VBM. Similar peaks are present during the initial stages of exposure to excited oxygen. This fits in with other data from chemical shift measurements

where it was shown that the result of exposure to excited or unexcited oxygen started in the same way, i.e., with a chemisorption stage.[5] However, in the case of excited oxygen, the surface is oxidized for exposures above 10^6 L. Thus, the peaks we see in the curves for exposures of 10^7 L of excited oxygen (Fig. 15) at 8.8 and 5 eV below the VBM should be oxide peaks. If the excited oxygen was found to be atomic rather than excited molecular oxygen, the similarity in the initial adsorption of the excited and the molecular oxygen would indicate that the molecular oxygen adsorbed dissociatively on the GaAs (110) surface. Thus, it would be very interesting to perform an experiment to determine the nature of the excited oxygen, as well as an adsorption experiment with atomic oxygen.

The simultaneous appearance and growth of the peaks 9.9, 8.2, and 4 to 5 eV below the VBM indicates that all three are due to a single adsorption process. The splitting between the shoulder and second peak is 3.2 to 4.2 eV and between the second and third peaks is 1.7 eV. It is interesting to compare these peaks to those seen in gas phase photoemission from molecular oxygen. The first three peaks in that case are the πg, πu, and $^4\Sigma g$ levels with splittings of 4 eV (πg and πu) and 2 eV (πu and $^4\Sigma g$).[23,24] If we associate the shoulder in our data with the πg level and the next two peaks with the πu and $^4\Sigma g$ levels, respectively, we see that the agreement is rather good. The first splitting between the πg and πu is within the range of values we see, and the second splitting is 0.3 eV larger than what is seen in our results. This is, by no means, conclusive evidence that the oxygen adsorbs as a molecule. However, the evidence is strong enough that the suggestion must be made.

The studies presented in this paper are rather exploratory in nature, and their importance lies, not only in what we have learned so far but, also, in suggestions for new work that will clarify some of the questions that remain unanswered. For example, more work must be done to correlate the pinning on clean surfaces with actual physical defects such as impurities or cleavage steps. As discussed above, these defects could also be the cause of surface strain and the resulting smearing of the EDC's. Once the relationship between these various effects is established, it will be possible to make better and more reproducible surfaces. LEED studies should be performed along with the photoemission to see if we can detect any change in the LEED I-V curves when we have changes in the EDC's. In order to gather more evidence as to the nature of the adsorbed oxygen, the three oxygen induced levels should be studied as a function of photon energy to see if their cross sections are the same as for molecular oxygen, and electron energy loss experiments to detect any molecular vibrational levels that might be present should also be undertaken.

Finally, since theoretical calculations on the rearranged GaAs (110) surface are starting to be published,[3] it should not be long until we can start making more detailed comparisons between our photoemission data and the calculated surface densities of states.

REFERENCES

1. A. R. Lubinsky, C. B. Duke, B. W. Lee, and P. Mark, Phys. Rev. Letters 36, 1058 (1976); C. B. Duke, A. R. Lubinsky, B. W. Lee, and P. Mark, J. Vac. Sci. Technol. 13, 761 (1976); A. R. Lubinsky, J. Vac. Sci. Technol. 14, 910 (1977).
2. W. A. Harrison, Surface Sci. 55, 1 (1976); J. Vac. Sci. Technol. 14, 883 (1977).
3. S. G. Louie, J. R. Chelikowsky, and M. L. Cohen, J. Vac. Sci. Technol. 13, 790 (1976); J. R. Chelikowsky, S. G. Louie, and M. L. Cohen, Phys. Rev. B (in press); C. Calandra, F. Manghi, and C. M. Bertoni (to be published).
4. Some preliminary work has been published in W. E. Spicer, I. Lindau, P. E. Gregory, C. M. Garner, P. Pianetta, and P. W. Chye, J. Vac. Sci. Technol. 13, 780 (1976) and W. E. Spicer, P. Pianetta, I. Lindau, P. W. Chye, J. Vac. Sci. Technol. 14, 885 (1977).
5. P. Pianetta, Ph.D. thesis, Stanford University (1976).
6. L. Ley, R. A. Pollak, F. R. McFeely, S. P. Kowalczyk, and D. A. Shirley, Phys. Rev. B 9, 600 (1974).
7. J. D. Joannopoulos and M. L. Cohen, Phys. Rev. B 10, 5075 (1974).
8. D. J. Chadi and M. L. Cohen, Phys. Stat. Sol. (b) 68, 405 (1975).
9. J. Chelikowsky, D. J. Chadi, and M. L. Cohen, Phys. Rev. B 8, 2786 (1973).
10. J. R. Chelikowsky and M. L. Cohen, Phys. Rev. B 14, 556 (1976).

11. P. E. Gregory and W. E. Spicer, Phys. Rev. B 13, 725 (1976); P. E. Gregory, W. E. Spicer, S. Ciraci, and W. A. Harrison, Appl. Phys. Letters 25, 511 (1974).

12. J. H. Dinan, L. K. Galbraith, and T. E. Fischer, Surface Sci. 26, 587 (1971).

13. J. van Laar and A. Huijser, J. Vac. Sci. Technol. 13, 769 (1976); A. Huijser and J. van Laar, Surface Sci. 52, 202 (1975).

14. W. Gudat and D. E. Eastman, J. Vac. Sci. Technol. 13, 831 (1976) and references contained therein.

15. D. E. Eastman and J. L. Freeouf, Phys. Rev. Letters 34, 1624 (1975).

16. G. J. Lapeyre and J. Anderson, Phys. Rev. Letters 35, 117 (1975).

17. Here, we are discussing only clean cleaved GaAs (110) surfaces since contamination can also cause pinning as will be discussed below.

18. The surfaces studied in Reference 11 showed Fermi level pinning but were not the result of "bad" cleaves, i.e., there was no surface roughness nor was there a large amount of microscopic steps.

19. For a detailed explanation of the justification for this method, see Reference 11 or G. F. Derbenwick, D. T. Pierce, and W. E. Spicer, Methods of Experimental Physics (Academic Press, New York, 1974), Vol. 11, pp. 89-92.

20. LD1C was called sample II cleave A, and MCPB was called sample III cleave B in Reference 4.

21. P. Pianetta, I. Lindau, C. M. Graner, and W. E. Spicer, Phys. Rev. Letters 37, 1166 (1976).

22. R. Ludeke and A. Koma, Crit. Rev. Solid State Sci. 5, 259 (1975); and J. Vac. Sci. Technol. 13, 241 (1976).

23. K. Siegbahn, C. Nordling, G. Johansson, J. Hedman, P. F. Hedén, K. Hamrin, U. Gelius, T. Bergmark, L. O. Werme, R. Manne, and Y. Baer, ESCA Applied to Free Molecules (North Holland, Amsterdam, 1969), pp. 69-73.

24. D. W. Turner, C. Baker, A. D. Baker, and C. R. Brundle, Molecular Photoelectron Spectroscopy (Wiley, New York, 1970), pp. 36-37, 52.

Table I

LIST OF SAMPLES. Entries include Fermi level location for each sample immediately after cleavage, classification of samples according to location of the Fermi level, and an indication as to the relative sharpness of the valence band before and after exposure to oxygen.

Sample		E_F Position[a]	Valence Band Structure[b]		Group[c]	Data Shown in Figure Numbers	
			After Cleavage	After $\lesssim 10^2$ LO_2		(Clean)	(+O_2)
LD1	A	midgap	smeared	sharpened	II	1	6
	B	midgap	smeared	no data	II	1	not shown
	C	CBM	sharp	same	I	1	7
	D	midgap	smeared	sharpened	II	1	8
LD2	A	midgap	sharp	sharper	II	2	13,15
	B	midgap	smeared	sharpened	II	not shown	not shown
	C	midgap	sharp	same	II	2	15,16
	D	midgap	sharp	same	II	2	not shown
	E	midgap	sharp	no data	II	not shown	no data
LD3	A	CBM	sharp	same	I	3	not shown
	B	CBM	sharp	same	I	3	not shown
	C	CBM	sharp	sharper	I	3	14
MCP	A	CBM	sharp	sharper	I	4	9
	B	midgap	smeared	sharpened	III	4	10
	C	midgap	smeared	sharpened	II	4	11
	D	midgap	no data	sharp	II	not shown	12

a. Approximate position, see Figs. 1-5 for exact position.

b. See text for discussion of what is meant by sharpness.

c. Group I indicate E_F at CBM, group II at midgap, group III at midgap then going to CBM with addition of oxygen.

FIGURE CAPTIONS

Fig. 1. EDC's taken at a photon energy of 21 eV for four cleaves from Sample LD1. The solid curve for sample LD1C was taken 12 hours after cleaving, whereas the dotted curve was taken within 45 minutes after cleaving.

Fig. 2. EDC's taken at $h\nu = 21$ eV for three cleaves from Sample LD2.

Fig. 3. EDC's taken at $h\nu = 20$ eV for three cleaves from Sample LD3.

Fig. 4. EDC's taken at $h\nu = 21$ eV for three cleaves from Sample MCP. The solid curve for sample MCPB was taken 20 hours after cleaving, whereas the dotted curve was taken within 30 minutes after cleaving.

Fig. 5. Summary of Fermi level movement versus exposure for some of the samples shown in Figs. 1 - 4. Here, we show the position of the Fermi level, E_F, with respect to both the valence band maximum, VBM (in the bottom set of curves) and peak "A" (in the top set of curves). The middle set of curves show the position of the VBM with respect to peak "A". Samples in group I show no Fermi level pinning after cleavage. Pinning is seen from group II and III samples, but, for the group III sample, it is removed by exposure to oxygen (see text).

Fig. 6. EDC's for Sample LD1A, i.e., Sample LD1 cleave A, as a function of oxygen exposure ($h\nu = 21$ eV).

Fig. 7. EDC's for Sample LD1C as a function of oxygen exposure ($h\nu$ = 21 eV).

Fig. 8. EDC's for Sample LD1D as a function of oxygen exposure ($h\nu$ = 21 eV).

Fig. 9. EDC's for Sample MCPA as a function of oxygen exposure ($h\nu$ = 21 eV).

Fig. 10. EDC's for Sample MCPB as a function of oxygen exposure ($h\nu$ = 21 eV).

Fig. 11. EDC's for Sample MCPC as a function of oxygen exposure ($h\nu$ = 21 eV).

Fig. 12. EDC's for Sample MCPD as a function of oxygen exposure ($h\nu$ = 21 eV). No spectra were taken of the clean sample.

Fig. 13. EDC's for Sample LD2A as a function of oxygen exposure ($h\nu$ = 21 eV).

Fig. 14. EDC's for Sample LD3C as a function of oxygen exposure. Note, here, $h\nu$ = 21 eV , but $h\nu$ = 20 eV in Fig. 3, so the clean spectra will be somewhat different due to direct transition effects.

Fig. 15. Comparison of Sample LD2A, exposed to molecular unexcited oxygen, with Sample LD2C, exposed to excited oxygen.

Fig. 16. EDC's for Sample LD2C exposed to excited oxygen ($h\nu$ = 25 eV).

Fig. 17. Partial yield measurements for (a) Sample MCPB and (b) Sample LD1C as a function of oxygen exposure.

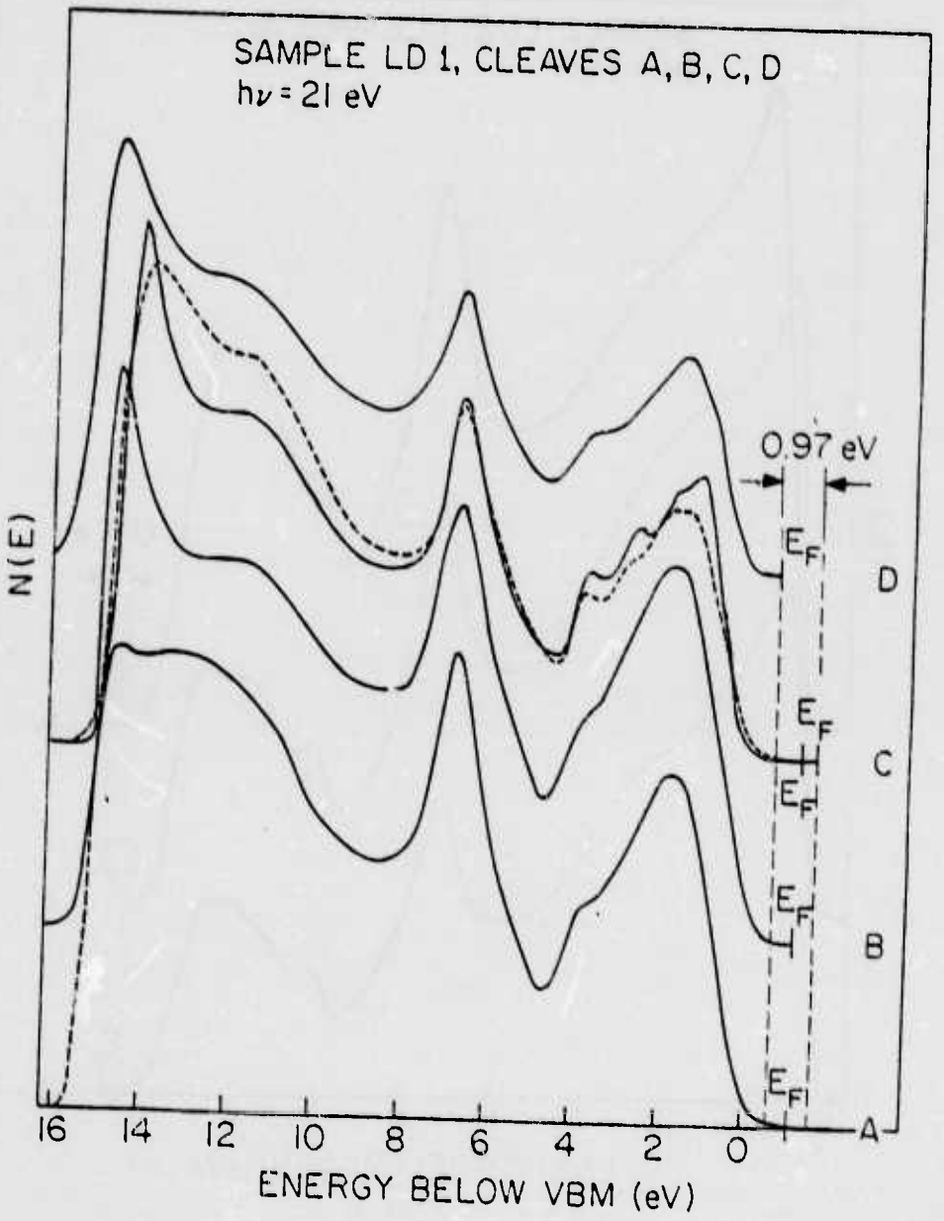
SAMPLE LD 1, CLEAVES A, B, C, D
hν = 21 eV
0.97 eV
N(E)
D
C
B
A
16
14
12
10
8
6
4
2
0
ENERGY BELOW VBM (eV)

Fig. 1

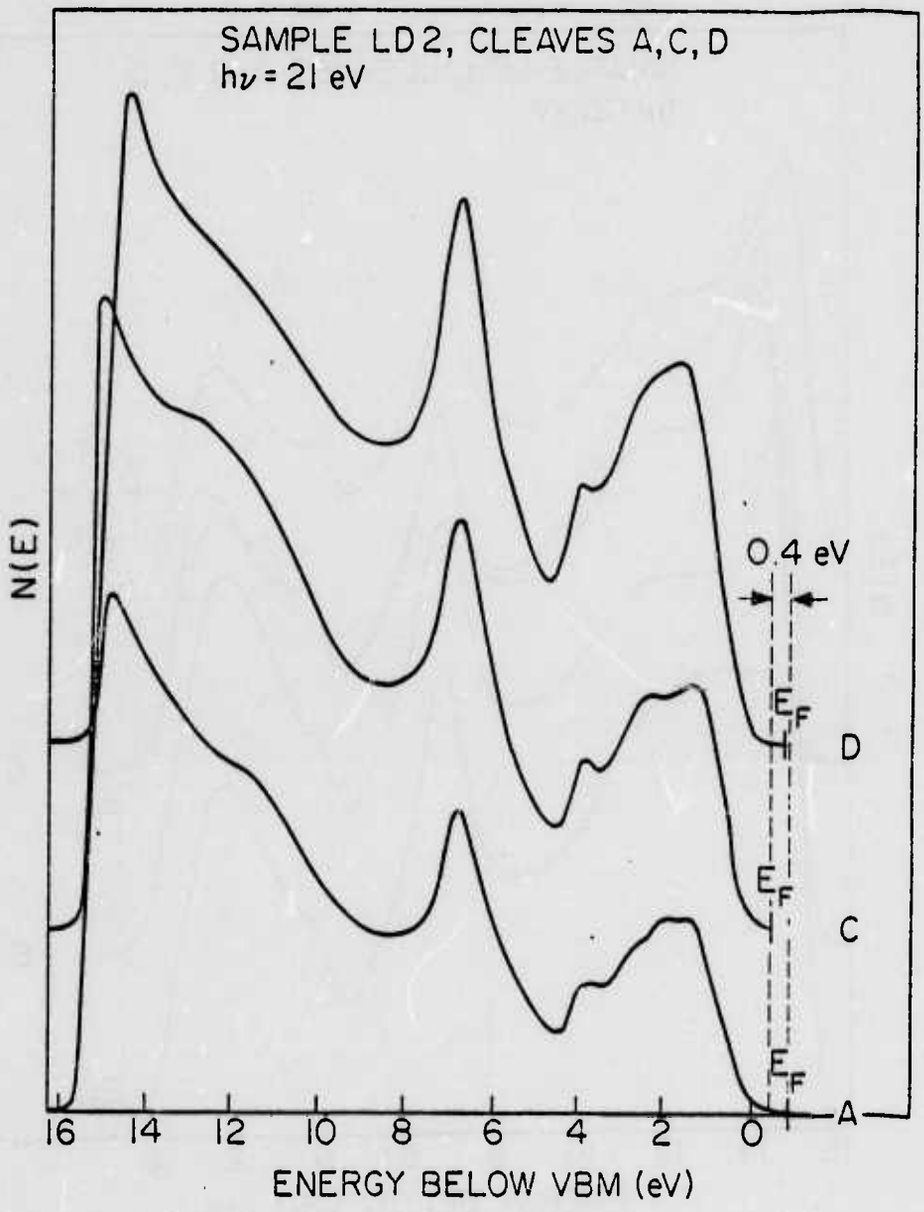
SAMPLE LD2, CLEAVES A,C,D
hν = 21 eV
N(E)
0.4 eV
E_F
D
E_F
C
E_F
A
16
14
12
10
8
6
4
2
0
ENERGY BELOW VBM (eV)

Fig. 2

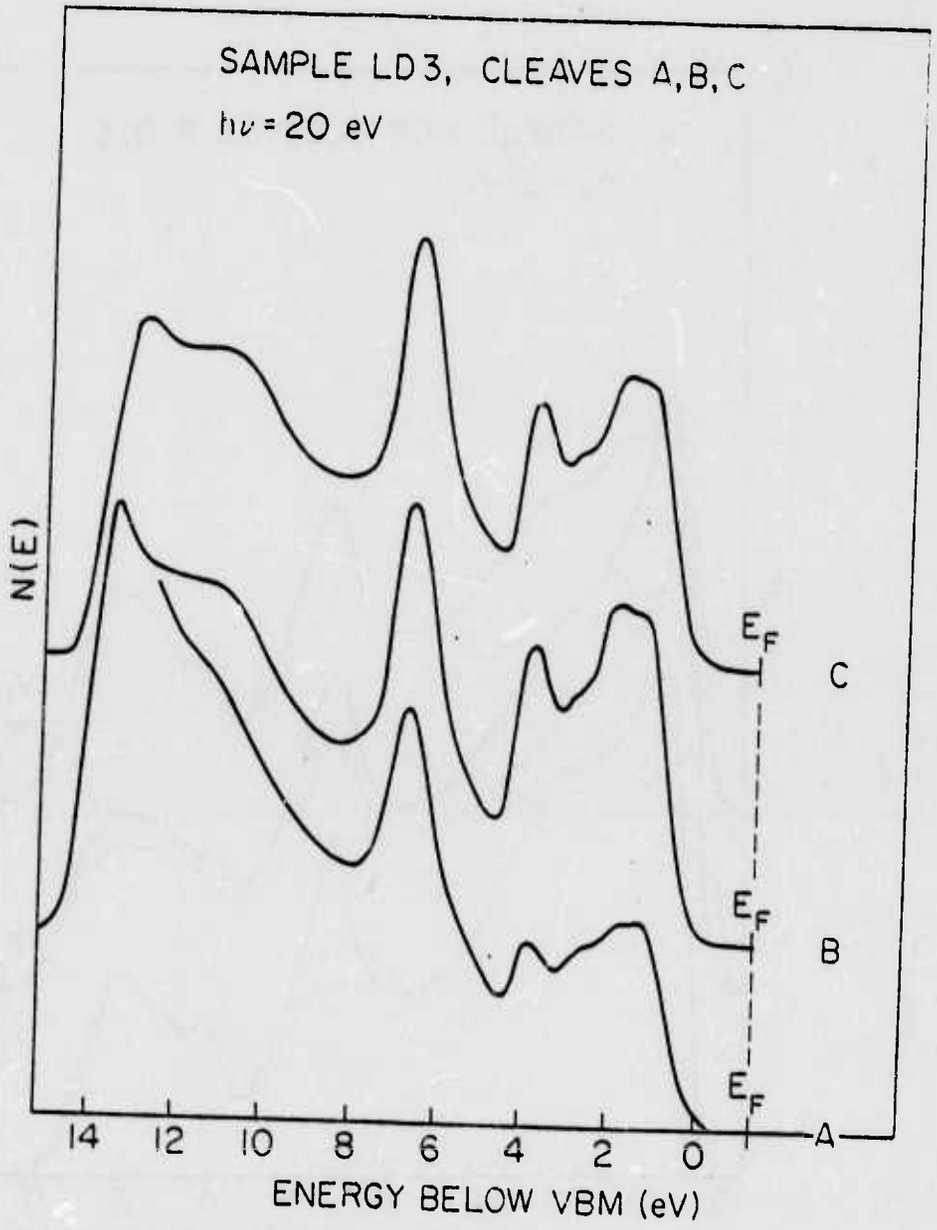
SAMPLE LD3, CLEAVES A, B, C
hν = 20 eV
N(E)
E_F
C
E_F
B
E_F
A
14
12
10
8
6
4
2
0
ENERGY BELOW VBM (eV)

Fig. 3

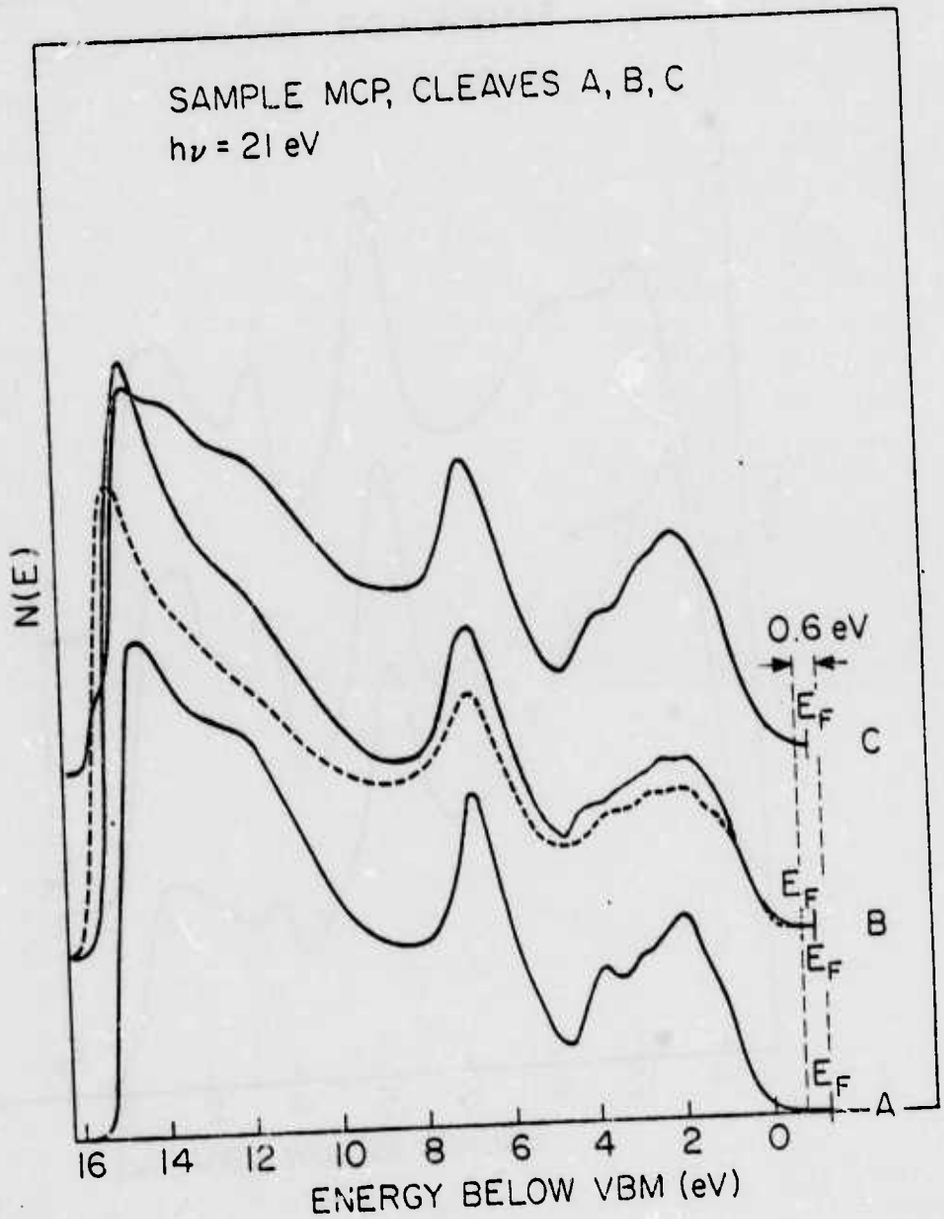
SAMPLE MCP, CLEAVES A, B, C
hν = 21 eV
N(E)
0.6 eV
E_F
C
E_F
B
E_F
E_F
A
16
14
12
10
8
6
4
2
0
ENERGY BELOW VBM (eV)

Fig. 4

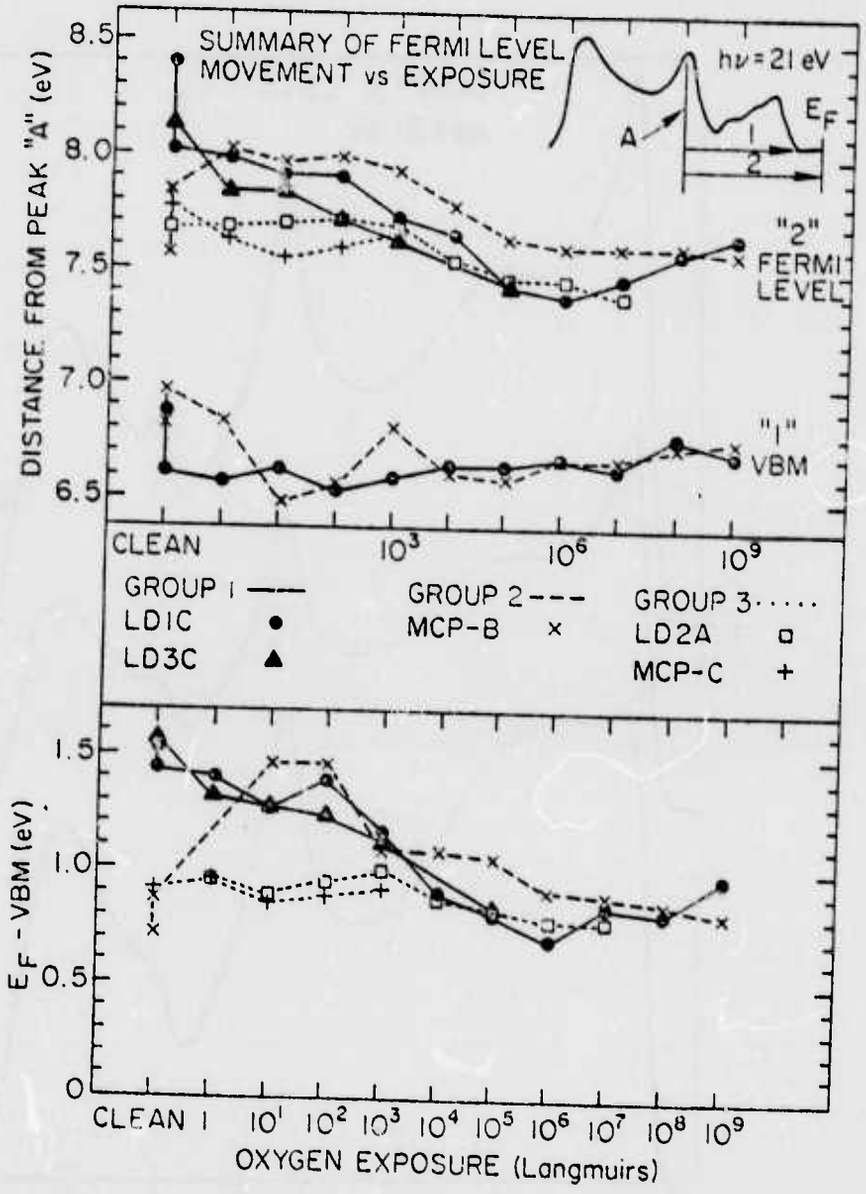
SUMMARY OF FERMI LEVEL MOVEMENT vs EXPOSURE
hν = 21 eV
A
E_F
1
2
"2" FERMI LEVEL
"1" VBM
DISTANCE FROM PEAK "A" (eV)
8.5
8.0
7.5
7.0
6.5
CLEAN
10^3
10^6
10^9
GROUP 1
LD1C
LD3C
GROUP 2
MCP-B
GROUP 3
LD2A
MCP-C
E_F - VBM (eV)
1.5
1.0
0.5
0
CLEAN 1
10^1 10^2 10^3 10^4 10^5 10^6 10^7 10^8 10^9
OXYGEN EXPOSURE (Langmuirs)

Fig. 5

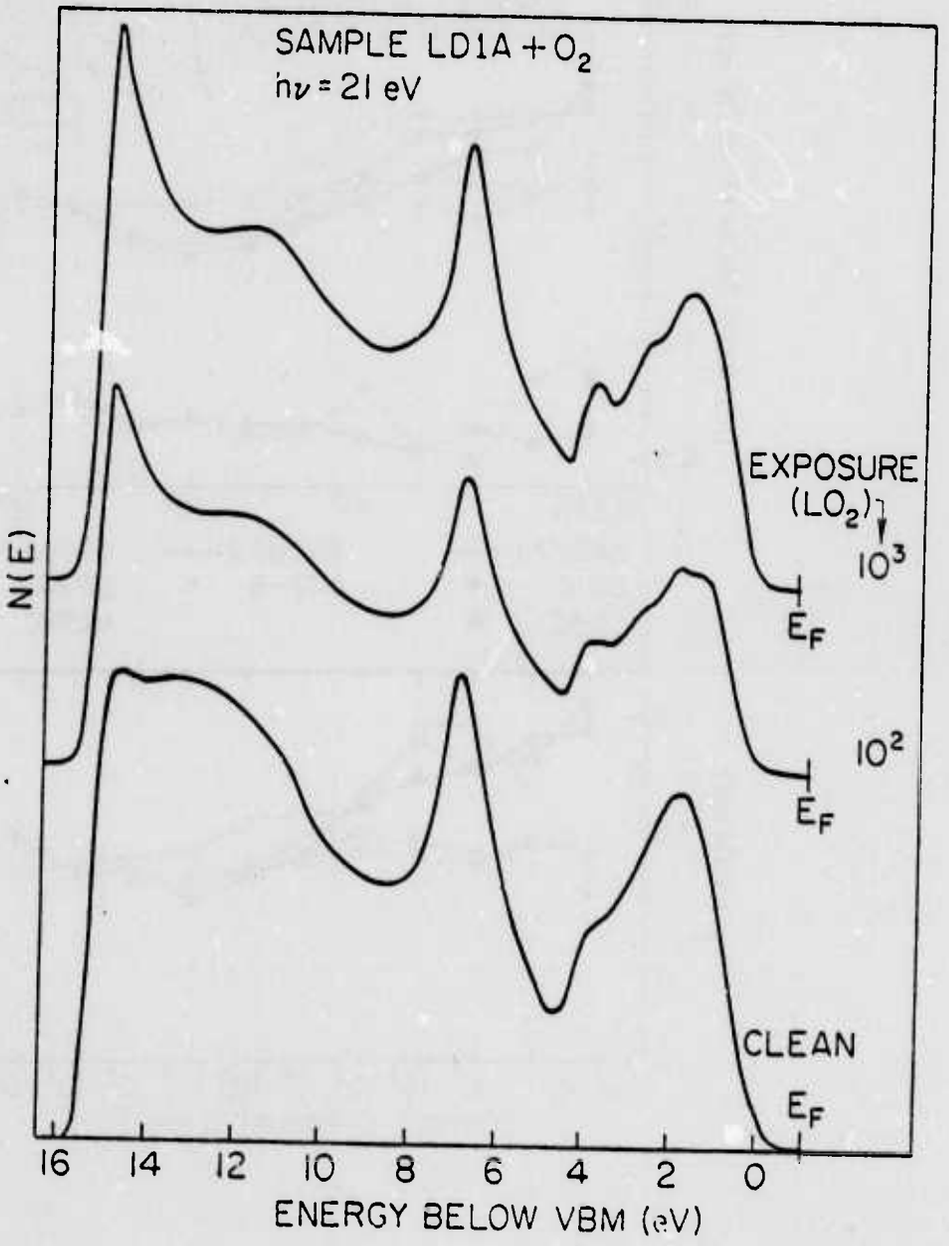
SAMPLE LD1A + O_2
$h\nu$ = 21 eV
EXPOSURE (LO_2)
10^3
E_F
10^2
E_F
CLEAN
E_F
N(E)
16
14
12
10
8
6
4
2
0
ENERGY BELOW VBM (eV)

Fig. 6

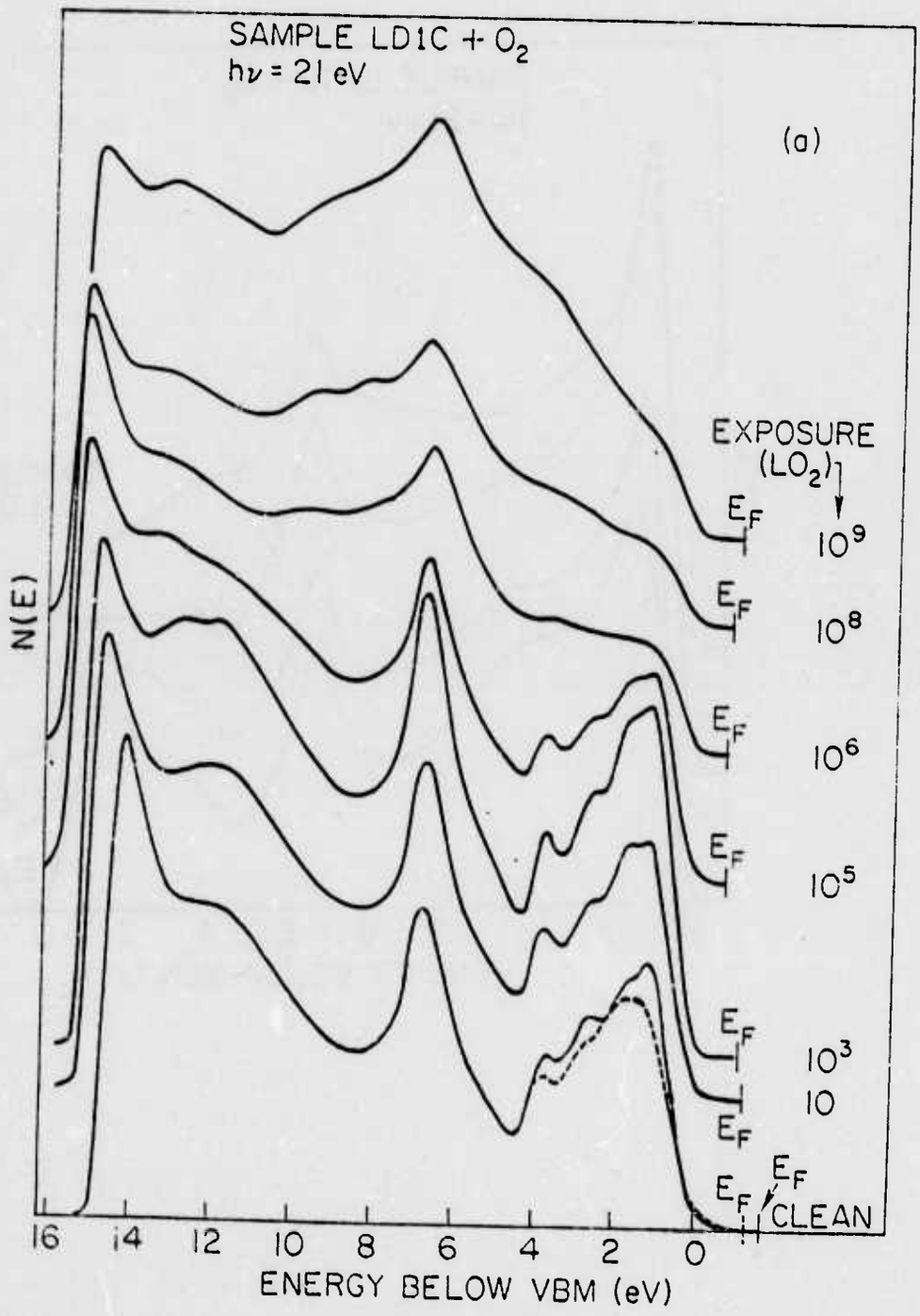
SAMPLE LD1C + O_2
$h\nu$ = 21 eV
(a)
EXPOSURE (LO_2)
E_F
10^9
10^8
10^6
10^5
10^3
10
CLEAN
N(E)
16
14
12
10
8
6
4
2
0
ENERGY BELOW VBM (eV)

Fig. 7

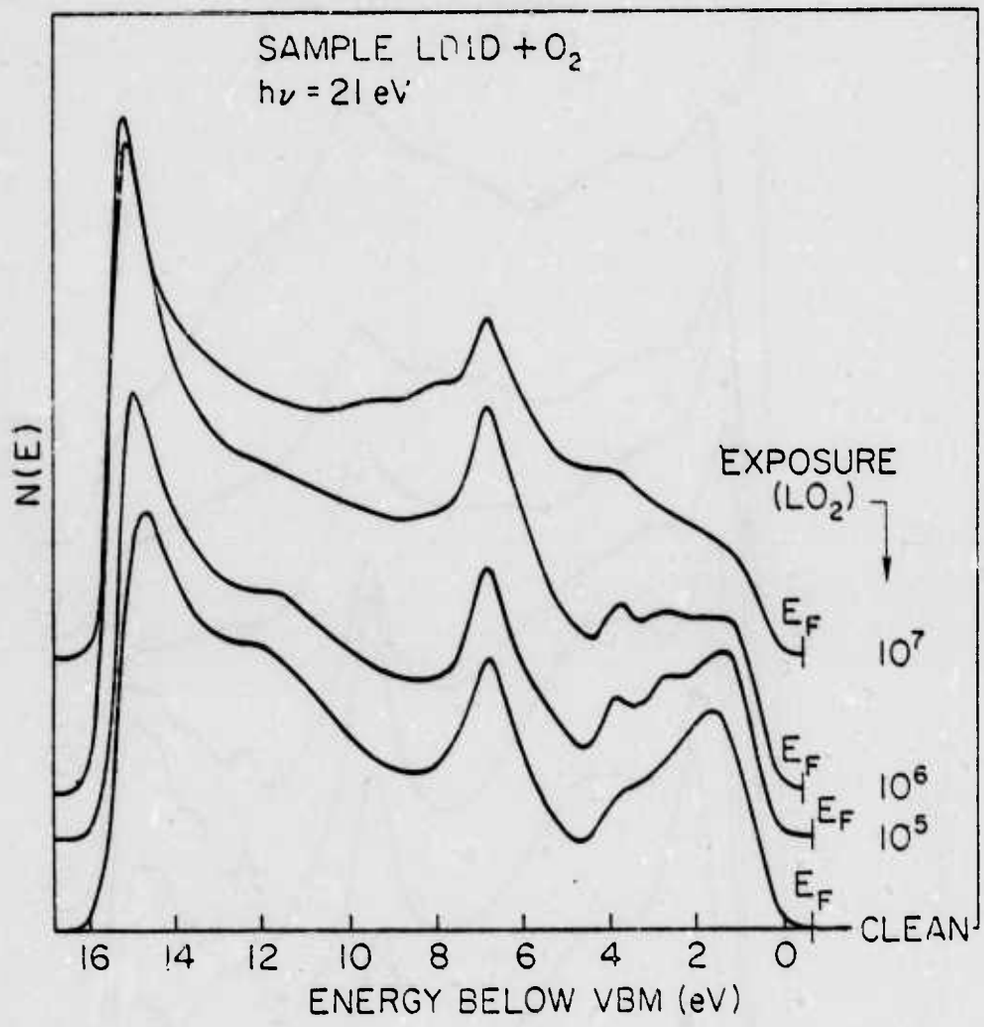
SAMPLE LD1D + O_2
$h\nu$ = 21 eV
N(E)
EXPOSURE
(LO_2)
E_F
10^7
E_F
10^6
E_F
10^5
E_F
CLEAN
16
14
12
10
8
6
4
2
0
ENERGY BELOW VBM (eV)

Fig. 8

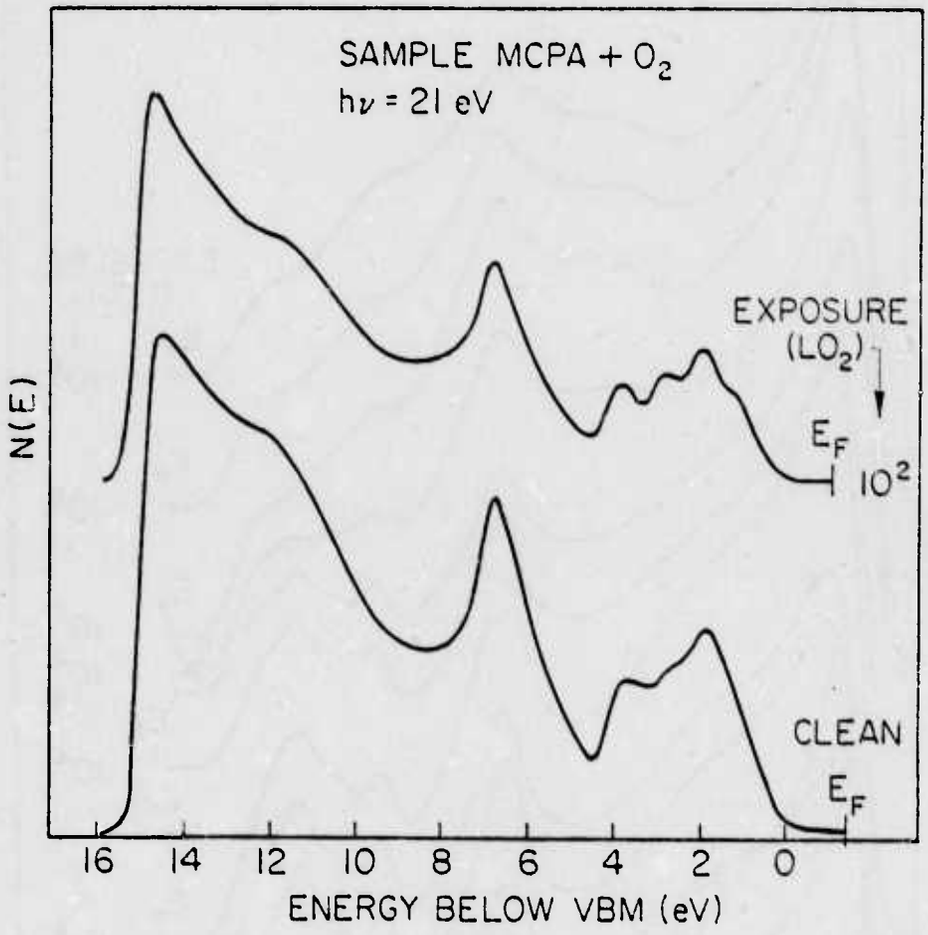
SAMPLE MCPA + O_2
$h\nu$ = 21 eV
EXPOSURE (LO_2)
E_F
10^2
CLEAN
E_F
N(E)
16
14
12
10
8
6
4
2
0
ENERGY BELOW VBM (eV)

Fig. 9

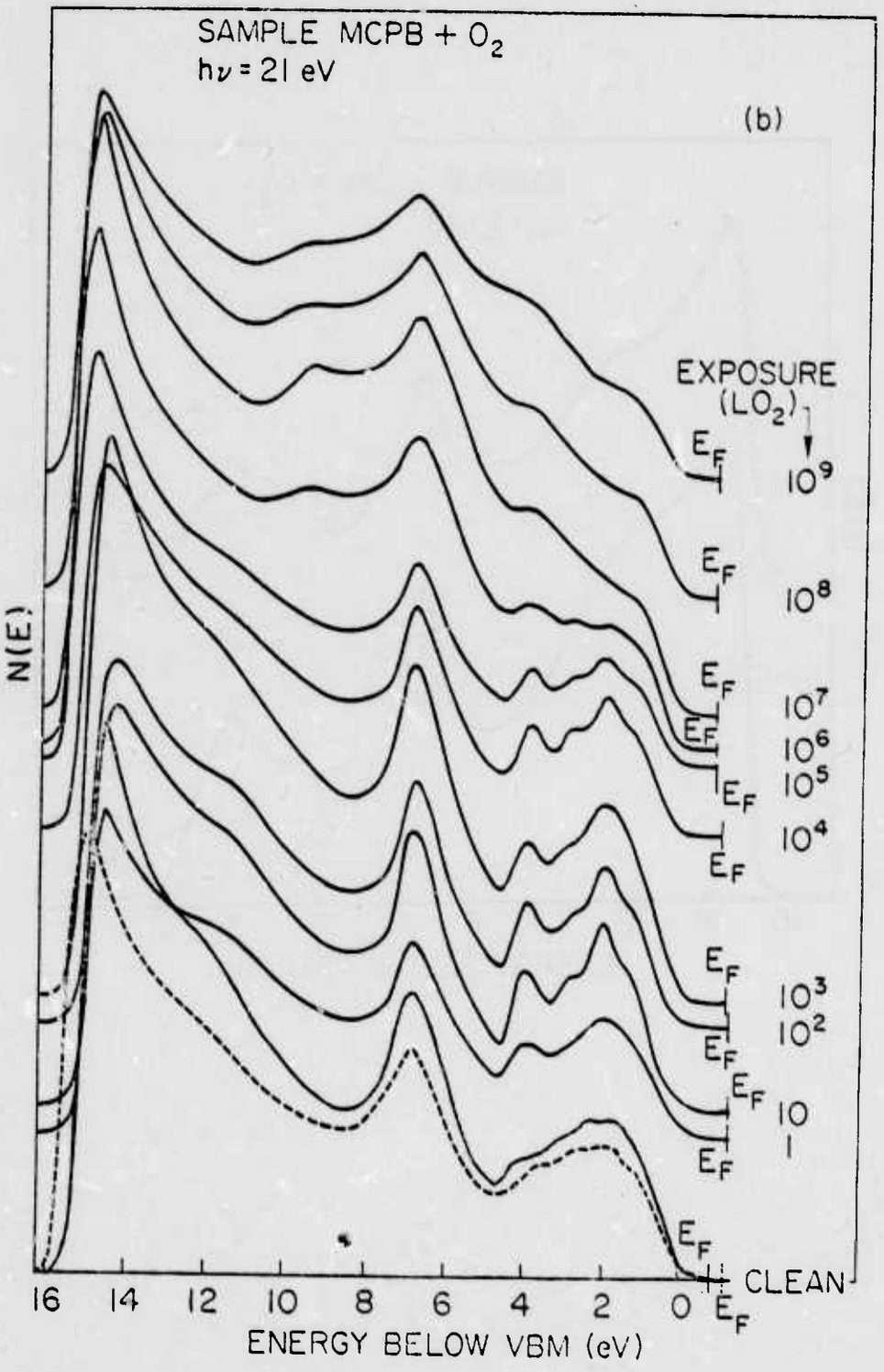
SAMPLE MCPB + O_2
$h\nu$ = 21 eV
(b)
EXPOSURE (LO_2)
E_F
10^9
10^8
10^7
10^6
10^5
10^4
10^3
10^2
10
1
CLEAN
N(E)
16 14 12 10 8 6 4 2 0 E_F
ENERGY BELOW VBM (eV)

Fig. 10

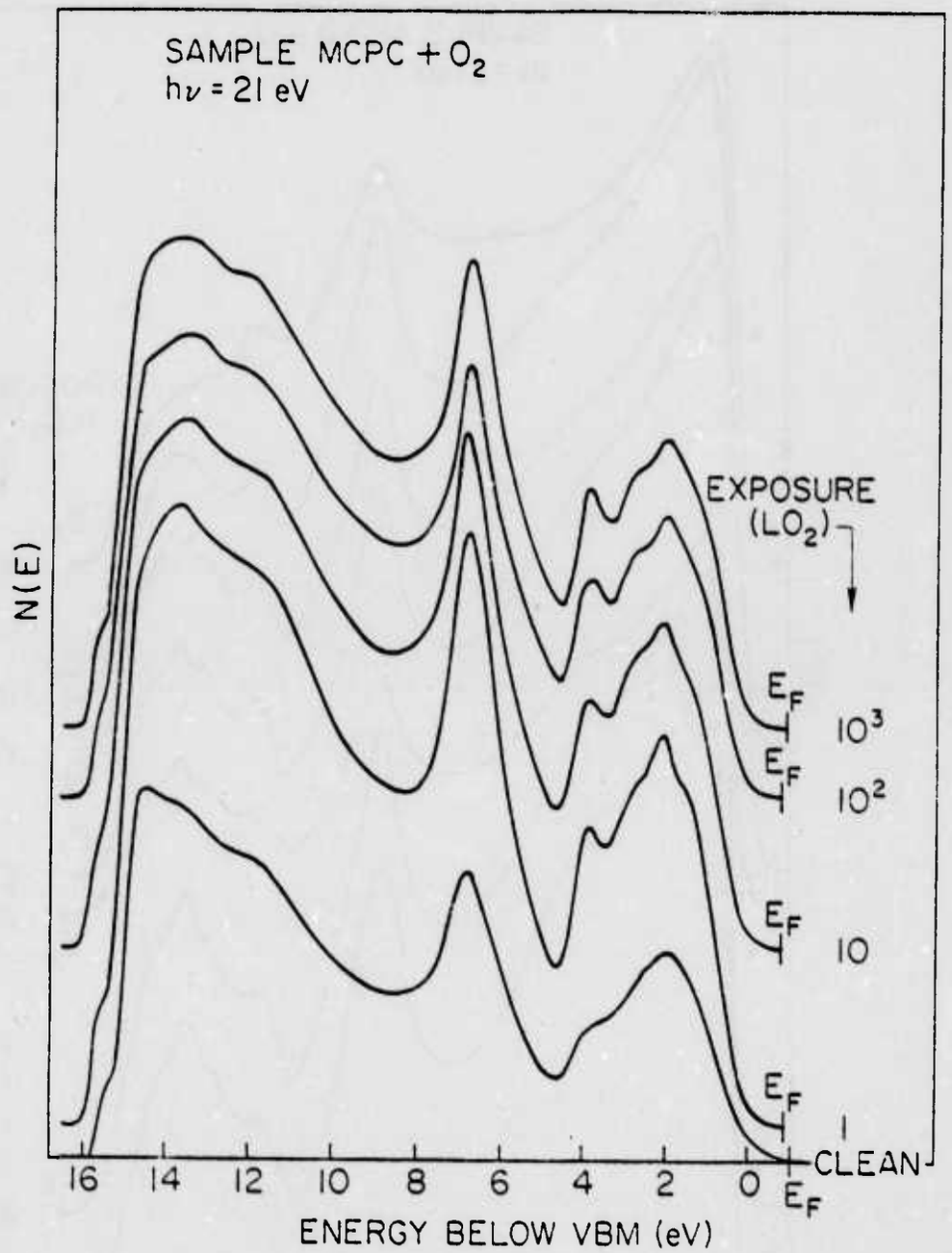
SAMPLE MCPC + O_2
$h\nu$ = 21 eV
N(E)
EXPOSURE (LO_2)
E_F
10^3
E_F
10^2
E_F
10
E_F
1
CLEAN
16
14
12
10
8
6
4
2
0
E_F
ENERGY BELOW VBM (eV)

Fig. 11

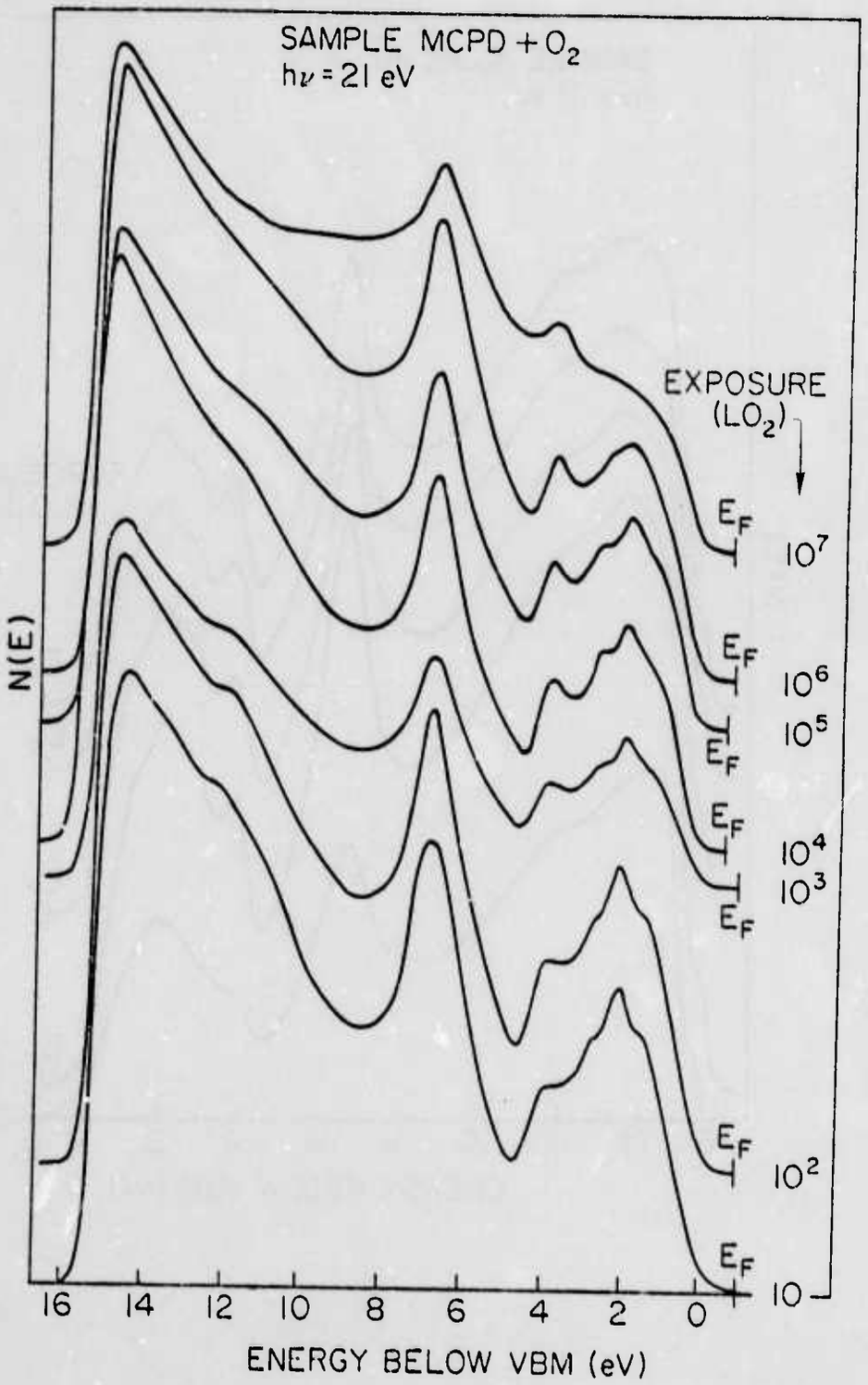
SAMPLE MCPD + O_2
$h\nu$ = 21 eV
EXPOSURE (LO_2)
E_F
10^7
10^6
10^5
10^4
10^3
10^2
10
N(E)
16
14
12
10
8
6
4
2
0
ENERGY BELOW VBM (eV)

Fig. 12

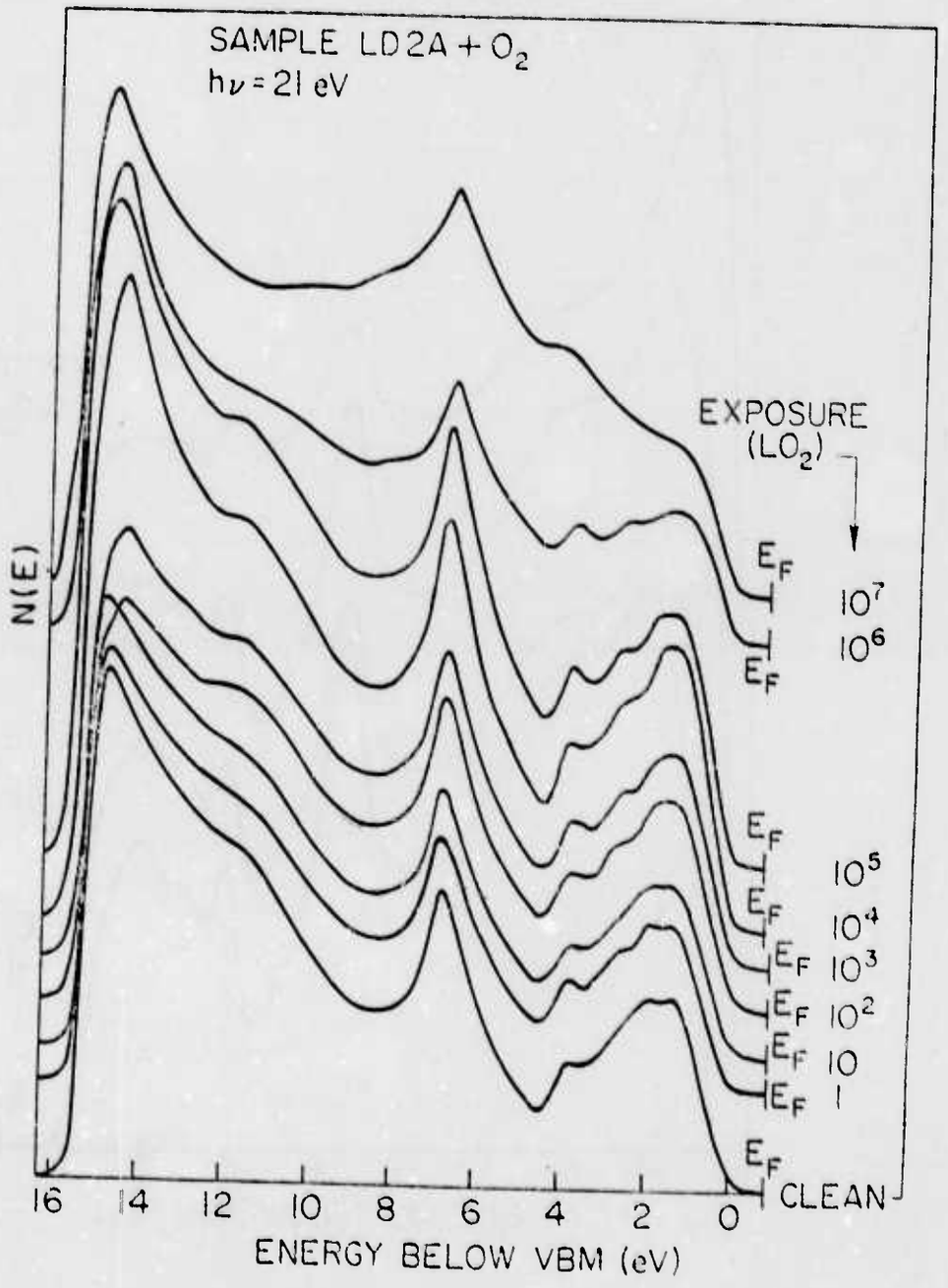
SAMPLE LD2A + O_2
$h\nu$ = 21 eV
EXPOSURE (LO_2)
N(E)
E_F
10^7
10^6
10^5
10^4
10^3
10^2
10
1
CLEAN
16
14
12
10
8
6
4
2
0
ENERGY BELOW VBM (eV)

Fig. 13

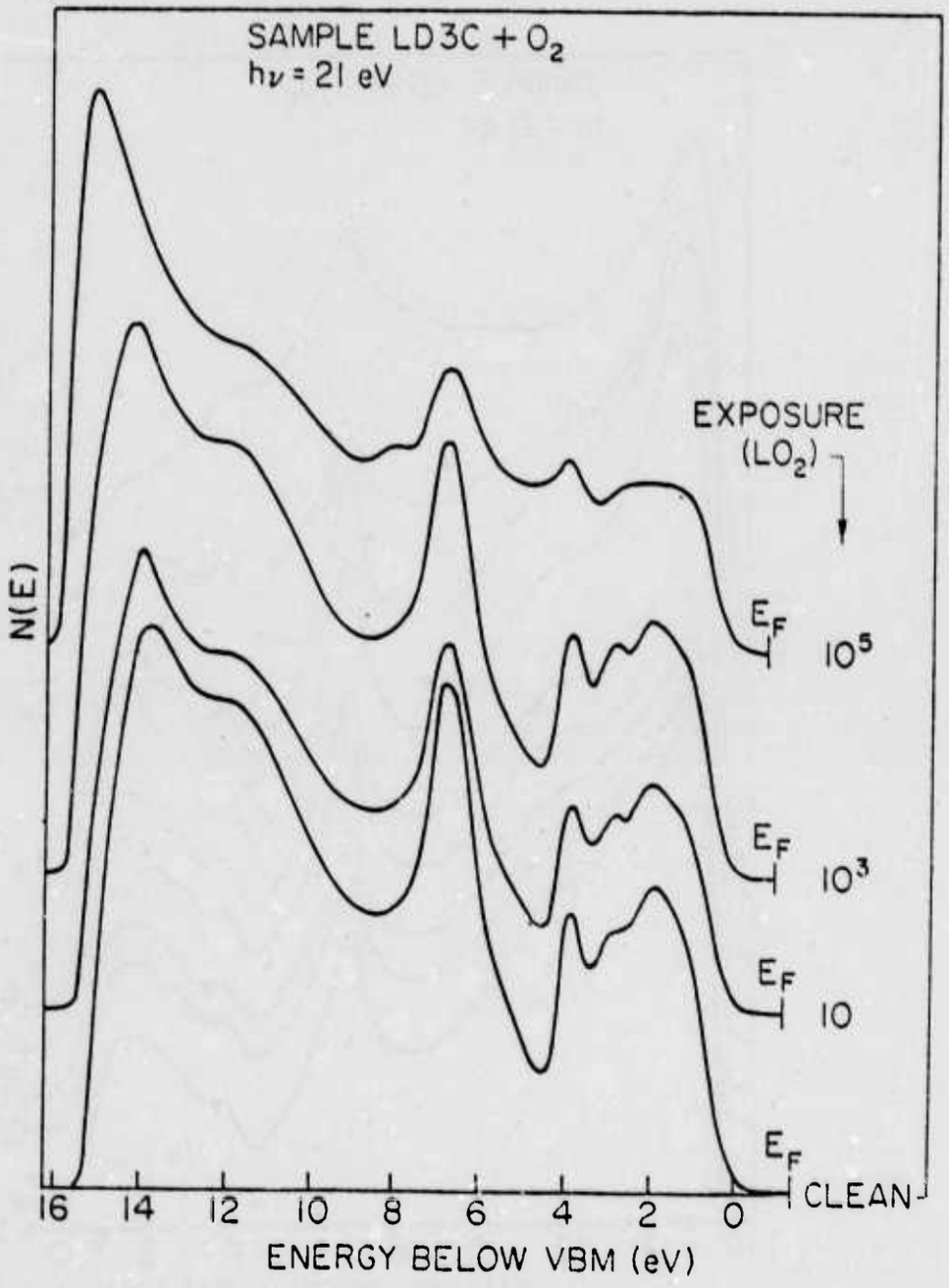
SAMPLE LD3C + O_2
$h\nu$ = 21 eV
EXPOSURE (LO_2)
E_F
10^5
E_F
10^3
E_F
10
E_F
CLEAN
N(E)
16
14
12
10
8
6
4
2
0
ENERGY BELOW VBM (eV)

Fig. 14

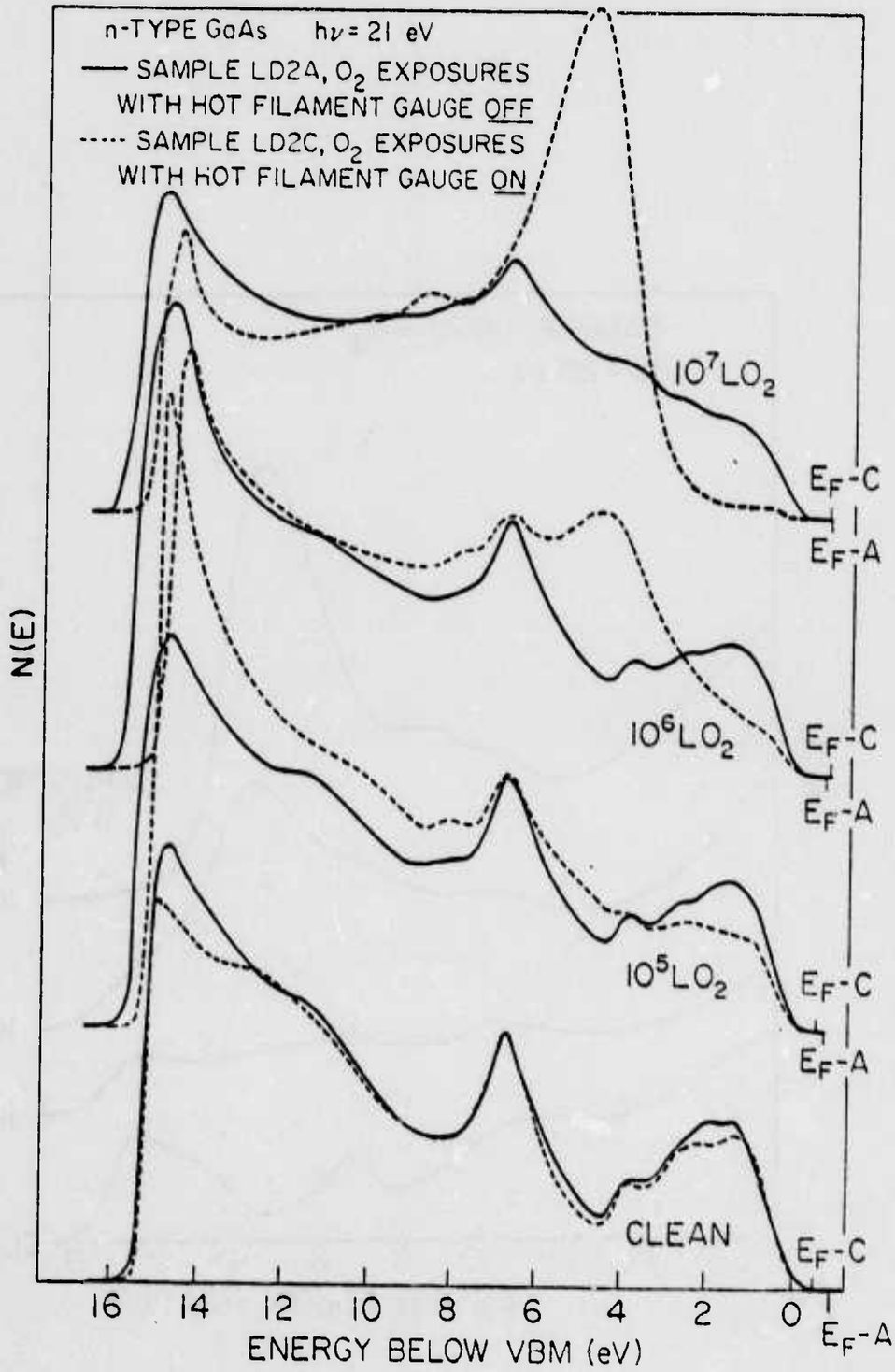
n-TYPE GaAs hν = 21 eV
SAMPLE LD2A, O2 EXPOSURES WITH HOT FILAMENT GAUGE OFF
SAMPLE LD2C, O2 EXPOSURES WITH HOT FILAMENT GAUGE ON
10^7 LO2
10^6 LO2
10^5 LO2
CLEAN
E_F-C
E_F-A
N(E)
16
14
12
10
8
6
4
2
0
ENERGY BELOW VBM (eV)

Fig. 15

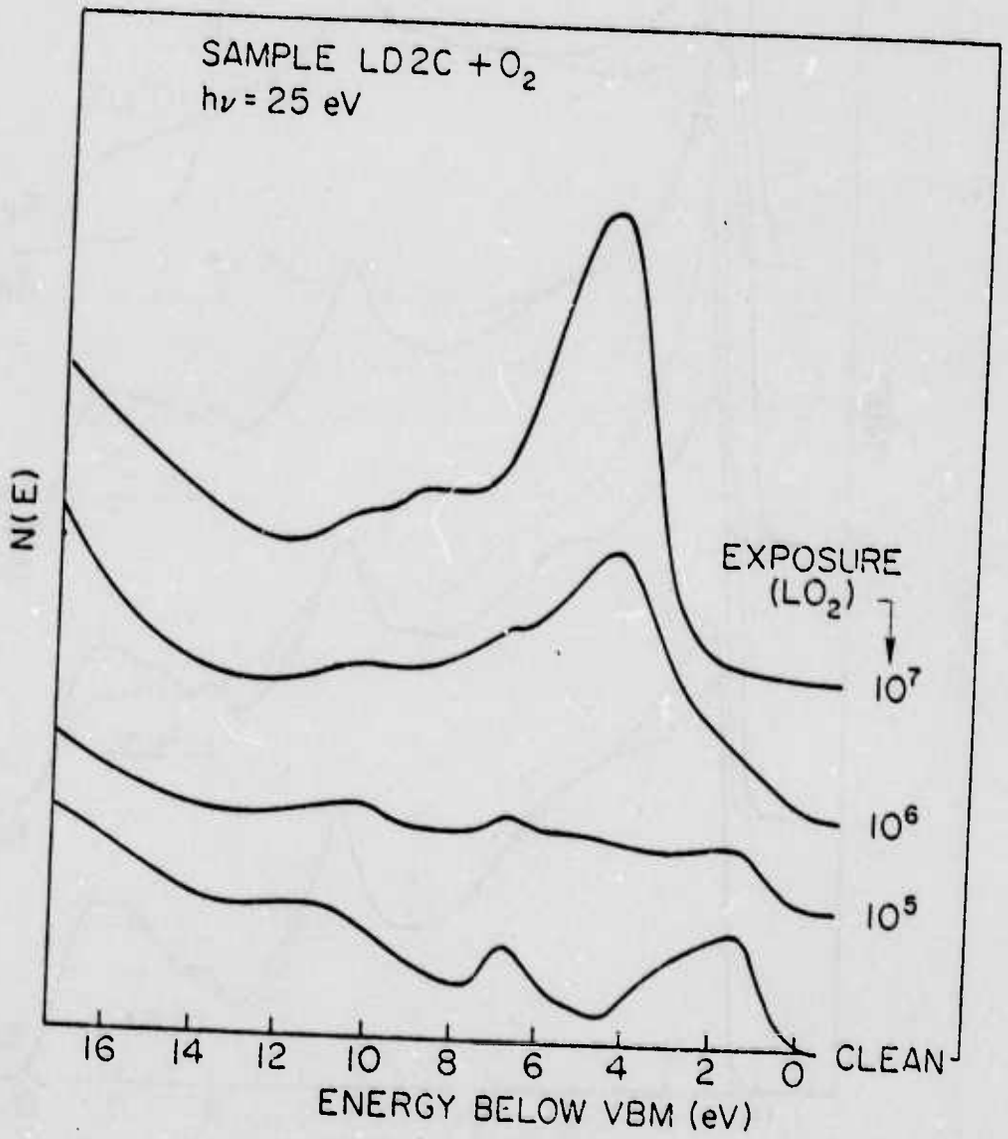
SAMPLE LD2C + O_2
$h\nu$ = 25 eV
N(E)
EXPOSURE (LO_2)
10^7
10^6
10^5
CLEAN
16
14
12
10
8
6
4
2
0
ENERGY BELOW VBM (eV)

Fig. 16

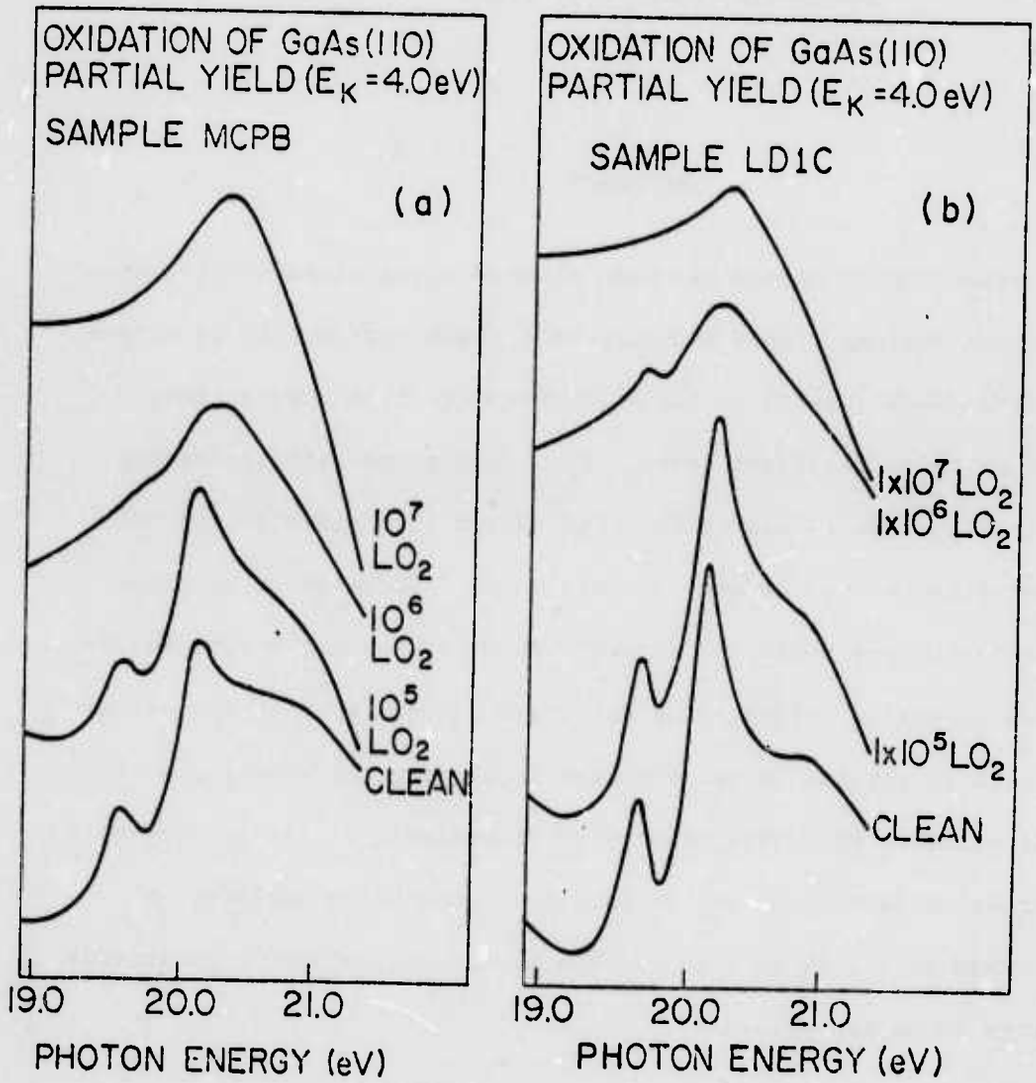
OXIDATION OF GaAs(110)
PARTIAL YIELD (E_K =4.0eV)
SAMPLE MCPB
(a)
10^7 LO_2
10^6 LO_2
10^5 LO_2
CLEAN
19.0
20.0
21.0
PHOTON ENERGY (eV)
OXIDATION OF GaAs(110)
PARTIAL YIELD (E_K =4.0 eV)
SAMPLE LD1C
(b)
$1x10^7$ LO_2
$1x10^6$ LO_2
$1x10^5$ LO_2
CLEAN
19.0
20.0
21.0
PHOTON ENERGY (eV)

Fig. 17 (a) & (b)

Chapter 8

THE OXIDATION OF Cs - UV PHOTOEMISSION STUDIES*

by

Paul E. Gregory, Patrick Chye, Hideo Sunami+ and W. E. Spicer
Stanford Electronics Laboratories
Stanford University, Stanford, Cal. 94305

+Present address: Central Research Laboratory of Hitachi. Ltd.
1-280 Higashikoigakubo
Kokubunji, Tokyo 185, Japan

ABSTRACT

The oxidation of cesium has been studied using ultraviolet photoemission spectroscopy. Upon exposure of a fresh cesium film to oxygen, a very narrow peak appears in the energy distribution curves (EDCs) about 2.6 eV below the Fermi level, E_f, and grows with increasing exposure. This peak is associated with oxygen ions dissolved in the cesium metal below the surface. After 3×10^{-5} Torr-sec of exposure, additional structure begins to appear. This is associated with the precipitation of cesium oxides. The structure associated with the oxides changes with increasing oxygen exposure indicating the appearance of different oxides. The oxide penetrates appreciably to the surface only after strong oxide buildup has taken place beneath the surface. A sharp minimum of 0.7 eV is found in the work function over a relatively small range of oxygen exposure.

*This research was supported by the Advanced Research Projects Agency of the Department of Defense and monitored by Night Vision Laboratory, USAECOM under Contract No. DAAK 02-74-C-0069.

I. INTRODUCTION

Recently it has become evident that ultraviolet photoemission spectroscopy can be used to study the process of oxidation of solids. Of particular importance to the present work was the study of the oxidation of Sr carried out by Helms and Spicer.[1] They showed that the oxygen ions formed in the oxidation process in the early stages of oxidation did not remain on the surface but, rather, were located below the surface layer of Sr atoms. On the basis of the Sr work, it was suggested that two important criteria for the occurrance of such behavior were: 1) that the oxide be ionic in nature since, in that case, the energy will be minimized when the oxygen ion sits beneath the surface so that it receives the maximum benefit from the surrounding positive charge of the lattice and 2) the lattice be sufficiently open so that the oxygen ion does not have to move through a large repulsive potential barrier to gain the interior of the sample. Both criteria were well satisfied in Sr . Concerning the second criterion, it should be noted that Sr has a fcc lattice and that the oxygen ions very neatly fill the interstitial sites forming a NaCl lattice. The Sr-Sr distance shrinks from 4.3 Å to 3.66 Å on oxidation. Thus, one would not expect an appreciable activation energy for the motion of oxygen ion into the bulk of the sample, and none was found.

Cesium also has quite an open fcc lattice and is ionic. Therefore, we would expect the oxygen to lie below a surface layer of Cs atoms. However, as can be seen[2] from Fig. 1, it has a very complex oxide phase diagram with an unusually large number of oxides.

Cesium oxide is also of interest because in thin layers it provides perhaps the lowest work function material known. However, little relationship has been established between the phase diagram and the work function. In particular, it has not been established which of the oxides corresponds to the low work function. Recently, interest in the low work function cesium oxide layers has been renewed because of the new class of negative electron affinity photoemitters which has been developed.[3] These emitters depend on obtaining optimum thin cesium oxide layers, and properties of these layers appear to limit the long wavelength threshold which can be obtained and the time-stability of the cathodes. It appeared useful to study the oxidation of thick films of Cs by UPS in order to provide background information which could be correlated with similar studies made on the cesium oxide produced on the surface on negative affinity photocathodes.

II. EXPERIMENTAL DETAILS

The experiment was carried out in a stainless steel ultra-high vacuum system with a base pressure of about 3×10^{-10} Torr as measured on a Redhead gauge. EDCs were measured using a standard retarding potential system.[4]

The cesium metal was contained in a vacuum sealed glass ampul. The ampul contained about 1/3 gram of Cs which had been vacuum distilled from a 1 gram Cs ampul purchased from Electronic Space Products, Inc. The 1/3 gram ampul was placed in a copper side arm of about 30 cm total length. After pump down and bakeout of the system the side arm was crushed to break the ampul. The Cs remained in the side arm after the

ampul was crushed. It was necessary to heat the side arm with heat tapes or a propane torch in order to evaporate cesium at a sufficiently rapid rate.

The cesium was evaporated onto a copper substrate which had been cooled to approximately 140 K with a liquid nitrogen cooled cold strap. After several hours of cooling the substrate temperature reached a minimum of 100 K. All data shown in this article was measured at a temperature between 100 K and 140 K on films which had never been warmed above 140 K.

It took approximately one hour to evaporate a sample sufficiently thick for measurements. It was not possible to measure the thickness of the cesium layer, but it was visible as a dull, dark layer on the substrate. During evaporation the yield was monitored at 7.7 eV. The yield first rose as a monolayer of Cs was deposited, and then fell as a bulk Cs layer formed. For the final layer only, emission from the metallic cesium was obtained.

During Cs evaporation the pressure rose to about 5×10^{-8} Torr. During measurement the pressure was approximately 3×10^{-9} Torr. The system was pumped by an Orb-Ion pump and a small VacIon pump. It was necessary to turn the Orb-Ion off during measurements because the light from its filaments caused photoemission from the Cs .

The Cs was oxidized while cold by admitting high purity (10 ppm impurities) oxygen into the system through a Varian leak valve. The presence of Cs in the system caused large reverse currents, which produced low energy peaks in the EDCs, similar to those shown in Fig. 1 of Reference 5. The reverse current peaks have been removed from the EDCs shown in this paper.

III. RESULTS

A. Introduction

Figure 2a shows the photoelectric yeild of the oxidized cesium film as a function of oxygen exposure. From it we see that the oxidation process up to 4×10^4 Langmuirs ($1L = 10^{-6}$ Torr-sec) may be divided approximately into four regions. In region I there is only a slight increase in yield with exposure. At about 10L a more rapid rate of increase is observed, up to about 100L, at which point the yield begins to rise rapidly. At 500L we enter region IV where the yield drops slowly with exposure.

EDCs of oxidized cesium are shown in Fig. 3 through 10. Two sets of EDCs are presented for $h\nu = 7.7$ and $h\nu = 10.2$ eV. The EDCs shown are taken from two different runs of the experiment. The EDCs were quite reproducible from the two runs. The EDCs are normalized so that the area under the curve equals the yield at the indicated photon energy. Note that there is a scale change between Figs. 3 and 4, 4 and 5, 7 and 8, and 8 and 9.

B. Low Oxygen Exposure (Regions I and II)

EDCs for clean Cs are shown in the bottom curves in Figs. 3 and 7. Peak A is due to unscattered electrons from the Cs valence band. These EDCs agree very well with previous work on clean Cs [5,6] except that the weak structure labeled B_1 in our curves is much weaker than the peak in the same position in the work of Smith et al. Since shoulder B_1 is at the same energy where the strong oxide peak B develops, we believe that the clean Cs investigated by Smith actually had a small oxygen contamination. Our curve for 1L exposure looks more like the EDCs of Smith than our EDCs from clean Cs. We believe that our Cs was

very clean because the Cs was distilled under vacuum once before the ampul was placed in the experimental chamber, and because the long path around two bends which the Cs had to traverse on its way to the substrate caused further purification of the Cs . On the other hand, Smith's apparatus featured a line-of-sight evaporation from the Cs ampul to the substrate.

Peak B_1 has previously been attributed to valence electrons which have been scattered by a surface plasmon.[5,6] Our data does not preclude that explanation; we still see a weak shoulder B_1 before oxidation. The shoulder is fairly broad and asymmetrical compared to the oxide peak B , which tends to suggest that the shoulder B_1 is not caused by oxygen contamination. The shoulder could be caused by the surface plasmon as originally proposed, or it could be due to small quantities of contaminants in the Cs .

In Figs. 3 and 4 it is important to note that the magnitude of peak A does not decrease for oxygen exposures up to 200L, although the growth of structure below -2 eV is very dramatic. Peak A is caused by unscattered electrons emitted from the conduction band of cesium. This is exactly the same behavior as was seen in the oxidation of Sr .[1] As mentioned in the introduction, in the study of oxidation of Sr it was found that, until oxidation neared completion, the oxide was located beneath the surface and the surface remained very metal rich. The first step in the oxidation process was the appearance of dissolved $O^=$ ions below the surface. The first step in the oxidation of Cs appears to be identical to that of Sr , i.e., $O^=$ ions are dissolved in the Cs metal. This stage is characterized

by a narrow oxide peak in the EDCs in both cases. This is followed by precipitation of crystallites. Here Sr differs from Cs in that it has one dominant oxide whereas Cs has many oxides (see Fig. 1). In this study a metallic Fermi edge was clearly visible in the EDCs on an expanded scale, at 300L exposure, and barely visible at 500L exposure. Beyond 500L exposure any Fermi edge was buried in the noise. Thus we believe that at least up to the 200L exposure, there is a layer of Cs metal on the surface, with the oxide lying in the bulk of the material. From 300 through 500L there is probably an increasing amount of oxide mixed with the cesium at the surface. Above 500L there is probably only oxide at the surface. As we will see later a sharp minimum appears in the work function near 500L exposure.

The extreme sharpness of the peak B for exposures up to 30L is also similar to the behavior of Sr oxidation,[1] and again we believe that the explanation is the same in both cases: for the first 20-30L the oxygen atoms are well separated so that the oxygen-oxygen overlap is very small. Thus the peak B is an atomic-like oxygen level. From 30-100L, peaks C and D develop, indicating that oxygen levels overlap at these exposures, i.e., formation of cesium oxygen compounds starts.

C. Regions of Large Oxygen Exposure (Regions II, III and IV)

As can be seen from Figs. 4-6 and 8-10, there are very distinct changes in the EDCs as the oxidation proceeds from 30 to 5000L. Based on phase diagrams and estimates of vapor pressure, Bell[7] has estimated that the phase important for activation of photocathodes is Cs_2O_2. Four other compositions lie on the cesium rich side of this composition.

Another important parameter is contained in Figs. 3-8. This is the work function $e\phi$, which is obtained from the EDCs by subtracting the width of the EDC (from the low energy cutoff to the Fermi level) from the photon energy used to produce the EDC. In Fig. 2b the work function is plotted versus oxygen exposure. At 500L oxygen exposure, the yield (Fig. 2a) reaches a maximum and the work function reaches a sharp minimum of about 0.7 eV. In addition a fairly distinct EDC is obtained at 500L. Note in particular that a distinct peak (C) is present at -4.5 eV in Fig. 3, which is not well defined for any nearby oxygen exposure. Thus it appears that a fairly distinct EDC occurs for the low work function form of cesium oxide. Note also that it was just above 500L exposure that the metallic Fermi edge completely disappeared.

IV. CONCLUSIONS

The oxidation of Cs proceeds in a manner which is in general similar to that of Sr. The first step in the oxidation is the appearance of dissolved oxygen ions inside the metal. This is followed by precipitation of oxides. However, Cs differs from Sr in two ways. First after oxide appears, the structure in the EDCs from the cesium oxide changes with oxygen exposure, indicating the appearance of different cesium oxides; whereas, in the oxidation of Sr, only one oxide is observed. Second, a sharp minimum appears in the cesium oxide work function with oxygen exposure. No similar sharp minimum was observed in the case of the Sr. This work provides a starting point in attempting to better understand the low work function of cesium oxide layers which are so important to III-V photocathodes and other electron emitting devices. The next step in this

investigation will be the examination of cesium oxide on practical emitting surfaces.

ACKNOWLEDGEMENTS

Valuable discussions with R. L. Bell and John Edgecomb of Varian are gratefully acknowledged.

REFERENCES

1. C. R. Helms and W. E. Spicer, Phys. Rev. Lett. 28, 565 (1972); 31, 1307 (1973); 32, 228 (1974); Appl. Phys. Lett. 21, 237 (1972).
2. Figure 1 is an approximate phase diagram compiled by R. L. Bell from several sources, in particular R. P. Elliott, Constitution of Binary Alloys, First Supplement, McGraw-Hill, (1965) and S. P. Bernardell, Ph.D. Thesis, University of Rhode Island (1971).
3. R. L. Bell, Negative Electron Affinity Devices, Clarendon Press, Oxford (1973); R. L. Bell and W. E. Spicer, Proc. IEEE 58, 1788 (1970); W. E. Spicer and R. L. Bell, Publ. of Astronomical Soc. of Pacific, 84, 110 (1972).
4. C. R. Eden, Ph.D. Thesis, Stanford University (unpublished); Rev. Sci. Inst. 41, 252 (1970).
5. N. V. Smith and G. B. Fisher, Phys. Rev. B3, 3662 (1971).
6. N. V. Smith and W. E. Spicer, Phys. Rev. Lett. 23, 769 (1969).
7. R. L. Bell, private communication.

FIGURE CAPTIONS

1. Approximate phase diagram for the Cs-O system (Ref. 1).

2a. Yield of cesium oxide versus oxygen exposure.

2b. Work function of cesium oxide versus oxygen exposure.

3. EDCs of cesium oxide at 7.7 eV for clean cesium through 30L oxygen exposure.

4. EDCs of cesium oxide at 7.7 eV for oxygen exposure from 30L to 200L.

5. EDCs of cesium oxide at 7.7 eV for oxygen exposure from 200L to 1000L.

6. EDCs of cesium oxide at 7.7 eV for oxygen exposure from 1000L to 40,000L.

7. EDCs of cesium oxide at 10.2 eV for oxygen exposure for clean cesium through 30L oxygen exposure.

8. EDCs of cesium oxide at 10.2 eV for oxygen exposures from 30L to 200L.

9. EDCs of cesium oxide at 10.2 eV for oxygen exposures from 200L to 1000L.

10. EDCs of cesium oxide at 10.2 eV for oxygen exposures from 1000L to 40,000L.

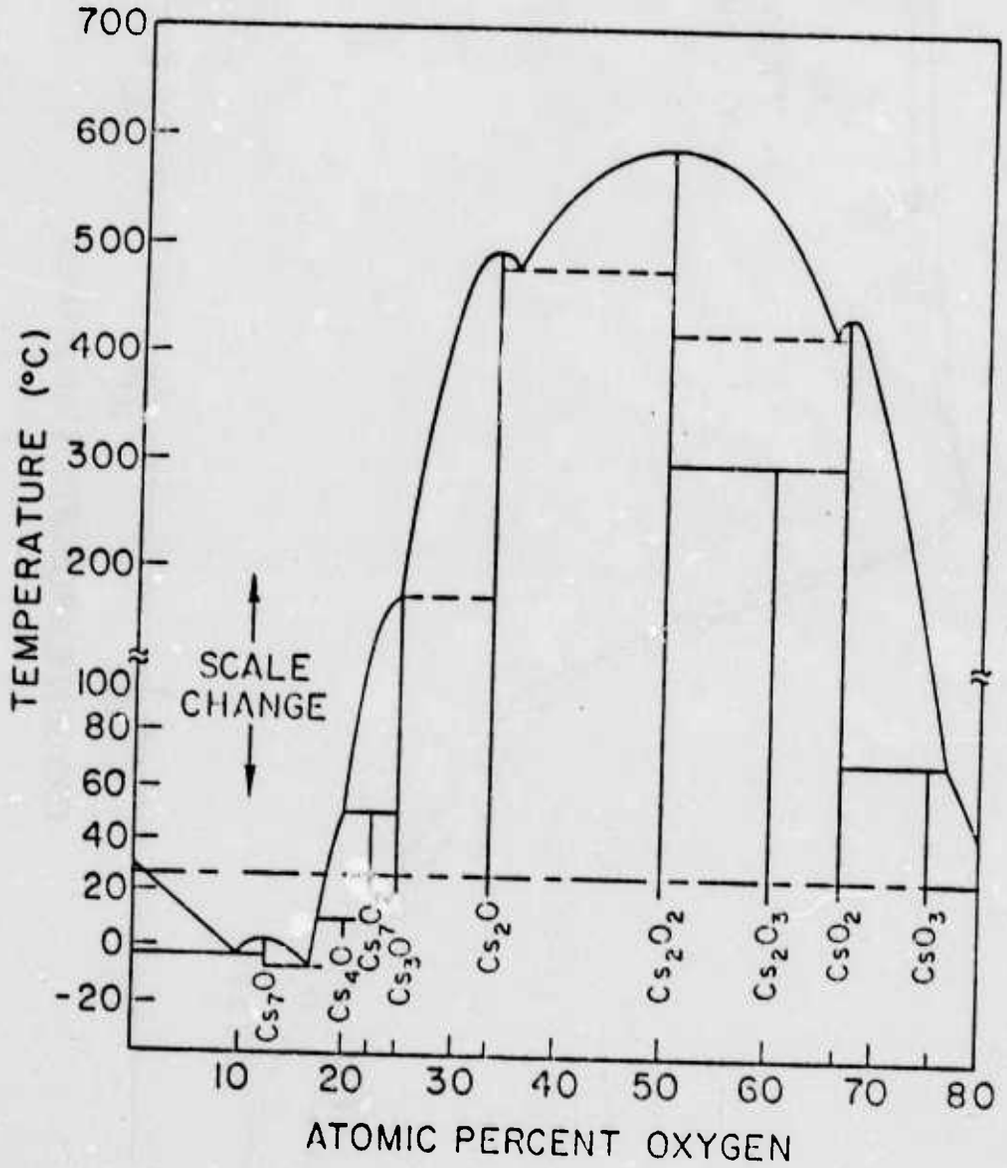
700
600
500
400
300
200
100
80
60
40
20
0
-20
TEMPERATURE (°C)
SCALE CHANGE
Cs_7O
Cs_4O
Cs_7O_2
Cs_3O
Cs_2O
Cs_2O_2
Cs_2O_3
CsO_2
CsO_3
10
20
30
40
50
60
70
80
ATOMIC PERCENT OXYGEN

Fig 1

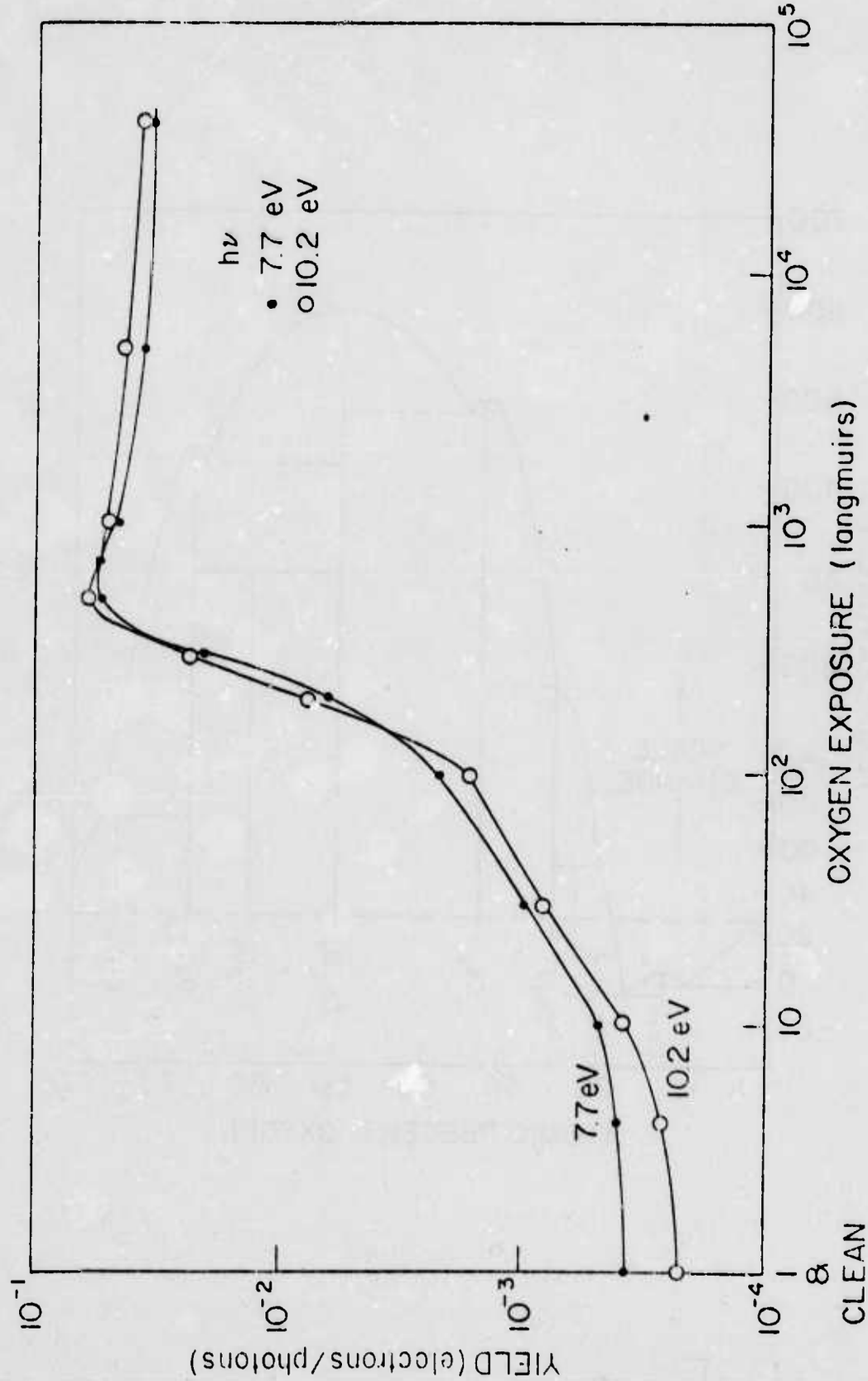
YIELD (electrons/photons)
10^{-1}
10^{-2}
10^{-3}
10^{-4}
hν
• 7.7 eV
○ 10.2 eV
7.7eV
10.2 eV
1
CLEAN
10
10^2
10^3
10^4
10^5
OXYGEN EXPOSURE (langmuirs)

Fig 2a

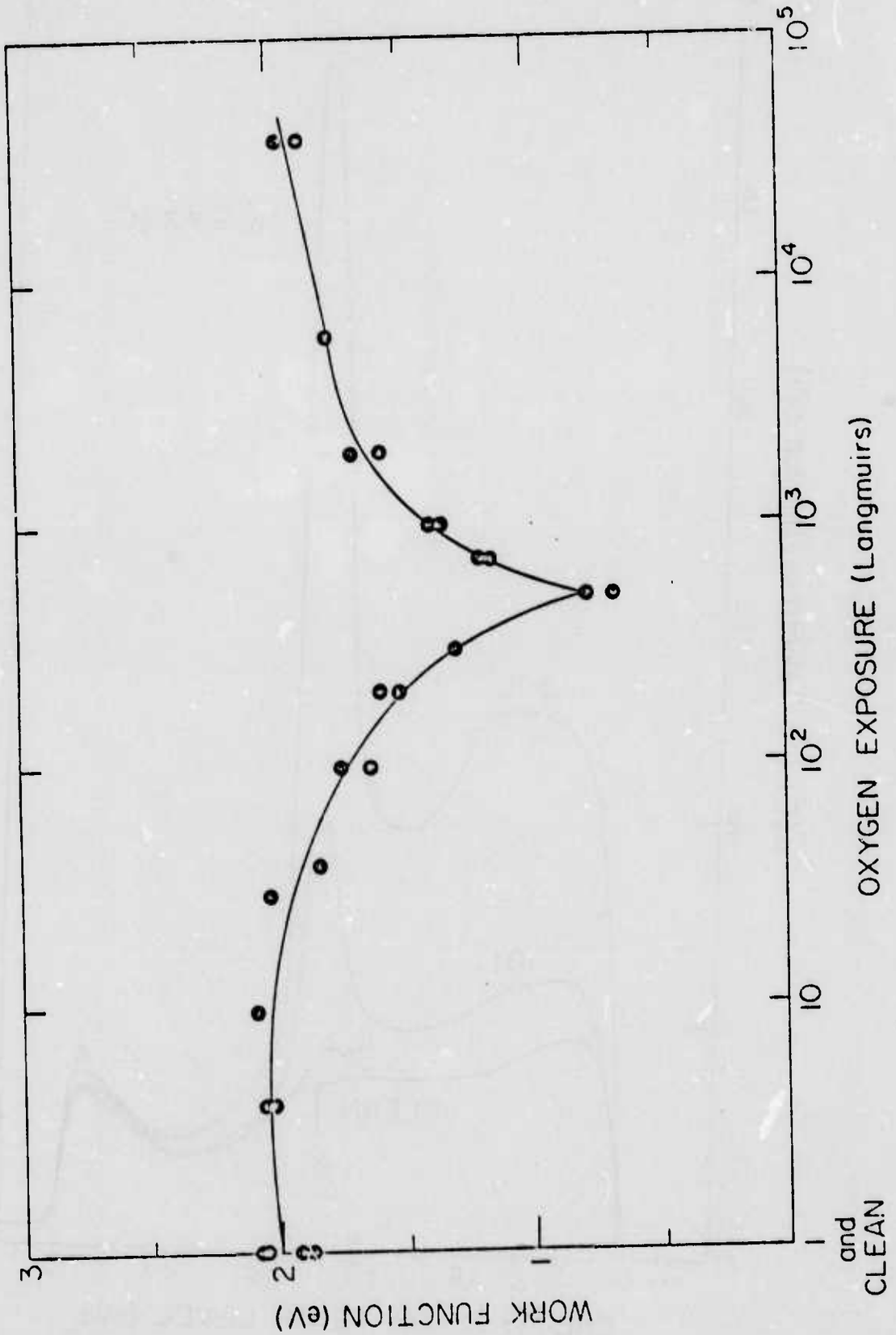
WORK FUNCTION (eV)
3
2
OXYGEN EXPOSURE (Langmuirs)
and CLEAN
1
10
10^2
10^3
10^4
10^5

Fig 2b

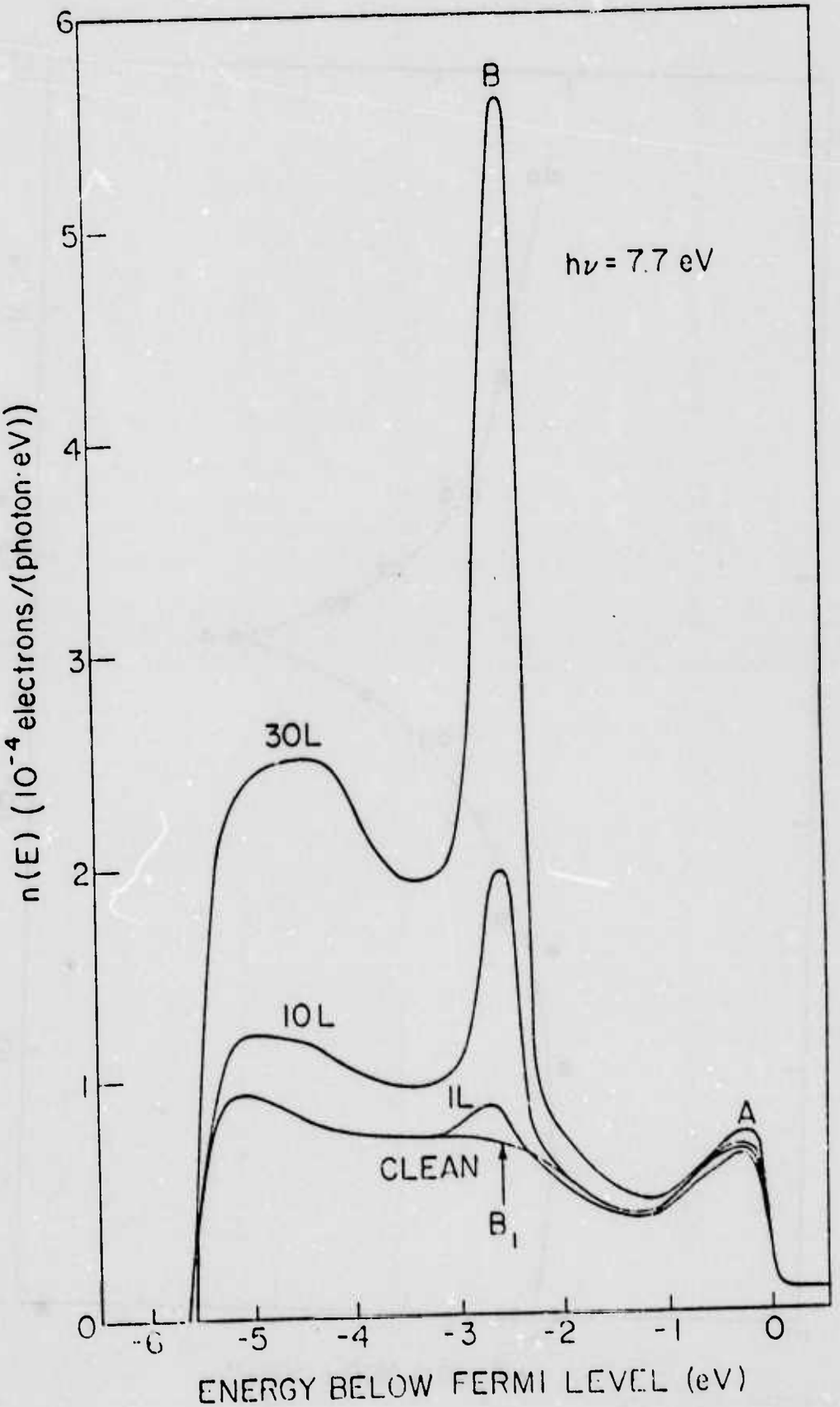
B
hν = 7.7 eV
30L
10L
1L
CLEAN
A
B1
n(E) (10-4 electrons/(photon·eV))
ENERGY BELOW FERMI LEVEL (eV)
0
1
2
3
4
5
6
-6
-5
-4
-3
-2
-1
0

Fig 3

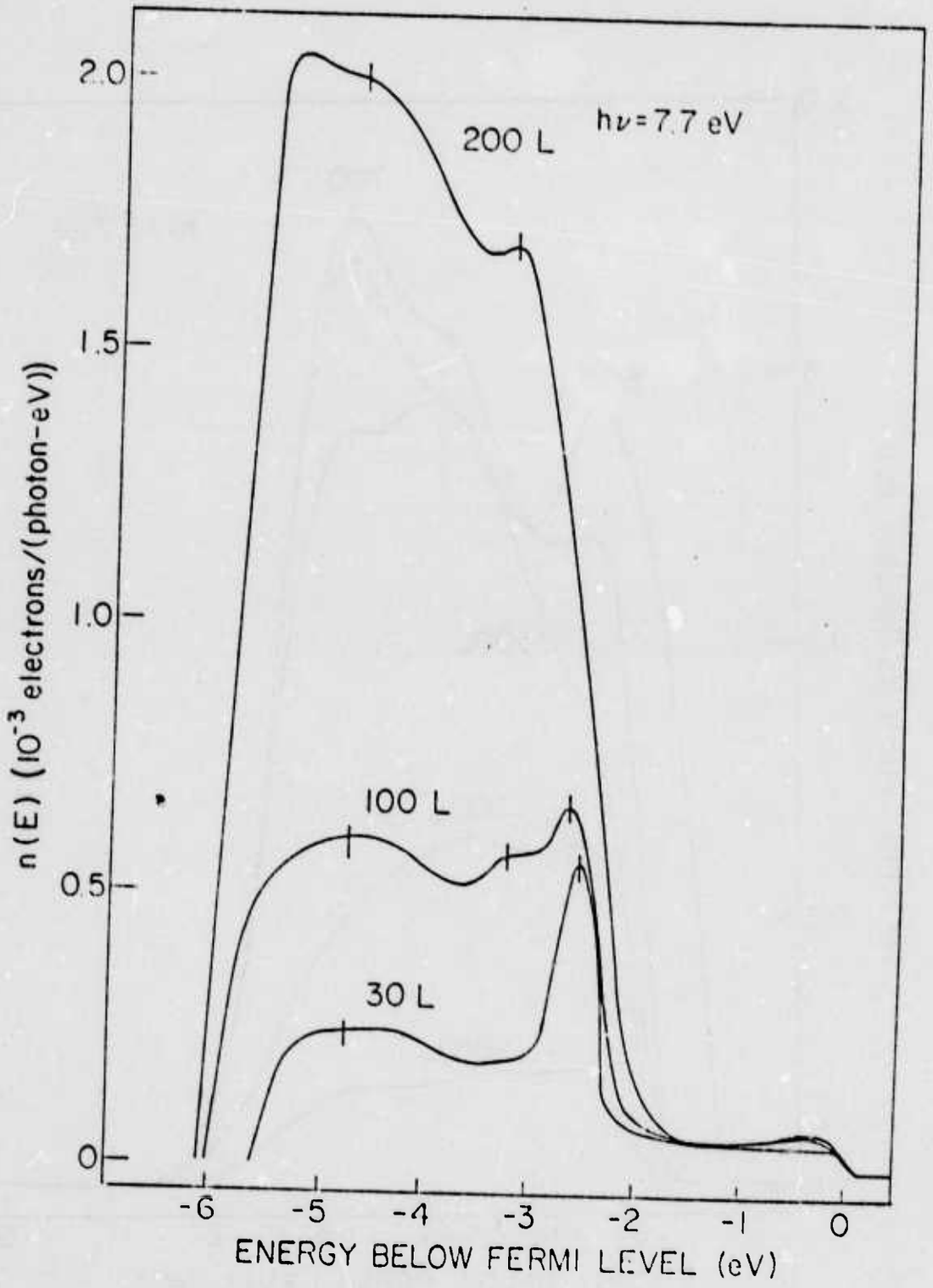
2.0
1.5
1.0
0.5
0
200 L
hν=7.7 eV
100 L
30 L
n(E) (10⁻³ electrons/(photon-eV))
-6
-5
-4
-3
-2
-1
0
ENERGY BELOW FERMI LEVEL (eV)

Fig 4

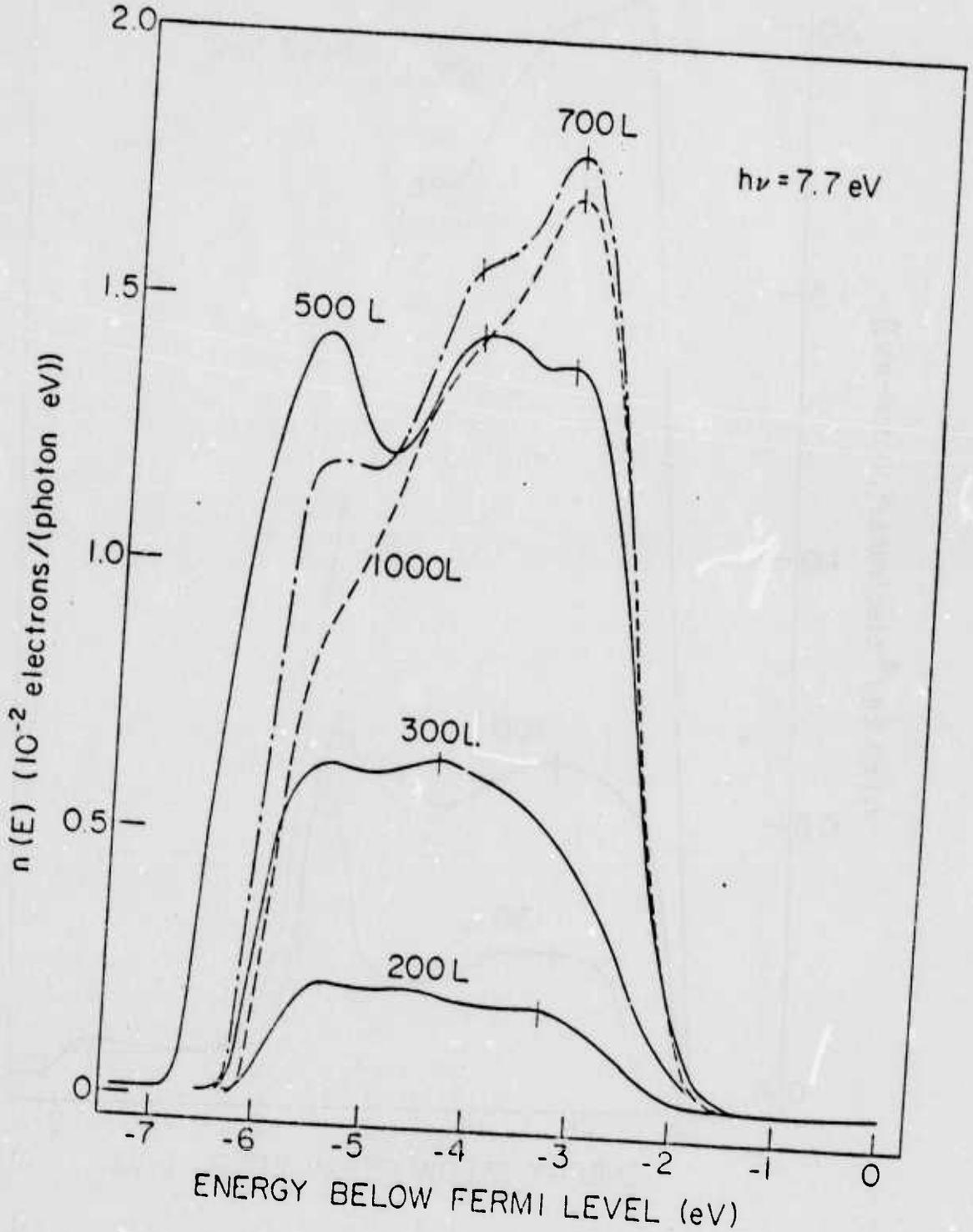
2.0
1.5
1.0
0.5
0
700 L
hν = 7.7 eV
500 L
1000L
300L.
200 L
n(E) (10⁻² electrons/(photon eV))
-7
-6
-5
-4
-3
-2
-1
0
ENERGY BELOW FERMI LEVEL (eV)

Fig. 5

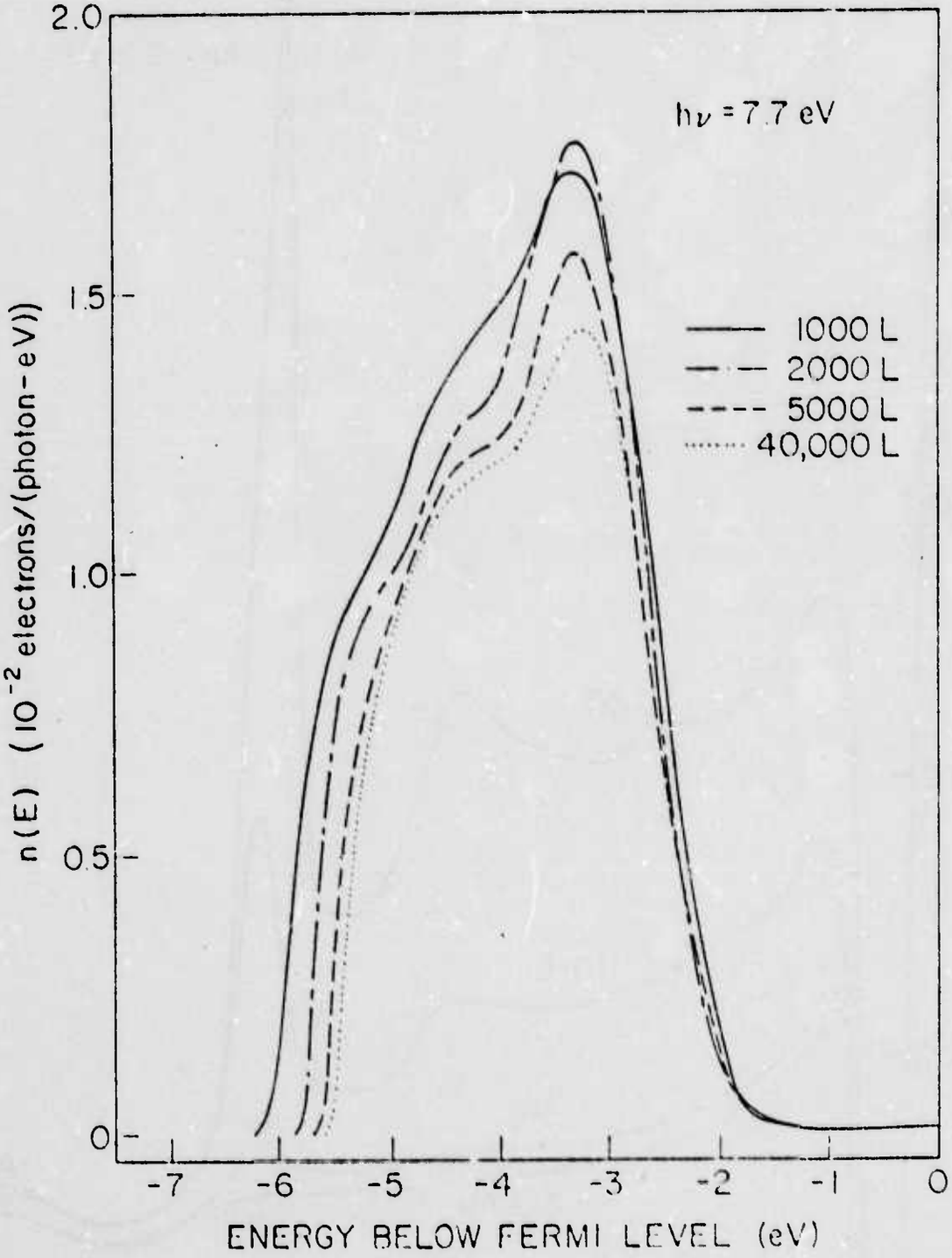
2.0
1.5
1.0
0.5
0
n(E) (10⁻² electrons/(photon-eV))
hν = 7.7 eV
1000 L
2000 L
5000 L
40,000 L
-7
-6
-5
-4
-3
-2
-1
0
ENERGY BELOW FERMI LEVEL (eV)

Fig 6

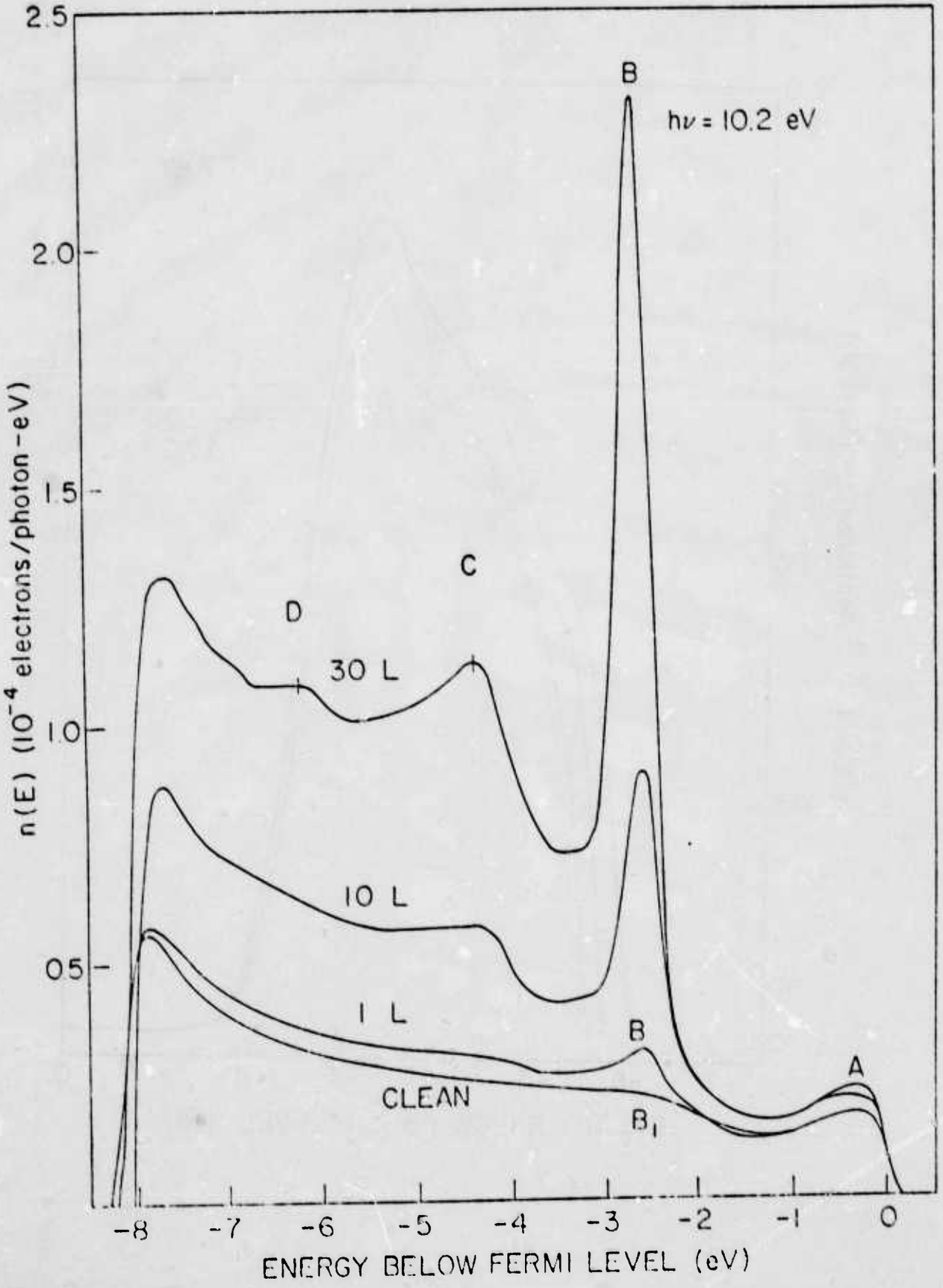
2.5
2.0
1.5
1.0
05
n(E) (10^{-4} electrons/photon-eV)
B
hν = 10.2 eV
C
D
30 L
10 L
1 L
CLEAN
B
A
B_1
-8
-7
-6
-5
-4
-3
-2
-1
0
ENERGY BELOW FERMI LEVEL (eV)

Fig 7

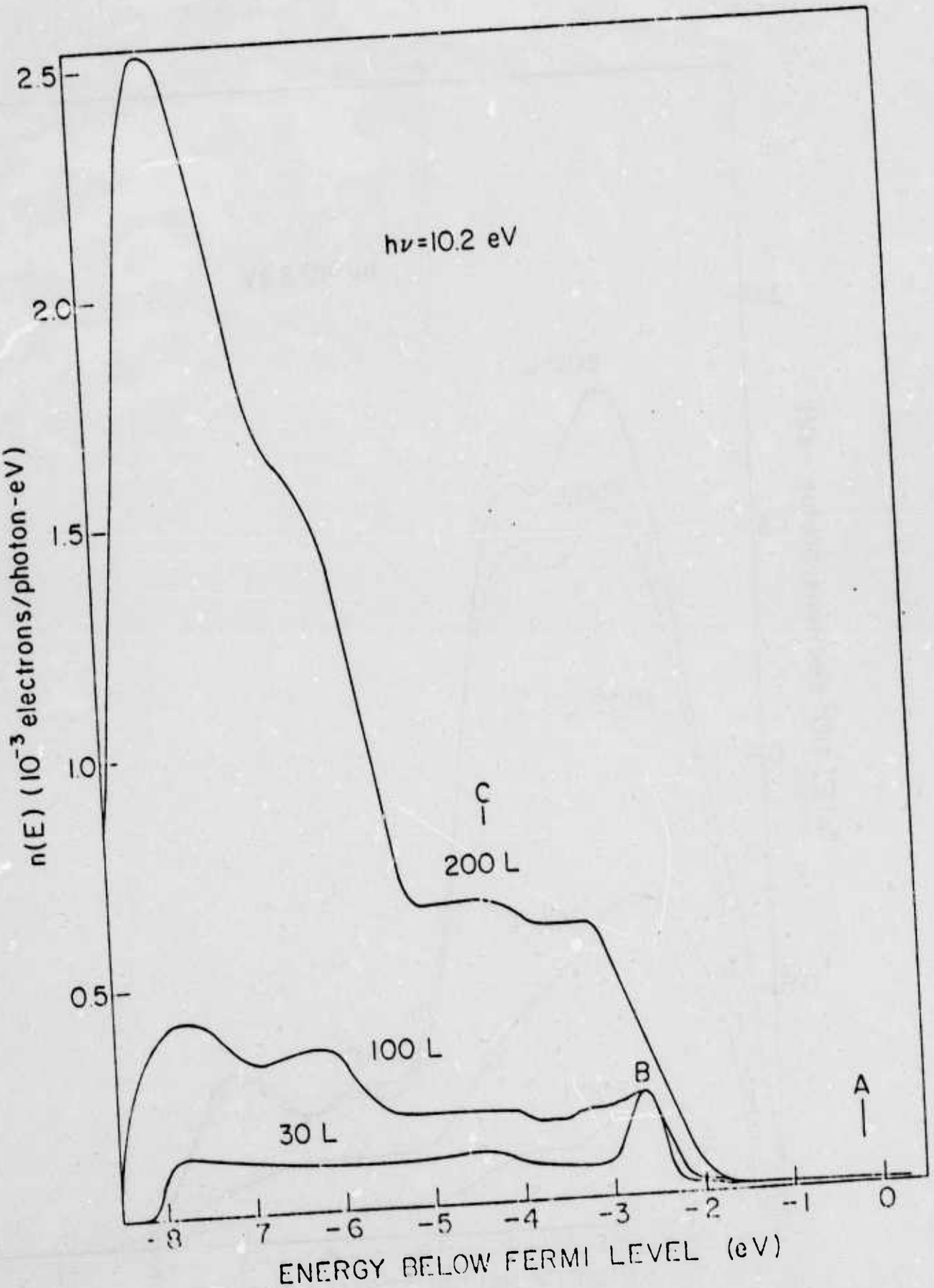
hν=10.2 eV
n(E) (10^{-3} electrons/photon-eV)
2.5
2.0
1.5
1.0
0.5
C
200 L
100 L
30 L
B
A
-8
-7
-6
-5
-4
-3
-2
-1
0
ENERGY BELOW FERMI LEVEL (eV)

Fig 8

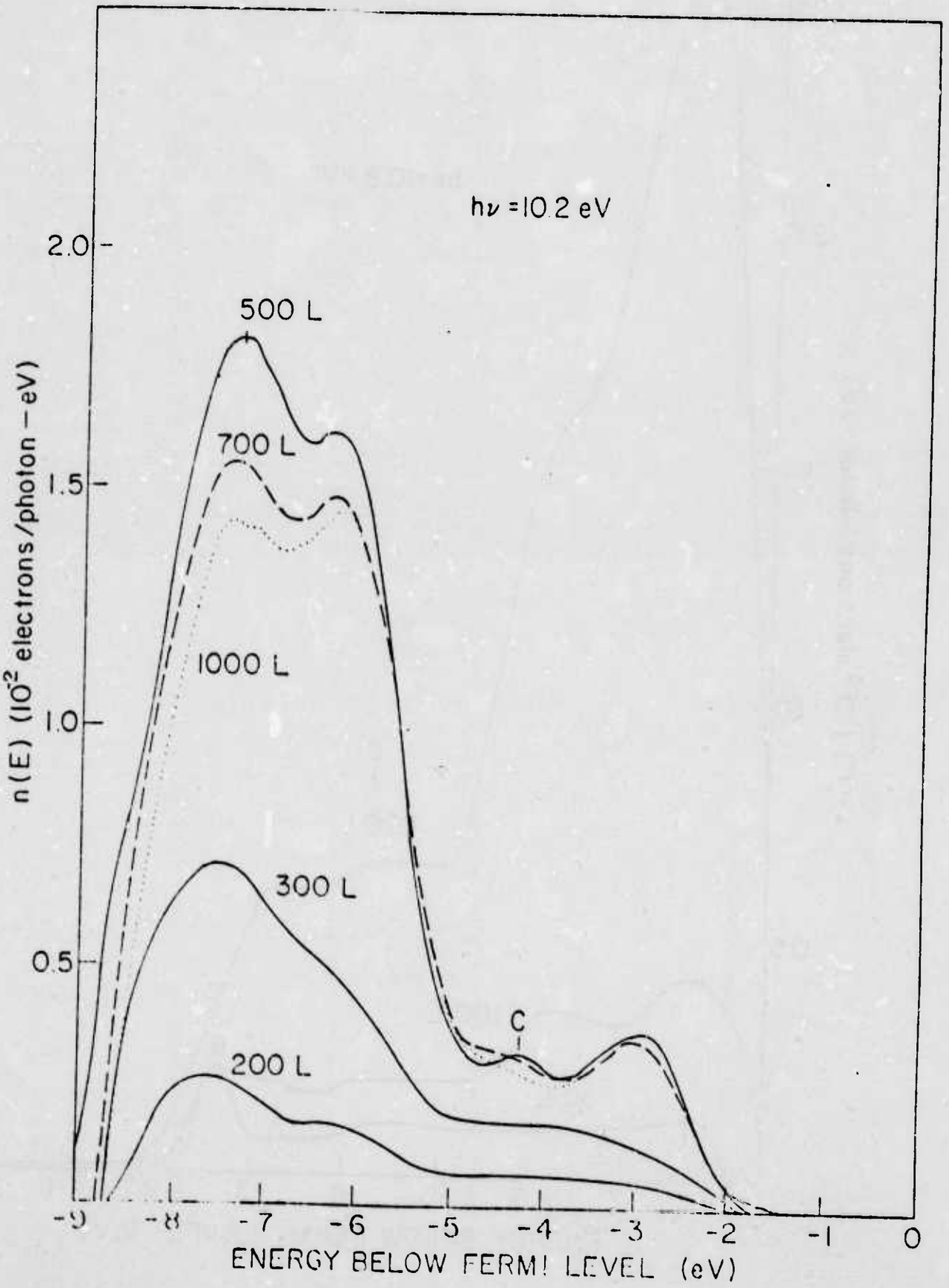
hν = 10.2 eV
500 L
700 L
1000 L
300 L
200 L
C
n(E) (10⁻² electrons/photon – eV)
2.0
1.5
1.0
0.5
-9
-8
-7
-6
-5
-4
-3
-2
-1
0
ENERGY BELOW FERMI LEVEL (eV)

Fig 9

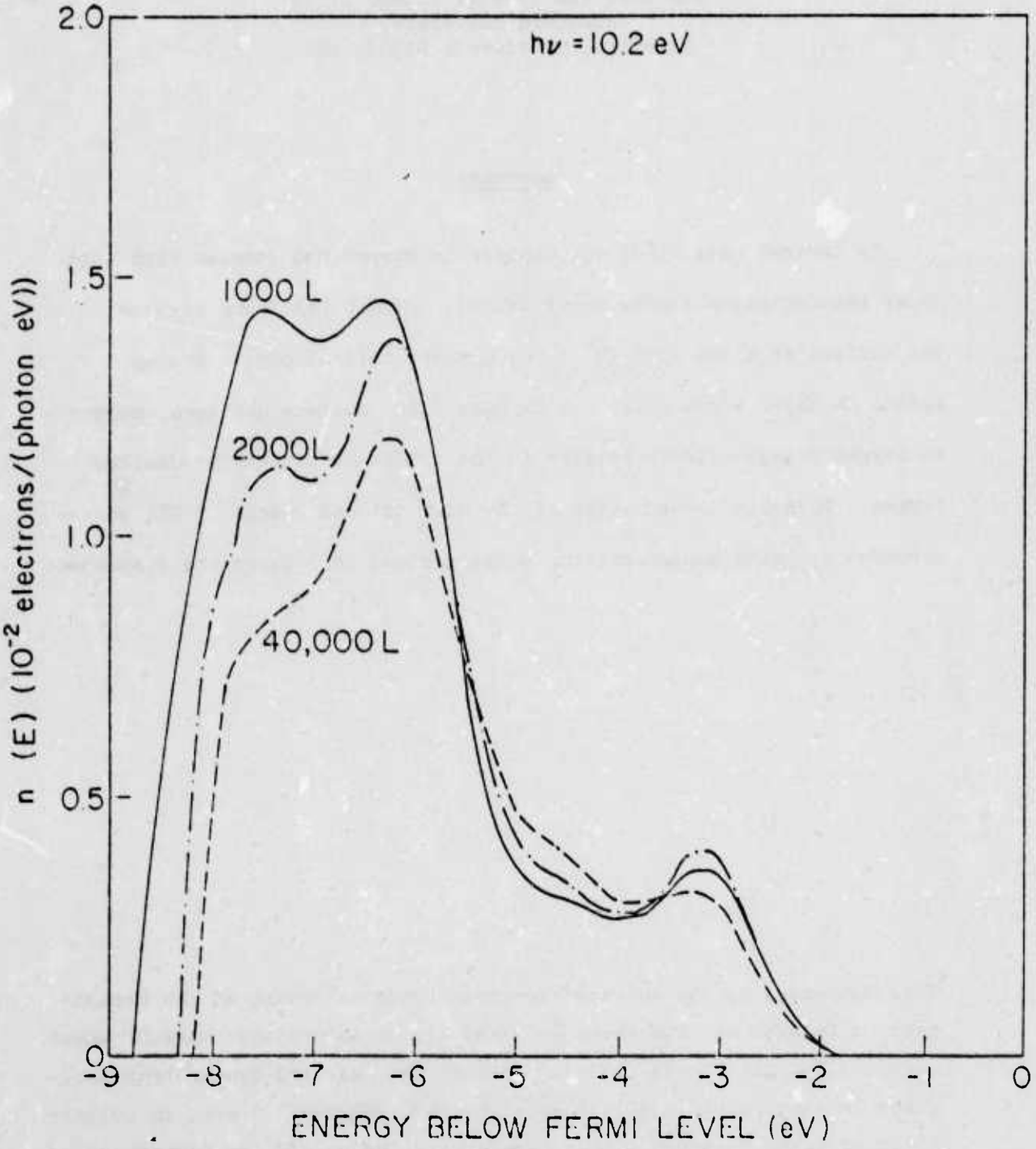
hν = 10.2 eV
1000 L
2000L
40,000 L
n (E) (10⁻² electrons/(photon eV))
2.0
1.5
1.0
0.5
0
-9
-8
-7
-6
-5
-4
-3
-2
-1
0
ENERGY BELOW FERMI LEVEL (eV)

Fig 10

Chapter 9

OXYGEN CHEMISORPTION ON Cs COVERED GaAs (110) SURFACES*

C. Y. Su, P. W. Chye, P. Pianetta,
I. Lindau, and W. E. Spicer
Stanford Electronics Laboratories
Stanford University
Stanford, California 94305, USA

Abstract

Cs covered GaAs (110) was exposed to oxygen and studied with soft X-ray photoemission spectroscopy (SXPS). Oxygen was found to bond to the surface As atoms with 10^6 times greater initial oxygen uptake. A second Cs layer added after the Cs/GaAs (110) surface had been exposed to oxygen brings effects similar to the oxidation of GaAs by excited oxygen. Possible inadequacies of the conventional models of NEA photocathodes assuming noninteracting substrate and Cs_2O layer are discussed.

*Work supported by the Advanced Research Projects Agency of the Department of Defense and monitored by Night Vision Laboratory, USAECOM under Contract No. DAAK 02-74-C-0069. Work at the Stanford Synchrotron Radiation Laboratory was also supported by NSF, DMR73-07692 A02, in cooperation with the Stanford Linear Accelerator Center and the Department of Energy.

Adsorption and initial oxidation of the III-V compound semiconductor are topics extensively discussed in the literature,[1] particularly for the case of GaAs. In this work, we coadsorbed Cs and oxygen on GaAs (110) in order to further probe the oxidation property of this surface. The results are compared to those for the oxidation of clean GaAs. A discussion will also be presented in relation to the negative electron affinity (NEA) photocathodes, where the process of coadsorption of Cs and oxygen is assumed to give a low work function coating of Cs_2O without involving the substrate.[2]

Experiments were done using synchrotron radiation at the Stanford Synchrotron Radiation Laboratory (SSRL) in the same sample chamber previously reported.[3] Cs from an atomic cesium source was evaporated onto a vacuum cleaved n-GaAs (110) crystal kept at room temperature until the photoemission of the Cs-4d level saturated, at which point a monolayer coverage had been reached. Additional Cs deposited beyond this coverage will be pumped away from the surface. Research grade oxygen was admitted into the vacuum through a bakable leak valve. Slightly different oxygen-cesium treatments were applied to three separate cleaves of the crystal with good reproducibility of the important features in the photoemission spectra.

Figure 1 shows the EDCs of a cleaved GaAs (110) surface exposed to unexcited molecular oxygen according to the work by Pianetta et al.[4] The shifted peak 2.9 eV below the As-3d peak (E_B = 40.8 eV) serves as a fingerprint for oxygen chemisorbed on the As of GaAs. Contrasted to these results, the EDCs obtained at different oxygen exposures on a cesiated GaAs (110) surface are shown in Fig. 2. At 10 L oxygen exposure (1 L = 10^{-6} torr-sec), we see the chemically shifted As-3d peak

characteristic of oxygen adsorbed on GaAs. As we go to higher exposures, the shifted As-3d peak and the O-2p peak grow simultaneously until saturation is reached between 40 and 1000 L. A striking contrast between the oxidation of clean GaAs and cesiated GaAs is immediately apparent here. The oxygen uptake is many orders of magnitude faster on the cesiated surface. Thus, the spectra at 20 and 5×10^7 L O_2 for the cesiated and clean surfaces, respectively, are comparable.

The effect of oxygen on Cs is to shift the Cs core levels (5s and 5p in Fig. 2, Cs-4d not shown) to lower binding energy with peak shapes unchanged. Accompanying the Cs core level shift is the continuous movement of the shifted As-3d peak to higher binding energy. Movement of both the Cs peaks and the shifted As-3d peak stabilize in energy position around 40 L O_2, at which point the growth in strength of the shifted As-3d peak also slows down. This correlation indicates interaction between the oxidizing substrate and the Cs/O overlayer. The nature of this complex interaction will be presented elsewhere.[5] As far as we are concerned here, it is sufficient to point out that the shifted As-3d peak with energy position from 2.9 to 3.3 eV below the unshifted peak represent the same chemisorption state of oxygen on GaAs, the shift being due to the Cs-oxygen interaction.

As shown by the curve second from the top in Fig. 2, the second Cs dose caused several prominent effects. First, the Cs peaks and the oxygen related peaks shifted to higher binding energy by 0.8 eV, i.e., back to the original binding energy for Cs on GaAs. We also see the shifted As-3d peak broaden into two peaks: a new peak 4.5 eV below the unshifted peak plus the original one at 3.3 eV. Furthermore, a small shoulder appears 1.1 eV below the Ga-3d peak, as indicated by the arrow under "A"

in Fig. 2. These two effects on the Ga and As core levels are very similar to that in the case of exposing clean GaAs to oxygen excited by an ion gauge, of which the EDCs are shown in Fig. 3. (There are also some subtle effects on the Ga-3d core level, which will be discussed in detail elsewhere.[5]) Thus, it appears that true arsenic and gallium oxides are being formed.

It is possible that the heat brought to the surface by the deposited Cs atoms could break back bonds and create effects very similar to that caused by excited oxygen. There is no evidence for breaking back bonds before putting down the second Cs overlayer despite the fact that the heat of adsorption should be comparable for the first and the second Cs dose. This again confirms that, in order to break back bonds of the GaAs (110) surface, we need oxygen chemisorbed on the As dangling bonds, as was first proposed by Pianetta et al.[4] After subjecting the Cs/O/Cs covered GaAs to a high oxygen exposure, the Cs peaks were shifted back 0.8 eV toward lower binding energy. In addition to this complex shift to be discussed elsewhere,[5] there are two effects concerning the oxidation of GaAs. First, if we take the relative area under shifted and unshifted As-3d peak as a measure of the oxygen coverage, we have oxidized more than one monolayer of GaAs. Moreover, the ΔE_B (change in binding energy) = 4.5 eV state corresponding to As_2O_5 has been converted to the lower oxide As_2O_3 with ΔE_B = 3.7 eV. These two effects, again, manifest the breaking of back bonds.

The large enhancement in the initial oxidation rate can be explained by the following picture. The oxygen molecules, which impinged on the Cs-covered parts of the GaAs, undergo a dissociative chemisorption on top of the Cs layer. Such dissociative chemisorption has been suggested

by Gregory et al[6] and Papageorgopoulos et al[7] on Cs and by Wijers et al[8] on Cs, Rb, and K. Once the oxygen is in atomic form, the Madelung energy makes it favorable for oxygen atoms to be distributed below the Cs adatoms. This was first proposed by Helms and Spicer,[9] and applied to Cs by Gregory et al,[7] who also pointed out the two conditions to be fulfilled for such mechanisms to work, namely, the high electronegativity difference between O and Cs and the relatively open structure of the Cs layer. Oxygen at such a position can readily bind to the As of GaAs. Since, to the first order, the Cs overlayer does not perturb the O-GaAs binding and causes a large enhancement in the initial oxidation rate of GaAs, we could propose the dissociation of molecular oxygen into atomic oxygen to be the rate limiting process in the initial oxidation of the GaAs (110) surface. This was also suggested from the experiments by Pianetta et al[4] using hot filament excited oxygen. In our case, the dissociation of the molecular oxygen is ascribed to the presence of the Cs layer on the surface.

Although we did not follow the exact procedures of activating GaAs in making real NEA photocathodes, the results of the present work bear some very important implications to the understanding of NEA photocathodes. Whether there is cesium oxide, Cs_2O, or suboxides forming can not be deduced unambiguously from our data. But, we have definitely demonstrated that the oxygen does not only interact with the Cs overlayer but also affects the substrate strongly. The irreversible oxidation of the substrate may be responsible for the interfacial barrier which sets the ultimate limit for the long wavelength response of NEA photocathodes, as will be discussed further elsewhere. Moreover, the correlation of the Cs core level shifts to the growth of the shifted As-3d peak, as described

above, suggests that the interaction between the substrate and the Cs/O overlayer is complex but important in determining the final surface conditions that control the work function.[2]

In summary, we have observed the important phenomenon of enhanced oxygen uptake on the GaAs (110) surface by the presence of a metal adlayer. From the observation that a cesium overlayer causes dissociative chemisorption of O_2, it is inferred that the rate limiting process in the initial oxidation of clean GaAs is the dissociation of molecular oxygen into atomic oxygen. The results also suggest possible inadequacies of those models for the NEA photocathodes, which leave out the role played by the chemically active substrate.

The authors would like to thank Mr. D. Ling and L. Derbenwick for setting up the computer data acqusition system.

References

1. See C. W. Wilmsen and S. Szpak, "MOS Processing for III-V Compound Semiconductors: Overview and Bibliography," Thin Solid Films, 46, 17 (1977).

2. See, for example, review by W. E. Spicer, Appl. Phys., 12, 115 (1977).

3. P. Pianetta, I. Lindau, and W. E. Spicer, Quantitative Surface Analysis of Materials, ASTM STP 643, N. S. McIntyre, Ed., American Soc. for Testing and Materials, 1978, pp. 105-123.

4. P. Pianetta, I. Lindau, C. M. Garner, and W. E. Spicer, Phys. Rev. Lett., 37, 1166 (1976); 35, 1356 (1975); Phys. Rev. B, in press.

5. W. E. Spicer, I. Lindau, C. Y. Su, P. W. Chye, and P. Pianetta, Appl. Phys. Lett., in press.

6. P. E. Gregory, P. Chye, H. Sunami, and W. E. Spicer, J. Appl. Phys., 46, 3525 (1975).

7. C. A. Papageorgopoulos and J. M. Chen, Surf. Sci., 39, 313 (1973).

8. C. Wijers, M. R. Adriaens, and B. Feuerbacher, to be published.

9. C. R. Helms and W. E. Spicer, Phys. Rev. Lett., 28, 565 (1972); 32, 228 (1974).

Figure Captions

1. EDCs of clean and oxygen exposed n-type GaAs (110) at $h\nu = 100$ eV. From Ref. 4.

2. EDCs of clean and Cs/O treated surface of n-type GaAs (110) at $h\nu = 120$ eV. The arrow under "A" points to an asymmetry in the Ga-3d peak. "*" represent equal energy spacing of 0.8 eV.

3. EDCs of clean p-type GaAs (110) and the clean surface exposed to excited oxygen at $h\nu = 100$ eV.

APPENDIX

II. Publications

1. Surface State Band on GaAs (110) Face, P. E. Gregory, W. E. Spicer, S. Ciraci, and W. A. Harrison, Applied Physics Letters 25, 511 (1974).

2. The Oxidation of Cs UV Photoemission Studies, P. E. Gregory, P. Chye, H. Sunami, and W. E. Spicer, Journal of Applied Physics 46, No. 8, 3525 (August 1975).

3. Photoemission Studies of the GaAs-Cs Interface, P. E. Gregory and W. E. Spicer, Physical Review B12, 2370 (September 1975).

4. Determination of the Oxygen Binding Site on GaAs (110) Using Soft X-Ray-Photoemission Spectroscopy, P. Pianetta, I. Lindau, C. Garner, and W. E. Spicer, Phys. Rev. Letters 35, 1356 (November 1975).

5. GaSb Surfaces States and Schottky-Barrier Pinning, P. W. Chye, I. A. Babalola, T. Sukegawa, and W. E. Spicer, Comments - Physical Review Letters 35, 1600 (December 1975).

6. Photoemission Study of the Formation of Schottky Barriers, W. E. Spicer, P. E. Gregory, P. W. Chye, I. A. Babalola, and T. Sukegawa, Applied Physics Letters 27, 617 (December 1975).

7. Photoemission Study of Surface States of the (110) GaAs Surface, P. E. Gregory and W. E. Spicer, Phys. Rev. B13, 725 (January 1976).

8. Ultraviolet Photoemission Study of Cesium Oxide Films on GaAs, P. E. Gregory and W. E. Spicer, Journal of Applied Physics 47, 510 (February 1976).

9. Photoemission Studies of Surface and Interface States on III-V Compounds, W. E. Spicer, P. W. Chye, P. E. Gregory, T. Sukegawa, and I. A. Babalola, J. Vac. Sci. Technol. 13, 233 (January/February 1976).

10. Photoemission Studies of Surface States and Schottky-Barrier Formation on InP, P. W. Chye, I. A. Babalola, T. Sukegawa, and W. E. Spicer, Phys. Rev. B13, 4439 (May 1976).

11. Synchrotron Radiation Studies of Electronic Structure and Surface Chemistry of GaAs, GaSb, and InP, W. E. Spicer, I. Lindau, P. E. Gregory, C. M. Garner, P. Pianetta, and P. W. Chye, J. Vac. Sci. Technol. 13, 780 (July/August 1976).

12. Photoemission Study of the Adsorption of O_2, CO and H_2 on GaAs (110), P. E. Gregory and W. E. Spicer, Surface Science 54, 229-258 (1976).

13. Oxidation Properties of GaAs (110) Surfaces, P. Pianetta, I. Lindau, C. M. Garner, and W. E. Spicer, Physical Review Letters 37, 1166 (1976).

14. Surface and Interface States of GaSb: A Photoemission Study, P. W. Chye, T. Sukegawa, I. A. Babalola, H. Sunami, P. Gregory, and W. E. Spicer, Physical Review B15, 2118 (February 1977).

15. Oxygen Sorption and Excitonic Effects on GaAs Surfaces, P. W. Chye, P. Pianetta, I. Lindau, and W. E. Spicer, J. Vac. Sci. Technol. 14, 917-919 (July/August 1977).

16. Surface and Interface States on GaAs (110): Effects of Atomic and Electronic Rearrangements, W. E. Spicer, P. Pianetta, I. Lindau, and P. W. Chye, J. Vac. Sci. Technol. 14, No. 4, 885-893 (July/August 1977).

17. Do the Au 5d-Bands Narrow at the Surface: Comparison with Au Alloys, P. W. Chye, I. Lindau, P. Pianetta, C. M. Garner, and W. E. Spicer, Physics Letters 63A, No. 3, (November 1977).

18. Studies of Surface Electronic Structure and Surface Chemistry Using Synchrotron Radiation, W. E. Spicer, I. Lindau, J. N. Miller, D. T. Ling, P. Pianetta, P. W. Chye, and C. M. Garner, Physica Scripta 16, 388 (November/December 1977).

19. Reply to "Oxidation Properties of GaAs (110) Surfaces", R. Ludeke, P. Pianetta, I. Lindau, C. M. Garner, and W. E. Spicer, Phys. Rev. B. 16, No. 12, 5600-5602 (December 1977).

20. Photoemission Studies of the Electronic Structure of III-V Semiconductor Surfaces, I. Lindau, P. Pianetta, C. M. Garner, P. W. Chye, P. E. Gregory, and W. E. Spicer, Surface Science 63, 45-55 (1977).

21. The Surface Electronic Structure and Surface Chemistry of GaAs (110), P. Pianetta, I. Lindau, W. E. Spicer, and C. M. Garner, Proc. 7th Intern. Vac. Congr. and 3rd Intern. Conf. Solid Surfaces, 615-618, Vienna, (1977).

22. Oxygen Adsorption and the Surface Electronic Structure of GaAs (110), I. Lindau, P. Pianetta, W. E. Spicer, P. E. Gregory, C. M. Garner, and P. W. Chye, J. of Electron Spectroscopy and Related Phenomena 13, 155-160 (1978).

23. Valence Band Studies of Clean and Oxygen Exposed GaAs (11C) Surfaces, P. Pianetta, I. Lindau, P. E. Gregory, C. M. Garner, and W. E. Spicer, Surface Science 72, 298-320 (1978).

24. Evidence for a New Type of Metal-Semiconductor Interaction on GaSb, P. W. Chye, I. Lindau, P. Pianetta, C. M. Garner, and W. E. Spicer, Phys. Rev. B. 17, No. 6, 2682-2684 (March 1978).

25. The Use of Soft X-Ray Photoemission Spectroscopy to Study the Adsorption of Oxygen on the (110) Surface of Gallium Arsenide and Gallium Antimonide, P. Pianetta, I. Lindau, and W. E. Spicer, Quantitative Surface Analysis of Materials, ASTM STP 643, N. S. McIntyre, Ed., American Society for Testing and Materials, 105-123, 1978.

26. New Phenomena in Schottky Barrier Formation on III-V Compounds, I. Lindau, P. W. Chye, C. M. Garner, P. Pianetta, C. Y. Su, and W. E. Spicer, J. Vac. Sci. Technol. 15(4), 1332-1339 (July/August 1978).

27. UPS and LEED Studies of GaAs (110) and (111) As Surfaces, P. Skeath, W. A. Saperstein, P. Pianetta, I. Lindau, and W. E. Spicer, J. Vac. Sci. Technol. 15(4), 1219-1222, (July/August 1978).

28. Chemisorption and Oxidation Studies of the (110) Surfaces of GaAs, GaSb, and InP, P. Pianetta, I. Lindau, C. M. Garner, and W. E. Spicer, Phys. Rev. B 18, No. 6, 2792-2806 (September 1978).

29. Photoemission Study of Au Schottky-Barrier Formation on GaSb, GaAs, and InP Using Synchrotron Radiation, P. W. Chye, I. Lindau, P. Pianetta, C. M. Garner, C. Y. Su, and W. E. Spicer, Phys. Rev. B 18, No. 10, 5545-5559 (November 1978).

30. Core-Level Photoemission of the Cs-O Adlayer of NEA GaAs Cathodes, W. E. Spicer, I. Lindau, C. Y. Su, P. W. Chye, and P. Pianetta, Appl. Phys. Lett. 33(11), 934-935 (December 1978).

31. Oxygen Chemisorption on Cs Covered GaAs (110) Surfaces, C. Y. Su, P. W. Chye, P. Pianetta, I. Lindau, and W. E. Spicer, Surface Science (Proc. from the ICSFS Conf., 5-8 July 1978, Tokyo).

32. The Surface Electronic Structure of 3-5 Compounds and the Mechanism of Fermi Level Pinning by Oxygen (Passivation) and Metals (Schottky Barriers), W. E. Spicer, P. W. Chye, C. M. Garner, I. Lindau, and P. Pianetta, Surface Science (Proc. from the ICSFS Conf., 5-8 July 1978, Tokyo).

33. Abrupt $Ga_{1-x}Al_xAs$-GaAs Quantum-Well Heterostructures Grown by Metal-organic Chemical Vapor Deposition, R. D. Dupuis, P. D. Dapkus, C. M. Garner, C. Y. Su, and W. E. Spicer, Appl. Phys. Lett. 34, No. 5, 338-340 (March 1979).

34. Fundamental Studies of III-V Surfaces and the 3-5 Oxide Interface, W. E. Spicer, I. Lindau, P. Pianetta, P. W. Chye, and C. M. Garner, Thin Solid Films, Vol. 56, No. 1, 2, 1-18 (1979).